

# **Molecular Basis of Recessively Inherited Eye Disorders in Pakistani Population**



**By  
Raesa Tehreem**

**Molecular Biology Lab  
Department of Zoology  
Faculty of Biological Sciences  
Quaid-i-Azam University,  
Islamabad  
2024**

# **Molecular Basis of Recessively Inherited Eye Disorders in Pakistani Population**

PhD Dissertation



**By**  
**Raeesa Tehreem**

**Supervised By**  
**Dr. Sabika Firasat**

Submitted in the partial fulfillment of the requirement for degree of Doctor of Philosophy in Molecular Biology

**Molecular Biology Lab**

**Department of Zoology**  
**Faculty of Biological Sciences**  
**Quaid-i-Azam University,**  
**Islamabad**  
**2024**

*"In the name of ALLAH, the most Beneficent,  
the most Merciful"*



# *Dedication*

This manuscript is entirely dedicated to my teachers, family, friends, my supporting husband and world's best parents especially my mother who will always have profound impact on my life and my father whose motivation and encouragement made me successful.

## Certificate of Approval

This is to certify that the research work presented in this thesis, entitled "Molecular Basis of Recessively Inherited Eye Disorders in Pakistani Population" was conducted by **Ms. Raeesa Tehreem** under the supervision of **Dr. Sabika Firasat**. No part of this thesis has been submitted anywhere else for any other degree. This thesis is submitted to the Department of Zoology of Quaid-i-Azam University, Islamabad in partial fulfillment of the requirements for the degree of Doctor of Philosophy in Zoology (Molecular Biology).

Student Name: **Ms. Raeesa Tehreem**

Signature: Raeesa

### Examination Committee:

a) External Examiner 1:

Signature: [Signature]

- 1. Dr. Mazhar Qayyum**  
Professor (Retd.)  
Department of Zoology, Wildlife  
and Fisheries, PMAS Arid  
Agriculture University, Rawalpindi

b) External Examiner 2:

Signature: [Signature]

- 2. Dr. Shamim Akhter**  
Professor (Retd.)  
Department of Zoology, Wildlife  
and Fisheries, PMAS Arid  
Agriculture University, Rawalpindi

- 3. Dr. Sabika Firasat**  
Research Supervisor

Signature: [Signature]

Name of HOD: **Dr. Kiran Afshan**

Signature: [Signature]

Date: 27.09.2024

CHAIRPERSON  
Department of Zoology  
Quaid-i-Azam University  
Islamabad,



## **Author's Declaration**

I **Ms. Raeesa Tehreem** hereby state that my PhD thesis titled “Molecular Basis of Recessively Inherited Eye Disorders in Pakistani Population” is my own work and has not been submitted previously by me for taking any degree from Quaid-i-Azam University, Islamabad, Pakistan.

At any time if my statement is found to be incorrect even after my Graduation the University has the right to withdraw my Ph.D. degree.

Signature     *Raeesa*    

**Ms. Raeesa Tehreem**

## **Plagiarism Undertaking**

I solemnly declare that research work presented in the thesis titled “Molecular Basis of Recessively Inherited Eye Disorders in Pakistani Population” is solely my research work with no significant contribution from any other person. Small contribution/ help wherever taken has been duly acknowledged and that complete thesis has been written by me.

I understand the zero tolerance policy of the HEC and Quaid-i-Azam University towards plagiarism. Therefore I as an Author of the above titled thesis declare that no portion of my thesis has been plagiarized and any material used as reference is properly referred/ cited.

I undertake that if I am found guilty of any formal plagiarism in the above titled thesis even after award of Ph.D degree, HEC and the University has the right to publish my name on the HEC/University Website on which names of students are placed who submitted plagiarized thesis.

Student / Author Signature: Racesa

Name: **Ms. Racesa Tehreem**

### **Plagiarism Undertaking**

I solemnly declare that research work presented in this thesis entitled “Molecular basis of recessively inherited eye disorders in Pakistani population” is my research work with no significant contribution from any other person. Contributions have been duly acknowledged and complete thesis is written by me.

I understand the zero-tolerance policy of HEC and Quaid-i-Azam University towards Plagiarism. Therefore, I as an author declare that no portion of my thesis is plagiarized, and any material used as a reference is properly cited.

Author Signature  
Raeesa Tehreem



## TABLE OF CONTENT

Sr. No	Title	Page no
<b>Chapter 1: INTRODUCTION</b>		
<b>Section I:</b>		
1.1	Brief anatomy of the human eye	1
1.2	Eye disorders	2
1.3	Autosomal recessive ocular disorders	3
1.4	Glaucoma	4
1.5	Anatomy and physiology of eye relevant to Glaucoma	4
1.6	Pathophysiology of Glaucoma	6
1.7	Classification of glaucoma	7
1.8	Examination and differential diagnosis	10
1.9	Genetics of primary congenital glaucoma	10
1.10	Treatment and disease management	13
<b>Section II:</b>		
1.11	Inherited Retinal dystrophies	14
1.12	Anatomy of photoreceptors	14
1.13	The visual cycle	14
1.14	Mechanisms involved in retinal degeneration	16
1.15	Retinitis pigmentosa	18
1.16	Types of retinitis pigmentosa	19
1.17	Other inherited retinal dystrophies	21
1.18	Genetics of retinal dystrophies	22
1.19	Diagnostic criteria	24
1.20	Treatment and disease management	26
<b>Section III:</b>		
1.21	Microphthalmia	27
1.22	Risk factors for microphthalmia	27
1.23	Development of human eye at molecular level	28
1.24	Types of microphthalmia	29
1.25	Diagnosis	30
1.26	Genetics of microphthalmia	31

---

1.27	Disease management and treatment	32
1.28	Molecular diagnosis in genetic disorders	34
1.29	Objectives of study	37
<b>Chapter 2: MATERIALS AND METHODOLOGY</b>		
2.1	Field work	39
2.2	Laboratory work	40
2.3	Molecular analysis of Primary congenital glaucoma	43
2.4	Molecular analysis of retinal dystrophies and microphthalmia	47
<b>Chapter 3: RESULTS</b>		
<b>Section I:</b>		
3.1	Clinical analysis of Primary congenital glaucoma	54
3.2	Molecular analysis of Primary congenital glaucoma patients	55
3.3	Polymorphisms identified in CYP1B1 gene	66
3.4	Conservation analysis of identified disease causing variants	68
3.5	Analysis of conservation and structure by HOPE	69
<b>Section II:</b>		
3.6	Clinical analysis of inherited retinal dystrophies	71
3.7	Molecular analysis of thirty five retinal dystrophy families	75
<b>Section III:</b>		
3.8	Clinical analysis of microphthalmia	100
3.9	Molecular analysis of Microphthalmia	101
<b>Chapter 4: DISCUSSION</b>		
4.1	Clinical and molecular study of primary congenital glaucoma in Pakistani population	105
4.2	Clinical and molecular analysis of inherited retinal dystrophies	107
4.3	Clinical and molecular analysis of microphthalmia	111
4.4	Conclusion and future perspective	112
<b>Chapter 5: REFERENCES</b>		
Annexure I		
Annexure II		
Publications		

---

## List of Tables

Table No.	Title	Page no
1.1	Chromosomal anomalies associated with microphthalmia.	30
2.1	Composition of solutions used for extraction of genomic DNA	42
2.2	List of primers used to amplify CYP1B1 gene in enrolled families	44
2.3	Components of PCR reaction and their quantity for 25 µL reaction mixture	44
2.4	List of 344 candidate genes screened in NGS panel capture sequencing	48
3.1	List of Novel disease causing variants identified in PCG patients	56
3.2	List of all the single nucleotide polymorphisms identified in current study	56
3.3	In-silico analysis of disease-causing variants identified in this study	57
3.4	In-silico analysis of polymorphisms identified in this study	67
3.5	Demographic and clinical data of thirty five inherited retinal dystrophies affected families enrolled for this study	72
3.6	List of previously reported and novel pathogenic variants identified in eighteen unrelated inherited retinal dystrophies families segregating with disease phenotype.	76
3.7	In silico analysis of nineteen, disease causing variants found in nineteen retinal dystrophies families	77
3.8	Novel missense variant identified in S1PR2 gene in RP 073	87
3.9	A list of primers used to amplify ALMS1 gene exonic region (13-16) deletion of chr2:73775682-73814328 in RP109	93
3.10	Details of pathogenic variant identified in FOXE3 encoding gene in current study	101
3.11	List of exonic splicing sites (ESE), exonic splicing silencer (ESS) created and ESE sites broken due to c.720 C>A disease causing variant	102

## List of Figures

Figure No.	Legend	Page no
1.1	Sagittal section of the human eye	3
1.2	Schematic illustration of the trabecular meshwork outflow pathway	5
1.3	Schematic diagram illustrating the uveoscleral outflow pathway	6
1.4	The normal anatomy of human optic nerve. B) Neurodegeneration in optic nerve in glaucoma.	6
1.5	Signaling pathway in unfolded proteins in response to ER-stress	7
1.6	Schematic illustration of normal human eye anatomy B) Regions of eye affected in POAG C) Obstruction of drainage pathway in primary angle closure glaucoma	9
1.7	Schematic view of CYP1B1 gene role in glaucoma	12
1.8	Anatomy of the cone and rod photoreceptor cells	15
1.9	The visual cycle in photoreceptor cells	16
1.10	The visual cycle in cone photoreceptors	16
1.11	Mechanism of cone cell death due to deficiency of rod-derived cone viability factor (RdCVF)	17
1.12	Role of oxidative stress in cone degeneration	18
1.13	Fundus showing bony spicules, pale optic disc and attenuated blood vessels in a retinitis pigmentosa patient	25
1.14	Clinical appearance of microphthalmia	28
1.15	Formation of lens and optic cup in developing human eye	29
1.16	A baby with unilateral microphthalmia. (a) Eye without cosmetic shell (b) An eye with cosmetic shell (c) appearance of child with cosmetic shell with growth	33
1.17	The method of Sanger sequencing in graphical form	36
3.1	The graph shows the number of PCG patients recruited in current study in different age groups	55
3.2	Pedigree drawing of family PCG 049	58
3.3	Chromatograms of two heterozygous variants c.457C>G and c.516C>A identified in family PCG 049 in CYP1B1 gene	59
3.4	Pedigree diagram of Family PCG 059	60

3.5	Chromatogram of frameshift variant c.758_759insA identified in family PCG 059.	60
3.6	Pedigree diagram of family PCG 060	61
3.7	Chromatogram of family PCG 060 showing missense variant c.722T>A	62
3.8	Pedigree drawing of family PCG 062	62
3.9	Chromatograms for compound heterozygous variants c.1263T>A and c.1314G>A identified in family PCG 062	63
3.10	Pedigree of family PCG 063	65
3.11	Chromatograms of compound heterozygous variants c.771T>G and c.789dup identified in family PCG 063.	65
3.12	Pedigree drawing of family PCG 067 showing four affected members	65
3.13	Chromatogram of normal and affected individual for variant c.724G>C in family PCG 067	66
3.14	Figure shows comparison of conservation of amino acids in CYP1B1 gene among homologs for unreported disease causing variants detected in current study.	69
3.15	The overview of CYP1B1 wild type protein	69
3.16	Position of amino acid residue and change in structure due to variant predicted by HOPE. Wild type amino acid residue is green in color while red color shows mutant amino acid.	70
3.17	Vertical graph shows the number of affected individuals in a particular age group among 35 enrolled families	74
3.18	Pie chart showing the percentage of stationary and progressive cases of night blindness among recruited families	74
3.19	Pedigree diagram of family RP 004	78
3.20	Chromatogram of family RP 004 (a) Control IV.II (heterozygous for the variant in AGL5 gene) (b) Proband V.I (c) affected siblings V.II and V.III	78
3.21	Pedigree diagram of family RP 005	79
3.22	Chromatograms for variant c.847C>T in family RP 005 in CERKL gene. a) Control III.XV b) Proband III.XVIII c) affected sister III.X d) affected sister III.XVII e-g) affected nephews and niece	80
3.23	Pedigree diagram of family RP 008	80
3.24	Chromatograms showing variant c.1429C>T in GPR179 gene in family RP 008. a) Heterozygous in III.II b) Homozygous in IV.XI c) Heterozygous in III.III d)	81

---

	Homozygous in IV.XII	
3.25	Pedigree diagram of Family RP 010	81
3.26	Chromatograms of c.874C>T variant in SAG gene in family RP 010. (a, c) Heterozygous variant in unaffected individuals (b, d, e) Homozygous variant in affected individuals.	82
3.27	Pedigree diagram of RP 019	82
3.28	Pedigree diagram of family RP 043	83
3.29	Chromatograms of heterozygous normal individuals and two affected individuals for family RP 043 in ARL6 gene	84
3.30	Chromatograms for variant c.1252T>C in CRB1 gene in family RP 044. a) II.I b) III.II c) III.V d) III.VI	85
3.31	Pedigree diagram of Family RP 044	85
3.32	Pedigree diagram of RP 073	85
3.33	Pedigree diagram showing segregation of novel S1PR2 gene variant c.388C>T. Individuals (symbols) colored in orange are suffering from profound deafness while black colored symbols depict RP affected individuals	86
3.34	Chromatogram for individual V.XII on the left and IV.XX on the right showing variant nucleotide in CNGB1 gene in family RP 073	86
3.35	Chromatogram for individual III.I on the left and IV.III on the right showing variant c.388C>T in S1PR2 gene in RP 073	87
3.36	Pedigree diagram of RP 102. (m2: c.187C>T)	87
3.37	Chromatograms for variant c.187C>T in RP 102 in USH2A gene	88
3.38	Chromatogram for variant c.1560C>A in gene USH2A in family RP 105. (unaffected (left) IV.I and affected (right) individual V.IV)	88
3.39	Pedigree drawing of family RP 105 (m3: c.1560C>A)	89
3.40	a) Fundus photograph of left and right eye of an affected individual (VI.VI of RP105) showing pale optic disc, bony spicules and thin blood vessels characteristic of RP phenotype. b) Audiometry report of an affected individual (VI.VI of RP105) performed at 14 years. The x-axis on graphs shows the frequency in hertz and the y-axis shows hearing level in decibels (dB). Note the hearing loss in the range of 50-80 dB in both ears of the Usher patient	89
3.41	Chromatogram of unaffected (left) and affected individual (right) for variant in NMNAT1 gene in family RP 106	90

---

3.42	Pedigree diagram of RP 106 (m4: c.547C>T)	90
3.43	Pedigree diagram of RP 107 family (m1: c.5571_5576delinsCTAGAT)	91
3.44	(a) Chromatogram of unaffected (left) and affected (right) family member (b) Segregation testing for novel homozygous deletion variant c.5571_5576delinsCTAGAT: p.Leu1858* found in EYS gene in RP107 in four affected (i, ii, iii, iv) and three unaffected (v, vi, vii) family members	92
3.45	Pedigree diagram of RP 109 (m1: c.9911_11550del)	92
3.46	Gel picture showing confirmation of deletion in unaffected and affected members.	93
3.47	Pedigree diagram of RP 110	94
3.48	(A) Chromatogram of unaffected and affected individual. (b) Segregation testing for heterozygous variant c.109del: p.Ala37fs*31 found in RP110 in PAX6 gene in two affected (i, ii) and two unaffected (iii, iv) family members	94
3.49	Chromatogram of unaffected and affected individual for variant c.471dup identified in family RP 112 and RP 113 in SPATA7 gene	95
3.50	Pedigree diagram (A) RP 112 (B) RP 113 (m1: c.471dup	96
3.51	Segregation testing results for homozygous duplication c.471dupG: p.Pro158Alafs*39 checked in RP113 in four affected (i, ii, iii, iv) and two unaffected (v, vi) family members	96
3.52	Chromatogram of unaffected and affected member of family RP 131 in ACOX3 gene	96
3.53	Pedigree diagram of RP 131	97
3.54	Segregation analysis of variant c.1459T>C in RP 131. (a,b,e,f) Unaffected (c,d) Affected	98
3.55	Chromatogram of affected IV.VI (right) and unaffected (left) III.II	98
3.56	Pedigree diagram of RP 144	99
3.57	Pedigree drawing of microphthalmia family (Micro-001) enrolled in this study showing autosomal recessive inheritance pattern of disease phenotype	99

---

3.58	A) Proband (VI.VIII in figure 1) an eleven years old female having microphthalmia, total sclerocornea and total blindness. (B) Uncle (V.VII in figure 1) of proband suffering from corneal opacities and microphthalmia since birth	100
3.59	Chromatogram of reported disease causing variant i.e., c.720C>A identified in homozygous state in proband (VI.VIII). Normal sequence is shown on left side while variant sequence is shown on right side of figure	101
3.60	(A) Clustal omega results showing comparison of FOXE3 gene sequence conservation among different homologs at variant site. (B) Web logo graphical representation of FOXE3 sequence proposing 100% conservation at variant i.e., p.Cys240* site. (Large size of amino acid abbreviation letter in Web logo result show full conservation while small size of letter shows less conserved position of amino acid among homologs)	103

---



## List of Abbreviations

---

UV radiations	Ultraviolet radiations
IOP	Intra ocular pressure
POAG	Primary open-angle glaucoma
UPR	Unfolded protein response
PAGC	Primary angle-closure glaucoma
<i>MMP9</i>	Matrix Metalloproteinase 9
<i>MTHFR</i>	Methylenetetrahydrofolate Reductase
<i>MFRP</i>	Membrane Frizzled-Related Protein
<i>HGF</i>	Hepatocyte Growth Factor
<i>ABCC5</i>	ATP Binding Cassette Subfamily C Member 5
<i>CYP1B1</i>	Cytochrome P450 Family 1 Subfamily B Member 1
<i>HSP70</i>	Heat Shock Protein Family A (Hsp70) Member 1A
PCG	Primary congenital glaucoma
<i>PGF</i>	Placental Growth Factor
<i>LTBP2</i>	Latent transforming growth factor- $\beta$ -binding protein-2
cGMP	Guanosine 3',5'-cyclic monophosphate
RdCVF	Rod derived cone viability factor
GLUT-1	Glucose transporter-1
mTOR	Mechanistic target of rapamycin
ROS	Reactive oxygen species
NADPH	Nicotinamide adenine dinucleotide phosphate
RP	Retinitis pigmentosa
USH	Usher syndrome
BBS	Bardet-Biedl syndrome
LCA	Leber congenital amaurosis
ARMD	Age- related macular degeneration
IRDs	Inherited retinal dystrophies

---

---

<i>PDE6C</i>	Phosphodiesterase 6C
<i>PDE6B</i>	Phosphodiesterase 6b
<i>CNGB1</i>	Cyclic nucleotide-gated channel protein 1
<i>CRB1</i>	Crumbs cell polarity complex component 1
<i>MYO7A</i>	Myosin, unconventional, family VII, member A
<i>ARL6</i>	ADP-ribosylation factor-like GTPase 6
<i>NMNAT1</i>	Nicotinamide nucleotide adenylyltransferase 1
<i>ABCA4</i>	Adenosine triphosphate-binding cassette transporter alpha 4 subunit
OCT	Optical coherence tomography
ERG	Electroretinogram
<i>OTX2</i>	Orthodenticle Homeobox 2
SHH	Sonic hedgehog
<i>BMP</i>	Bone morphogenetic protein
<i>VAX1</i>	Ventral Anterior Homeobox 1
<i>TMEM98</i>	Tumor-Suppressor Gene Transmembrane Protein 98
NGS	Next generation sequencing
dNTPs	Deoxynucleotides triphosphate

---

## ACKNOWLEDGEMENTS

All praises, thanks and acknowledgements to **ALLAH ALMIGHTY**, the most beneficent, the most merciful, Who provided me strength and capability to undertake and carry out this research project. Countless praises to our **HOLY PROPHET HAZRAT MUHAMMAD** (Peace be upon HIM), who is forever a torch of guidance and the embodiment of knowledge for enlightening humanity as a whole.

I would like to extend my deepest appreciation to those people, who helped me in one way or another to finish the task at hands, this thesis manuscript. It is a pleasure to convey my gratitude to all of them in my humble acknowledgment.

I feel deep sense of gratitude to my supervisor, **Dr. Sabika Firasat**, Associate Professor, Department of Zoology, Quaid-i-Azam University, Islamabad for her valuable guidance and suggestions throughout the study and presentation of this dissertation. I am thankful to her for her inspiration and counseling from time to time and providing a friendly environment.

I am obliged to **Dr. Kiran Afshan**, Chairperson, Department of Zoology, Faculty of Biological Sciences, Quaid-i-Azam University, Islamabad for extending the research facilities of the department to accomplish this work. I express my deepest gratitude to the whole faculty and all those teachers who had always been a source of motivation and inspiration for me and whose support and guidance helped me to get through all the difficulties.

I would like to thank **Prof. Dr. Sumaira Altaf** from Al Shifa Eye Trust Hospital, Rawalpindi, Pakistan. I would like to thank all the patients and their families whose participation helped me in making this work possible.

I would like to express my gratitude to my seniors for their guidance, valuable suggestions and support. I am thankful to my lab fellows and wish to extend a special thanks to Maria Komal who was always there to share my troubles and joys during the research work.

In the end, I gratefully acknowledge and thank my family and **Parents** especially my Mother whose contribution in our education is remarkable and cannot be explained in words. I would like to thank my **sisters** for their love, care and my husband for his support, encouragement and prayers that have enlightened my way throughout every task of life.

I am also thankful to **Higher Education Commission of Pakistan, Indigenous 5000 PhD Fellowship Program Phase II** and **International Research Support Initiative Program for funding and support** for this research project.

Finally, I thank again **Allah** the **Almighty**, the constant Guider, and the source of all good, Who listened to my prayers and destined the accomplishment of this task.

**Raeesa Tehreem**

## Abstract

Eye disorders can occur due to genetic variations that can be inherited. Autosomal recessive eye disorders are considered rare, but their prevalence increases significantly in regions where consanguineous marriages are common. The current study was designed to investigate the molecular basis of recessively inherited eye disorders in Pakistani population. After approval of this study from Bioethical Committee of Faculty of Biological Sciences, Quaid-i-Azam University, Islamabad Pakistan, various hospitals in different cities were visited and samples were collected from twenty primary congenital glaucoma (PCG) families, thirty-five retinal dystrophy families and one microphthalmia family with the help of ophthalmologists. Whole genomic DNA was extracted from each sample and Sanger's sequencing was carried out for *CYP1B1* gene in PCG patients while retinal dystrophy and microphthalmia samples were sent for next generation sequencing to screen for pathogenicity. The identified variants were checked for segregation in family members. Various in-silico tools such as PROVEAN, SIFT, Mutation taster, CADD, REVEL, PolyPhen-2, PANTHER and MutPred were used to analyze the pathogenicity of identified variants.

In twenty consanguineous PCG families Sanger sequencing of *CYP1B1* gene revealed nine disease causing variants included five missense variants c.457C>G, c.724G>C, c.516C>A, c.740T>A, c.1263T>A, two frameshift variants c.758-759insA, c.789dup and two silent variants c.1314G>A, c.771T>G. Out of these variants, six heterozygous and three homozygous variants were not reported before in any study. During molecular screening of these twenty families seven polymorphisms c.1347T>C, c.1294G>C, c.2244\_2245insT, c.1358A>G, c.355G>T, c.142C>G and g.35710\_35711insT were also identified one of which was not reported before (g.35710\_35711insT).

In thirty five retinal dystrophy families' disease causing variant were identified in eighteen families by next generation panel sequencing and whole exome sequencing for four families. The eighteen variants identified in current study were c.842G>A in *AGBL5* gene, c.847C>T in *CERKL* gene, c.1429C>T in *GPR179* gene, c.874C>T in *SAG* gene, c.559T>C in *RHO* gene, c.281T>C in *ARL6* gene, c.1252T>C, c.1728del and c.1459T>C in *CRB1* gene, c.413-1G>A in *CNGB1* gene, c.187C>T and c.1560C>A in *USH2A* gene, c.547C>T in *NMNAT1* gene, c.5571\_5576delins

CTAGAT in EYS gene, chr2:73775682-73814328 in ALSM gene, c.109del in PAX6 gene, c.471dup in SPATA7 gene, c.1163A>G in ACOX3 gene. Four variants c.1728del (p.Asp576GlufsTer20) in CRB1 gene, c.5571\_5576delinsCTAGAT (p. Leu1858\*) in EYS gene, c.471dup (p. Pro158Alafs\*39) in SPATA7 gene and c.1163A>G (p.Asp388Gly) in ACOX3 gene are not reported earlier in any study. Three of these novel variants were homozygous except for c.1728del (p.Asp576GlufsTer20) that was found in heterozygous condition. One novel variant p. Pro158Alafs\*39 was identified in two families RP 112 and RP 113. In family RP 073 a novel homozygous variant c.388C>T; p.Arg130Cys was identified in S1PR2 gene in three deaf and dumb family members who were found normal for retinal disorder.

In congenital bilateral microphthalmia family, a previously reported stop gain variant c.720C>A; p. Cys240\* was identified in FOXE3 gene during panel capture sequencing. This variant leads to early truncation of protein that cause developmental defects in size of eye socket and was segregated in recessive manner. The stop gain variant affected the exonic splicing enhancer sites and exonic splicing silencer sites and was found to be 100% conserved in similar species.

This study provides insight into the highly heterogeneous spectrum of eye disorders in consanguineous families from Pakistan. Genetic counseling was provided to all enrolled families. In PCG families, identification of disease-causing variant in *CYP1B1* gene in 45% recruited families draw attention to the involvement of non- coding region of *CYP1B1* gene and other genes like *LTBP2*, *TEK*, and *MYO7A* in our population. Identification of different gene mutations in eighteen inherited retinal dystrophy families and no variant in remaining seventeen recruited families stresses on need of whole genome sequencing of these families. Our findings necessitate effective screening of inherited eye disorders in Pakistani families using state of art technologies to reduce disease incidence in upcoming future through genetic counseling to refrain from practicing consanguinity and performing premarital screening as a control measure in upcoming generations.



**Chapter 1**  
**INTRODUCTION**

## **Section I:**

The human eye is highly specialized and one of the most complex organs in the human body. It is capable of receiving information in the form of visual images and sending it to the brain to process. The normal human has a diameter of 22-27 mm and a circumference of about 69-85 mm (Kels, Grzybowski, & Grant-Kels, 2015).

### **1.1. Brief anatomy of the human eye:**

The human eye has a protective covering that is made up of the palpebral conjunctiva, muscle, skin fold, and tarsus known as the eyelid (Shumway, Motlagh, & Wade, 2018). A cross-sectional view of the eye shows three different layers and chambers. The external layer is formed by the cornea and sclera, and the internal layer is comprised of retina, which has sensory receptors. There is an intermediate layer between these two layers that is formed anteriorly by the iris and ciliary body and posteriorly by the choroid (Kolb, 2011).

The fluid chamber between the cornea and iris is known as the anterior chamber. The posterior chamber is formed between the iris and lens. The vitreous chamber is the third compartment formed between the lens and retina (Figure 1.1) (Canning, Greaney, Dewynne, & Fitt, 2002). The socket protects the eyeball and is made up of the maxilla, palatine, and zygomatic bones at the bottom. At the top orbit is composed of the frontal bone and a wing of the sphenoid. The optic nerve runs into the brain through the optic foramen. The almond-shaped lacrimal glands keep the eye moist and are located at the outer corner of each eye. They comprise upper and lower duct systems (Ducker & Rivera, 2022).

There are six extraocular muscles involved in the movement of the eye among which four are rectus muscles and two are oblique muscles. The rectus muscles included are the superior, inferior, lateral, and medial muscles, whereas the two oblique muscles involved are the superior and inferior muscles (Shumway et al., 2018). The ophthalmic artery, a branch from the carotid artery, supplies blood to the eye muscles and divides into superior and inferior muscular branches. Another artery known as the lacrimal artery provides blood to the lateral rectus muscles, while two anterior ciliary arteries supply blood to all the remaining rectus muscles (Tibrewal & Kekunnaya, 2018).



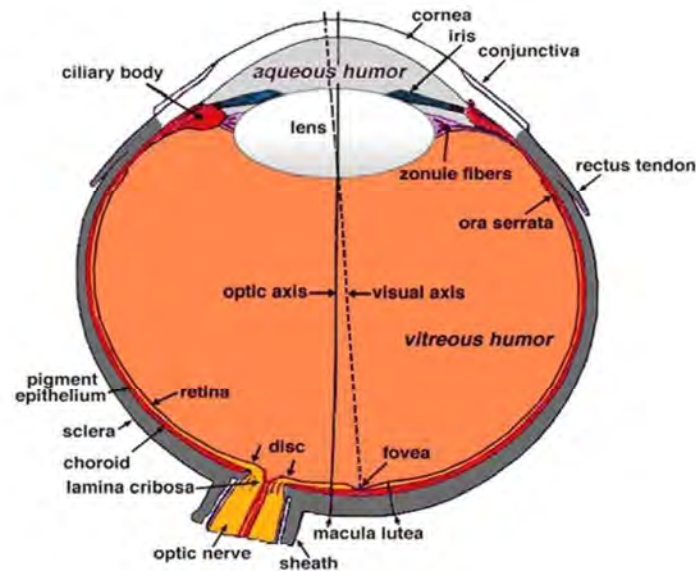


**Figure 1.1:** Sagittal section of the human eye (Kolb, 2011).

## 1.2. Eye disorders:

Impairment in visual acuity severely affects the life of an individual (Park, Ahn, Woo, & Park, 2015). Various genetic and environmental factors can contribute to a decrease or complete loss of vision. Some environmental factors contributing to vision loss include: UV radiations, exposure to toxic pollutants, harmful gases, chemicals, bacteria, viruses, smoking, drugs, reading or working in environment with poor light and physical injury (Yadav, 2019).

The genetic causes of eye diseases show variable inheritance patterns. The diseases that manifest in old age or later part of life usually do not have a clear pattern of inheritance although they seem to run in families such as age related macular degeneration (W. Chen et al., 2010), cataract, polypoidal choroidal vasculopathies and uveal melanoma (Singh & Tyagi, 2018).

The mitochondrial inheritance, autosomal dominant (aniridia, Axenfeld-Rieger anomaly, and neurofibromatosis type I), autosomal recessive (congenital hereditary endothelial dystrophy), X-linked dominant (Nance-Horan syndrome) and X-linked recessive (Lowe syndrome) pattern is observed in syndromes associated with glaucoma (Abu-Amero & Edward, 2017). The diseases that show autosomal recessive inheritance pattern are quite rare, although in populations where high interbreeding is

practiced many cases are observed. According to Dineen et al., 2007, cataract (51.5%) is the most common cause of blindness in adults ( $\geq 30$ ) followed by corneal opacity, aphakia, and glaucoma, in a comprehensive study he conducted on 16507 individuals (Dineen et al., 2007). Not much data is available on the most common causes of visual impairment and blindness in infants, children, and young adults in Pakistan.

### **1.3. Autosomal recessive ocular disorders:**

It is observed that consanguinity is deeply rooted in many parts of the world, and around one billion people live in communities that prefer intra-familial unions (Hamamy et al., 2011). Most of these disorders manifest in the first or second decade of individuals life span. Until now, an autosomal recessive pattern of disease has been observed in many ocular disorders.

In Pakistan, high risk of inherited autosomal recessive eye disorders is identified more frequently in families with consanguineous marriages. Consanguineous and first-degree nuptials are reported in approximately 60-80 % of the population (Hussain & Bittles, 1998).

The present study was aimed at identifying the most common autosomal recessive eye disorders in the Pakistani population and to find out the molecular determinants involved in disease development. Among autosomal recessive eye disorders present in Pakistani population case of primary congenital glaucoma and inherited retinal dystrophies were more common.

### **1.4. Glaucoma:**

The term glaucoma is coined for a group of heterogeneous disorders that can cause loss of the retinal ganglion cells, cupping of the optic disc, and thinning of fiber of the retinal layer (Jonas et al., 2018). It is classified according to etiology, age of onset and the iridocorneal angle (Sarfarazi, Stoilov, & Schenkman, 2003). In early stages of disease only peripheral visual image is lost without any other visible symptoms.

### **1.5. Anatomy and physiology of eye relevant to Glaucoma:**

Damage to the optic nerve is often associated with the elevation of intra-ocular pressure that occurs due to impaired outflow of aqueous humour. Aqueous humour

nourishes the eye with nutrients, and oxygen is produced by the ciliary body (Goel, Picciani, Lee, & Bhattacharya, 2010). The normal range of IOP is between 10-21 mm Hg. The ciliary body is a ring of tissues that is divided into ciliary epithelium, ciliary muscles, and ciliary body stroma. The non-pigmented cells (pars plana) of the ciliary epithelium secrete collagen, hyaluronic acid, and zonular fibers. The aqueous humour is derived from blood plasma by both active and passive transport (Goel et al., 2010).

Limbus, which is present at the border between sclera and cornea, performs many roles, like providing nourishment, corneal healing, hypersensitivity response, and immunosurveillance of the ocular region. It also controls the outflow of aqueous humour. In healthy eye about 80 to 90% of aqueous humour is discharged through Schlemm's canal/ trabecular meshwork (Figure 1.2) and 10 to 20% by uveoscleral outflow (Figure 1.3) (Sunderland & Sapro, 2022).

Aqueous humour moves from the anterior chamber through trabecular spaces of sponge-like trabecular meshwork. This meshwork is lined by cells that remove debris from aqueous humour as they have phagocytic and trapping activity. After reaching Schlemm's canal, aqueous humour is delivered to the blood stream (Sunderland & Sapro, 2022).

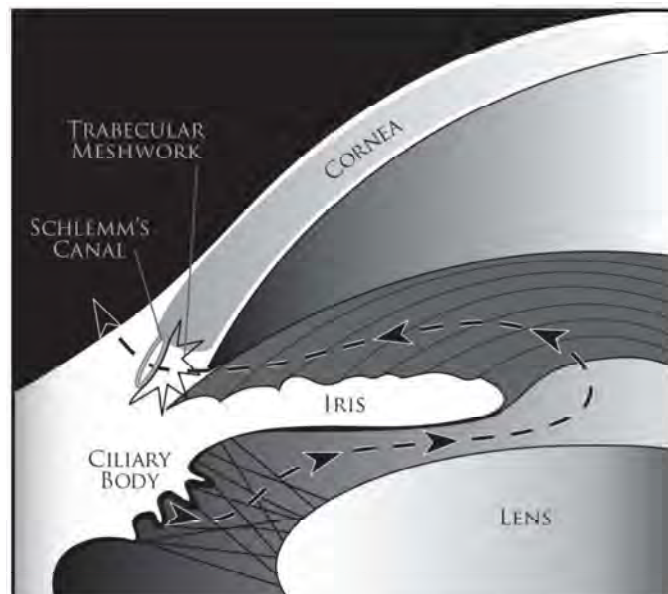


**Figure 1.2:** Schematic illustration of the trabecular meshwork outflow pathway (Goel et al., 2010).

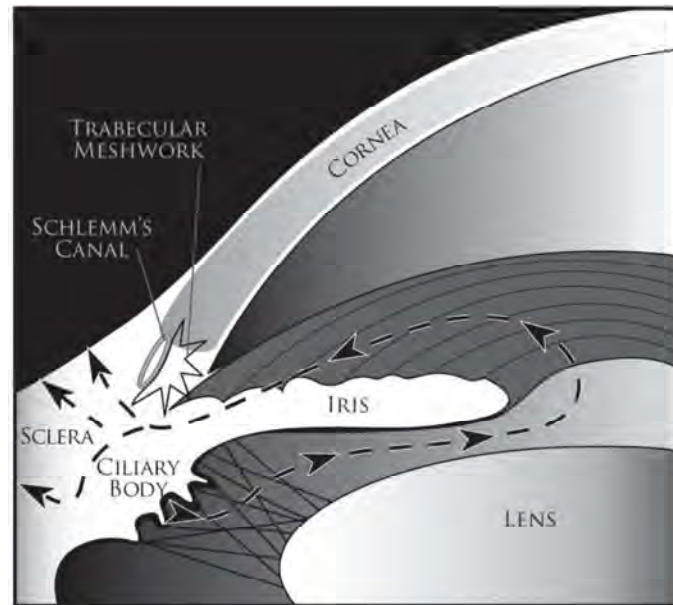


**Figure 1.3:** Schematic diagram illustrating the uveoscleral outflow pathway (Goel et al., 2010).

### 1.6. Pathophysiology of Glaucoma:

Although the exact pathogenesis of glaucoma is not fully known, the death of retinal ganglion cells due to increased IOP is related to it (Weinreb, Aung, & Medeiros, 2014). When the balance between production and drainage of aqueous humor is disturbed it causes the optic disc to compress. The compression of the optic disc hinders the flow of cytoplasm into the axon that leads to ischemia.

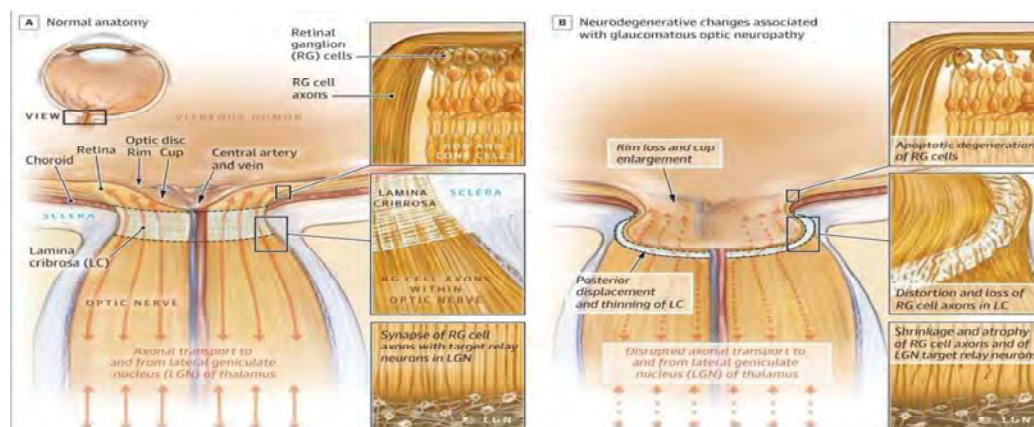


**Figure 1.4:** A) The normal anatomy of human optic nerve. B) Neurodegeneration in optic nerve in glaucoma. (Weinreb et al., 2014)

The affected individual can lose vision and can even go blind as the optic nerve is deprived of nutrients and oxygen (Sunderland & Sapiro, 2022) (figure 1.4). According to Anholt & Carbone, 2013, in POAG, myocilin is released by the trabecular meshwork into the aqueous humor. This myocilin helps in cell migration and cell adhesion (Anholt & Carbone, 2013). When compression causes increased stress, high cortisol results in a rise of myocilin production as a defense. The enzyme endoprotease calpain II, with the aid of calcium, cleaves myocilin. If these unfolded proteins are not removed through proteolysis, reduction, or ubiquitination, it causes ER stress. This is considered a leading cause of POAG. Disease-causing variations in different cellular components make it further difficult for the unfolded protein response (UPR) pathway to function, hence contributing to disease (Anholt & Carbone, 2013) (figure 1.5).

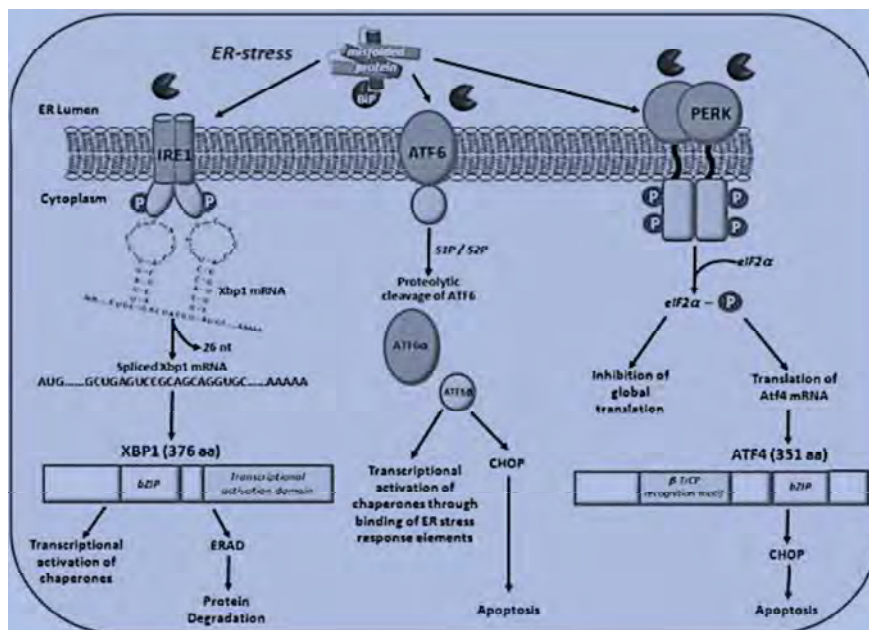


**Figure 1.5:** Signaling pathway in unfolded proteins in response to ER-stress. (Anholt & Carbone, 2013)

### 1.7. Classification of glaucoma:

Glaucoma can also be associated with other genetic abnormalities in development that occur due to anterior segment dysgenesis such as aniridia, Rieger's anomaly, Peter's anomaly, and Axenfeld's anomaly (Gould & John, 2002). Glaucoma is classified as primary when no other known etiology is identified and secondary when earlier

damage is reported that is contributing to disease. The major categories of glaucoma are:

### **1.7.1. Primary open angle glaucoma:**

Primary open-angle glaucoma (POAG) is a complex, chronic, and progressive optic neuropathy that damages optic nerve fibers (figure 1.6). In POAG, the anterior chamber angles are open that increases intra ocular pressure and loss of visual field. Most of the time the patients remain asymptomatic until a significant and an irreversible damage has occurred to the optic nerve (Taqi, Fasih, Jafri, & Sheikh, 2011). Some cases of POAG are observed in which the intra-ocular pressure (IOP) was low or normal. The optic nerve was still damaged even IOP was normal, this type of glaucoma is called as normal-pressure glaucoma (Anderson, Drance, & Schulzer, 2003). Genetics of POAG includes several genes: myocilin (*MYOC*) at *GLC1A* loci, optineurin (OPTN) at *GLC1E* and a repeat domain WD 36 at *GLC1G* loci are associated with autosomal dominant monogenic disease (Monemi et al., 2005; Rezaie et al., 2002; Stone et al., 1997).

### **1.7.2. Secondary open angle glaucoma:**

In this type of glaucoma, the resistance to the outflow of aqueous humour is increased in the trabecular meshwork and Schlemm's canal due to some detectable cause. This condition is also known as pigmentary glaucoma and exfoliative glaucoma (Moroi et al., 2003).

### **1.7.3. Primary angle closure glaucoma:**

The primary angle-closure glaucoma (PACG) occurs due to iridocorneal contact as the peripheral iris is pushed forward as a result of increased IOP in the posterior chamber and decreased pressure in the anterior angle (figure 1.6). The reason behind this pressure is the increased flow resistance through the slit between the lens and the iris that in turn damages the optic nerve (Nongpiur et al., 2011).

PACG is mostly associated with variants in *PLEKHA7* (Pleckstrin Homology Domain Containing, Family A Member 7, OMIM: 612686), *COL11A1* (Collagen Type XI Alpha 1 Chain, OMIM: 120280), *PCMTD1* (Protein-L-Isoaspartate O-Methyltransferase Domain-Containing Protein, OMIM: 620091), *ST18* (ST18

C2H2C-Type Zinc Finger Transcription Factor, OMIM: 617155) (Vithana et al., 2012), *MMP9* (Matrix Metalloproteinase 9, OMIM: 120361) (Awadalla, Burdon, Kuot, Hewitt, & Craig, 2011), *MTHFR* (Methylenetetrahydrofolate Reductase, OMIM: 607093) (Micheal et al., 2009), *MFRP* (Membrane Frizzled-Related Protein, OMIM: 606227) (I.-J. Wang et al., 2008), *CHX10* (Visual System Homeobox 2, OMIM: 142993) (Aung et al., 2008), *HGF* (Hepatocyte Growth Factor, OMIM: 142409) (Awadalla et al., 2011), *ABCC5* (ATP Binding Cassette Subfamily C Member 5, OMIM: 605251) (Nongpiur et al., 2014), *CYP1B1* (Cytochrome P450 Family 1 Subfamily B Member 1, OMIM: 601771) (Chakrabarti et al., 2007) and *HSP70* (Heat Shock Protein Family A (Hsp70) Member 1A, OMIM: 140550) (Ayub et al., 2010).

#### 1.7.4. Secondary angle closure glaucoma:

In secondary angle-closure glaucoma due to some ischemic retinopathy, vascular endothelial growth factor is overproduced that causes the iridocorneal contact (Ferrara, 2009).

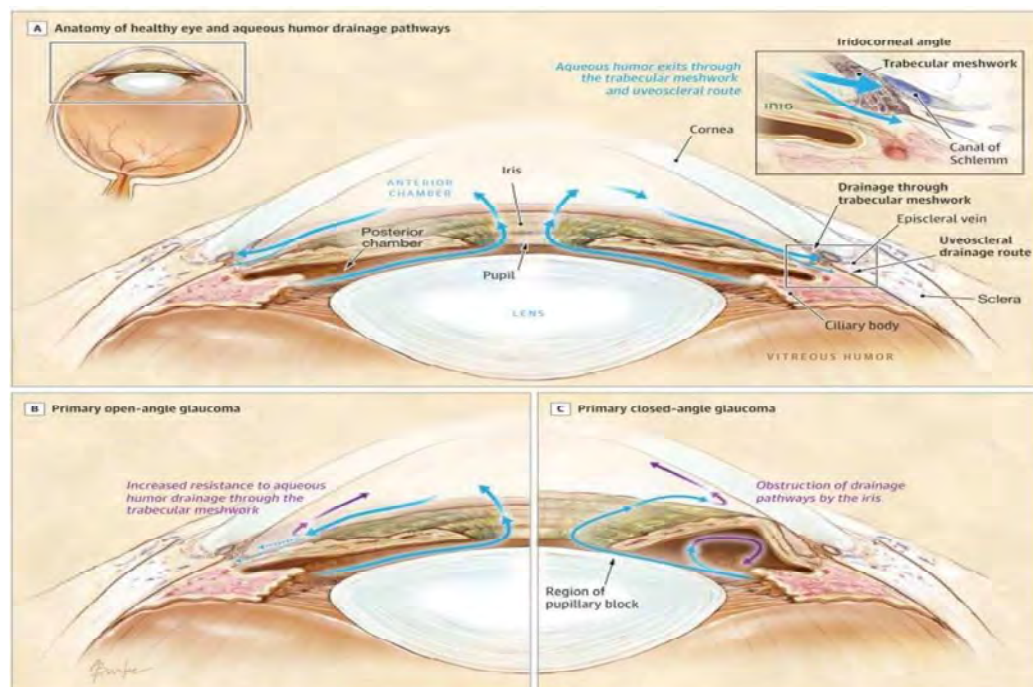


**Figure 1.6:** A) Schematic illustration of normal human eye anatomy B) Regions of eye affected in POAG C) Obstruction of drainage pathway in primary angle closure glaucoma (Weinreb et al., 2014).

### **1.7.5. Primary congenital glaucoma:**

Primary congenital glaucoma (PCG; OMIM 231300) is an infantile-stage disease showing symptoms like damage to Descemet's membrane, an enlarged globe, and opacification of the cornea (Sarfarazi & Stoilov, 2000). In PCG, irreversible loss of retinal ganglion cells leads to complete blindness in most cases. The disease is characterized by elevated intraocular pressure (IOP) and blockage in the flow of aqueous humor due to abnormalities in the anterior chamber angle and trabecular meshwork (Huang et al., 2014). Other clinical manifestations of PCG include buphthalmos, photophobia, blepharospasm, epiphora and hyperlacrimation (Barkan, 1955).

Worldwide data suggests that the disease is more prevalent in males as compared to females, at 65% and 35%, respectively (Vasiliou & Gonzalez, 2008). In Pakistan, glaucoma is reported as the third most common reason for bilateral blindness in individuals belonging to diverse ethnic origins (Mahar & Shahzad, 2008).

### **1.8. Examination and differential diagnosis:**

At an early stage of glaucoma it is completely painless and no measurable loss in visual field can be detected by patient (Jonas et al., 2018). Ocular enlargement occurs in PCG due to increased IOP by stretching, which results in the growth of collagen in the sclera and cornea. The normal corneal diameter (horizontal) is 9.5–10.5 mm for infants and 10–11.5 mm by the age of 1 year, which can reach 13 mm in cases of glaucoma (Beck, 2011).

The IOP range in healthy newborn babies is 10–12 mmHg, which becomes 20 mmHg or greater in case of disease that can be measured by tonometry and is considered as main criteria for diagnosis (Jonas et al., 2018). A complete ophthalmic examination also includes gonioscopy, a refraction test, and an assessment of the optic nerve. Looking for asymmetry in the cup-to-disc ratios and inspecting the cornea for clarity are also important in the accurate diagnosis of disease (Beck, 2011).

### **1.9. Genetics of primary congenital glaucoma:**

Genetic analysis of PCG patients manifests heterogeneity; so far, it is mapped on four loci for autosomal recessive inheritance. At the GLC3A locus, disease-causing



variants are identified in *CYP1B1*, a member of the cytochrome P450 enzyme family (OMIM: 601771) located at 2p21. It codes a metabolic enzyme and is considered the most common cause of PCG (Stoilov, Akarsu, & Sarfarazi, 1997). Two loci, *GLC3B* (1p36) and *GLC3C* (14q24.3), do not have any PCG genes associated with them, but recently, in a study on 100 unrelated PCG patients, variants were identified in *ZC2HC1C* (Zinc Finger C2HC-Type Containing 1C), *VPS13D* (Vacuolar Protein Sorting 13 Homolog D), and *PGF* (Placental Growth Factor) in these loci (Qiao et al., 2023).

Another gene *LTBP2* (latent transforming growth factor- $\beta$ -binding protein-2, OMIM: 602091) located at the fourth locus *GLC3D* (14q24.2-q24.3) has been identified to cause glaucoma in infants (Ali et al., 2009). An extracellular matrix protein is encoded by *LTBP2* that helps to maintain the structure of connective tissues and functions in cell adhesion (C. J. Lewis et al., 2017). The disease-causing variants are also found in four other genes in individuals with congenital glaucoma which include *TEK* (ANGPT1 receptor tunica interna endothelial cell kinase, OMIM: 617272) (Thomson et al., 2017), *MYOC* (myocilin, OMIM: 601652) (K Kaur et al., 2005), *ANGPT1* (angiopoietin-1, OMIM: 601667) (Souma et al., 2016), and *PXDN* (peroxidasin, OMIM: 605158) (K. Khan et al., 2011).

### 1.9.1. *CYP1B1* Gene:

Disease causing variants in cytochrome P450, subfamily 1, polypeptide 1 (*CYP1B1*) gene that encodes a 543 amino acid protein are known to cause congenital ocular anomalies (Vasiliou & Gonzalez, 2008). Homozygous or compound heterozygous mutant amino acids in *CYP1B1* gene are established to play a role in PCG by decreasing the activity of protein or by making it unstable (López-Garrido et al., 2010). According to the Human gene mutation database (HGMD) 315 disease causing variants are reported in *CYP1B1* gene until now for PCG, POAG, Peter's anomaly, congenital heart defects and hepatocellular adenoma. Various studies have revealed that this monooxygenase is involved in oxidative metabolism in a number of substrates both endogenous and exogenous (Vasiliou & Gonzalez, 2008). In ocular tissues *CYP1B1* protein is expressed in cornea, iris, retina and ciliary body. Its role in PCG was first studied by Stoilov et al., in families with bilateral eye anomalies and an autosomal recessive inheritance pattern of disease (Stoilov et al., 1997). The

hydroxylase activity of CYP1B1 for 17 $\beta$ -estradiol is primarily believed to be effected by disease causing variant leading to glaucoma (B. R. Shah, Xu, & Mraz, 2019) (figure 1.7). It can also help in the metabolism of retinol to retinoic acid that regulate morphogenesis (Kiranpreet Kaur, Mandal, & Chakrabarti, 2011).

In knockout studies in mice the CYP1B1 deficiency resulted in abnormalities in the trabecular meshwork. Detailed analysis revealed irregularities in collagen distribution, high oxidative stress, elevated peroxidation of lipids, and reduced level of periostin (Zhao et al., 2013).

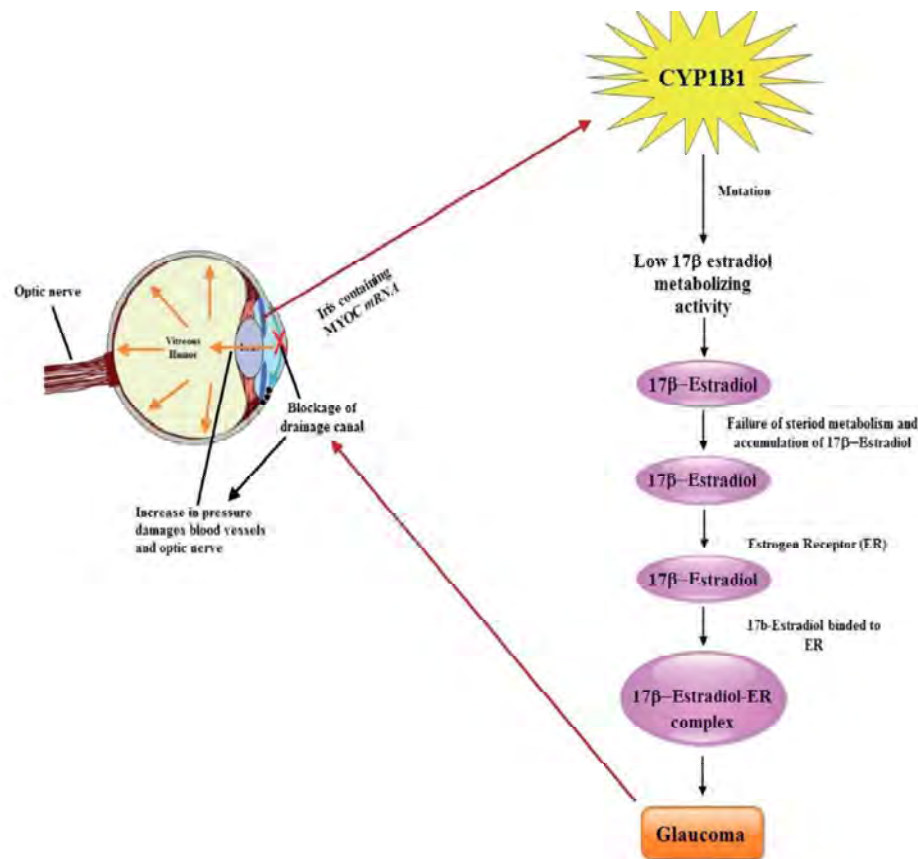


**Figure 1.7:** Schematic view of *CYP1B1* gene role in glaucoma (B. R. Shah et al., 2019).

### 1.9.2. *LTBP2* gene:

Latent transforming growth factor beta binding protein 2 (*LTBP2*), is located on locus GLC3D on chromosome 14q24. *LTBP2* gene is a member of transforming growth factor- $\beta$  (TGF- $\beta$ ) latent complex and codes a matrix protein (Ali et al., 2009). It

contains 36 exons and is identified as a strong candidate gene in many cases of primary congenital glaucoma. It is involved in the structural formation of microfibrils that are involved in cell adhesion.

Firasat et al. (2008) and Ali et al. (2009) identified mutations in LTBP2 gene in studies on consanguineous Pakistani families with PCG (Ali et al., 2009; Firasat, Riazuddin, Hejtmancik, & Riazuddin, 2008).

#### **1.10. Treatment and disease management:**

Unfortunately until now no cure is discovered for this chronic condition. The only option is disease management and timely diagnosis for better results (H. Yang, Lu, & Sun, 2023). Trabeculotomy is performed to reduce the elevated IOP and is considered the gold standard procedure in disease management (H. Yang et al., 2023). Other approach to lower the pressure of aqueous humor at an early stage of disease is reducing its production by using drugs like alpha-adrenergic agonists and beta-blockers (R. A. Lewis et al., 2017).

**SECTION II:****1.11. Inherited Retinal dystrophies**

An important cause of substantial vision loss and sometimes blindness is degenerative retinal dystrophies. These genetically heterogeneous disorders and have a range of phenotypic manifestation, but the most common symptoms include night blindness, color blindness and loss of peripheral vision (Nash, Wright, Grigg, Bennetts, & Jamieson, 2015). As the time progress the disease becomes worse and can lead to complete blindness. High variability is reported in inheritance pattern of familial cases of retinal dystrophies including autosomal dominant, autosomal recessive, X-linked dominant and X-linked recessive (Bowne et al., 2002). The estimated prevalence of retinal abnormalities is 1 in every 4000 individuals (Haim, 2002). To date multiple causative genes have been identifies to be associated the retinal disorders. In the retina the degeneration of the photoreceptor cells due to harmful mutations is considered the cause of many inherited retinal dystrophies and various knockout studies on mouse models have also confirmed it (Perkins, Fadool, & Dowling, 2004).

**1.12. Anatomy of photoreceptors:**

The photoreceptor cells are highly specialized cells consisting of an outer segment, a cilium that connects outer segment to the inner segment, cell body and synaptic region (Perkins et al., 2004) (figure 1.8). The outer segment in cones is different in cones as compared to rods. It contains tightly stacked discs having phototransduction proteins in them. The intraflagellar transport in cilia takes the pigment protein formed in inner segment to the outer segment. The inner segment of photoreceptor cells also contains mitochondria to fulfill the energy demands for production and transport of pigment protein. Spherules (synaptic terminal of rods) and pedicles (synaptic terminals of cones) have synaptic vesicles and synaptic ribbons. Both pedicles and spherules are presynaptic to horizontal cells and bipolar cells (Insinna & Besharse, 2008).

**1.13. The visual cycle:**

When a photon of light enters the eye it triggers a series of reactions in retina with the help of a G-protein coupled receptor known as opsin to convert that photon into an electrical signal (Allwardt, Lall, Brockerhoff, & Dowling, 2001). When 11-cis retinal

chromophore present in opsin is activated by the photon of light it isomerizes to all-trans retinal (figure 1.9).

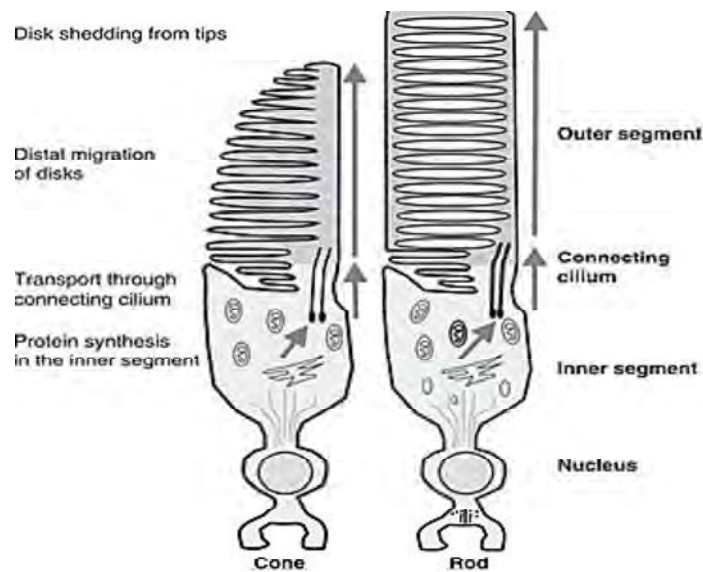


**Figure 1.8:** Anatomy of the cone and rod photoreceptor cells (Perkins et al., 2004).

This action leads to the hyperpolarization of the photoreceptor cell as the cGMP gated channels are closed. All this change of potentials in photoreceptor cells causes the brain to receive nerve impulse and an image is generated. To receive another image to repeat the process the all-trans retinal is converted to all-trans retinol. Another enzyme lecithin-retinol acyltransferase then change it to retinyl ester in retinal pigment epithelium.

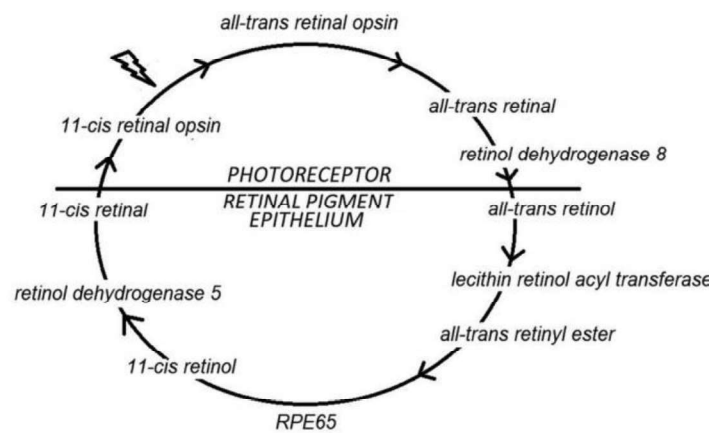


**Figure 1.9:** The visual cycle in photoreceptor cells (Tsin, Betts-Obregon, & Grigsby, 2018).

Isomerase I then convert retinyl ester to 11-cis-retinol which is later oxidized to 11 cis-retinal. It is then combined with opsin to form rhodopsin in rods and cones. The cones in photoreceptor cell responds to different wave length of light and are responsible for the perception of color vision. The visual cycle in cones begin when all-trans retinal is released by photo isomerization from cone pigment (figure 1.10). In the retina it is transferred to Muller cells when reduced to all-trans retinol. It is then isomerized to 11-cis retinol and later esterified. When hydrolyzed it is returned to photoreceptor cells in the form of 11-cis retinol where it is further oxidized to 11-cis retinal. In the photoreceptor cells it is conjugated to opsin for pigment formation.

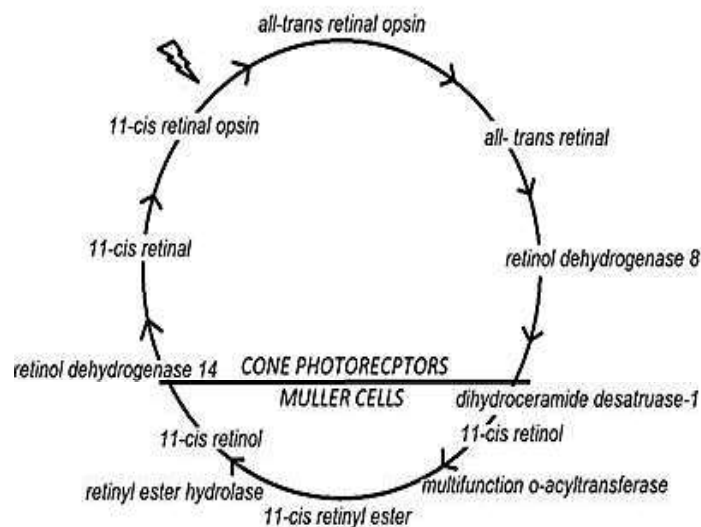


**Figure 1.10:** The visual cycle in cone photoreceptors (Tsin et al., 2018).

#### 1.14. Mechanisms involved in retinal degeneration:

The mechanisms involved in the degeneration of rods and cones are studied with the help of animal models. These studies have proposed five mechanisms that may be contributing to the degeneration of retina.

##### 1.14.1. Tropic factors:

Tropic factors are various molecules that are synthesized in the body that contribute in growth, proliferation, maturation and development of neurons. In an in vivo study on

R10 mice the long term exposure to GDNF (galial-derived neurotrophic factor) can help increase the cone density (Ohnaka et al., 2012). Fibroblast (FGF-2), epidermal growth factors (Traverso, Kinkl, Grimm, Sahel, & Hicks, 2003) and rod derived cone viability factor (RdCVF) (Léveillard et al., 2014) also produced promising results in photoreceptor growth in various studies.

#### 1.14.2. Cone starvation:

Punzo et al. (2009), proposed a theory that cone degeneration occurs due to starvation of cone when proper nutrient supply is affected (Punzo, Kornacker, & Cepko, 2009) Figure (1.11). According to his research if the rod-derived cone viability factor (RdCVF) is deficient it will decrease its binding to Basigin-1 that is crucial for the proper functioning of GLUT-1 (glucose transporter-1). The impaired function of GLUT-1 will prevent glucose from entering in to the cone cells that will starve the cell. In turn the mechanistic target of rapamycin (mTOR) signaling pathway, will not be activated that will lead to autophagy of cone cells (Venkatesh et al., 2015).

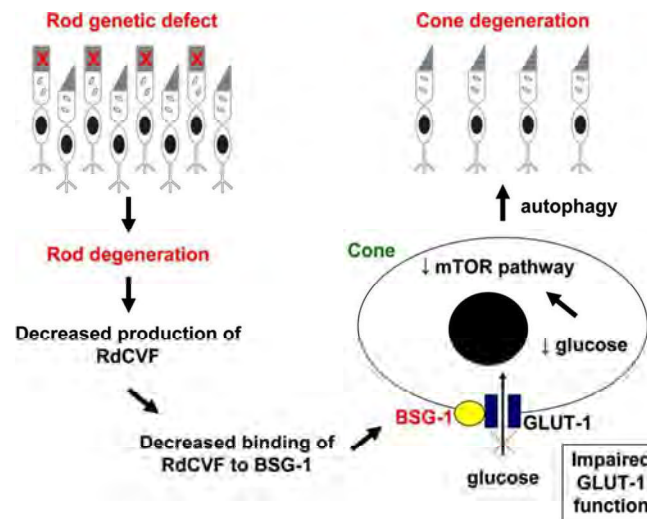


**Figure 1.11:** Mechanism of cone cell death due to deficiency of rod-derived cone viability factor (RdCVF) (Venkatesh et al., 2015).

#### 1.14.3. Oxidative stress:

A cell can undergo oxidative stress when the balance between production of reactive oxygen species (ROS) and their elimination is disturbed (Narayan, Wood, Chidlow, & Casson, 2016) (figure 1.12). If due to any genetic variability the density of rods

decrease it will increase the oxygen level in choroid vessels. Increased oxygen level will in turn increase the level of reactive oxygen species and nicotinamide adenine dinucleotide phosphate (NADPH). Increased level of these factors will cause the cell to undergo oxidative stress that will trigger cone degeneration (Lee et al., 2011).

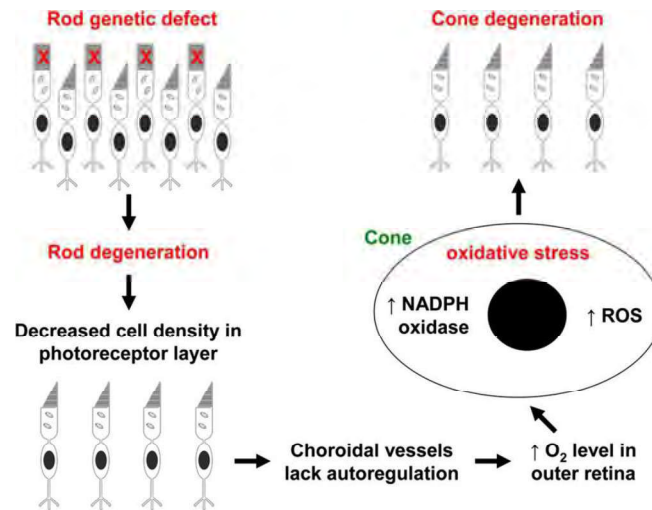


**Figure 1.12:** Role of oxidative stress in cone degeneration (Venkatesh et al., 2015).

### 1.15. Retinitis pigmentosa:

Among retinal dystrophies, retinitis pigmentosa (RP) is the major cause of visual abnormalities and sometimes blindness (Strong, Liew, & Michaelides, 2016). It is characterized by primary degeneration of rods and secondary progressive degeneration of cones photoreceptors. The retinal degeneration typically starts at mid-peripheral region and leads towards macula and fovea in later stages of disease. The disease follow multiple Mendelian inheritance patterns with X-linked RP being the most dangerous type as compared to autosomal recessive RP, autosomal dominant RP and X-linked dominant RP (Russell et al., 2017).

#### 1.15.1. Age of onset:

The age of onset in RP patients is variable as some individuals might develop no night blindness symptoms until they reach adulthood while some present symptoms in early childhood. Depending on age of onset, progression of disease and severity of symptoms, RP is divided in to various subtypes (Davies & Pineda II, 2017).



**1.15.2. Clinical manifestation:**

The disease manifests as decreased or poor night vision or Nyctalopia, progressive degeneration of retinal pigmented epithelium and photoreceptors, tunnel vision and reduced visual acuity (Marc, Jones, Watt, & Strettoi, 2003). Some patients with RP may experience color blindness and photophobia (Marc et al., 2003). It is observed in RP patients that the rods are affected in the earlier stage of disease and later cones are also degenerated that explains the appearance of night blindness first in patients then a secondary visual impairment (Hamel, 2006). In few affected individuals other symptoms are also observed with retinitis pigmentosa that is why it is divided into non-syndromic retinitis pigmentosa and syndromic retinitis pigmentosa (Hamel, 2006).

**1.16. Types of retinitis pigmentosa:****1.16.1. Non-syndromic retinitis pigmentosa:**

It is the typical form of retinitis pigmentosa that may be present in early years of life or may appear in second decade of life. Some people show signs of stationary night blindness while others have a progressive form of disease (Fahim, Daiger, & Weleber, 2023). First night blindness or mild mid night blindness appears but after some time defects in peripheral vision can be observed. In the mid stage of disease a complete phenotypic picture of night blindness develops (Talib, Van Cauwenbergh, & Boon, 2022).

Patient feels difficulty while driving or walking at night or in darkness. The loss of peripheral vision can be seen in broad day light when patient cannot detect objects and movement in surroundings. In addition to these symptoms the patient might become photophobic, can develop reading difficulty, and dyschromatopsia (Verbakel et al., 2018).

**1.16.2. Syndromic retinitis pigmentosa:**

In syndromic type of retinitis pigmentosa the patient develops other disabilities with night blindness. The most frequently occurring types of syndromic form of disease are: Usher syndrome and Bardet Biedl syndrome (Pierrottet et al., 2014). Some less frequent types of syndromic RP includes Jeune syndrome, Cockayne syndrome,

Alport syndrome, Senior loken syndrome (Ronquillo, Bernstein, & Baehr, 2012) and Cohen syndrome (Hamel, 2006). RP is also reported in some metabolic disorders and central nervous system disorders. The metabolic cases of RP include peroximal disorders, Refsum disease (Kumar, Srivastava, & Muhammad, 2022), mucopolysaccharidoses, cystinosis and bietti's disease (Vargas, Mitchell, Yang, & Weleber, 2019). The neurological diseases associated with RP are neuronal ceroid lipofuscinosis, Joubert syndrome (Sturm et al., 2010), autosomal dominant cerebellar ataxia type II and myotonic dystrophy (Kimizuka, Kiyosawa, Tamai, & Takase, 1993).

#### **1.16.2.1. Usher syndrome:**

This is the most frequently found (18% cases) form of syndromic RP (Koenig, 2003) and is inherited in an autosomal recessive pattern (Yoon, 2022). Usher syndrome (USH) is characterized by retinal dystrophy and hearing loss. It is further classified into three types on the bases of age of onset and severity of disease (Yoon, 2022).

In type 1 of USH a congenital sensorineural hearing loss, retinal disease, vestibular dystrophy and speech loss is observed in early childhood (Koenig, 2003). In patients with USH 1 the speech does not develop unless at an early stage of disease a cochlear implant is not fitted (Koenekoop, Arriaga, Trzupek, & Lentz, 2020). Usher syndrome type II (USH2) is clinically characterized by bilateral, congenital sensorineural hearing loss and progressive retinitis pigmentosa (J. Yang, Wang, Song, & Sokolov, 2012). The hearing loss can be mild to moderate at lower frequency but can be profound at higher frequencies (J. Yang et al., 2012). The vestibular response remains intact in most cases but some variability is also observed in cases. Early fitting of hearing as well as speech therapy can help better manage disease. USH2A is usually misdiagnosed as non-syndromic hearing disorder until the symptoms of retinitis pigmentosa starts developing (Sadeghi et al., 2004). In Usher syndrome type III the patient experience progressive postlingual hearing disability, late onset of retinitis pigmentosa and variable vestibular damage. Affected individuals have normal hearing, develop speech and vision at birth but as the person enter its second decade of life progressive damage to hearing and retina occurs (Fields et al., 2002).

### **1.16.2.2. Bardet-Biedl syndrome:**

Bardet-Biedl syndrome (BBS) has a prevalence of 1/150000 (Beales, Elcioglu, Woolf, Parker, & Flinter, 1999) and is characterized by retinitis pigmentosa, postaxial polydactyly and obesity. In some severe cases of BBS cognitive impairment, hypogonadism and renal abnormalities are also reported (Forsyth & Gunay-Aygun, 2020). Other symptoms associated with BBS are strabismus, facial dimorphisms, hearing disability, ataxia and developmental delay (Shoemark, Dixon, Beales, & Hogg, 2015).

### **1.17. Other inherited retinal dystrophies:**

#### **1.17.1. Leber congenital amaurosis:**

Leber congenital amaurosis (LCA) is a rare retinal dystrophy that is often confused with RP and is inherited in an autosomal recessive manner (Gregory-Evans, Pennesi, & Weleber, 2012) although some autosomal dominant cases have also been reported (Perez-Lanzon, Kroemer, & Maiuri, 2018). The only distinction between RP and LCA is that LCA is manifested within months after birth. It is considered the most common cause of childhood blindness with a prevalence rate of 1 in 800000 individuals. The phenotypic manifestation of disease includes features like vision loss, nystagmus, photophobia and keratoconus (Lyons & Lambert, 2022).

#### **1.17.2. Macular dystrophy:**

The inherited macular dystrophies harm the central region of retina and are associated with degeneration of retinal pigment epithelium (Schum, 2013). The macular dystrophies are reported to be monogenic and have an autosomal dominant inheritance pattern. Age-related macular degeneration (ARMD) is mostly reported in elderly individuals mostly in their sixties and is responsible for 8.7% of worldwide vision loss (Wong et al., 2014). Some studies have found higher number of women affected by age related macular degeneration as compared to men (Seddon, Reynolds, Yu, Daly, & Rosner, 2011).

### **1.17.3. Stargardt disease:**

The most common form of macular dystrophy in a young age is Stargardt disease. People affected with this condition have vision loss around twenty years of age. This disease is transmitted autosomal recessively in familial cases and has a prevalence of about 0.8% (Jadoon et al., 2006). The disease manifests as progressive loss of central vision (bilateral). Some less common features of disease include photopsia, blind spot formation, photophobia and loss of color vision (Kohli & Kaur, 2023).

### **1.17.4. Aniridia:**

Aniridia, an autosomal disease is characterized by bilateral iris hypoplasia resulting in ophthalmological abnormalities. Patient can also develop complete or partial foveal and optic nerve hypoplasia, nystagmus, cataract, glaucoma, clouding of cornea and vascular retinopathy (Black, Ashworth, & Sergouniotis, 2022). In up to 85% of congenital cases of Aniridia autosomal dominant inheritance pattern is observed while in 1-3% of cases autosomal recessive inheritance is reported. In autosomal recessive Aniridia it is often associated with Gillespie syndrome if cerebral ataxia and mental abnormality is also present (Tripathy & Salini, 2023).

### **1.17.5. Alstrom syndrome:**

Alstrom syndrome present as multi-organ genetic disorder that is inherited in an autosomal recessive way (Collin et al., 2005). Its clinical features encompass an early rod cone abnormality, obesity, hearing difficulty, insulin resistance, short stature, cardiomyopathy, liver and kidney dysfunction. The symptoms start appearing in infancy but their severity increases with time and result in life threatening condition in adults (Marshall et al., 2005).

### **1.18. Genetics of retinal dystrophies:**

The genetics of inherited retinal dystrophies is highly heterogeneous like its clinical manifestation. To date more than 300 genes have been associated with IRDs (Eker, 2023). The mode of inheritance of retinal diseases is also variable with fifteen to twenty percent autosomal dominant cases and five to twenty cases are autosomal recessive (Daiger, Bowne, & Sullivan, 2007). X-linked inheritance is also reported in 5-20% cases (Daiger et al., 2007) while in case of RP digenic inheritance is also

observed where two genes with heterozygous mutation are responsible for disease (Nash et al., 2015). To date more than 80 genes have been reported for non-syndromic RP (Verbakel et al., 2018). These genes are known to be involved in variable functions like phototransduction, RNA splicing, maintenance, metabolism and development of retinal cells (Nash et al., 2015).

Retinitis pigmentosa genes commonly reported in Pakistani population includes *PDE6C* (phosphodiesterase 6C), *TULP1* (tubby-like protein 1), *MERTK* (mer tyrosine kinase proto-oncogene), *RHO* (Marwan et al., 2023), *CERKL* (ceramide kinase-like), *RPI* (axonemal microtubule-associated protein) (Nadeem et al., 2020), *PDE6B* (phosphodiesterase 6b), *CNGBI* (cyclic nucleotide-gated channel protein 1), *CRBI* (crumbs cell polarity complex component 1) (Azam et al., 2011),

For syndromic forms of RP like Usher syndrome (USH) 15 genes (Daiger et al., 2007) are known to be the cause of disease among which *MYO7A* (Myosin, unconventional, family VII, member A), *USH2A* (usherin gene), *USH1C* (PDZ domain-containing protein), *CDH23* (cadherin-related family, member 23), *PCDH15* (protocadherin 15) and *SANS* (scaffold protein containing Ankyrin repeats and Sam domain) are associated with USH type 1, *ADGRV1* (Adhesion G protein-coupled receptor V1) and *WHRN* (Whirlin) for USH type 2; *CLRN1* (Clarin-1) for USH type 3 (Nash et al., 2015).

In Bardet-Biedl syndrome (BBS) biallelic loss of function is reported in 26 genes (Niederlova, Modrak, Tsyklauri, Huranova, & Stepanek, 2019). Some of the most reported variants are found in BBS1 (23.4%), BBS2 (9.6%), ARL6 (ADP-ribosylation factor-like GTPase 6) (5.15%), BBS10 (14.5%) and CEP290 (290-kD centrosomal protein) (6.3%) (Forsyth & Gunay-Aygun, 2020). CEP290 is also reported for Joubert syndrome, Senior Loken syndrome and Leber congenital amaurosis (Forsyth & Gunay-Aygun, 2020). Other genes identified in LCA includes: *GUCY2D* (GUANYLATE CYCLASE 2D), *CRBI* (crumbs cell polarity complex component 1), *AIP1* (arylhydrocarbon-interacting receptor protein-like 1), *NMNAT1* (nicotinamide nucleotide adenylyltransferase 1), *RPE65* (retinoid isomerohydrolase), *SPATA7* (spermatogenesis-associated protein 7), and *MERTK* (mer tyrosine kinase protooncogene) (den Hollander, Roepman, Koeneke, & Cremers, 2008).

The first homeobox gene *PAX6* is reported to cause Aniridia when mutated. It has 4 exons and is located on chromosome 11p13. Until now scientists have discovered 400 heterozygous disease causing variants in *PAX6* gene (Hingorani, Hanson, & Van Heyningen, 2012). *ALMS1* gene is located on chromosome 2p13, and is reported to cause Alstrom syndrome if a mutation occurs in it. It is composed of 23 exons and is expressed in retina, renal tubules, hypothalamus, pancreas and organ of corti (Jagger et al., 2011). The adenosine triphosphate-binding cassette transporter alpha 4 subunit (*ABCA4*) gene consists of 50 exons and is located on chromosome. An abnormality in *ABCA4* gene due to variant can cause inherited cases of macular dystrophy or Stargardt Disease (Glazer & Dryja, 2002).

### **1.19. Diagnostic criteria:**

There are various methods that are used for the diagnosis of retinal dystrophies. Some of them are explained in detail.

#### **1.19.1. Ophthalmic examination:**

A funduscopy exam of the affected individual is done by an ophthalmologist to find out any changes that might indicate retinal damage. The three classical clinical features observed during the fundus examination of a person with mild or late stage of RP are: attenuation of retinal blood vessels, a waxy pallor of the optic nerve and formation of bony spicules (Thenappan, Nanda, Lee, & Lee, 2023) (figure 1.13). In some patients hyperpigmentation of the fundus is also observed.

Other ocular findings in patients with retinal dystrophies include nystagmus and refractive error (Flitcroft, Adams, Robson, & Holder, 2005). Retinal dystrophies that cause macular complications can show hole in macula, macular scar and edema (Sultana, 2023).

#### **1.19.2. Perimetry:**

To assess the loss of peripheral vision Goldmann perimeter or static perimetry is used (Pineles et al., 2006). Microperimetry or fundus driven perimetry is introduced relatively recently that provides assessment of loss of central vision. It enables the assessment of image of posterior pole and helps correlate it to the function (Acton & Greenstein, 2013).



**Figure 1.13:** Fundus showing bony spicules, pale optic disc and attenuated blood vessels in a retinitis pigmentosa patient (Hamel, 2006).

### 1.19.3. Color vision:

Color vision is not affected in all retinal dystrophies but sometimes if the visual acuity decreases below 20/40 this abnormality is reported. Higher order color detection tests like Berson plates are used for blue color monochromes (Chawla & Vohra, 2023).

### 1.19.4. Optical coherence tomography:

In case of thinning of retina like in retinitis pigmentosa optical coherence tomography (OCT) can provide evaluation of retinal damage (Hood et al., 2011). In advanced stage of disease this thinning can progress towards macula. OCT can also detect edema in macula thus eliminating the need of fundus angiography for detecting cystoid edema in macula. Foveal hypoplasia and membrane damage in sub foveal region in case of achromatism may be identified using OCT (Thiadens et al., 2010).

### 1.19.5. Electroretinography:

Electroretinography not helps in diagnosis of retinal disorder but also provides assessment for disease progression (Thiadens et al., 2010). The electroretinogram

(ERG) can detect the disease at early stage than fundus examination. The delayed or diminished scotopic response of rods can be detected in full-field ERG. A highly abnormal ERG or even an extinguished ERG is observed in cases of Leber congenital amaurosis (Thiadens et al., 2010).

### **1.20. Treatment and disease management:**

Regardless of advances in science and technology no cure is discovered for retinal dystrophies. Support treatments like vision aid are provided in case of low visual acuity and flashlights can help individuals suffering from night blindness.

#### **1.20.1. Gene therapy:**

Genetic therapies are difficult to perform and expensive but in case of retina it can be possible as it is easily accessible for surgical procedure and the barrier between blood and retina provides ocular immunity (Russell et al., 2017). Some clinical trials are under progress for sub retinal injections for disease management.

#### **1.20.2. Retinal implants:**

Retinal implant therapies are being introduced to replace the phototransduction in eye with artificial devices. In patients with retinal dystrophies the degenerated photo receptor cells cannot send signal to brain but these implants can help trigger signals that will be transmitted to brain (Musarella & MacDonald, 2011).

#### **1.20.3. Retinal transplantation:**

Another approach to treat retinal dystrophies is transplantation of retinal pigment epithelium cells or developing retina into sub retinal space. A study was conducted on ten AMD and RP patients having visual acuity 20/200. Seven out ten showed slight improvement in vision with implantation of fetal retina (Radtke et al., 2008). Scientists are also trying to develop an alternative approach of using photoreceptor precursor cells (MacLaren et al., 2006) or incubated human stem cell (Lamba, Karl, Ware, & Reh, 2006) to restore vision in individuals with retinal disorders.

#### **1.20.4. Vitamin therapy:**

The role of vitamin A in protection of photoreceptors from antioxidants makes vitamin A therapy an effective approach to treat the dystrophies. Data from long term



studies have revealed that a high dosage (15000IU) of vitamin a can slow down the loss of ERG amplitudes if taken for 5 to 15 years (Berson et al., 2010). Many scientists are still debating the role vitamin A therapy can play to improve vision.

#### **1.20.5. Drug delivery:**

An alternative approach under consideration is to treat retinal degeneration by direct drug induction through the sclera. Different methods to deliver drugs can be use of electric field, microneedles and collagen gels (Jiang, Geroski, Edelhauser, & Prausnitz, 2006).

### **Section III:**

#### **1.21. Microphthalmia**

Microphthalmia is a congenital condition in which one or both eyes are smaller at birth than <15mm. The normal human eye ranges between 16 to 19 mm in the neonatal stage. In this rare developmental disorder the post-natal growth of eye that occurs in the early years of life within the posterior region is also affected (figure 1.14). The corneal diameter in microphthalmia is <10mm while the diameter of eye globe <20mm. Microphthalmia can present with other developmental disorders of eye including deformity in optic fissure closure and coloboma (S. P. Shah et al., 2011). It may also affect sclera, lens, cornea and anterior and posterior region of eye (Verma & FitzPatrick, 2007). Some studies have reported other than ocular abnormalities in microphthalmia patients like facial deformities, renal damage, microcephaly and cardiac anomalies (Skalicky et al., 2013).

The prevalence of microphthalmia is 30 affected individuals in 100000 births and is reported to cause blindness in almost 11% of affected children (Verma & FitzPatrick, 2007).

#### **1.22. Risk factors for microphthalmia:**

Data from epidemiological studies reveal some risk factors might contribute to defects in ocular development. A smaller gestational time and underweight infant are more prone to microphthalmia. Environmental factors, excessive alcohol drinking by mother and her age (>40) are also considered risk factors (Verma & FitzPatrick,

2007). In alcoholic mothers infant can be born with fetal alcoholic syndrome and a small eye globe (Brennan & Giles, 2014). During pregnancy gestational infections such as cytomegalovirus, rubella, varicella and toxoplasma have also been reported as important environmental cause of disease (Mauri et al., 2015). Other contributing factors include harmful drugs, vitamin A deficiency and exposure to damaging radiations (Mauri et al., 2015).

The genetically inheritable causes of disease are not any less common. Microphthalmia is genetically heterogeneous and can be inherited in an autosomal dominant pattern, autosomal recessive pattern, X-linked disease, de novo sporadic cause, and chromosomal abnormality syndrome (Morle et al., 2000).



**Figure 1.14:** Clinical appearance of microphthalmia (Verma & FitzPatrick, 2007).

### **1.23. Development of human eye at molecular level:**

In humans ocular development starts in the anterior region of neural plate at 3 weeks in fetus. Orthodenticle Homeobox 2 (OTX2) initiates the specification with coordination of SIX Homeobox 3 (SIX3), Retina and Anterior Neural Fold Homeobox (RAX) and Paired box protein Pax-6 (PAX6) (Sinn & Wittbrodt, 2013; Zagozewski, Zhang, & Eisenstat, 2014). A forkhead transcription factor (FOXD3) plays an important role in the formation and maintenance of neural crest cells and allow its derivatives to develop (Barenbaum & Bronner-Fraser, 2005). After 22 days of gestation SIX3 regulates SHH (sonic hedgehog) to form the mid line and it stimulates the migration of prospective hypothalamic cells to anterior end leading to

splitting the eye field into two. SIX3 also activates PAX6 and SOX2 to form lens preplacodal region (Sinn & Wittbrodt, 2013). This developing lens placode release retinoic acid and bone morphogenetic protein (BMP) to stimulate the invagination at 33 days gestation to form the optic vesicle that results in the formation of bi-layered optic cup (Cvekl & Wang, 2009). Signaling of TGF $\beta$  from the extraocular mesenchyme layer maintains OTX2 and MITF expression in optic cup to form retinal pigment epithelium (Cvekl & Wang, 2009). Ventral Anterior Homeobox 1 and 2 (VAX1/VAX2) are regulated by SHH to induce the expression of PAX2 for formation of optic stalk (Take-uchi, Clarke, & Wilson, 2003). At four weeks of gestation formation of an optic fissure help supply nutrients to the developing eye (Richardson, Tracey-White, Webster, & Moosajee, 2017) (figure 1.15).

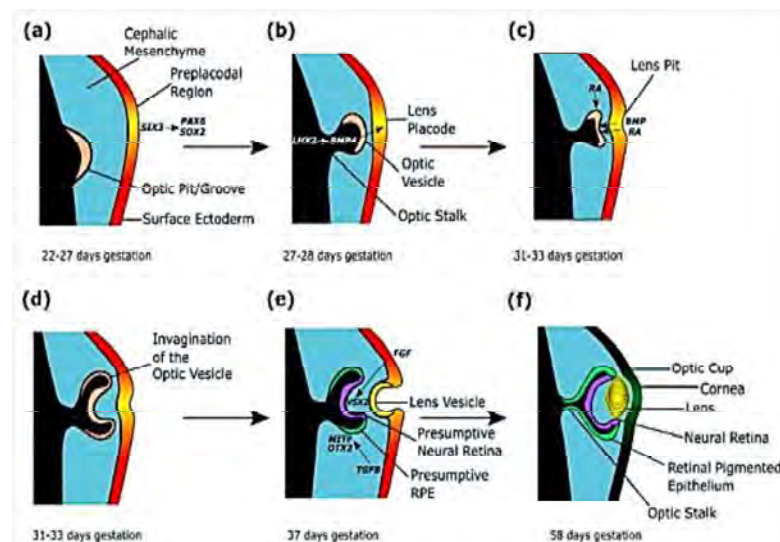


**Figure 1.15:** Formation of lens and optic cup in developing human eye (Harding & Moosajee, 2019)

#### 1.24. Types of microphthalmia:

Three types of microphthalmia are recognized:

##### 1.24.1. Simple microphthalmia:

It is also known as pure microphthalmos or nanomicrophthalmos. In simple microphthalmia the eye is smaller than normal size and no other abnormality is associated with it. Such eyes may have a thickened sclera and sometimes a cyst. *TMEM98* gene located at chromosome 17p12-q12 is often linked to pure

microphthalmia and is inherited in an autosomal dominant pattern (Yanoff & Sassani, 2018).

#### 1.24.2. Systemic anomalies and microphthalmia:

It is associated small eyes and anomalies like trisomy 13 and infections such as congenital rubella (Yanoff & Sassani, 2018). Some anomalies associated with microphthalmia are listed in table.

**Table 1.1:** Chromosomal anomalies associated with microphthalmia are listed in table below.

Chromosomal abnormality	Disease features
Triploidy syndrome	Large placenta, syndactyly, brain anomalies, heart defects
Duplication 3q syndrome	Growth deficiency, genital defect, cardiac anomalies, hypertrichosis
4p- (Wolf-Hirschhorn syndrome)	Microcephaly, learning difficulty, epilepsy, cleft lip, growth deficiency
Trisomy 18 (Edwards syndrome)	Learning difficulty, single umbilical artery, cardiac defect, microgathia, hypoplasia of skeletal muscles.
Duplication 4p syndrome	Epilepsy, obesity, microcephaly, genital abnormalities
Duplication 10q syndrome	Ptosis, microcephaly, growth deficiency, learning difficulty
Trisomy 9 mosaic syndrome	Microgathia, growth deficiency, learning disability, heart defect.

#### 1.24.3. Complicated or complex microphthalmia:

In this type cases of epibulbar choristomas are reported with microphthalmia. Other ocular abnormalities like opaque cornea, Aniridia, retinal dysplasia and corectopia are generally found in clinical examination (Yanoff & Sassani, 2018).

#### 1.25. Diagnosis:

The measurement of the total length of eyeball is the standard way of diagnosis for microphthalmia. The total axial length of the eye ball both in posterior region and anterior region is measured including corneal diameter, chamber depth, and length of

the lens (Qidwai & Shaikh, 2015). Visual acuity test is performed to check for reduced vision due to small eye ball.

A fundus examination can help to identify any blurred margins of the optic disc. The optical coherence tomography (OCT) is performed in rare cases to study the elevated retinal fold (Qidwai & Shaikh, 2015). A fetal ultrasound can be performed to identify any abnormality in fetus following international ultrasound protocols (Searle, Shetty, Melov, & Alahakoon, 2018). These guidelines also provide overview on orbital measurements and diagnosis. The diagnosis is usually made on identification of decreased orbital diameter and examining the intra orbital structures such as lens, optic nerve and pupil (Searle et al., 2018).

### **1.26. Genetics of microphthalmia:**

To date almost 100 genes are identified in syndromic and non-syndromic cases of microphthalmia (Harding & Moosajee, 2019). According to Harding & Moosajee, 2019, these genes mostly fall in two categories: *SOX2*, *OTX2*, *PAX6*, *RAX*, *FOXE3* and *VSX2* fall in transcription factors that contribute to ignition of eye development (Harding & Moosajee, 2019). The second category include *ALDH1A3*, *RAR* and *STRA6* genes that are component of retinoic acid signaling pathway (Harding & Moosajee, 2019).

#### **1.26.1. *SOX2* gene:**

In genetic cases of bilateral microphthalmia heterozygous mutations found in *SOX2* gene contribute to most cases (15-40%) (Fares-Taie et al., 2013) (Slavotinek, 2019). This gene is also associated with syndromic form of microphthalmia where extra ocular findings such as seizures, brain anomalies, hearing loss, short stature and genetic abnormalities are also present (Slavotinek, 2019). Missense mutations in *SOX2* gene are also reported to affect the DNA binding domains resulting in a milder presentation of disease such as developmental abnormalities, coloboma and growth retardation (Williamson & FitzPatrick, 2014).

#### **1.26.2. *OTX2* gene:**

Reported heterozygous variants in *OTX2* include missense, nonsense, frameshift and indels (Williamson & FitzPatrick, 2014) that are estimated to be a cause of disease in

2-8% cases of microphthalmia (Wyatt et al., 2008). Highly variable phenotype is found in patients with disease causing variant in *OTX2* gene such as anterior segment deformities, hypoplasia and retinal dystrophies (Schilter et al., 2011).

### **1.26.3. *FOX3* gene:**

Autosomal dominant variant in *FOX3* gene was first identified in a patient with myopia, cataracts, and embryotoxon (Semina, Brownell, Mintz-Hittner, Murray, & Jamrich, 2001). In 2006, Valleix et al., identified autosomal recessive variant in *FOX3* gene in siblings born in a consanguineous union with aphakia, microphthalmia, and aplasia of anterior region (Valleix et al., 2006).

### **1.26.4. *PAX6* gene:**

This transcription factor is mostly associated with aniridia but in a study on more than 500 patients of microphthalmia, anophthalmia and coloboma 1-2% cases were found to be related to *PAX6* gene (Williamson & FitzPatrick, 2014). Complex phenotypic presentation of disease is reported for microphthalmia patients with mutation in *PAX6* gene such as aniridia, coloboma, and optic nerve damage (Williamson & FitzPatrick, 2014).

## **1.27. Disease management and treatment:**

As no cure is available for microphthalmia, only shared approach of care for affected individuals can help to manage disease. Children are prescribed glasses in case a significant error in refraction is identified or only one eye is affected (Ragge, Subak-Sharpe, & Collin, 2007).

### **1.27.1. Expansion of eye socket:**

An early expansion of eye socket in severe microphthalmia can help minimize the facial disfigurement. When a child is born the size of eye is 70% of the size in an adult human eye and it keeps growing as the face of child grows with age until it reaches its maximum size (Ragge et al., 2007). A reduced volume in ocular region due to underdeveloped eyelids, orbit and fornices will affect the normal facial development (figure 1.16).



**Figure 1.16:** A baby with unilateral microphthalmia. (a) Eye without cosmetic shell (b) An eye with cosmetic shell (c) appearance of child with cosmetic shell with growth (adopted from (Ragge et al., 2007).

If the progressive growth of the socket is not facilitated by adding socket expanders, the individual will not be able to wear prosthesis and will have an asymmetric face (Ragge et al., 2007). In microphthalmic eyes where there is vision and the axial length is less than 16 mm, a purpose made cosmetic shell is fitted to promote orbital growth (Ragge et al., 2007).

### **1.27.2. Long term disease management:**

After first five years of life with socket expansion a yearly review will be required of growing eye. In some cases an angle closure glaucoma (Demirci, Singh, Shields, Shields, & Eagle, 2003) and retinal detachment (Daufenbach, Ruttum, Pulido, & Keech, 1998) is developed over time. Patients are advised to visit an ophthalmologist promptly if they find any change in their vision.

### **1.27.3. Therapeutics:**

Trial studies are being conducted to evaluate the efficiency and safety of intravenous administration of stem cells for various diseases (Harding & Moosajee, 2019). Small molecular drugs are being developed for aniridia that interfere with the fidelity of ribosomes to produce full length proteins in mouse models (X. Wang et al., 2017). In future if successful these techniques might be used for congenital ocular disorders like microphthalmia.

## **1.28. Molecular diagnosis in genetic disorders:**

With advancements in molecular genetics DNA based diagnostics techniques are used for early diagnosis of disease causing variants in affected individuals (Carss et al., 2017). An early identification of pathogenic variant especially in familial cases of disease can help in better disease management. Genetic studies on disease causing variants in a population also provide the data for genes actively involved in diseases in a region and highlights the worldwide variability in genome. Sanger sequencing is the most widely used approach in molecular diagnosis even after 40 years of discovery but this technique has some limitations such as it is time consuming and cannot be used for longer fragments of DNA. Another limitation of Sanger sequencing is that it cannot be used for heterogeneous diseases such as retinitis pigmentosa and various other retinal dystrophies.

Considering high genetic variability in ocular diseases genetic testing using next generation sequencing (NGS) approach is becoming more common. This technology enables us to acquire molecular diagnosis for large number of patients. An accurate diagnosis of disease provides basis for disease prognosis and genetic counseling. NGS has been applied primarily to Mendelian disorders as it makes analysis simple and accurate (Lopez Jimenez et al., 2011a). In current study we will be using molecular diagnostic techniques like Sanger sequencing and next generation exome sequencing for identification of pathogenic variants in autosomal recessive inherited eye disorders in Pakistani population.

### **1.28.1. Techniques used for identification of disease causing variants in eye disorders:**

#### **1.28.2. Sanger sequencing:**

In 1970, Frederick Sanger and colleagues developed a first-generation sequencing method for DNA sequencing (Solomon, 2018). Even to this day, with all the advancements in sequencing techniques, Sanger sequencing retains its essential position as a diagnostic technique in clinical genomics (Hagemann, 2015). It also provides an orthogonal way to confirm the variants identified in modern next generation sequencing techniques (Hagemann, 2015).



This method uses a pair of targeted oligonucleotide primers for a specified region of DNA. The process starts with the denaturation of double-stranded DNA, and then the oligonucleotide primer is annealed to targeted region. An elongated strand is formed complementary to the parent strand using a mixture of deoxynucleotides triphosphate (dNTPs) such as adenine (A), guanine (G), thymine (T) and cytosine (C). The mixture of dNTPs also includes some small quantity of dideoxynucleotide triphosphates (ddNTPs) that acts as a chain terminator. Due to these ddNTPs chains will terminate at different lengths. These ddNTPs also include a fluorescent marker that produces fluorescence when attached to elongating strand. Each ddNTP is indicated by a different color such as green for A, red for T, blue for C and black for G that is detected by a laser in an automated machine and is translated into a peak (figure 1.17). This method can detect a silent mutation, missense variants, nonsense variants, deletions, splice variants, insertions and truncating frameshift variants (Gomes & Korf, 2018).

### **1.28.3. Next-generation sequencing:**

A comparatively new DNA sequencing technology that has revolutionized the sequencing of DNA and RNA is next-generation sequencing (NGS). With the help of NGS, hundreds and thousands of samples can be sequenced deeply in a parallel manner. It has made the sequencing of the entire human genome possible in just a single day (Qin, 2019).

NGS can be used to interrogate exomes or full genomes to identify reported and novel disease-causing variants. DNA fragmentation is the first major step in the NGS that breaks the DNA into short segments ranging from 100 to 300 bp in length (Knierim, Lucke, Schwarz, Schuelke, & Seelow, 2011). Fragmentation can be achieved by using enzymes or sonication. Following fragmentation segments are usually pulled out using a hybridization capture assay or amplicon assay. The next step is the preparation of library in which samples are given a sample specific index to identify each sample. This also allows primers to bind specifically to a sequence for sequencing in later steps. The DNA library is then uploaded to a matrix in sequencer to allow parallel sequencing of all samples.

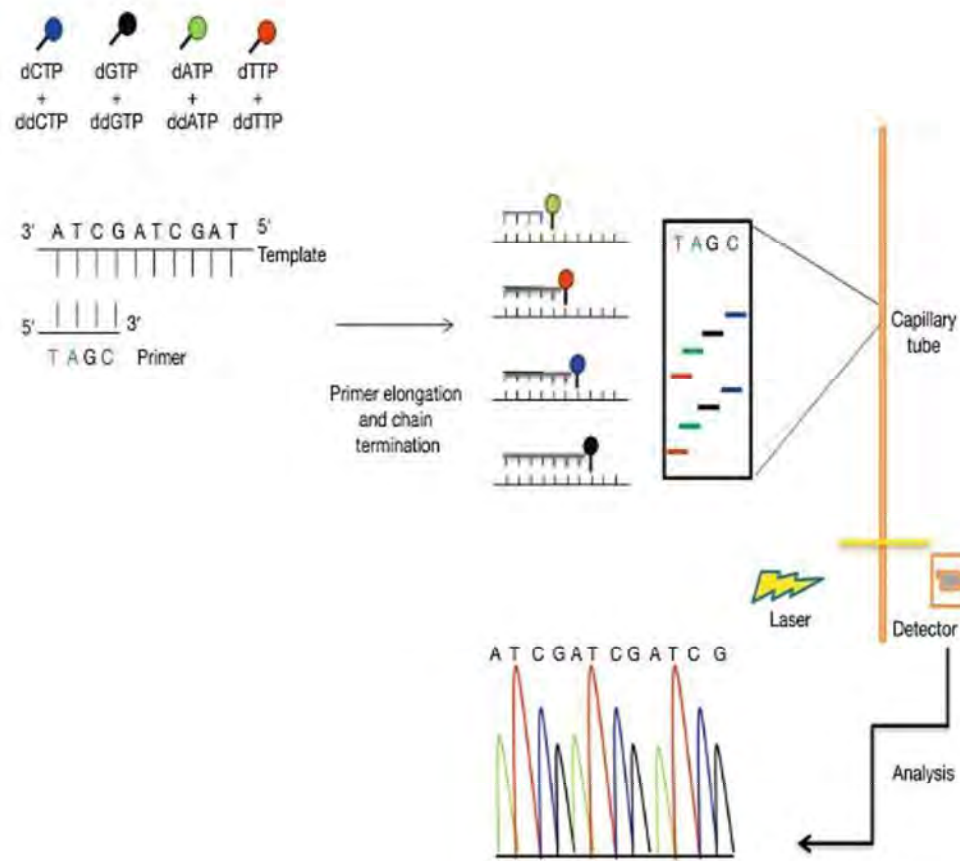


**Figure 1.17:** The method of Sanger sequencing in graphical form (Zhang, Seth, & Fernandes, 2014).

The data generated is subjected to bioinformatics analysis in next step that involves base calling, alignment of read, identification of variants and lastly annotation of variants. During these steps a human genome is used as a reference for identification of variants in data (Qin, 2019). NGS can identify disease-causing variants despite the type of variant, inheritance pattern of disease and its genotype (Russnes, Navin, Hicks, & Borresen-Dale, 2011).

The main disadvantage of NGS is the infrastructure and expertise that is required for subsequent data generation and variant analysis. To make it cost effective large batches of samples should be run to offer benefits in patients' health. Whole exome sequencing also has some disadvantages such as it does not cover exon with high GC content like first exon and non-coding RNAs (Topper, Ober, & Das, 2011).

### **1.29. Objectives of study:**

The main objectives of present study were following:

1. Enroll families affected with selected autosomal recessive eye disorders (primary congenital glaucoma, inherited retinal dystrophies and microphthalmia) from different regions of Pakistan.
2. Identification of disease causing mutations in enrolled primary congenital glaucoma families through Sanger's sequencing method.
3. Next generation sequencing including panel and whole exome sequencing (as per availability) of enrolled microphthalmia and inherited retinal dystrophies families to identify mutant gene and variant/s.
4. Bioinformatics analysis of all identified variants, definitive molecular diagnose of various eye diseases and provision of information to the families and clinicians for better management and genetic counseling.

**Chapter 2**  
**MATERIALS AND**  
**METHODOLOGY**

To identify the genetic and molecular basis of autosomal recessive eye disorders in Pakistani population the study was divided into field work and laboratory work. The study was approved by Bioethics Committee of Faculty of Biological Sciences, Quaid-i-Azam University (QAU) Islamabad, Pakistan (Annexure I).

## **2.1. Field work:**

### **2.1.1. Identification and enrollment of eye disorders families:**

The field work comprised identification of families affected with autosomal recessive eye disorders, enrollment of families, collection of blood samples and data collection about affected family. Patients with primary congenital glaucoma (PCG), retinal dystrophies and microphthalmia were recruited from different eye hospitals in Pakistan during October 2019 to December 2021. A detailed history of disease in patient was recorded on specially designed comprehensive questionnaire (Annexure II). If the affected individual was a minor information and consent was obtained from parents or guardians. All the families were briefed about the disease and purpose of research before recruiting them. Only those families were recruited which had more than one affected individuals born to consanguineous parents. The performa included details about the names, relationship to proband, address, contact details, detailed pedigree, caste, ethnicity and phenotype in patient. All the personal data of patients was kept highly confidential. If a family had affected individuals in extended family, they were also contacted and samples were obtained considering their availability and willingness to participate in research. Pictures of clinical reports and patients were taken in case of any apparent developmental anomaly. All the enrolled patients were clinically assessed by ophthalmologists for PCG, retinal dystrophies and microphthalmia.

### **2.1.2. Sample collection:**

After informed written consent, a blood sample was collected in 5 ml Ethylene Di-amine-Tetra acetic acid (EDTA) vacutainer tubes from 20 primary congenital glaucoma families, 35 retinal dystrophy families, 1 microphthalmia family. For genetic analysis, all these samples were dispatched to Molecular Biology Lab, Department of Zoology, Faculty of Biological Sciences, Quaid-i-Azam University and were store at 4 °C.

### **2.1.3. Pedigree design:**

Pedigree for each proband was drawn using HaploPainter software <https://haploPainter.sourceforge.net/> (Thiele & Nürnberg, 2005) according to the information provided at the time of data collection. A square in the pedigree represents male while a female is represented by a circle. A small fill symbol represents affected individual. Consanguineous marriage in the pedigree is shown by double line. A diagonal line above the symbol represents a deceased individual.

### **2.1.4. Clinical evaluation:**

Detailed medical history of each enrolled family was collected such as age of onset, sex, age at time of examination and clinical presentation of disease.

For primary congenital glaucoma patients were evaluated for changes in intra ocular pressure (IOP), damage to the optic nerve and reduced visual acuity. Only those families were recruited with had increased IOP than 22 mmHg and showed autosomal recessive inheritance pattern.

In case of retinal dystrophies, patients were checked for reduced night vision, tunnel vision, color blindness, cataract, photophobia and nystagmus by expert ophthalmologists. Fundus examination of all the patients were performed to find changes like macular scar, pale optical disc, attenuated retinal vessels and pigmentation. Families were also inquired for any surgeries for retinal detachment and cataract. Further information was collected regarding hearing issues, mental abnormality, kidney problems, increased blood pressure, obesity, polydactyly, dental anomalies, reproductive system abnormalities, speaking disability and cardiovascular defects. As microphthalmia is a congenital disorder patients were evaluated for corneal diameter to be less than 10 mm and diameter of eye orbit to be less than 20 mm. They were also questioned about any other deformities or abnormalities such as facial, renal and cardiac defect.

### **2.2. Laboratory work:**

In the laboratory all the collected data was organized in excel files and each family was labeled properly with a unique anonymous identification number (UAI) to further process the samples. The extraction of genomic DNA for all the PCG samples was

carried out using organic method of DNA extraction. For retinal dystrophies and microphthalmia families QIAamp DNA extraction kit was used.

### **2.2.1. DNA extraction using Phenol Chloroform method:**

EDTA tubes were taken out and placed at room temperature for 30 minutes to start cell lysis. The composition of all the solutions used is mentioned in table 2.1.

- 1) 50 ml falcon tubes were labeled with patient UAI and 5 mL blood was transferred to the falcon tube.
- 2) In each falcon tube 40 ml of TE buffer was added and then after 30 minutes they were centrifuged at 3000rpm for 20 minutes.
- 3) The centrifugation will form 2 layers. Discard the upper layer with autoclaved glass pipette to make the remaining volume 20 ml.
- 4) Refill each falcon tube with washing buffer to make total volume up to 40 ml. Gently tap and shake the falcon tube to dissolve the pellet. Centrifuge the tubes again at 3000 rpm for 20 minutes.
- 5) The upper layer was discarded up to mark of 10 ml this time and again washing buffer was added to make total volume 40 ml. Centrifugation was repeated at 3000 rpm for 20 minutes.
- 6) In last step of day one all the supernatant was discarded and a calculated amount of 6 mL TNE, 200  $\mu$ L SDS and 20  $\mu$ L PK was added in each tube and was incubated at 37 °C.
- 7) On next day falcon tubes were removed from incubator and were placed at room temperature. In each tube 500  $\mu$ L of Sodium chloride was added. The tubes were shaken vigorously and placed in ice for 10-15 minutes.
- 8) 1 ml of prepared mixture of phenol, chloroform and iso-amyl alcohol was poured in each tube and centrifugation was performed at 3000 rpm for 20 minutes.
- 9) After centrifugation two layers were formed. The upper layer of aqueous DNA was collected and transferred to a clean labeled falcon tube.
- 10) In each tube 60  $\mu$ L of isopropanol was added to precipitate the DNA. At this stage a thread of DNA can be seen in tube.
- 11) Precipitated DNA was centrifuged at 3000 rpm for 20 minutes again to make pellet of DNA. The supernatant was discarded.

- 12) In next step 5 ml of 70% ethanol was added to wash the DNA. All the supernatant was discarded after centrifugation.
- 13) Falcon tubes were inverted on a clean tissue paper to dry the pellet. 200  $\mu$ L of TE buffer was added in each tube and they were incubated at 37 °C overnight.

**Table 2.1:** Composition of solutions used for extraction of genomic DNA

<b>Solution</b>	<b>Composition</b>
TE Buffer	2mM EDTA, 10 mM Tris HCL, pH 8.0
Proteinase K	10 mg/ml
SDS	20%
TNE Buffer	10 mM Tris HCL, 400 mM NaCl, 2 mM EDTA
NaCl	6 M
Ethanol	70 %

### 2.2.2. DNA extraction using QIAamp extraction kit:

- 1) In a clean UAI labeled Eppendorf tube 20  $\mu$ L proteinase K was added. 200  $\mu$ L of blood sample was added in each tube.
- 2) Lysis buffer (AL) 200  $\mu$ L each was added in tubes and vortex was performed for 15 seconds. Tubes were incubated at 56 °C for 10 minutes.
- 3) After incubation centrifugation was done at 3000 rpm for 2 minutes. 200  $\mu$ L of ethanol was added to tubes and brief centrifugation was done.
- 4) All the mixture from Eppendorf was transferred to a clean labeled column and centrifugation was performed at 8000rpm for 1 minute.
- 5) In next step 500  $\mu$ L of washing buffer (AW1) was added and samples were centrifuged at 8000 rpm for 1 minute. The filtrate was removed.
- 6) In second washing add 500  $\mu$ L of washing buffer (AW2) and centrifuge at 14000 rpm for 3 minutes.
- 7) Column was shifted to a clean UAI labeled Eppendorf tube and collecting tube was discarded.
- 8) On the column 200  $\mu$ L of elution buffer (AE) was added and samples were incubated at room temperature for 1 minute.



- 9) Centrifugation at 8000 rpm was done for 1 minute in last step to collect clean DNA attached to filter.

To prevent DNA from denaturation, DNA vials were sealed with parafilm were subjected to heat shock in a water bath (70 °C for 1 hour).

### **2.2.3. Quantification and qualification of DNA:**

The integrity of extracted DNA was analyzed by two methods: agarose gel electrophoresis and Nano Drop.

### **2.2.4. Agarose gel electrophoresis:**

To prepare the gel for DNA, 0.8 g of agarose was dissolved in 100 ml of 1X TBE buffer. The mixture was heated for 2 minutes and 3  $\mu\text{L}$  of Ethidium bromide was added to stain the DNA so that it can be observed under ultra violet light. The mixture was poured in the casting tray and allowed to set for 30 minutes. After 30 minutes stopper and combs were removed from gel and tray with gel was placed in gel tank (Clever Scientific Limited, CS-3000V) for loading samples. In each well 1  $\mu\text{L}$  of loading dye (bromophenol blue) and 5  $\mu\text{L}$  of DNA was added after mixing. The gel was run for 30 minutes at 120 voltages and 120 Amperes current. The gel was removed after 30 minutes and was observed under UV light using Gel documentation system (Clever Scientific Limited).

### **2.2.5 DNA quantification by Nano drop:**

To measure the quantity of DNA and check its purity absorbance of samples was measured at 260/280, 260/230 and 260/325 using Nano drop machine. For blank 2  $\mu\text{L}$  of TE buffer was used and 2  $\mu\text{L}$  of DNA sample was loaded after that to record its values. A lint free wipe was used after every sample to prevent contamination.

## **2.3. Molecular analysis of Primary congenital glaucoma:**

For molecular analysis of 20 PCG patients (PCG 047-049, 051, 055-057, 059-069,101,102) *CYP1B1* gene was analyzed for disease causing variants. Each identified variant was checked against 96 control samples for confirmation.

### **2.3.1. Amplification of *CYP1B1* gene:**

To amplify the coding exons and intron exon boundaries primers described by (Afzal et al., 2019) (Table 2.2) were used. DNA was amplified using 200  $\mu$ L PCR tubes (Axygen, USA) and a reaction volume of 25  $\mu$ L was prepared by using quantity of reagents (Thermo Scientific Kit) mentioned in Table 2.3.

**Table 2.2:** List of primers used to amplify CYP1B1 gene in enrolled families.

Primer Name	Sequence	Exon	Temperature	Product size
2aF	ACCCAACGGCACTCAGTC	2	59 °C	517 bp
2aR	CCGAGTAGTGGCCGAAAG	2	59 °C	
2bF	CCCCATAGTGGTGCTGAATG	2	61 °C	512 bp
2bR	CTCGAATTCGCGGAAAAC	2	59 °C	
2cF	TCAGCCACAACGAAGAGTT	2	56 °C	531 bp
2cR	CACTGTGAGTCCCTTTACCG	2	58 °C	
3aF	GCAAGGCCTATTACAGGAAA	3	57 °C	463 bp
3aR	TTCACAGACCACTGGTTGAC	3	56°C	
3bF	TATGTCCTGGCCTTCCTTA	3	57 °C	512 bp
3bR	AGCTTGCCTCTTGCTTCTTA	3	57 °C	
3cF	AATGAGCCTGCGAAAATG	3	57 °C	513 bp
3cR	ATGGCCTGGTTACCAAATA	3	56 °C	

**Table 2.3:** Components of PCR reaction and their quantity for 25  $\mu$ L reaction mixture

PCR Reagent	Quantity in each reaction
1. DNA	2 $\mu$ L
2. MgCl <sub>2</sub>	2 $\mu$ L
3. PCR buffer	2.5 $\mu$ L
4. dNTPs Mixture	2.5 $\mu$ L
5. PCR water	14.7 $\mu$ L
6. Taq DNA Polymerase	0.3 $\mu$ L
7. Forward primer	0.5 $\mu$ L
8. Reverse primer	0.5 $\mu$ L
<b>Total</b>	<b>25 <math>\mu</math>L</b>

After adding the PCR reagents in quantity mentioned in table 2 PCR tubes were spun at 3000 rpm for 1 minute for mixing before putting the tubes in thermocycler for amplification. In thermocycler amplification were performed on set conditions such as initial denaturation at 95 °C for five minutes 1 time. After denaturation 35 cycles of denaturation at 95 °C for 45 seconds, annealing at variable temperatures for 45 second, followed by extension at 72 °C for 90 sec were carried out. In final extension temperature was set at 72 °C for 10 minutes and then samples were at infinite hold at 25 °C at end of PCR.

### **2.3.2. Analysis of amplified PCR product:**

For this purpose 2% agarose gel was used. In 2% gel 1g of agarose powder was added in 100 ml of 1X TBE buffer. To visualize the bands in gel 3 µL of ethidium bromide was added. When gel was solidified after 30 minutes it was transferred to gel tank. While loading 3 µL of PCR product and 2 µL of loading dye was used. The loaded gel was exposed to 120 volts and 120 ampere current for 25 minutes and observed for bands under Gel documentation system.

### **2.3.3. Purification of PCR product:**

The amplified PCR product was purified using Wizrep Purification Mini kit using the manual provided by manufacturer:

1. In the first step 20 µL PCR product was added to 2 ml Eppendorf tube and 100 µL of GP buffer was added in each tube.
2. The mixture was transferred to labeled spin columns that were attached to collection tubes.
3. Centrifugation at 13000 rpm for 2 minutes was performed and then 350 µL of washing buffer was added in each column and samples were centrifuged again.
4. In following step the filtrate was discarded and again 350 µL of washing buffer was added in spin column.
5. After centrifugation the filtrate was discarded and elution buffer that was pre heated in incubator at 70 °C for 10 minutes was added.
6. The addition of 50 µL of elution buffer was followed by centrifugation to remove DNA attached to the filter in a clean Eppendorf tube.

### 2.3.4. Sanger sequencing and result analysis:

The amplified PCR product along with primers was sent for sequencing by big dye terminator ready reaction mix at DNA Core Facility, Center for Applied Molecular Biology, CAMB Lahore. For sequencing at CAMB an automated ABI-3730 Genetic Analyzer was used. For sequencing of all exons forward primers were sent with the product.

### 2.3.5. Sequence visualization and in silico analysis:

Sequencing results were visualized using Chromas v 2.6.6 <https://technelysium.com.au/wp/chromas/>. Sequence for each sample was aligned with reference sequence of *CYP11B1* gene NM\_000104.4 obtained from Ensembl genomic browser, using Sequencher software (v 5.4.6) and Codon Code Aligner program to identify the variants.

For in silico analysis of identified variants Mutation taster <https://www.mutationtaster.org/> (Schwarz, Cooper, Schuelke, & Seelow, 2014) was used. Significance of each identified variant was checked according to guidelines of Human Genome Variation Society HGVS <http://www.hgvs.org/>. To further evaluate the variants Mutalyzer (v 2.0.35) <https://mutalyzer.nl/> (Lefter et al., 2021) and Varsome <https://varsome.com/> (Kopanios et al., 2019) was used. Any effect of the variant on splicing was investigated with HSF (Human Splicing Finder version 3.1) <https://www.genomnis.com/access-hsf> (Desmet et al., 2009). PolyPhen-2 <http://genetics.bwh.harvard.edu/pph2/> (Adzhubei et al., 2010), SIFT <https://sift.bii.a-star.edu.sg/> (P. C. Ng & Henikoff, 2003) and PROVEAN Protein Variation Effect Analyzer) [http://provean.jcvi.org/seq\\_submit.php](http://provean.jcvi.org/seq_submit.php) (Choi, Sims, Murphy, Miller, & Chan, 2012) was used to predict the effects of all non-synonymous variants identified in the data. To identify any changes in the thermodynamics due to variants I-Mutant v2.0 <https://folding.biofold.org/i-mutant/i-mutant2.0.html> (Rodrigues, Pires, & Ascher, 2018) and MUpro <http://mupro.proteomics.ics.uci.edu/> (Cheng, Randall, & Baldi, 2006) softwares were used. Both these softwares predict stability using support vector method (SVM) and give value for Gibbs free energy  $\Delta\Delta G$ . Conservation of variant amino acid between different mammalian species was analyzed by Clustal omega <https://www.ebi.ac.uk/Tools/msa/clustalo/> (Sievers et al., 2011) and data was

presented in a graphical form using WebLogo software <https://weblogo.berkeley.edu/> (Crooks, Hon, Chandonia, & Brenner, 2004). To predict the biochemical changes in CYP1B1 protein HOPE software <https://www3.cmbi.umcn.nl/hope/> was used (Venselaar, Te Beek, Kuipers, Hekkelman, & Vriend, 2010).

#### **2.4. Molecular analysis of retinal dystrophies and microphthalmia:**

For the retinal dystrophies proband of 35 enrolled families their affected and unaffected members were tested for disease-causing variants using NGS because retinal dystrophies are highly heterogeneous. All the probands had congenital bilateral night blindness and consanguineous parents. 35 enrolled families were given a UAI, and extracted DNA samples from 35 families were sent to foreign collaborators Baylor College of Medicine, USA for capture panel sequencing, and Wellcome Wolfson Medical Research Centre, UK, and the National Eye Institute, USA, for whole exome sequencing.

##### **2.4.1. Next Generation sequencing:**

The DNA was extracted and quantified at Molecular biology Lab, QAU and were sent to foreign collaborators for NGS capture panel sequencing and whole exome sequencing.

##### **2.4.2. Whole exome sequencing:**

Whole exome sequence analysis was performed using NextSeq500; Illumina, San Diego, CA, USA. It also involved Agilent Sureselect Whole Exome v6 targeting, mate pair fixing, read alignment and removal of duplicates. InDel were realigned and base quality was recalibrated (GATK v3.7.0), SNV (single nucleotide variants) and indel detection was performed with variant annotation and depth assessment (GATK DepthOfCoverage). Savvy CNV was used to detect Copy number variants CNVs (Laver et al., 2022).

CNVs with <5 reads and an allele frequency >0.01 in gnomAD v4, v3.1 and v2.1.1 and 1000 Genomes Project was excluded. All the synonymous and non-synonymous variants that were homozygous and compound heterozygous with any predicted impact on splicing were evaluated and cross referenced against the published SNP

data in Wellcome Wolfson Medical Research Centre, UK and National Eye Institute, USA.

### 2.4.3. NGS capture panel sequencing:

In functional Genomics Core at Baylor College of Medicine, USA the sequencing library was generated by KAPA HyperPrep Kit following the protocol provided by manufacturer (Roche, Basel, Switzerland). The library was then pooled for targeted enrichment of a panel of 344 candidate genes for inherited retinal diseases (Table 2.4) using the SureSelect Target Enrichment system for the Illumina Platform (F. Wang et al., 2014) (Agilent, Santa Clara, CA, USA). The Novaseq 6000 (Illumina, San Diego, CA, USA) was used to quantify and sequence captured DNA.

**Table 2.4:** List of 344 candidate genes screened in NGS panel capture sequencing

ABCA4	ARL6	BEST1	CDH23	CLN6
ABCC6	ASIC2	C12orf65	CDH3	CLN8
ABHD12	ASIC3	C1QTNF5	CDHR1	CLRN1
ACBD5	ATF6	C21orf2	CEP164	CLUAP1
ADAM9	ATOH7	C2orf71	CEP290	CNGA1
ADAMTS18	ATP1B2	C5orf42	CEP41	CNGA3
ADGRA3	ATXN7	C8orf37	CERKL	CNGB1
ADGRV1	BBIP1	CA4	CFH	CNGB3
AGTPBP1	BBS1	CABP4	CHM	CNNM4
AHI1	BBS10	CACNA1F	CIB2	COL11A1
AIFM1	BBS12	CACNA2D4	CISD2	COL2A1
AIPL1	BBS2	CAPN5	CLCN2	COL9A1
ALMS1	BBS4	CC2D2A	CLCN3	CRB1

---

ARL13B	BBS5	CCDC66	CLCN7	CRB2
ARL2BP	BBS7	CCL2	CLN3	CROCC
ARL3	BBS9	CCR2	CLN5	CRX
CSPP1	FAM161A	GRM6	INVS	LZTFL1
CTSD	FBLN5	GUCA1A	IQCB1	MAK
CTSF	FLVCR1	GUCA1B	ITM2B	MCOLN1
CYP4V2	FSCN2	GUCY2D	JAG1	MDM1
DFNB31	FZD4	GUCY2F	KCNJ13	MERTK
DHDDS	GBF1	HARS	KCNV2	MFN2
DHX38	GDF6	HK1	KIAA1549	MFRP
DMD	GJA10	HMCN1	KIF11	MFSD8
DNAJC5	GNAT1	IDH3B	KIF7	MITF
DTHD1	GNAT2	IFT140	KIZ	MKKS
EFEMP1	GNGT1	IFT172	KLHL7	MKS1
ELOVL4	GNPTAB	IFT27	LCA5	MPP5
EMC1	GNPTG	IMPDH1	LPCAT1	MTTP
ERCC6	GPR125	IMPG1	LRAT	MVK
ERCC8	GPR179	IMPG2	LRIT3	MYO7A
EYS	GRK1	INPP5E	LRP5	NDP
NEK2	NPHP1	NR2E1	NRL	NYX
NEUROD1	NPHP3	NR2E3	NXNL1	OAT
NMNAT1	NPHP4	NR2F1	NXNL2	OFD1

---

---

OPA1	PEX1	PITPNM3	RD3	RPGR
OPA3	PEX10	PLA2G5	RDH11	RPGRIP1
OPN1LW	PEX11B	POMGNT1	RDH12	RPGRIP1L
OPN1MW	PEX12	PPT1	RDH5	RRAS2
OPN1SW	PEX13	PRCD	RDH8	RS1
OTX2	PEX14	PRKCZ	REEP6	SAG
PANK2	PEX16	PROM1	RGR	SDCCAG8
PAX2	PEX19	PRPF3	RGS9	SEMA4A
PAX6	PEX2	PRPF31	RGS9BP	SLC24A1
PCDH15	PEX26	PRPF4	RHO	SLC38A8
PCYT1A	PEX3	PRPF6	RIMS1	SLC4A7
PDCL	PEX5	PRPF8	RLBP1	SLC6A6
PDE6A	PEX6	PRPH2	ROM1	SLC7A14
PDE6B	PEX7	RAB28	RP1	SNRNP200
PDE6C	PFDN5	RAX2	RP1L1	SPATA7
PDE6G	PGK1	RB1	RP2	SRD5A3
PDE6H	PHYH	RBP3	RP9	TCTN1
PDZD7	PIN1	RBP4	RPE65	TCTN3
TEAD1	TIMM8A	TIMP3	TMEM126A	TMEM138
TMEM216	UNC119	MIR204	NBAS	PROX1
TMEM231	USH1C	PLK4	PRDM13	BMP2
TMEM237	USH1G	PNPLA6	RTN4IP1	UCHL3

---



TMEM67	USH2A	POC1B	SLC25A46	LAMA1
TOPORS	VCAN	PRPS1	SPP2	MAPKAPK3
TPP1	VLDLR	TUBGCP4	TRNT1	PITX1
TREX1	VPS13B	GPR143	FBN1	SF3B4
TRIM32	WDPCP	PLA2G6	CEP78	GNB3
TRPM1	WDR19	TRAF3IP1	CWC27	HMX1
TSPAN12	WFS1	C10orf11	ZGPAT	TULP1
TTC21B	ZNF408	TYR	IDH3A	BMP4
TTC8	ZNF423	APOB	IFT81	EXOSC2
TTLL5	ZNF513	AGBL5	FRMD7	HGSNAT
TTPA	CEP250	ADIPOR1	MC4R	TUBGCP6
TUB	DRAM2	CTNNA1	MSX2	

#### 2.4.4. Bioinformatics analysis:

Sequencing data was processed by method defined by Wang et al., (F. Wang et al., 2014). The fastq files generated were aligned to human reference genome hg 19 using bwa. GATK was used to recalibrate, realign reads and call variants. Following the ACMG standards variants were filtered against dbSNP, gnomAD 1000 Genomes Project and BCM-HGSC internal database. All the reported variants were identified by checking HGMD, ClinVar and LOVD databases. In silico tools were used to analyze the novel variants. Missense variants were analyzed based on sequence conservation and nonsense, splicing and frameshift variants were classified as potential loss of function alleles.

#### 2.4.5. Validation and segregation testing by Sanger sequencing:

All the identified candidate variants were validated by Sanger testing using an ABI PRISM 3130 automated DNA analysis system (Applied Biosystems). Primer 3 plus

<https://www.primer3plus.com/index.html> was used to design primers (Untergasser et al., 2012) with at least 50 flanking bases. Proband, affected family members and unaffected family members were subjected to Sanger testing for variant validation. For family RP 109, primers were adopted from Nikopoulos et al., 2016 to confirm break points of a reported deletion (Nikopoulos et al., 2016).

#### 2.4.6. Pathogenicity prediction of identified variants:

PolyPhen-2 (Polymorphism phenotyping V2) <http://genetics.bwh.harvard.edu/pph2/> (Adzhubei et al., 2010), SIFT (Sorting intolerant from tolerant) <https://sift.bii.a-star.edu.sg/> (P. C. Ng & Henikoff, 2003), and PROVEAN (Protein variation effect analyzer) <https://provean.jcvi.org/> (Choi & Chan, 2015) were used to predict the effect of variant on protein structure using sequence homology. Mutation taster <https://www.mutationtaster.org/> differentiate benign variants from disease causing variants using data generated from Human 1000 Genomes project, gnomAD and ExAC (Steinhaus et al., 2021). PANTHER-PSEP <https://www.pantherdb.org/tools/csnpscoreform.jsp> was used to calculate conservation score of variant amino acid (Mi, Guo, Kejariwal, & Thomas, 2007). FATHMM <https://fathmm.biocompute.org.uk/> can identify a disease causing variant from neutral variant by analyzing its effect on protein function (Shihab et al., 2015). The effect of the variant on molecular pathway of the protein was analyzed by MutPred2 <http://mutpred.mutdb.org/index.html> (Pejaver et al., 2020). Combined Annotation Dependent Depletion (CADD) <https://cadd.gs.washington.edu/> (Rentzsch, Witten, Cooper, Shendure, & Kircher, 2019) and Rare exome variant ensemble learner (REVEL) <https://sites.google.com/site/revelgenomics/> (Ioannidis et al., 2016) score was calculated to obtain pathogenicity prediction of variant.

The changes in stability of protein structure was analyzed using MUpro <https://mupro.proteomics.ics.uci.edu/> (Cheng et al., 2006), iStable <http://predictor.nchu.edu.tw/iStable/> (C.-W. Chen, Lin, Liao, Chang, & Chu, 2020) and I-Mutant 2.0 <https://folding.biofold.org/cgi-bin/i-mutant2.0.cgi> (Capriotti, Fariselli, & Casadio, 2005). These softwares use Support Vector Machine (SVM) and Neural Network to calculate free energy change  $\Delta\Delta G$ .

# **Chapter 3**

## **RESULTS**

The present study was designed for genetic screening and clinical analysis of inherited autosomal recessive disorders such as primary congenital glaucoma, retinal dystrophies and microphthalmia. For this purpose patients were enrolled from various hospitals of Pakistan through ophthalmologists. A total of 20 primary congenital glaucoma families, 35 retinal dystrophies families and 1 microphthalmia family were recruited. Data from all the families was collected via specially designed questionnaires and blood samples were obtained for molecular analysis. Primary congenital glaucoma patients were screened using the Sanger sequencing technique for variants in the *CYP11B1* gene considering its status as a most commonly mutated gene in PCG patients. Segregation of identified disease causing variants was checked in 96 control samples for PCG. As retinal dystrophies are highly heterogeneous Next generation sequencing was done to identify disease causing genes and variants. Variants for retinal dystrophies and microphthalmia were segregated in affected and unaffected family members as tested by direct Sanger sequencing.

## **SECTION I:**

### **3.1. Clinical analysis of Primary congenital glaucoma:**

For this study twenty families affected from primary congenital glaucoma were enrolled. In these 20 families eight families were from Punjab, one from Kashmir, nine from Khyber Pakhtunkhwa and two from Balochistan province of Pakistan. Among these families PCG 049, PCG 051, PCG 057, PCG 056, PCG059 had two affected individuals, PCG 064, PCG 067 had four affected members while remaining fourteen families PCG 047, PCG 048, PCG 055, PCG 056, PCG 060- 063, PCG 066, PCG 068, PCG069, PCG 101 and PCG 102 had only one affected individual born to consanguineous parents.

Each enrolled proband had bilateral congenital glaucoma and age of onset of disease was between 3 to 6 months. At the time of enrolment average age of each proband was 12 years. The age group in which each enrolled proband was can be seen in figure 3.1. About 45% of the recruited PCG patients were in their first decade of life, 35% in second decade of life, 15% in third decade of life and 5% in their seventh decade of life. The clinical findings in recruited PCG patients included congenital glaucoma, buphthalmos, nystagmus and photophobia. The intraocular pressure in affected individuals was >21 mmHg.

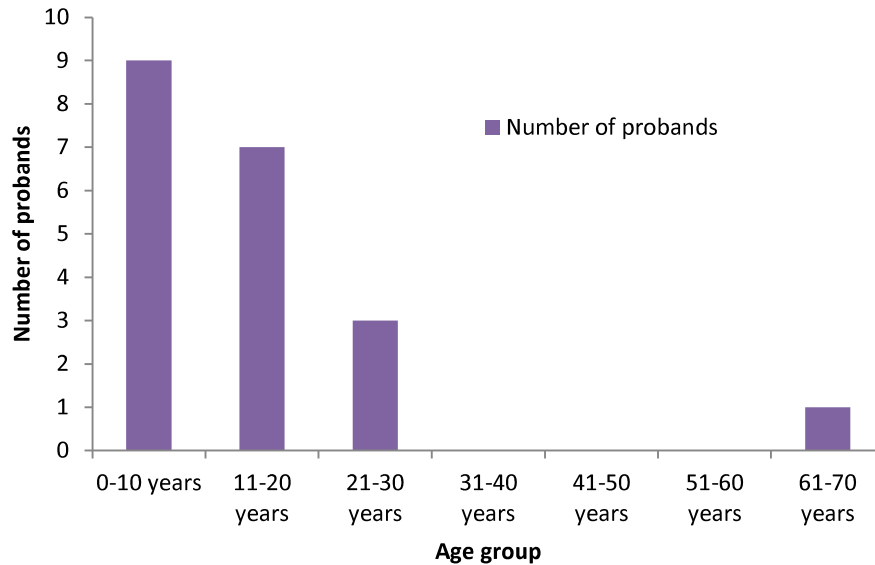


**Figure 3.1:** The graph shows the number of PCG patients recruited in current study in different age groups.

### 3.2. Molecular analysis of Primary congenital glaucoma patients:

Molecular screening of 20 PCG families for *CYP11B1* gene and its flanking region of 50 base pairs revealed nine disease causing variants in coding region of gene (Table 3.1).

Among these nine variants six were heterozygous and three were homozygous for the variant. The variants found included c.457C>G (p.Arg153Gly) and c.516C>A (p.Ser172Arg) in PCG 049, c.758-759insA (p.Val254Glyfs\*73) in PCG 059, c.740T>A (p.Leu247Gln) in PCG 060, c.1263T>A (p.Phe421Leu) and c.1314G>A in PCG 062, c.771T>G and c.789dup (p.Leu264Alafs\*63) in PCG 063 and c.724G>C (p.Asp242His) in PCG 067. All the identified variants are not reported before in PCG patients in *CYP11B1* gene. These variants included five missense variants c.457C>G, c.516C>A, c.740T>A, c.1263T>A, c.724G>C, two frameshift variants c.758-759insA, c.789dup and two silent variants c.1314G>A, c.771T>G.

In addition to disease causing variants seven polymorphisms were also detected: c.1347T>C, c.1294G>C, c.1358A>G, c.2244\_2245insT, c.355G>T, c.142C>G and g.35710\_35711insT (Table 3.2).

**Table 3.1:** List of Novel disease causing variants identified in PCG patients.

Family ID	Position	Nucleotide change	Protein change	Zygoty	Mutation taster prediction	dbSNP Status
PCG049	EXON 2	c.457C>G	p.Arg153Gly	Heterozygous	Disease causing	Not reported
	EXON 2	c.516C>A	p.Ser172Arg	Heterozygous	Disease causing	Not reported
PCG059	EXON 2	c.758-759insA	p.Val254Glyfs*73	Homozygous	Disease causing	Not reported
PCG060	EXON 2	c.740T>A	p.Leu247Gln	Heterozygous	Disease causing	Not reported
PCG062	EXON 3	c.1263T>A	p.Phe421Leu	Heterozygous	Disease causing	Not reported
	EXON 3	c.1314G>A	p.(=)	Heterozygous	Disease causing	Not reported
PCG063	EXON 2	c.771T>G	p.(=)	Heterozygous	Disease causing	Not reported
	EXON 2	c.789dup	p.Leu264Alafs*63	Homozygous	Disease causing	Not reported
PCG067	EXON 2	c.724G>C	p.Asp242His	Homozygous	Disease causing	Not reported

**Table 3.2:** List of all the single nucleotide polymorphisms identified in current study

Family ID	Position	Nucleotide change	Zygoty	Mutation taster	Protein change	dbSNP
PCG 047, 102, 060, 061, 062, 063, 064, 069	EXON 3	c.1347T>C	Homozygous	Polymorphism	p.(=)	rs1056837
PCG049, 055, 057	EXON 3	c.1294G>C	Homozygous	Polymorphism	p.Val432Leu	rs1056836
PCG051, 063	EXON 3	c.1358A>G	Homozygous	Polymorphism	p.Asn453Ser	rs1800400
PCG 102, 064, 065	3'UTR	c.2244_2245insT	Homozygous	Polymorphism	p.(=)	rs4646431
PCG 069, 056	EXON 2	c.355G>T	Homozygous	Polymorphism	p.Ala119Ser	rs1056827
PCG 056	EXON 2	c.142C>G	Homozygous	Polymorphism	p.Arg48Gly	rs10012
PCG 062	Intron	g.35710_35711insT	Homozygous	Polymorphism	p.(=)	Not reported

All these polymorphisms were reported previously except for an intronic variant g.35710\_35711insT in PCG 062. These polymorphisms were identified in a homozygous state in all individuals.

All the identified disease causing variants and polymorphisms were subjected to in silico analysis to predict the result of variant on *CYP11B1* protein. Results of the in silico analysis are described in Table 3.3.

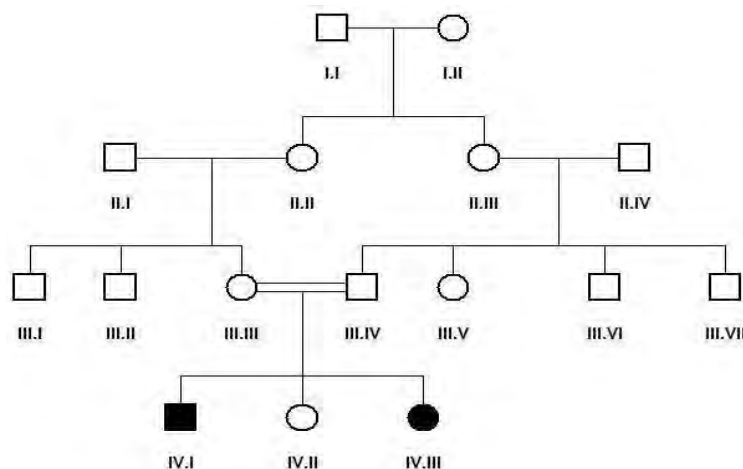
**Table 3.3:** In-silico analysis of disease-causing variants identified in this study

Nucleotide change	Protein change	Polyphen-2	Provean	Varsome	I mutant		MUpro		HOPE Conservation prediction	
					$\Delta\Delta G$ (kcal/mol) DDG value	Stability Prediction SVM2	$\Delta\Delta G$ (kcal/mol)	Stability Prediction SVM2		
c.457C>G	p.Arg153Gly	Probably damaging 1.00	Deleterious - 5.21	Likely Pathogenic	Decreased Stability	-1.47	Decreased Stability	-1.1669	Decreased Stability	Probably stable
c.516C>A	p.Ser172Arg	Possibly damaging 0.685	Neutral - 1.167	Pathogenic	Decreased Stability	-0.03	Decreased Stability	-0.2848	Decreased Stability	Probably stable
c.758-759insA	p.Val254Glyfs*73	Probably damaging 1.00	Deleterious - 3.95	Pathogenic	Decreased Stability	-3.18	Decreased Stability	-2.691	Decreased Stability	Damaging
c.740T>A	p.Leu247Gln	Probably damaging 1.00	Deleterious - 5.45	Likely Pathogenic	Decreased Stability	-2.14	Decreased Stability	-1.1804	Decreased Stability	Probably stable
c.1263T>A	p.Phe421Leu	Probably damaging 1.00	Deleterious - 5.43	Likely Pathogenic	Decreased Stability	-1.06	Decreased Stability	-0.4212	Decreased Stability	Stable
c.1314G>A	p.(=)	N/A	N/A	Likely Benign	N/A	N/A	N/A	N/A	N/A	N/A
c.771T>G	p.(=)	N/A	N/A	Likely Benign	N/A	N/A	N/A	N/A	N/A	N/A
c.789dup	p.Leu264A <sub>lafs</sub> *63	Probably damaging 0.998	Deleterious - 3.62	Likely Pathogenic	Decreased Stability	-1.59	Decreased Stability	-1.5125	Decreased Stability	Deleterious

\*N/A Not available

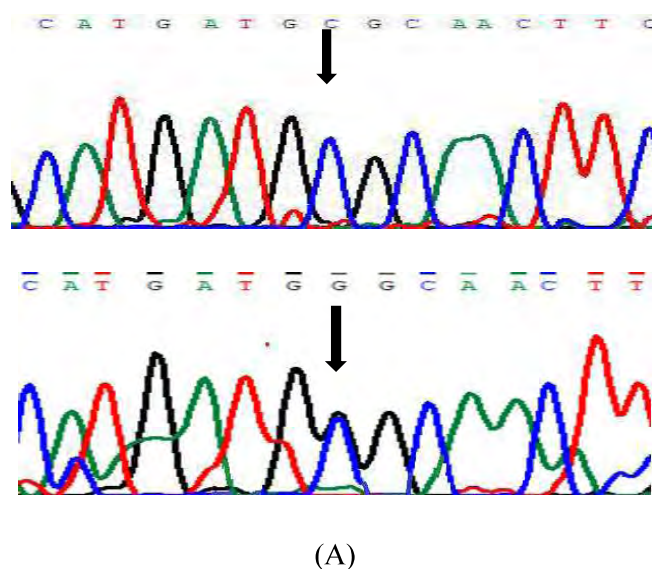
### 3.2.1. Family PCG 049:

In family PCG 049 (Figure 3.2) two heterozygous disease causing variants were detected in a consanguineous family with two affected siblings (3.1).

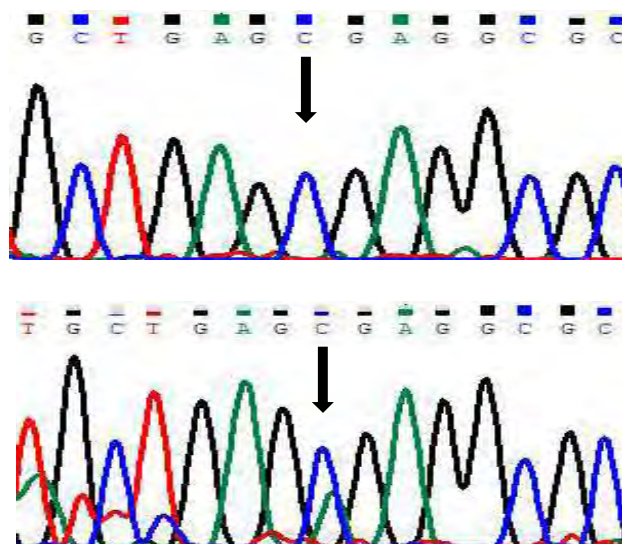


**Figure 3.2:** Pedigree drawing of family PCG 049.

At position 457 the substitution of single base i.e., c.457C>G, changed arginine to glycine p.Arg153Gly in CYP1B1 protein. Another heterozygous variant, i.e., c.516C>A, led to the substitution of arginine at position 172 in protein. In-silico analysis of both variants by Provean revealed c.457C>G to be deleterious and c.516C>A as neutral with a score of -5.21 and -1.67 respectively (table 3.3). The chromatogram of the identified variant can be seen in figure 3.3 (A, B).







(B)

**Figure 3.3:** Chromatograms of two heterozygous variants c.457C>G and c.516C>A identified in family PCG 049 in *CYP11B1* gene.

PolyPhen-2 predicted the change of arginine at position 153 as probably damaging with a score of 1.00 while change of serine at position 172 was predicted as possibly damaging (score: 0.685). Varsome predicted both variants as pathogenic. I-Mutant calculated negative value (-1.47, -0.03) of  $\Delta\Delta G$  for both variants and MUpro also predicted both variants will decrease the stability of protein structure (-1.1669, -0.2848).

Human splicing finder predicted that a new site for auxiliary factors like exonic splicing suppresser (ESS) hnRNPA1, Fas ESS, IIE, Sironi\_motif2, exonic splicing enhancer (ESE) 9G8 will be created and break sites for Sironi\_motif1, EIE, ESE\_SRp55 will be created if glycine at position 153 is added instead of arginine.

### 3.2.2. Family PCG 059:

A 1.5 years old female (figure 3.4) patient was enrolled from Punjab, Pakistan and a frameshift variant c.758-759insA was identified when screened for variant in *CYP11B1* gene (Table 3.1) (Figure 3.5). The insertion of adenine resulted in frame shift of 73 bases and valine at position 254 was replaced by glycine. In-silico tools predicted this variant as highly pathogenic (table 3.3). PolyPhen-2 and Provean gave it a pathogenicity score of 1.00 and -3.95 respectively.

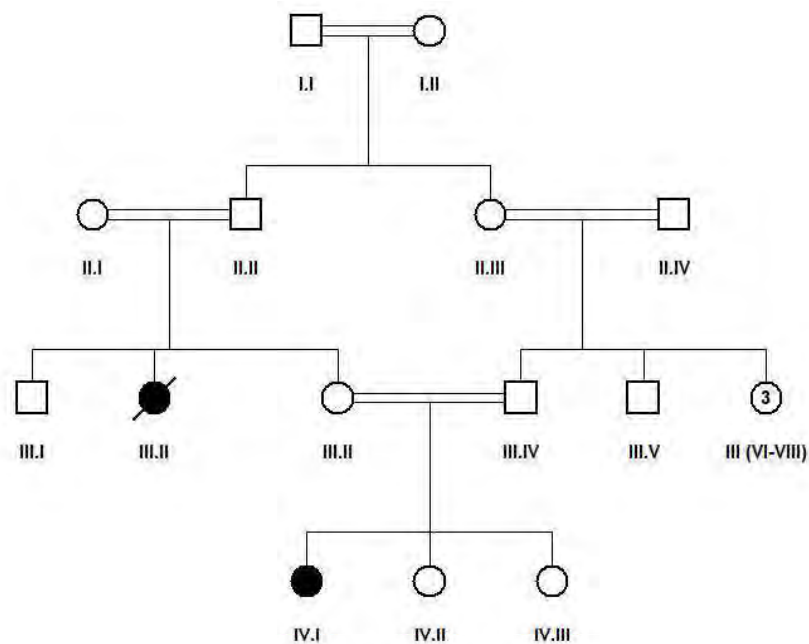


**Figure 3.4:** Pedigree diagram of Family PCG 059.

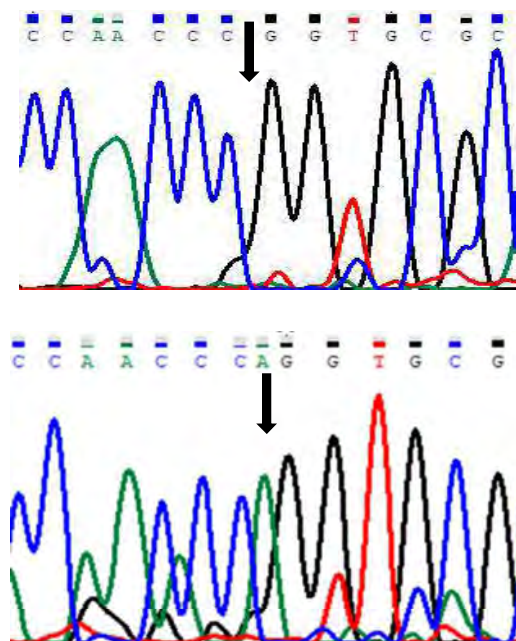
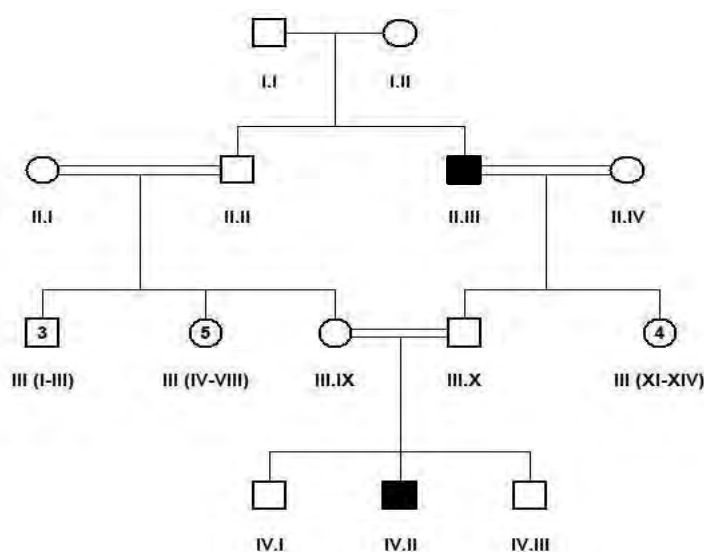


**Figure 3.5:** Chromatogram of frameshift variant c.758\_759insA identified in family PCG 059.

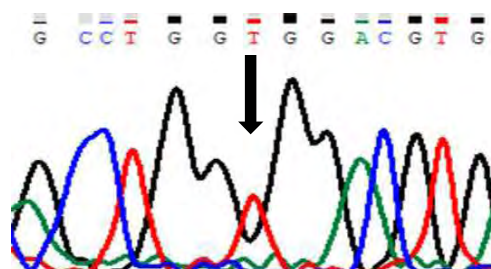
MUpro (-2.691) and I-Mutant (-3.18) predicted that insertion of adenine at position 758-759 will result in decreased stability of protein structure. Varsome predicted this insertion to be pathogenic.

### 3.2.3. Family PCG 060:

Family PCG 060 had high consanguinity and a 6 month old baby boy born with bilateral congenital glaucoma (figure 3.6). On screening of *CYP11B1* gene a novel missense variant c.740T>A was identified in proband (table 3.1) (figure 3.7). This heterozygous variant was responsible for change of leucine at position 247 to glutamine that was predicted as deleterious by Provean with a score of -5.45 (table 3.3). PolyPhen-2 and Varsome also predicted this variant to be pathogenic. According to I-Mutant and MUpro this variant will decrease the stability of protein structure thus affecting its function.



**Figure 3.6:** Pedigree diagram of family PCG 060.



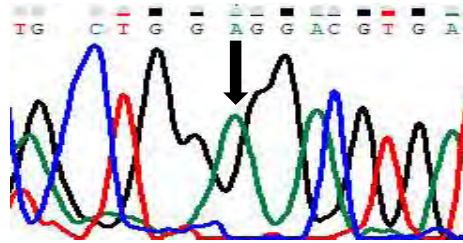
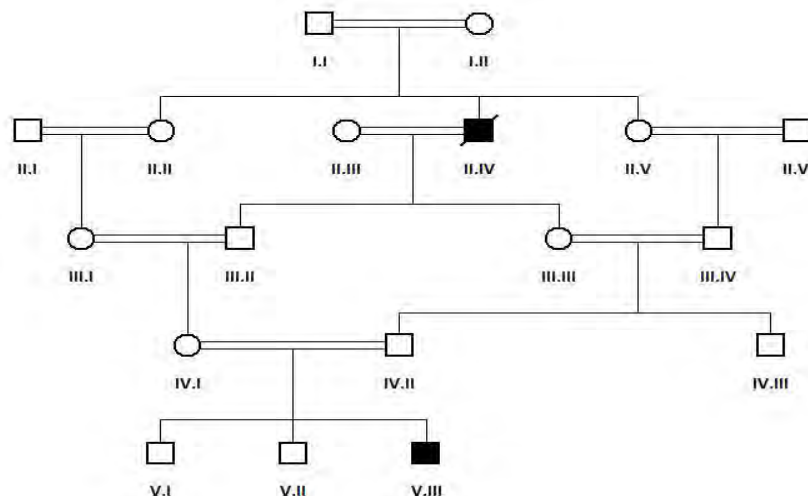


**Figure 3.7:** Chromatogram of family PCG 060 showing missense variant c.722T>A

Identification of only a single heterozygous variant leaves space for molecular analysis of intronic region of CYP1B1 gene and other PCG related genes to identify other pathogenic variants in this family. Due to limited resources available for the study a more detailed molecular analysis could not be performed for PCG 060.

#### 3.2.4. Family PCG 062:

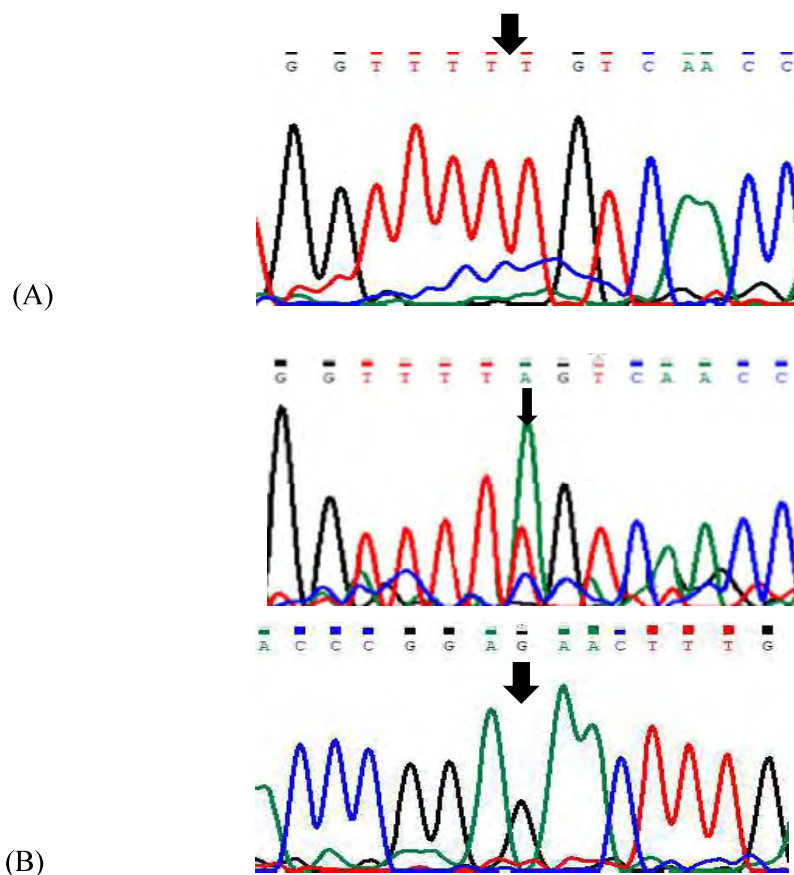
Proband of family PCG 062 (figure 3.8) had bilateral primary congenital glaucoma and two heterozygous variants were identified in it (Table 3.1). On molecular analysis a missense variant c.1263T>A (p.Phe421Leu) and a silent variant c.1314G>A (p.=) was identified in exon 3 (figure 3.9). Both variants were not reported before in any study for primary congenital glaucoma. First variant c.1263T>A replaced phenylalanine at position 421 with leucine and was reported as deleterious (-5.43) by Provean (table 3.3).

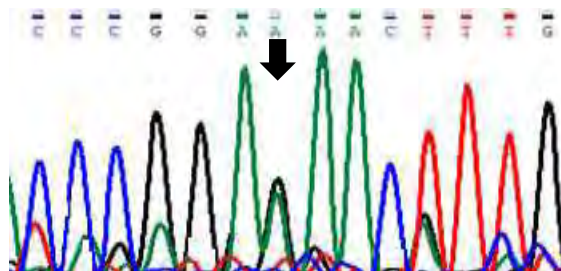


**Figure 3.8:** Pedigree drawing of family PCG 062.

PolyPhen-2 also reported this variant as damaging with a score of 1.00. Analysis of amino acid change on stability of protein by I-Mutant and MUpro revealed a decreased stability and predicted value of  $\Delta\Delta G$  (kcal/mol) as -1.06 and -0.4212.

Human splicing finder results for variant c.1263T>A predicted formation of a new acceptor site TGTGGTTTTGTC>CTGTGGTTTTAGTC with a consensus value (CV) of 78.78. As the CV value for new site is less than 80 so it is not a very strong acceptor site. Although the second heterozygous variant c.1314G>A (p.=) was reported as disease causing by Mutation taster but other related PCG genes including *MYOC*, *FOXC1* and *TEK* should be analyzed to find out any other variants in unlinked PCG genes. Segregation of both variants c.1263T>A and c.1314G>A needs to be tested in parents to find out the inheritance pattern of identified variants but unfortunately they were not available.

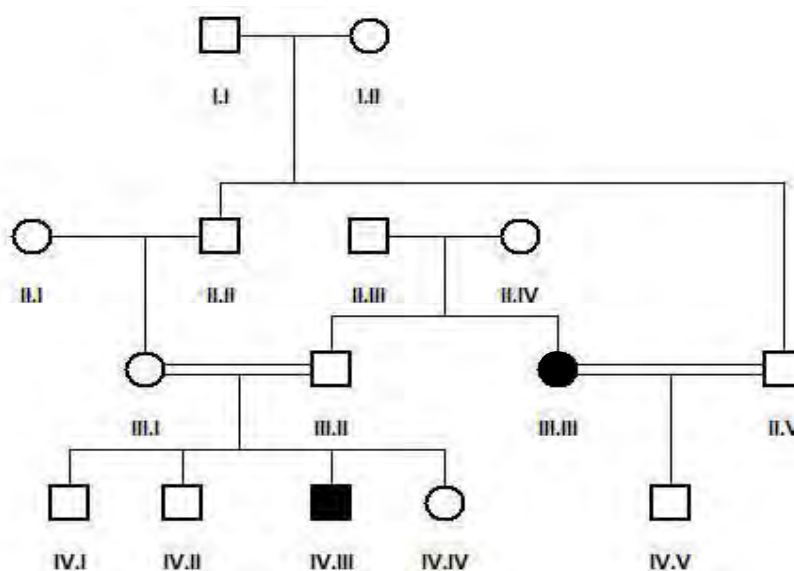




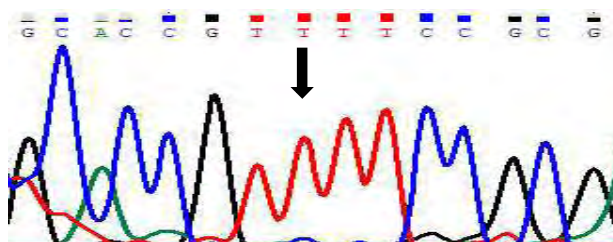
**Figure 3.9:** Chromatograms for compound heterozygous variants c.1263T>A and c.1314G>A identified in family PCG 062.

### 3.2.5. Family PCG 063:

In family PCG 063, an 11 year old boy born to consanguineous parents was affected from primary congenital glaucoma with no previous history of disease in family (figure 3.10). Two variants were found on molecular analysis, one silent variant c.771T>G and a frame shift disease causing variant c.789dup in homozygous state (table 3.1) (figure 3.11).



**Figure 3.10:** Pedigree of family PCG 063



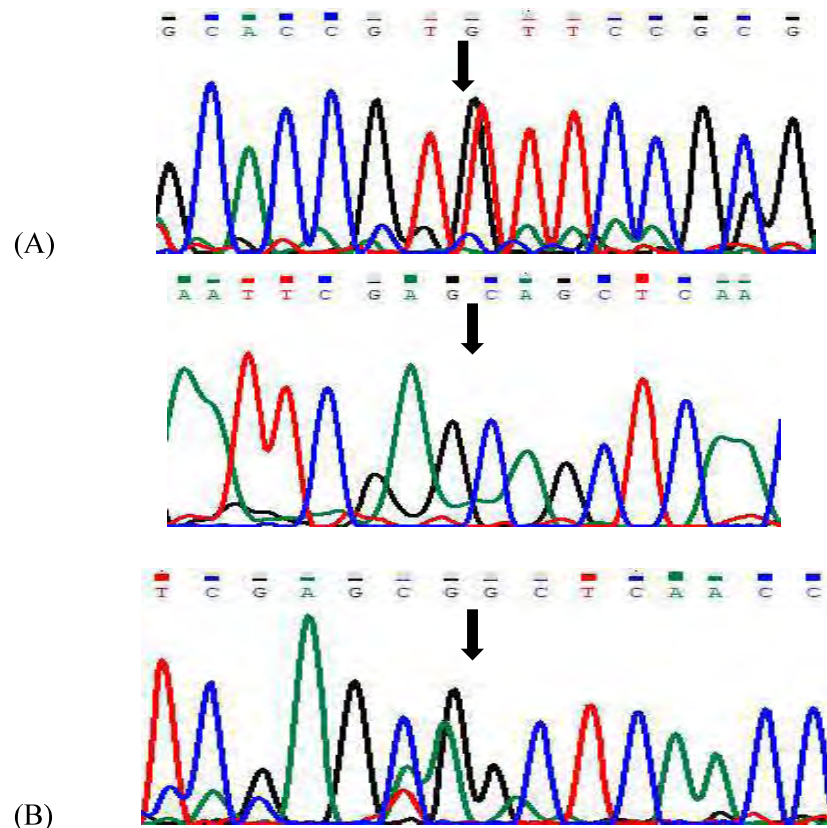


**Figure 3.11:** (A) Chromatograms of heterozygous variant c.771T>G. (B) A homozygous variant c.789dup identified in family PCG 063.

Due to frame shift variant c.789dup (p.Leu264Alafs\*63) a shorter protein was formed. Both Provean (score: -3.62) and Polyphen-2 (score 0.998) predicted this homozygous frameshift variant as damaging (table 3.4). A decreased stability was predicted by I-Mutant and MUpro with value for  $\Delta\Delta G$  (kcal/mol) as -1.59 and -1.51 respectively. An analysis of splicing region with Human splicing finder showed that for ESS\_hnRNPA1 CAGGCT site was created, GCAGGC for ESE\_9G8 CAGGCTCA for PESE. Two sites AGCAGC required for auxiliary factors ESE\_SRp55, AGCAGCTC for PESE was broken due to frameshift. The silent heterozygous variant was predicted as likely benign by varsome that is why it would not be contributing to the pathogenicity of the disease.

### 3.2.6. Family PCG 067:

In family PCG 067 the proband was a 13 years old boy affected from PCG. He also has an affected brother and two affected cousins (one male, other female) (Figure

3.12). A missense variant c.724G>C (p.Asp242His) (table 3.1) (figure 3.13) was identified in proband and was predicted as highly deleterious by PROVEAN -6.50 (table 3.3).

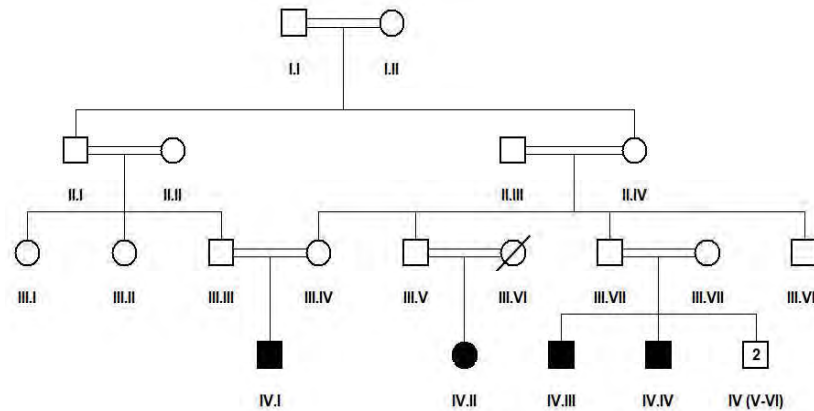


**Figure 3.12:** Pedigree drawing of family PCG 067 showing four affected members.

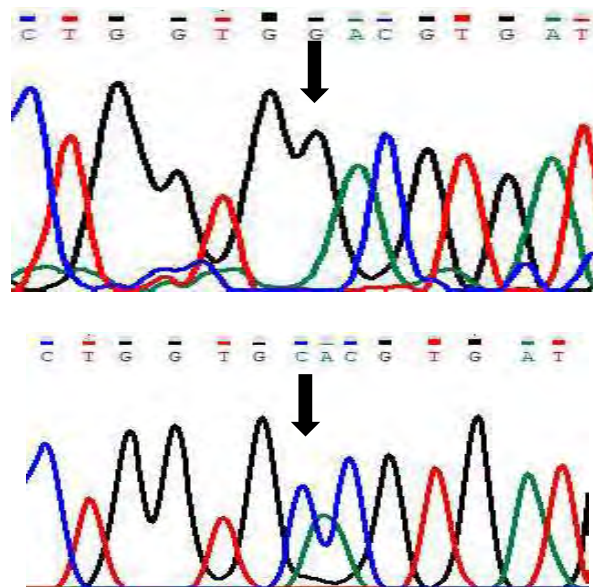


**Figure 3.13:** Chromatogram of normal and affected individual for variant c.724G>C in family PCG 067.

PolyPhen-2 predicted this change of aspartate at position 242 to histidine as damaging (score: 1). The value of  $\Delta\Delta G$  (kcal/mol) was predicted as -2.35 by I-Mutant and -0.7293 by MUpro that suggests a decreased stability of protein. This change of amino acid can also affect the splicing sites such as a new site was created for



ESE\_SRp55CACGTG and sites for Sironi\_motif2, Sironi\_motif1, ESE\_9G8, PESE, and EIE was broken.

### 3.3. Polymorphisms identified in *CYP11B1* gene:

Seven single nucleotide polymorphisms (SNP) were identified in current study in PCG gene during molecular analysis in twenty recruited families (Table 3.4). One SNP c.1347T>C (rs1056837) was identified in 45% of affected individuals (PCG 047,056, 060, 061, 062, 063, 064, 069) that were enrolled in current study. Another SNP c.1294G>C was identified in 15% of recruited individuals (PCG 049, 055, 057). This substitution of cytosine at position 1294 changed amino acid valine at position 432 to leucine p.Val432Leu (rs1056836). In two families PCG 051 and 063 a SNP c.1358A>G (rs1800400) changed aspartate to serine at position 453. This change of amino acid was predicted as deleterious by PROVEAN (score, -3.24) and PolyPhen-2 (possibly damaging, 0.906).

In the 3'UTR region of three samples PCG 064, 065, 102 a homozygous SNP c.2244\_2245insT was identified that was reported in previous data rs4646431. In family PCG 056 and 069 a homozygous SNP c.355G>T (rs10012) was found in exon 2. This SNP also changed the amino acid at position 119 to serine and was predicted as tolerated by SIFT, benign by Poly-Phen-2 and neutral (-0.085) by PROVEAN. Family PCG 062 had an insertion of thymine in intronic region g.35710\_35711insT in homozygous state. This variation was predicted as polymorphism by Mutation taster and was not reported before.

**Table 3.4:** In-silico analysis of polymorphisms identified in this study

Family ID	Position	Nucleotide change	Zygoty	Protein change	Mutation taster	Polyphen-2	SIFT	Provean	dbSNP
<b>PCG 047, 056, 102, 060, 061, 062, 063, 064, 069</b>	EXON 3	c.1347T>C	Homozygous	p.(=)	Polymorphism	N/A	N/A	N/A	rs1056837
<b>PCG 049, 055, 057</b>	EXON 3	c.1294G>C	Homozygous	p.Val432Leu	Polymorphism	Benign 0.00	Tolerant 1.00		rs1056836
<b>PCG 051, 063</b>	EXON 3	c.1358A>G	Homozygous	p.Asn453Ser	Polymorphism	Possibly damaging 0.906	Tolerant 1.00	Deleterious- 3.24	rs1800400
<b>PCG 102, 064, 065</b>	3'UTR	c.2244_2245insT	Homozygous	p.(=)	Polymorphism	N/A	N/A	N/A	rs4646431
<b>PCG 069, 056</b>	EXON 2	c.355G>T	Homozygous	p.Ala119Ser	Polymorphism	Benign 0.00	Tolerant 1.00	Neutral 1.51	rs1056827
<b>PCG 056</b>	EXON 2	c.142C>G	Homozygous	p.Arg48Gly	Polymorphism	Benign 0.00	Tolerant 0.82	Neutral 0.085	rs10012
<b>PCG 062</b>	Intron	g.35710_35711insT	Homozygous	p.(=)	Polymorphism	N/A	N/A	N/A	Not reported

### 3.4. Conservation analysis of identified disease causing variants:

The conservation analysis of nine identified variants was performed using Clustal Omega multiple sequence alignment tool. Homologous *CYP1B1* gene sequences for different species with high similarity index to *Homo sapiens* were identified using BLAST. Depending upon the result of BLAST these species were selected i.e., *Nomascus leucogenys* (XP\_003262792.2), *Pan troglodytes* (XP\_001167556.1), *Mus musculus* (NP\_001075448.1), and *Pongo abelii* (XP\_009235654.1).

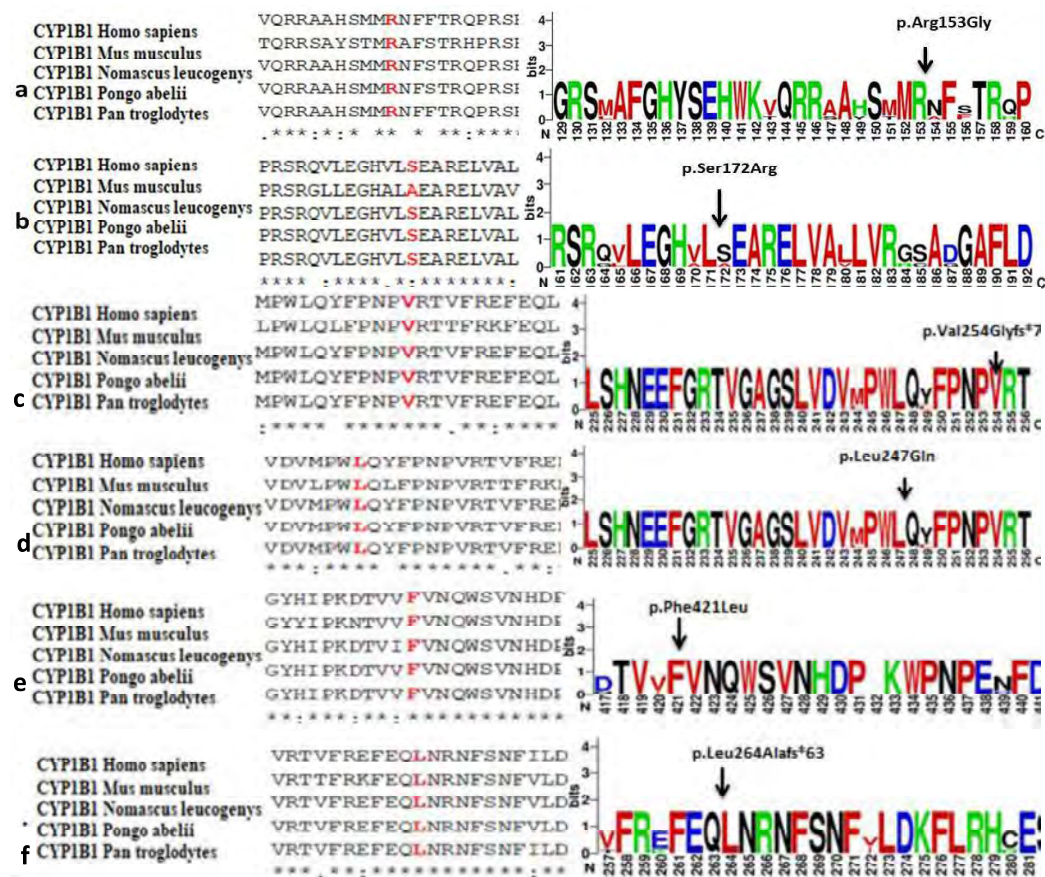


**Figure 3.14:** Figure shows comparison of conservation of amino acids in *CYP1B1* gene among homologs for unreported disease causing variants detected in current study. WebLogo results of all novel *CYP1B1* protein variants showing comparison of conservation among homologs are on right side of the figure. Large size of amino acid abbreviation letter show full conservation while small size shows less conserved position among homologs.

The result of conservation analysis can be seen in figure 3.14. The variant p.Arg153Gly detected in family PCG 049 was found to be 100% conserved in all homologous species depicting its role in proper functioning of CYP1B1 protein (figure 3.14 a). In family PCG 059 multiple sequence alignment results for frameshift variant p.Val254Glyfs\*73 showed complete conservation in all species figure 3.14 b). In family PCG 060 variant p. Leu247Gln, in PCG 062 variant p.Phe421Leu, in PCG 063 variant p.Leu264Alafs\*63 and in PCG 067 variant p.Asp242His were 100% conserved in all homologs.

### 3.5. Analysis of conservation and structure by HOPE:

The structure of CYP1B1 protein predicted by HOPE is presented in figure 3.15. HOPE predicted the variant amino acid (p.Arg153Gly) glycine in family PCG 049 as not damaging because other residues are also found in homologous proteins (figure 3.16 a) (table 3.3).

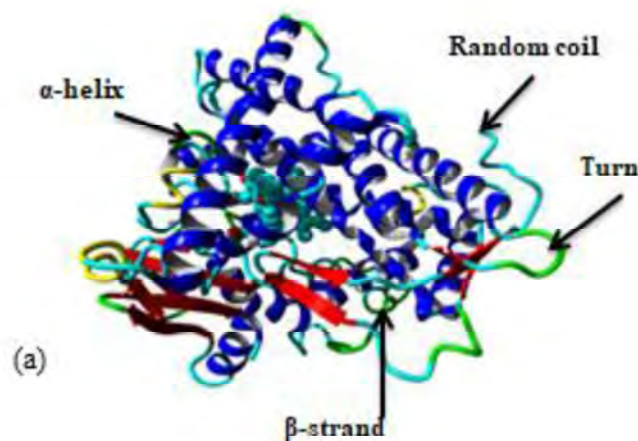


**Figure 3.15:** The overview of CYP1B1 wild type protein

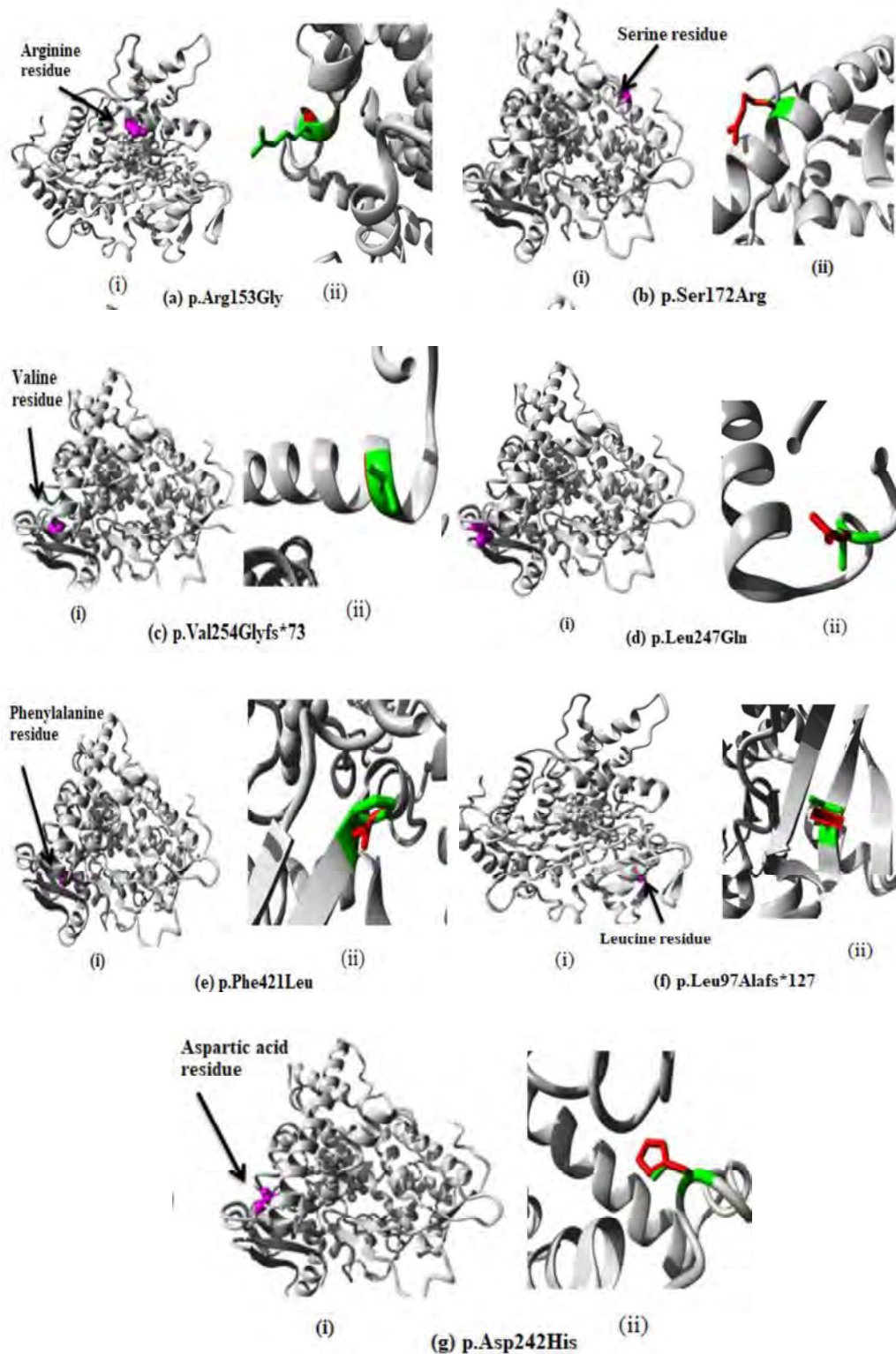


**Figure 3.16:** Position of amino acid residue and change in structure due to variant predicted by HOPE. Wild type amino acid residue is green in color while red color shows mutant amino acid.

The second heterozygous variant p.Ser172Arg in PCR 049 family was also predicted as not highly conserved by HOPE as other amino acids are reported in homologs (figure 3.16 b). The change of amino acid due to a frame shift variant Leu264Alafs\*63, in family PCG 063 was considered as deleterious by conservation analysis (figure 3.16 f). This position was found as 100% conserved in homologs. The three remaining missense variants found in current study p.Leu247Gln (figure 3.16 d), p.Phe421Leu (figure 3.16 e), and p.Asp242His (figure 3.16 g) was also predicted as not harmful for protein structure by HOPE. In family PCG 059 the insertion of adenine that led to frameshift of 73 amino acids (p.Val254Glyfs\*73) was damaging for CYP1B1 protein according to conservation analysis (figure 3.16 c).

## **SECTION II:**

In current study 35 large families affected with retinal dystrophies and high consanguinity was recruited from different hospitals with Pakistan. Among these families, ten families RP 004, 005, 007, 008, 010, 012, 013, 019, 033, 043 belonged to Punjab, twenty one families RP 044, 047, 050, 062, 101, 105, 106, 107, 109, 110, 112, 113, 118, 122, 141, 142, 144, 147, 150, 153, 154 were from Khyber Pakhtunkhwa, three families RP 068, 069, 073 from Sindh and only one RP 131 was from Kashmir, Pakistan.

Each of the recruited family had multiple affected individuals. The affected individuals had bilateral retinal dystrophies while some were syndromic for their condition.

### **3.6. Clinical analysis of inherited retinal dystrophies:**

The clinical features of all the enrolled families can be observed in Table 3.5. The common clinical feature in all enrolled individuals was Bilateral Night blindness. Three families RP 004, 043 and 131 had polydactyly while RP 047, 102, 105, 109, 144, 150, 153, 154 had proband with hearing loss and speaking disability. Mental disability was present in family RP 008, 144, 153 and 154. All the enrolled patients were in different age group with an average age of  $26 \pm 6$  (figure 3.17). Family history of disease was positive for all affected individuals. The enrolled families showed 100% consanguinity. Pie chart shows the number of families with progressive and stationary RP (figure 3.18).

**Table 3.5: Demographic and clinical data of thirty five inherited retinal dystrophies affected families enrolled for this study.**

Family ID	Proband ID	Age of onset	AGE	No of affected	Consanguinity	Family history	RP type	Symptoms
RP 004	V.I	By birth	23 Years	4	YES	Positive	Stationary	Night blindness, polydactyly
RP 005	III.XVIII	15 Years	31 Years	11	YES	Positive	Stationary	Bilateral Night blindness, Nystagmus
RP 007	III.I	By birth	19 Years	8	YES	Positive	Progressive	Bilateral Night blindness, Nystagmus
RP 008	IV.VI	By birth	22 Years	5	YES	Positive	Stationary	Night blindness, Low IQ.
RP 010	IV.I	By birth	34 Years	5	YES	Positive	Stationary	Bilateral Night blindness
RP 012	III.II	By birth	26 Years	4	YES	Positive	Stationary	Bilateral Night blindness, Photophobia
RP 013	.VIII	By birth	16 Years	4	YES	Positive	Stationary	Bilateral Night Blindness, Photosensitive
RP 019	IV.VI	By birth	62 Years	5	YES	Positive	Stationary	Night blindness, Photophobia
PR 033	IV.VI	By birth	21 Years	8	YES	Positive	Progressive	Night blindness, Poor day vision
RP 043	IV.IV	By birth	26 Years	3	YES	Positive	Progressive	Night blindness, polydactyly
RP 044	III.II	By birth	32 Years	6	YES	Positive	Progressive	Night blindness
RP 047	III.VII	By birth	17 Years	5	YES	Positive	Stationary	Night blindness, Hearing disability, Cataract
RP 050	III.II	By birth	12 Years	7	YES	Positive	Progressive	Bilateral Night blindness
RP 062	V.VIII	By birth	27 Years	4	YES	Positive	Progressive	Bilateral Night blindness, Nystagmus
RP 068	III.II	By birth	9 Years	6	YES	Positive	Progressive	Bilateral Night blindness, Photosensitive
RP 069	V.II	By birth	24 Years	6	YES	Positive	Progressive	Bilateral Night blindness
RP 073	IV.X	By birth	72 Years	10	YES	Positive	Progressive	Bilateral Night blindness, Severe vision loss
RP 102	VIII.I	9 years	40 Years	5	YES	Positive	Stationary	Night blind, Hearing loss
RP105	VI.VIII	14 years	26 Years	3	YES	Positive	Progressive	Night blind, Myopia, Hearing loss
RP106	VIII.I	By birth	7 Years	6	YES	Positive	Stationary	Night blind, uncontrolled body movement

<b>RP107</b>	IV.IX	12 years	30 Years	9	YES	Positive	Progressive	Night blind, Epiphora, Myopia, Blurred vision
<b>RP109</b>	VI.X	2-6 years	15 years	3	YES	Positive	Progressive	Night blind, Nystagmus, Hearing problem, Poor day vision
<b>RP110</b>	VI.V	By birth	32 years	5	YES	Positive	Progressive	Night blind, Photosensitive, Nystagmus, Poor day vision
<b>RP112</b>	V.V	By birth	45 years	4	YES	Positive	Progressive	Night blind, Maculopathy
<b>RP113</b>	IV.III	By birth	22 years	5	YES	Positive	Progressive	Night blind, Maculopathy
<b>RP 118</b>	III.III	By birth	29 Years	4	YES	Positive	Stationary	Night blindness
<b>RP 122</b>	IV.IV	By birth	10 Years	4	YES	Positive	Stationary	Night blindness, Nystagmus
<b>RP 131</b>	IV.III	By birth	34 Years	4	YES	Positive	Progressive	Night blindness, polydactyly
<b>RP 141</b>	III.VII	By birth	54 Years	5	YES	Positive	Progressive	Bilateral Night blindness
<b>RP 142</b>	IV.III	By birth	38 Years	5	YES	Positive	Progressive	Bilateral Night blindness, Nystagmus
<b>RP 144</b>	IV.VI	By birth	26 Years	8	YES	Positive	Stationary	Bilateral Night blindness, Deaf and Dumb, Mental disability
<b>RP 147</b>	III.I	By birth	14 Years	5	YES	Positive	Progressive	Bilateral Night blindness
<b>RP 150</b>	III.I	By birth	35 Years	3	YES	Positive	Progressive	Bilateral Night blindness, Deaf and Dumb
<b>RP 153</b>	III.XIX	By birth	35 Years	5	YES	Positive	Stationary	Bilateral Night blindness, Deaf and Dumb, Mental disability
<b>RP 154</b>	IV.I	By birth	9 Years	5	YES	Positive	Progressive	Bilateral Night blindness, Deaf and Dumb, Mental disability, Ataxia, Small head.



disease (figure 3.18). The onset of disease in all recruited families was by birth except for five families: RP 005 at age of 15 years, RP 102 at the age 9 years, RP 105 at the age of 14 years, RP 107 at the age of 12 years and RP 109 approximately at age of 2-6 years.

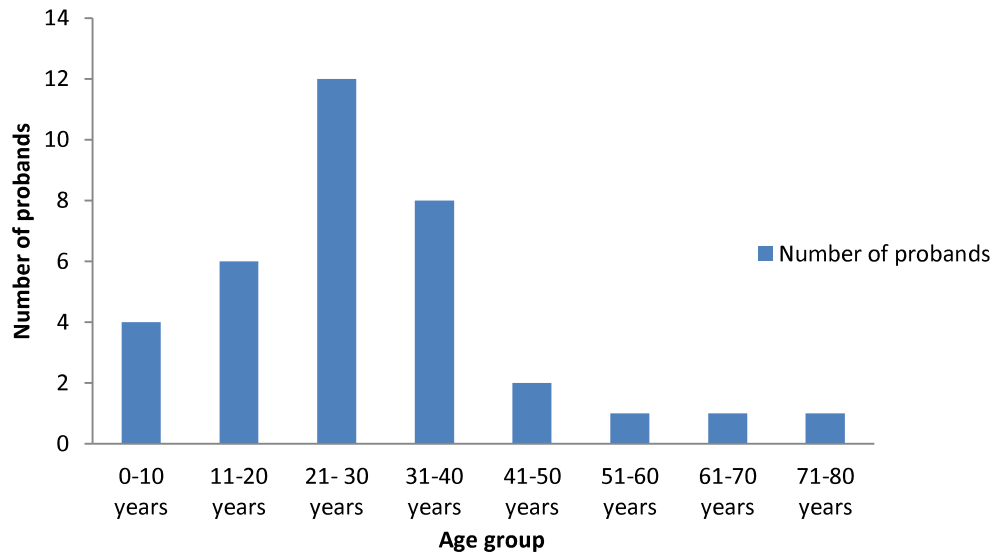


**Figure 3.17:** Vertical graph shows the number of affected individuals in a particular age group among 35 enrolled families.

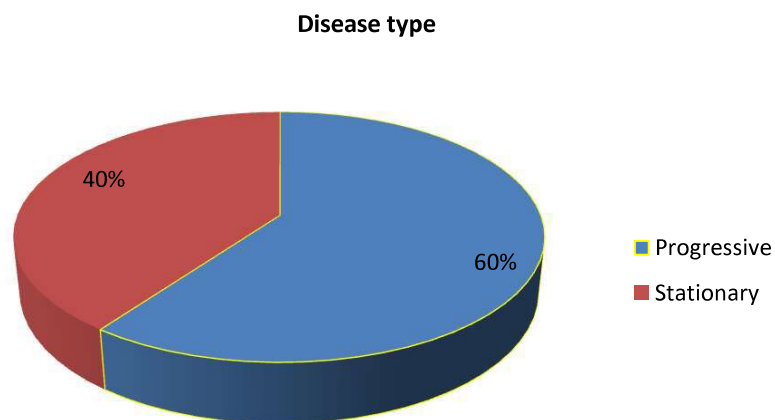


**Figure 3.18:** Pie chart showing the percentage of stationary and progressive cases of night blindness among recruited families.

### 3.7. Molecular analysis of thirty five retinal dystrophy families:

To identify the disease causing variants in 35 enrolled families, Whole exome sequencing was performed for RP 047, RP 073, RP 131, RP 144 and NGS panel sequencing was performed against a panel of 344 known genes for retinal dystrophies for remaining 31 families. Eighteen disease causing variants were identified in eighteen families (Table 3.6). No variant was identified in 17 families in known 344 genes for retinal dystrophies. These families will be processed for whole genome sequencing to identify disease causing variants.

Among eighteen variants 7 variants p.Arg281His, p.Cys187Arg, p.Ile94Thr, p.Ser418Pro, p.Leu183Phe, p.Asp388Gly, p.Ser487Pro were missense, six variants p.Arg283\*, p.Arg477\*, p.Arg292\*, p.Arg63\*, p.Cys520\* p.Leu1858\* were stop-gain, four were frameshift p.Asp576Glu>Ter20, p.Asn3306Lysfs\*7, p.Ala37Profs\*17 and p.Pro158Alafs\*39. The frameshift variant p.Pro158Alafs\*39 in *SPATA7* gene was found in two families RP 112 and RP 113. A splice variant c.413-1G>A was identified in family RP 144. All these variants were homozygous except for compound heterozygous variants c.1252T>C and c.1728del in *CRB1* gene identified in family RP 044.

In silico analysis of all missense variants was performed using provean (deleterious  $\geq$  -3.0), SIFT (tolerated or not tolerated), PolyPhen-2 (probably damaging), and mutation taster (variant listed as disease causing). The Protein ANalysis THrough Evolutionary Relationships (PANTHER) classified amino acids conserved for > 450my as probably damaging. MutPred2 predicted amino acid changes with value > 0.50 as pathogenic and fathmm described variants as damaging with high negative value. For CADD a value >25 and for REVEL a higher score for missense variants was predicted to be damaging for protein structure.

The variants c.842G>A, c.847C>T, c.1429C>T, c.874C>T, c.559T>C, c.281T>C, c.1252T>C, c.413-1G>A, c.187C>T, c.1560C>A, c.547C>T, chr2:73775682-73814328, c.109del, c.1459T>C were reported in previous studies. Remaining 4 variants c.1728del, c.5571\_5576delinsCTAGAT, c.471dup and c.1163A>G were identified for the first time in current study.

**Table 3.6:** List of previously reported and novel pathogenic variants identified in eighteen unrelated inherited retinal dystrophies families segregating with disease phenotype.

Family ID	Proband ID	Disease	NM_ID	cDNA change	Protein change	Gene	Genotype status	Allele Type	Reference (PMID)
RP 004	V.I	RP	NM_021831.6	c.842G>A	p.Arg281His	<i>AGBL5</i>	Homozygous	Known missense	rs1448861312
RP 005	III.XVIII	RP	NM_001030311.3	c.847C>T	p.Arg283*	<i>CERKL</i>	Homozygous	Known stop-gain	rs121909398
RP 008	IV.VI	RP	NM_001004334.4	c.1429C>T	p.Arg477*	<i>GPR179</i>	Homozygous	Known stop-gain	rs764877172
RP 010	IV.I	RP	NM_000541.5	c.874C>T	p.Arg292*	<i>SAG</i>	Homozygous	Known stop-gain	rs397514681
RP 019	IV.VI	RP	NM_000539.3	c.559T>C	p.Cys187Arg	<i>RHO</i>	Heterozygous	Known missense	rs2084785760
RP 043	IV.IV	BBS	NM_001278293.3	c.281T>C	p.Ile94Thr	<i>ARL6</i>	Homozygous	Known missense	rs771054395
RP 044	III.II	RP	NM_001257965.2	c.1252T>C	p.Ser418Pro	<i>CRBI</i>	Heterozygous	Known missense	
				c.1728del	p.Asp576GlufsTer20	<i>CRBI</i>	Heterozygous	Novel missense	
RP 073	IV.X	RP	NM_001297.5	c.413-1G>A	exon 7	<i>CNGB1</i>	Homozygous	Known splice variant	rs189234741
RP 102	IV.I	USH	NM_206933	c.187C>T	p.Arg63*	<i>USH2A</i>	Homozygous	Known stop-gain	rs781223647
RP105	VI.VIII	USH	NM_206933	c.1560C>A	p.Cys520*	<i>USH2A</i>	Homozygous	Known stop-gain	30190494, 276901, 613809
RP106	VIII.I	RP	NM_022787.4	c.547C>T	p.Leu183phe	<i>NMVA1</i>	Homozygous	Known missense	rs1337014971
RP107	IV.IX	RP	NM_001142800	c.5571_5576delinsCTAGAT	p.Leu1858*	<i>EYS</i>	Homozygous	Novel stop-gain	N/A
RP109	VI.X	AS		chr2:73775682-73814328	p.Asn3306Lysfs*7	<i>ALSM</i>	Homozygous	Known deletion	N/A
RP110	VI.V	Aniridia	NM_001310159	c.109del	p.Ala37Profs*17	<i>PAX6</i>	Heterozygous	Known frameshift	11479730/rs1057517780
RP112	V.V	LCA	NM_001040428	c.471dup	p.Pro158Alafs*39	<i>SPATA7</i>	Homozygous	Novel frameshift	N/A
RP113	IV.III	LCA	NM_001040428	c.471dup	p.Pro158Alafs*39	<i>SPATA7</i>	Homozygous	Novel frameshift	N/A
RP 131	IV.III	RP	NM_003501.3	c.1163A>G	p.Asp388Gly	<i>ACO3</i>	Homozygous	Novel missense	N/A
RP 144	IV.VI	RP/LCA	NM_201253.3	c.1459T>C	p.Ser487Pro	<i>CRBI</i>	Homozygous	Known missense	

\* RP: Retinitis Pigmentosa,USH: Usher Syndrome, BBS Bardet Biedl syndrome, LCA: Leber's Congenital Amaurosis, AS: Alstrom Syndrome, N/A: Not Available.

**Table 3.7:** In silico analysis of nineteen, disease causing variants found in nineteen retinal dystrophies families.

Gene	Protein change	Poly Phen-2	Sift	Provean	Mutation taster	PANTHER	Fathmm	MutPred	CADD	REVEL	ClinVar
<i>AGBL5</i>	p.Arg281His	1	1 Not tolerated	Deleterious -4.81	Disease causing	4200	2.75	0.836	34	0.64	Uncertain
<i>CERKL</i>	p.Arg283*	-	-	-	Disease causing	-	-	-	31	-	Pathogenic
<i>GPR179</i>	p.Arg477*	-	-	-	Disease causing	-	-	-	37	-	Pathogenic
<i>SAG</i>	p.Arg292*	-	-	-	Disease causing	-	-	-	38	-	Pathogenic
<i>RHO</i>	p.Cys187Arg	1	1 Not tolerated	Deleterious -6.78	Disease causing	1037	0.02	0.911	24.8	0.914	Likely Pathogenic
<i>ARL6</i>	p.Ile94Thr	0.997	1 Not tolerated	Deleterious -4.04	Disease causing	-	-0.4	0.753	25.9	0.878	Pathogenic
<i>CRBI</i>	p.Ser418Pro	1	1 Not tolerated	Deleterious -4.58	Disease causing	361	-1.43	0.52	19.05	0.851	Likely Pathogenic
<i>CRBI</i>	p.Asp576Glu&Ter20	1	1 Not tolerated	-	Disease causing	842	-	-	-	-	-
<i>CNGB1</i>	Exon 7	-	-	-	Disease causing	-	-	-	-	-	Pathogenic
<i>USH2A</i>	p.Arg63 *	1	-	-	Disease causing	-	-	-	-	-	Pathogenic
<i>USH2A</i>	p.Cys520*	-	-	-	Disease causing	-	-	-	-	-	-
<i>NMNAT1</i>	p.Leu183phe	0.995	1 Tolerated	Deleterious -3.46	Disease causing	176	-4.44	0.57	21.3	0.672	Uncertain
<i>EYS</i>	p.Leu1858*	-	-	-	Disease causing	-	-	-	-	-	-
<i>ALMS1</i>	p.Asn3306Lysfs *7	-	-	-	Disease causing	-	-	-	-	-	-
<i>PAX6</i>	p.Ala37Profs *17	1	0.13 Not tolerated	-	Disease causing	1036	-	-	-	-	Pathogenic
<i>SPATA7</i>	p.Pro158Alafs *39	0.995	-	-	Disease causing	324	-	-	-	-	-
<i>SPATA7</i>	p.Pro158Alafs *39	0.995	-	-	Disease causing	324	-	-	-	-	-
<i>ACOX3</i>	p.Asp388Gly	0.741	0.43 Tolerated	Deleterious -4.83	Disease causing	-	-0.61	0.332	18.95	0.271	-
<i>CRBI</i>	p.Ser487Pro	0.999	1 Not tolerated	Deleterious -4.58	Disease causing	361	-1.43	0.52	19.05	0.851	Likely Pathogenic

### 3.7.1. Family RP 004:

In RP 004 a variant c.842G>A was found in *AGBL5* gene in exon 6 by whole exome analysis of proband V.I (figure 3.19). This known missense variant (rs1448861312) was identified in homozygous condition and changed arginine at position 281 to histidine p.Arg281His (Table 3.6). This homozygous variant was later segregated in 2 affected siblings and mother was found to be heterozygous for the variant (figure 3.20). The in silico analysis of variant by provean predicted it as damaging (-4.81) and not tolerated by SIFT (Table 3.7).

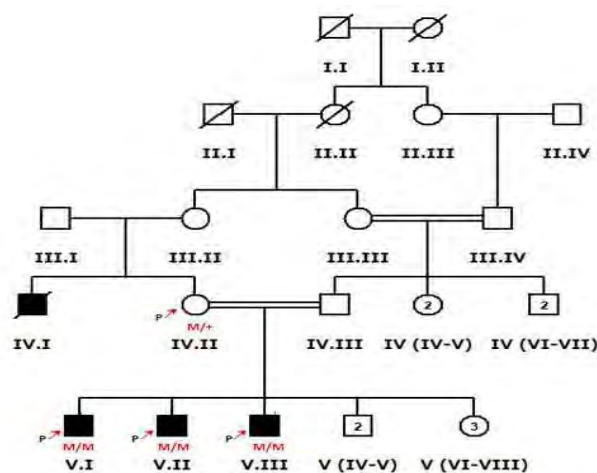


**Figure 3.19:** Pedigree diagram of family RP 004.

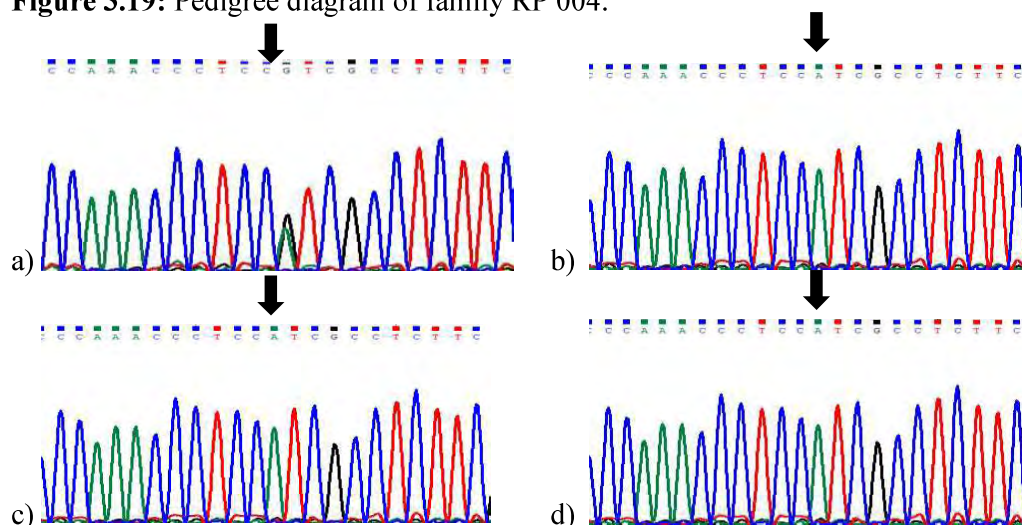
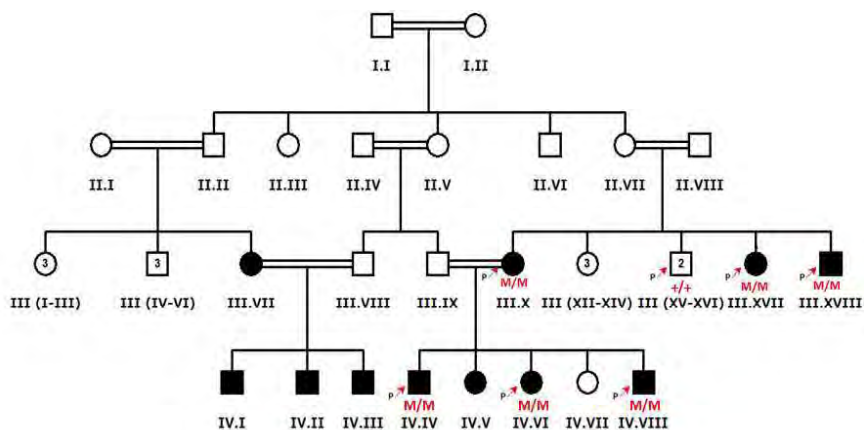


**Figure 3.20:** Chromatogram of family RP 004 (a) Control IV.II (heterozygous for the variant in *AGBL5* gene) (b) Proband V.I (c) affected siblings V.II and V.III.

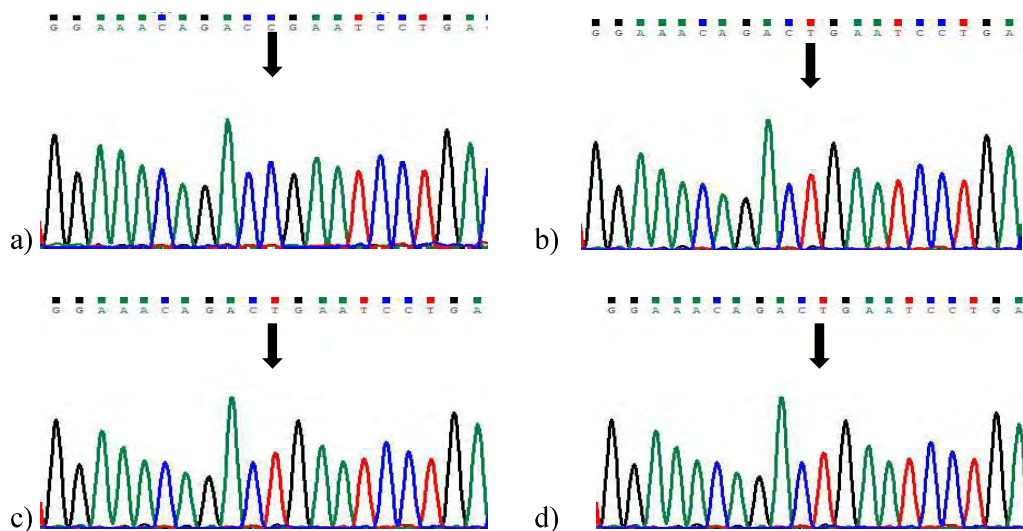
When the change of arginine at position 281 to histidine p.Arg281His was analyzed for its effect on stability of protein structure by iStable, a decrease in stability was predicted with a confidence score of 0.6763. MUpro and I-Mutant also predicted the change will result in less stable structure of AGL5 protein.

### 3.7.2. Family RP 005:

A known stop gain variant c.847C>T was found in family RP 005 by NGS in *CERKL* gene (figure 3.21). This variant changed amino acid p.Arg283\* and led to a truncated protein. This variant is reported as pathogenic in ClinVar (table 3.6). On segregation analysis four affected members of family were found to be homozygous for the variant while one unaffected member was homozygous for the wild type variant (figure 3.22).



**Figure 3.21:** Pedigree diagram of family RP 005.



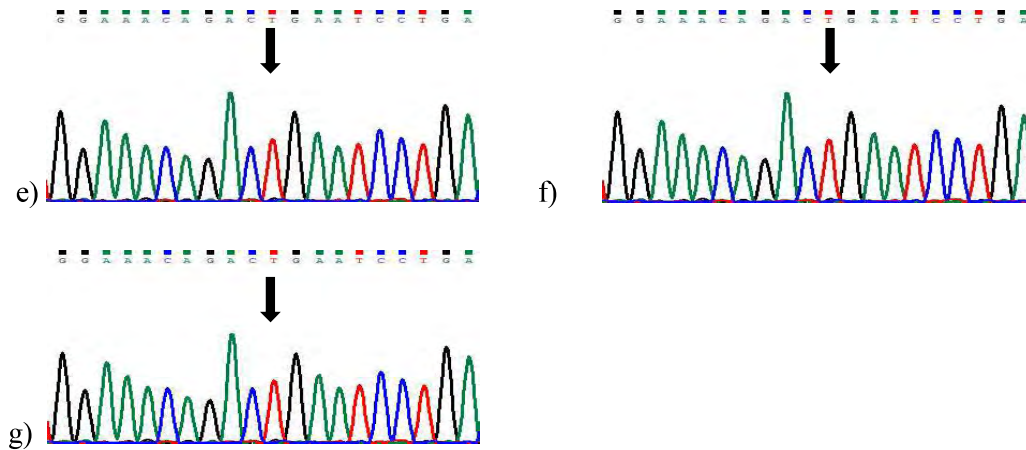


**Figure 3.22:** Chromatograms for variant c.847C>T in family RP 005 in CERKL gene. a) Control III.XV b) Proband III.XVIII c) affected sister III.X d) affected sister III.XVII e-g) affected nephews and niece.

### 3.7.3. Family RP 008:

In RP 008 five members of an extended highly consanguineous family were affected from Bilateral RP (figure 3.23). Exome analysis revealed a stop gain variant c.1429C>T (p.Arg477\*) segregating in family in *GPR179* gene in homozygous condition causing early truncation of protein (Figure 3.24) (Table 3.6). This variant was reported to be pathogenic on ClinVar (Table 3.7).

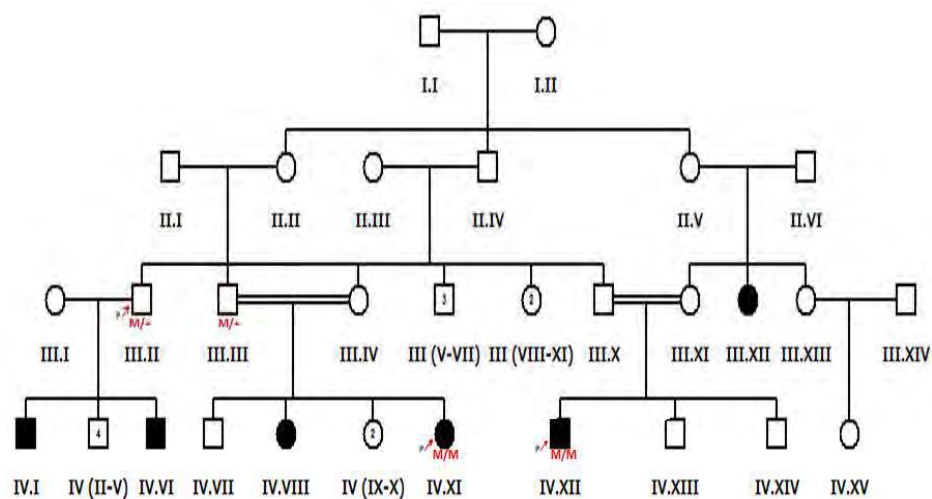


**Figure 3.23:** Pedigree diagram of family RP 008.

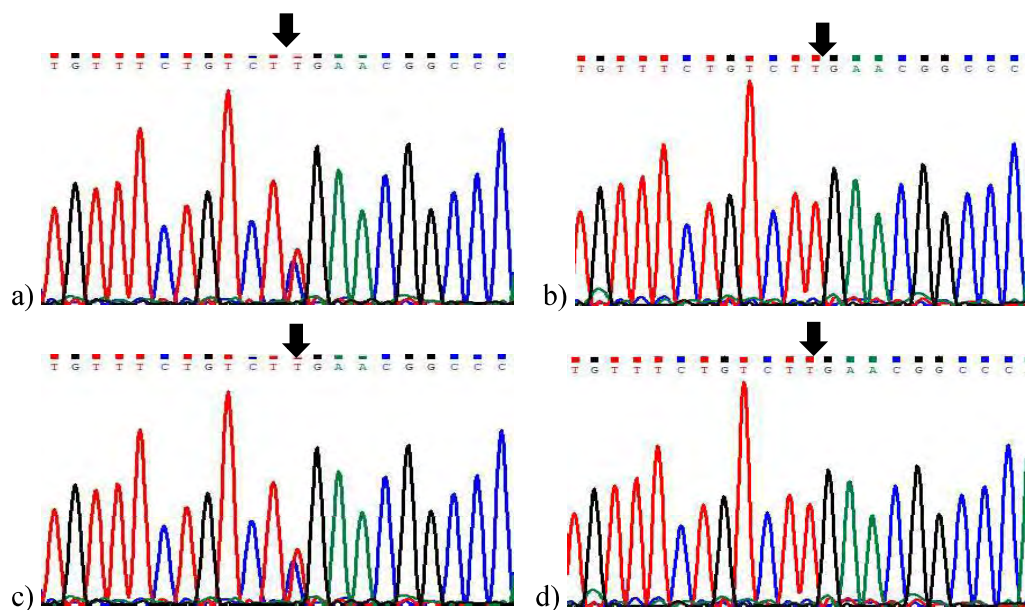


**Figure 3.24:** Chromatograms showing variant c.1429C>T in GPR179 gene in family RP 008. a) Heterozygous in III.II b) Homozygous in IV.XI c) Heterozygous in III.III d) Homozygous in IV.XII.

#### 3.7.4. Family RP 010:

In this family another stop gain variant c.874C>T (p.Arg292\*) was identified in *SAG* gene (Table 3.6) (figure 3.25, 3.26). The proband had stationary night blindness. His two siblings and two maternal aunts were also affected by the same disease.

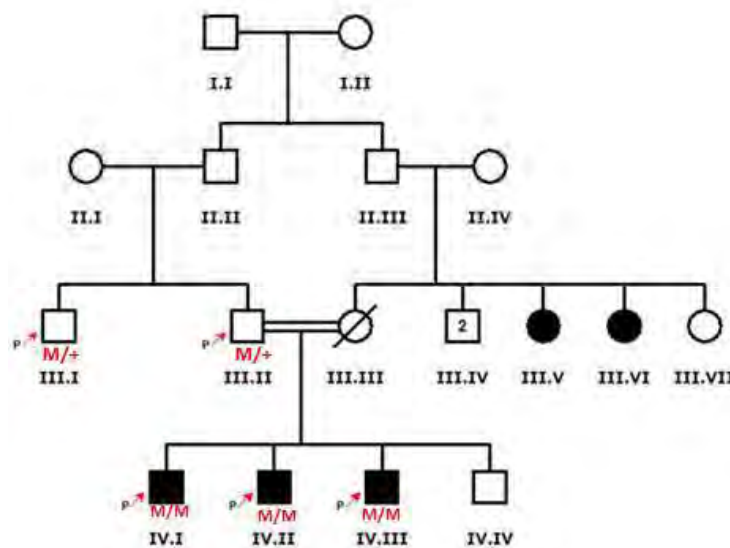


**Figure 3.25:** Pedigree diagram of Family RP 010.



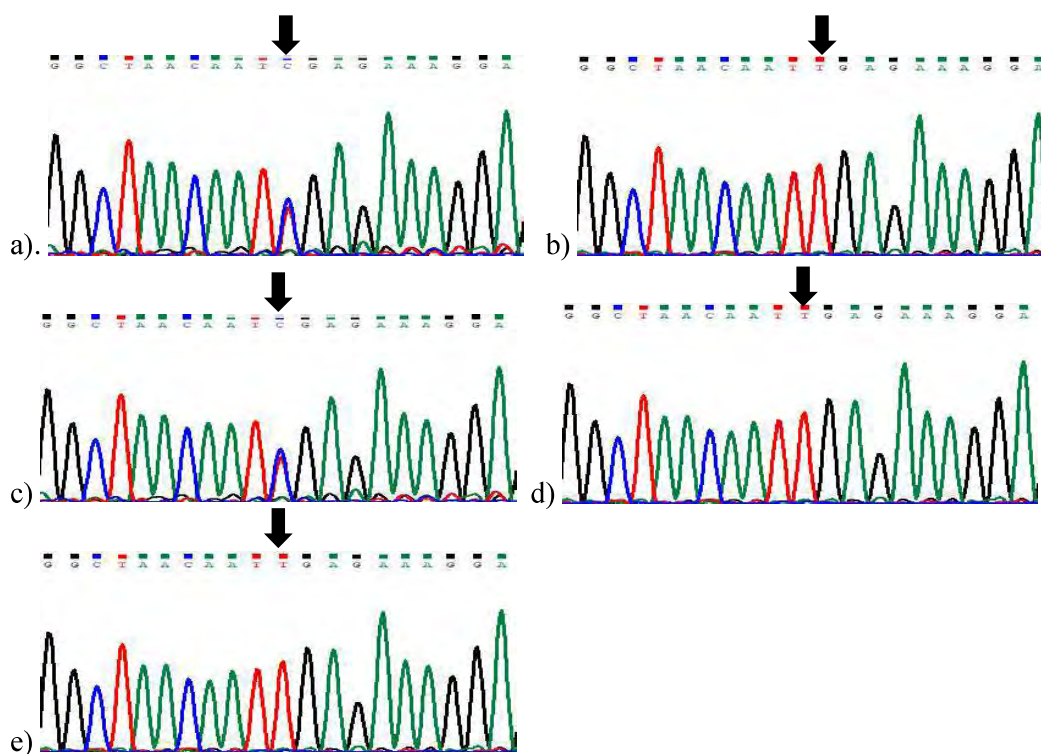


**Figure 3.26:** Chromatograms of c.874C>T variant in SAG gene in family RP 010. (a, c) Heterozygous variant in unaffected individuals (b, d, e) Homozygous variant in affected individuals.

### 3.7.5. Family RP 019:

In RP 019 a heterozygous variant c.559T>C was identified in *RHO* gene (table 3.6). Patient was a 27 years old boy suffering from stationary night blindness and photo-

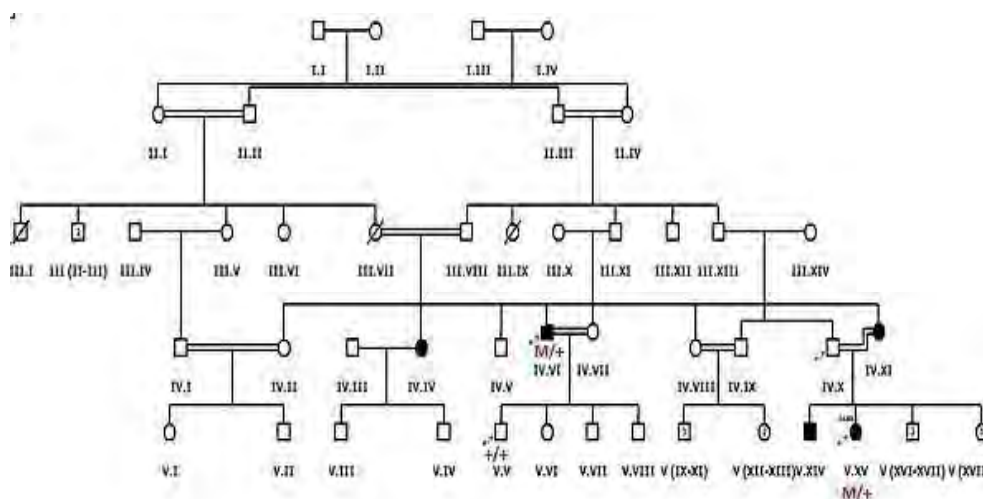


**Figure 3.27:** Pedigree diagram of RP 019.

phobia since birth. The variant changed amino acid at position 187 to arginine p.Cys187Arg that was predicted as damaging by provean (-6.78) and not tolerated by SIFT (figure 3.27). PolyPhen-2 and mutation taster listed the variant as disease causing. In silico tool MutPred gave it a score of 0.911, CADD 24.8 and REVEL 0.91 that highlights the high pathogenicity of this variant (table 3.7). ClinVar defined the variant as likely pathogenic. I-Mutant predicted a decrease in stability due to missense variant while iStable (confidence score 0.666) and MUpro (confidence score 0.487) predicted increased stability. A second pathogenic variant could not be identified in RHO gene that could mean a dominant variant is causing disease in this family regardless of consanguinity. The dominant variant might be do novo or it could be present in deceased mother of affected siblings as the RHO gene is commonly reported for dominant pattern of disease.

### 3.7.6. Family RP 043:

In family RP 043 a 26 years old boy was suffering from Bardet Biedl syndrome. The clinical symptoms in patient included progressive RP and polydactyly (figure 3.28). Whole exome analysis identified a homozygous missense variant c.281T>C in *ARL6* gene (table 3.6). This previously reported variant rs771054395 changes amino acid isoleucine at position 94 to threonine (figure 3.29). This change in amino acid was predicted as disease causing by mutation taster and Polyphen-2 (score 1). SIFT described this change as not tolerated and provean gave it a score of -4.04. High pathogenicity score was also predicted by REVEL 0.8 and CADD 25.9 (table 3.7).

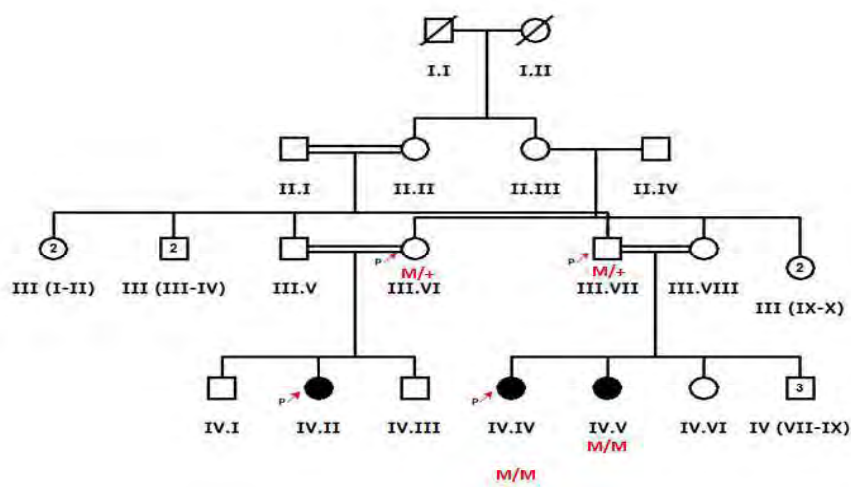


**Figure 3.28:** Pedigree diagram of family RP 043.

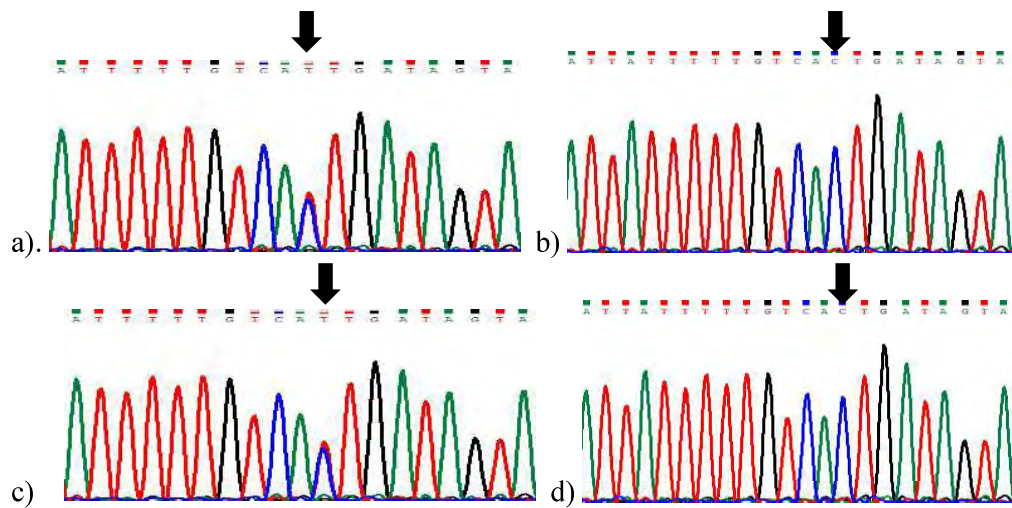
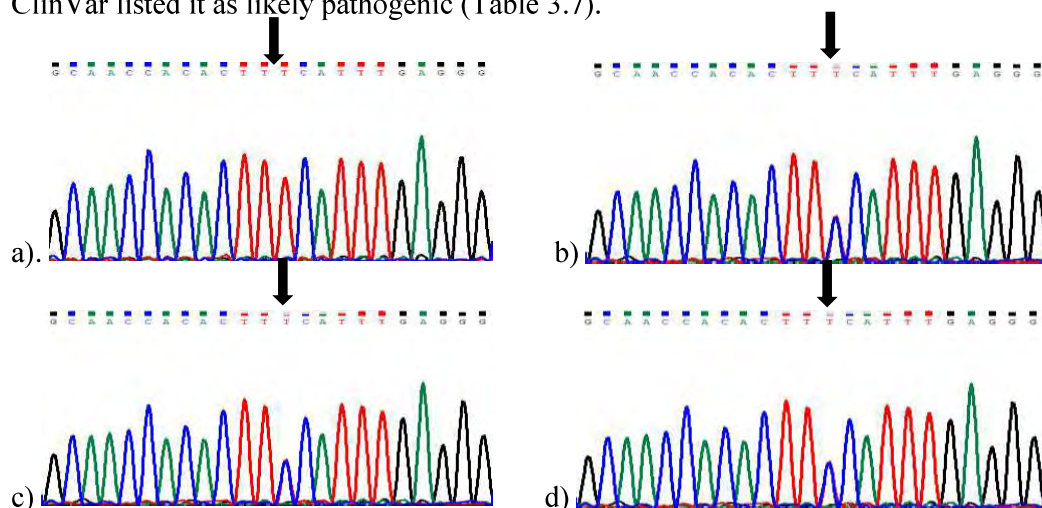


**Figure 3.29:** Chromatograms of heterozygous normal individuals and two affected individuals for family RP 043 in ARL6 gene.

The protein change p.Ile94Thr was predicted to decrease the stability of protein structure by I-Mutant, MUpro (score -1) and iStable (0.778).

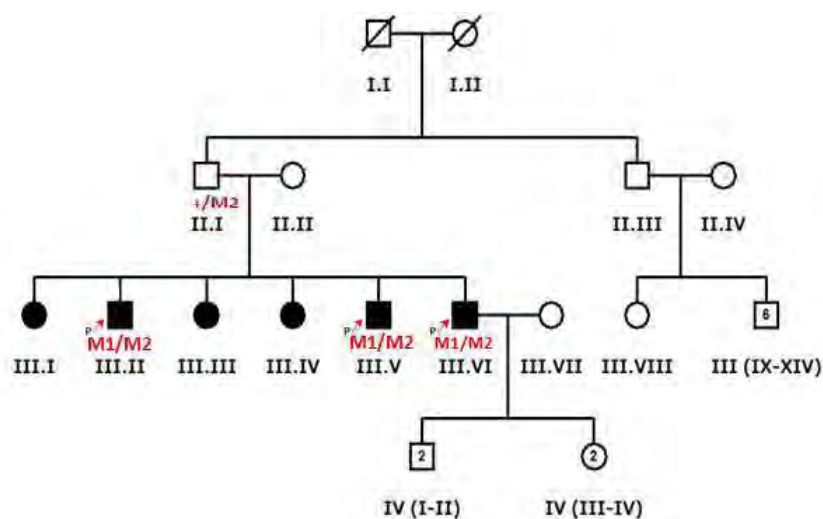
### 3.7.7. Family RP 044:

In this family individual III.II was screened for disease causing variant by NGS. The exome sequencing data revealed two heterozygous variants c.1252T>C (p.Ser418Pro) and c.1728del (p.Asp576GlufsTer20) in *CRBI* gene (figure 3.30) (table 3.6). The 32 years old proband had 5 affected siblings born to a consanguineous marriage (3.31). In silico analysis of missense variant by provean predicted it as damaging with score of -4.58. Analysis of variant c.1252T>C by PolyPhen-2 and Mutation taster predicted it to be disease causing. REVEL gave it a high pathogenicity score of -0.851 and ClinVar listed it as likely pathogenic (Table 3.7).

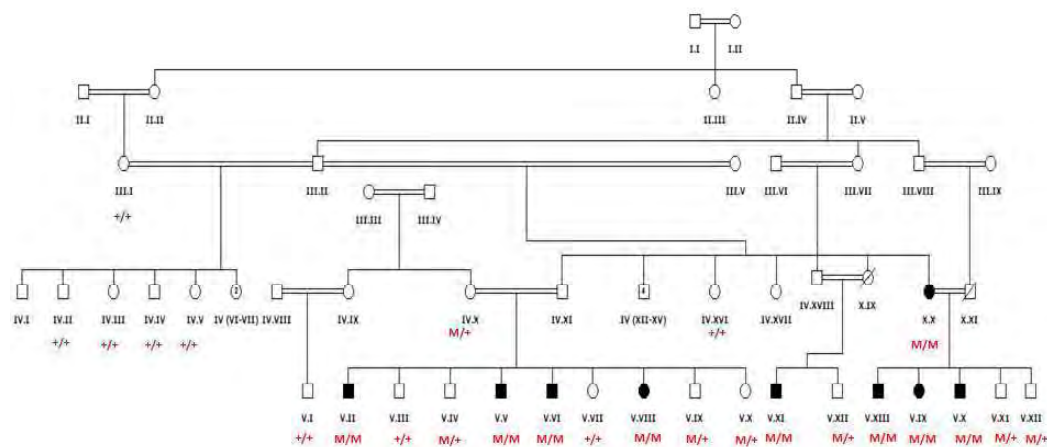


**Figure 3.30:** Chromatograms for variant c.1252T>C in *CRB1* gene in family RP 044.

a) II.I b) III.II c) III.V d) III.VI

**Figure 3.31:** Pedigree diagram of Family RP 044.**3.7.8. Family RP 073:**

Family RP 073 was a large consanguineous family with 10 affected individuals. All the affected members had night blindness since birth while three individuals (IV.III, IV.IV, and IV.V) had profound hearing loss and speaking disability (figure 3.33).

**Figure 3.32:** Pedigree diagram of RP 073.

During exome analysis a reported splice variant c.413-1G>A in *CNGB1* gene was identified in RP affected individuals. This variant segregated in all affected

individuals except for IV.II (Figure 3.34). This patient was negative for all the variants found in 344 RP related genes in panel and will be sent for whole genome sequencing. While data analysis a novel variant c.388C>T (p.Arg130Cys) in *SIPR2* gene was identified that segregated in all individuals with profound hearing loss and speaking disability (figure 3.35) (Table 3.8).

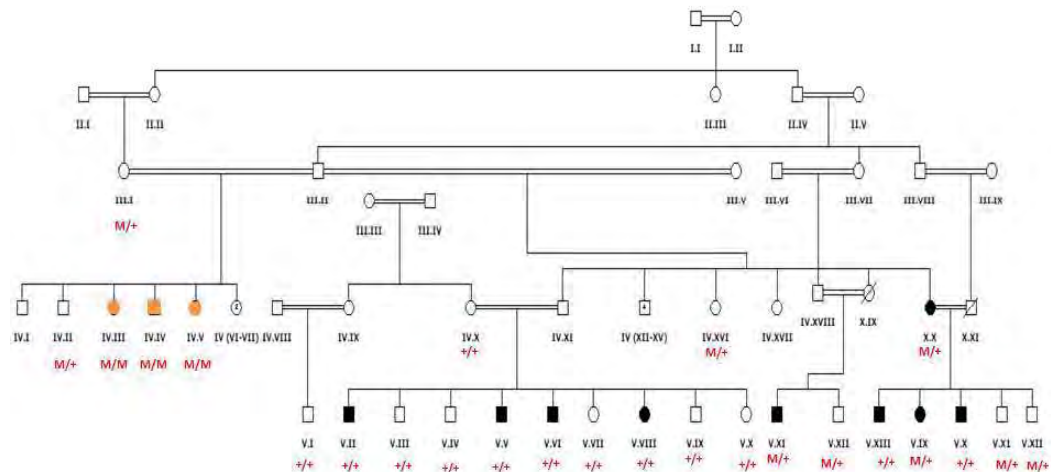


**Figure 3.33:** Pedigree diagram showing segregation of novel *SIPR2* gene variant c.388C>T. Individuals (symbols) colored in orange are suffering from profound deafness while black colored symbols depict RP affected individuals.

This gene is well associated with autosomal recessive hearing and speaking disorders. Segregation of variant c.388C>T was checked in all extended phenotypically normal family members and was found negative (Figure 3.33). MUpro (score -1), iStable (score 0.717) and I-Mutant (DDG -0.48) predicted the variant as cause of decreased stability.

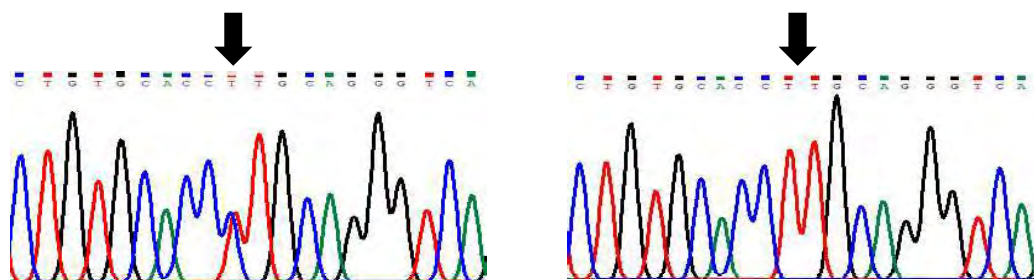


**Figure 3.34:** Chromatogram for individual V.XII on the left and IV.XX on the right showing variant nucleotide in *CNGBI* gene in family RP 073.

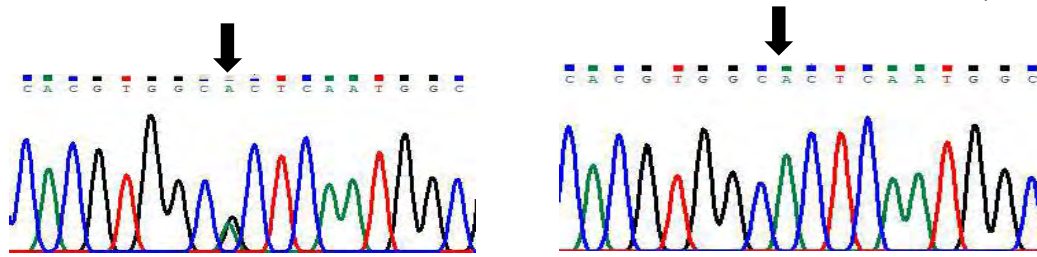


**Figure 3.35:** Chromatogram for individual III.I on the left and IV.III on the right showing variant c.388C>T in *SIPR2* gene in RP 073.

The homozygous splice variant c.413-1G>A in *CNGB1* gene is reported as pathogenic by ClinVar. The missense variant in *SIPR2* gene is found for the first time in homozygous state in Pakistan.

**Table 3.8:** Novel missense variant identified in *SIPR2* gene in RP 073

Family ID	Proband ID	Disease	cDNA change	Protein change	Gene	Genotype status	Allele Type	Reference (PMID)
RP 073	IV.III	Profound deafness	c.388C>T	p.Arg130Cys	<i>SIPR2</i>	Homozygous	Novel missense	N/A

### 3.7.9. Family RP 102:

A homozygous nonsense mutations in the *USH2A* gene c.187C>T: p.Arg63\* was found in RP102 (figure 3.36, 3.37). Consistent with the molecular diagnosis, patients from the family exhibit RP and hearing loss.

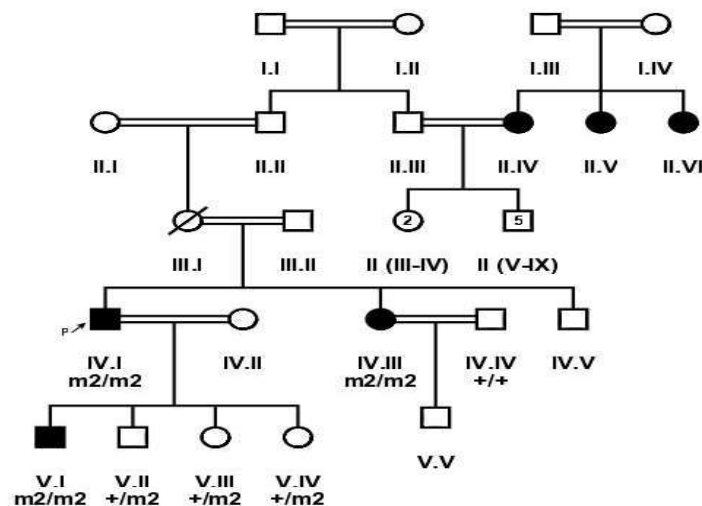


**Figure 3.36:** Pedigree diagram of RP 102. (m2: c.187C>T)

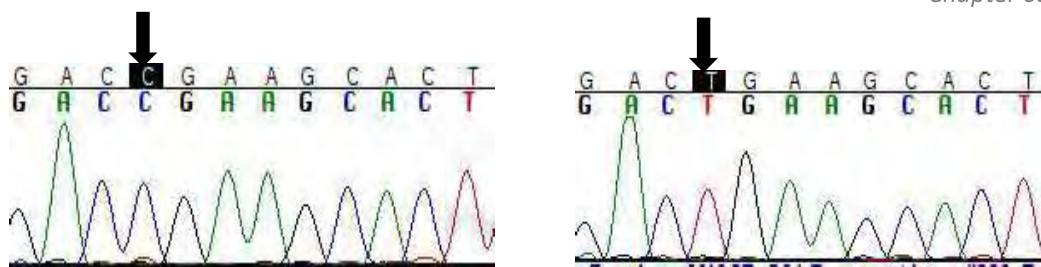


**Figure 3.37:** Chromatograms for variant c.187C>T in RP 102 in *USH2A* gene.

The p.Arg63\* variant in RP102 is a reported pathogenic mutation with a low population frequency of 0.001% in gnomAD. Segregation testing was carried out for the three affected and five unaffected family members and perfect segregation between the mutations with the disease phenotype was observed. One RP-affected (V.I) and two unaffected (V.III and a paternal aunt of IV.I) family members had mental retardation phenotype, which needs further investigation to find its causes.

### 3.7.10. Family RP 105:

The stop-gain mutation (c.1560C>A) p.Cys520\* identified in family RP105 in *USH2A* suffering from Usher syndrome is also previously reported and likely to be pathogenic as it is predicted to result in a truncated protein that is approximately 10% of the normal size (figure 3.38, 3.40). As a premature truncation, the mRNA is likely to undergo nonsense-mediated decay. Segregation testing for the RP105 family was carried out in three affected and three phenotypically normal family members, and the mutation co-segregated with all patients (figure 3.39).



**Figure 3.38:** Chromatogram for variant c.1560C>A in gene *USH2A* in family RP 105. (unaffected (left) IV.I and affected (right) individual V.IV)

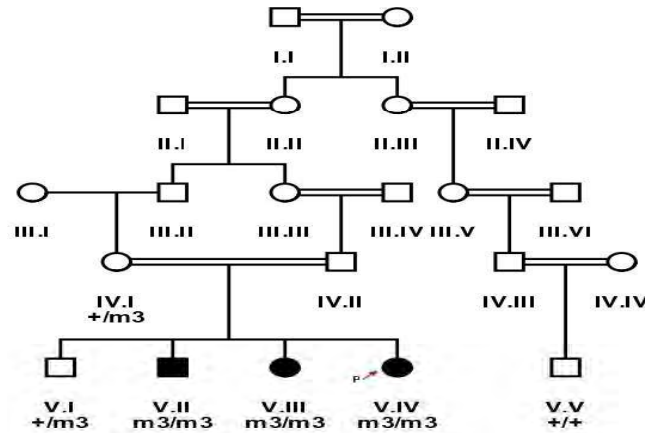


**Figure 3.39:** Pedigree drawing of family RP 105 (m3: c.1560C>A).

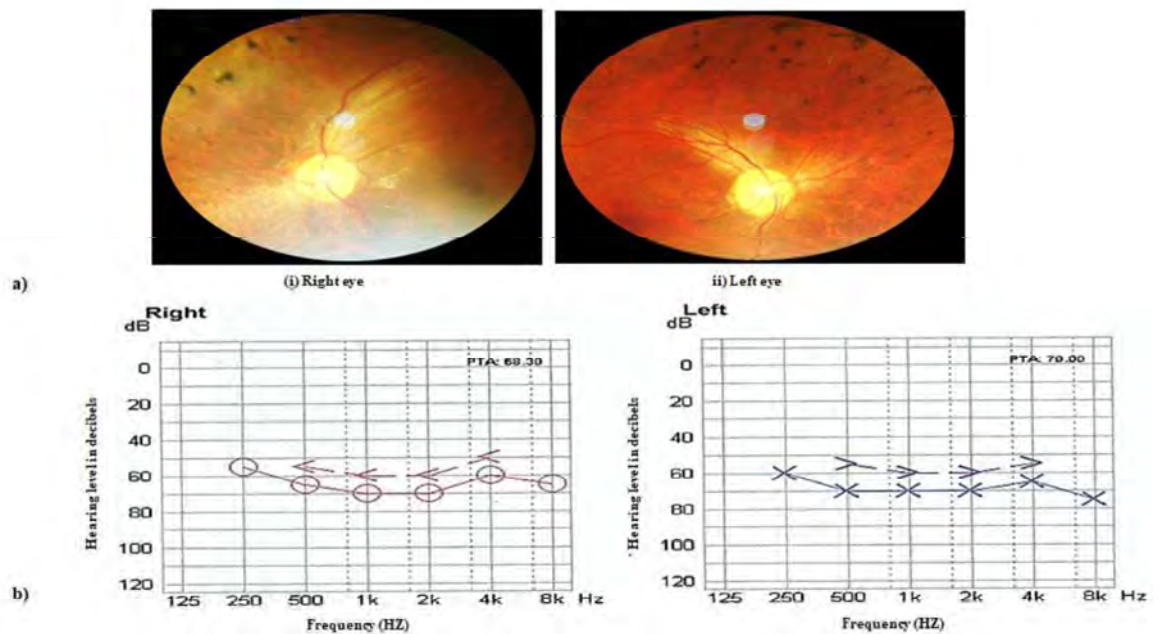


**Figure 3.40:** a) Fundus photograph of left and right eye of an affected individual (VI.VI of RP105) showing pale optic disc, bony spicules and thin blood vessels characteristic of RP phenotype. b) Audiometry report of an affected individual (VI.VI of RP105) performed at 14 years. The x-axis on graphs shows the frequency in hertz and the y-axis shows hearing level in decibels (dB). Note the hearing loss in the range of 50-80 dB in both ears of the Usher patient.

### 3.7.11. Family RP 106:

The affected individual of family RP106 carried a known homozygous missense variant, i.e., c.547C>T; p.Leu183Phe in the *NMNAT1* gene (Figure 3.41). This



variant is likely to be pathogenic as (1) it is rare in population and is only observed once in the gnomAD database with an estimated frequency of 0.0004%; (2) the variant is conserved from chicken to human; (3) multiple in silico prediction programs suggested it is deleterious with a CADD score of 22.

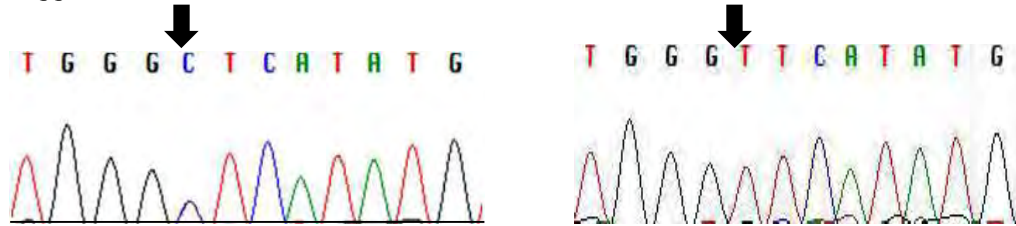


**Figure 3.41:** Chromatogram of unaffected (left) and affected individual (right) for variant in NMNAT1 gene in family RP 106.

Consistently, segregation testing in four affected and five unaffected members of the family showed that this variant co-segregates with the disease phenotype (Figure 3.42).

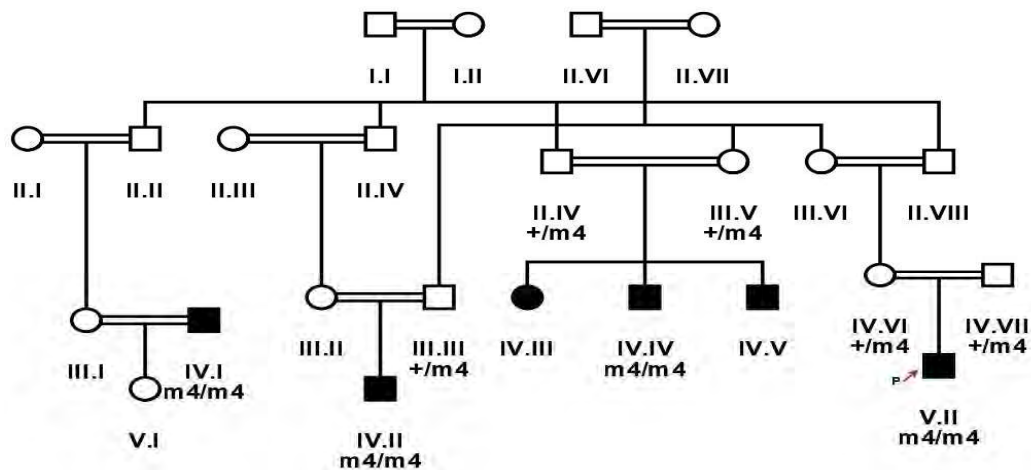


**Figure 3.42:** Pedigree diagram of RP 106 (m4: c.547C>T)

### 3.7.12. Family RP 107:

A novel homozygous variant in exon 6 in the EYS gene, i.e., c.5571\_5576delinsCTAGAT: p.Leu1858\*, that leads to a premature stop codon was identified in RP107 (Figure 3.43). This variant is likely to be pathogenic as the early termination removes approximately 40% of the protein, including all the laminin G-like domains. Alternatively, due to the premature stop codon, the mRNA may undergo nonsense-mediated decay.

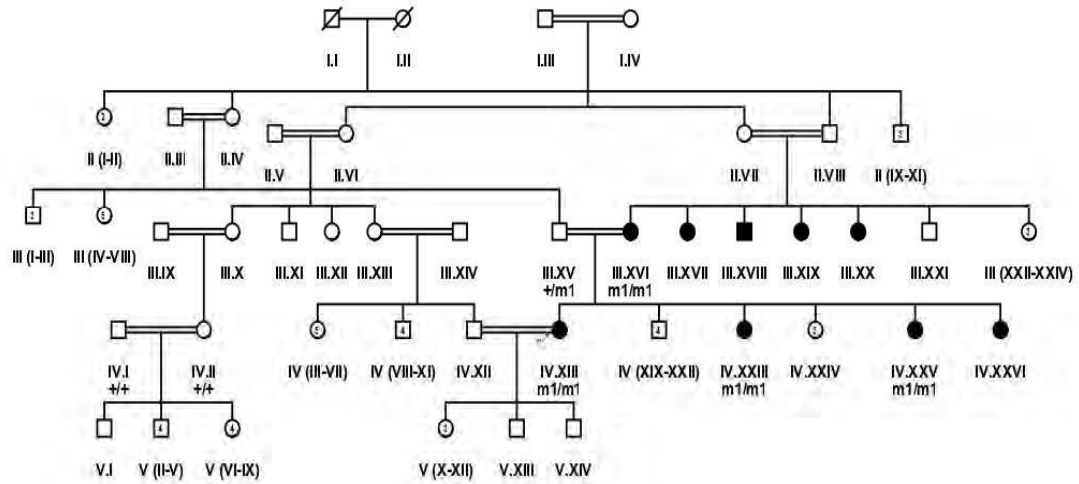


**Figure 3.43:** Pedigree diagram of RP 107 family (m1: c.5571\_5576delinsCTAGAT)

This variant is rare in population, and it has not been observed in the gnomAD database. Segregation of the mutation with the disease is observed for this family by genotyping four affected and three unaffected family members, further supporting the pathogenicity of this variant (Figure 3.44).

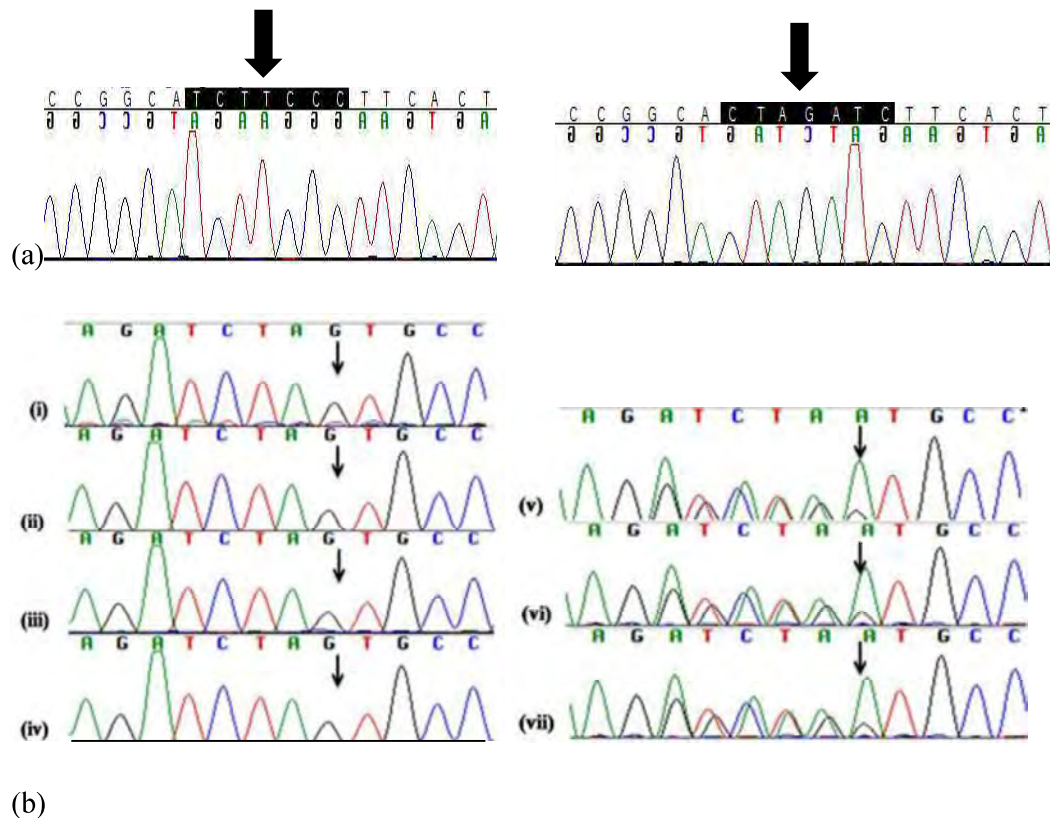


**Figure 3.44:** (a) Chromatogram of unaffected (left) and affected (right) family member (b) Segregation testing for novel homozygous deletion variant c.5571\_5576delinsCTAGAT: p.Leu1858\* found in EYS gene in RP107 in four affected (i, ii, iii, iv) and three unaffected (v, vi, vii) family members.

### 3.7.13. Family RP 109:

One homozygous previously reported large deletion, i.e., c.9911\_11550del, resulting in loss of four exons (exons 13–16) causing p.Asn3306Lys\*7 was identified in the ALMS1 gene in family RP109 (Figure 3.45). This deletion was validated by performing PCR testing using a pair of primers adopted from Nikopoulos et al., 2015 and four primer pairs, one for each of exon 13–16 (table 3.9).

These PCRs confirmed the exact break points of the deleted sequence (chr2: 73,772,326–73,813,432) as well as failure to obtain the band of the targeted region with patients' DNA as a template confirmed segregation of mutation (figure 3.46). This variant has not been observed in the gnomAD database and is pathogenic according to ACMG classification.

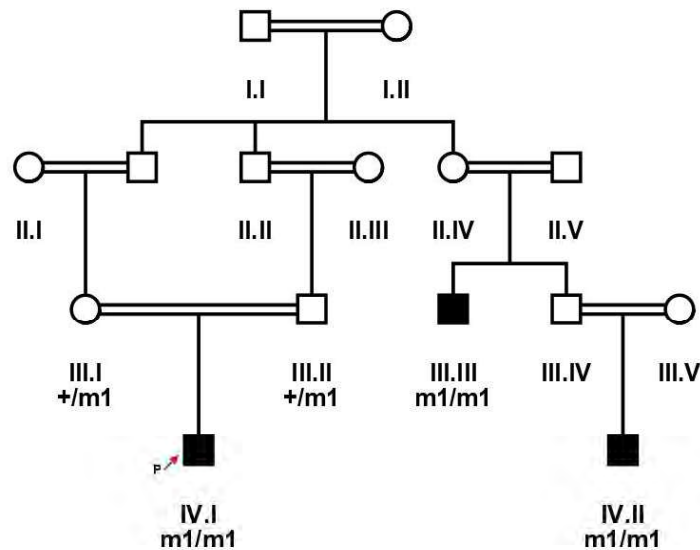


**Figure 3.45:** Pedigree diagram of RP 109 (m1: c.9911\_11550del)

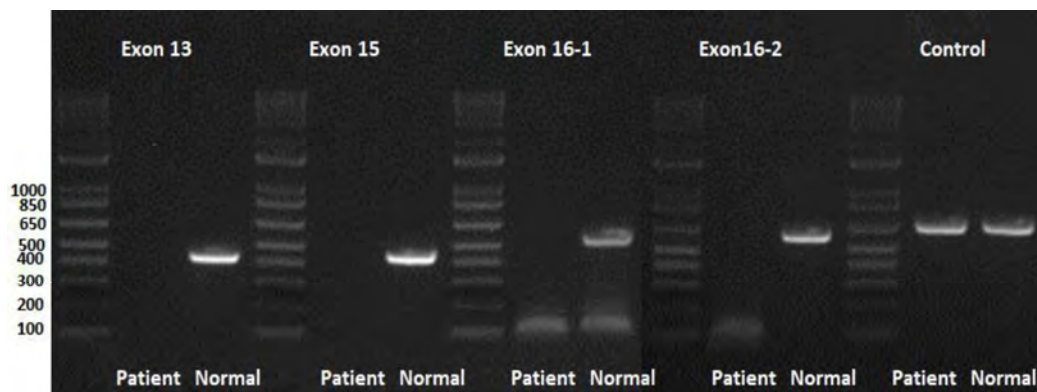


**Figure 3.46:** Gel picture showing confirmation of deletion in unaffected and affected members.

**Table 3.9:** A list of primers used to amplify ALMS1 gene exonic region (13-16) deletion of chr2:73775682-73814328 in RP109

Exon No	Primer	Sequence
<b>Exon 13</b>	Forward	CTCGTGTA AAAACGACGGCCAGTCATAGAATTGGTCTAAGAGGCAAA
	Reverse	CTGCTCAGGAAACAGCTATGACATGCTCAATATAACAGCAAGGAGA
<b>Exon 15</b>	Forward	CTCGTGTA AAAACGACGGCCAGTCCGCTACCTCTTTTTCTGACTG
	Reverse	CTGCTCAGGAAACAGCTATGACACCCAATCCCATTACCTCAA
<b>Exon 16-1</b>	Forward	CTCGTGTA AAAACGACGGCCAGTCTACCCGTTCTGTCTTCAGGTC
	Reverse	CTGCTCAGGAAACAGCTATGACTGAGACCTGGAGAGAATGTGTG
<b>Exon 16-2</b>	Forward	CTCGTGTA AAAACGACGGCCAGTACAAAGGGATCAGAAGGTCACC
	Reverse	CTGCTCAGGAAACAGCTATGACATTCGACAGTAGAAGTGGTGCC

### 3.7.14. Family RP 110:

The affected patient in RP110 carried a known heterozygous frameshift mutation, i.e., c.109del; p.Ala37Profs\*17 in PAX6 gene (Figure 3.47).

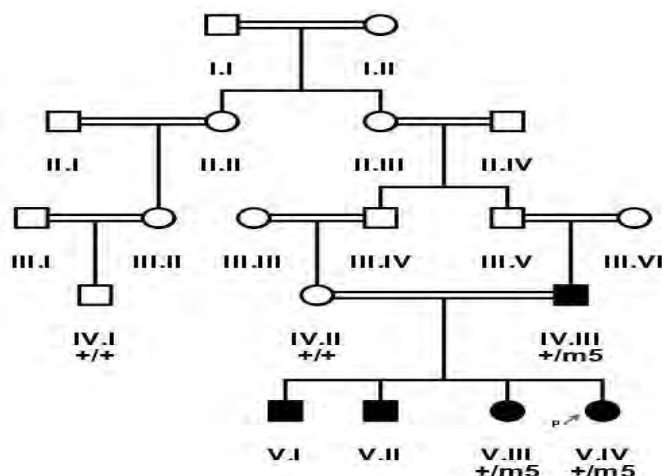


**Figure 3.47:** Pedigree diagram of RP 110.

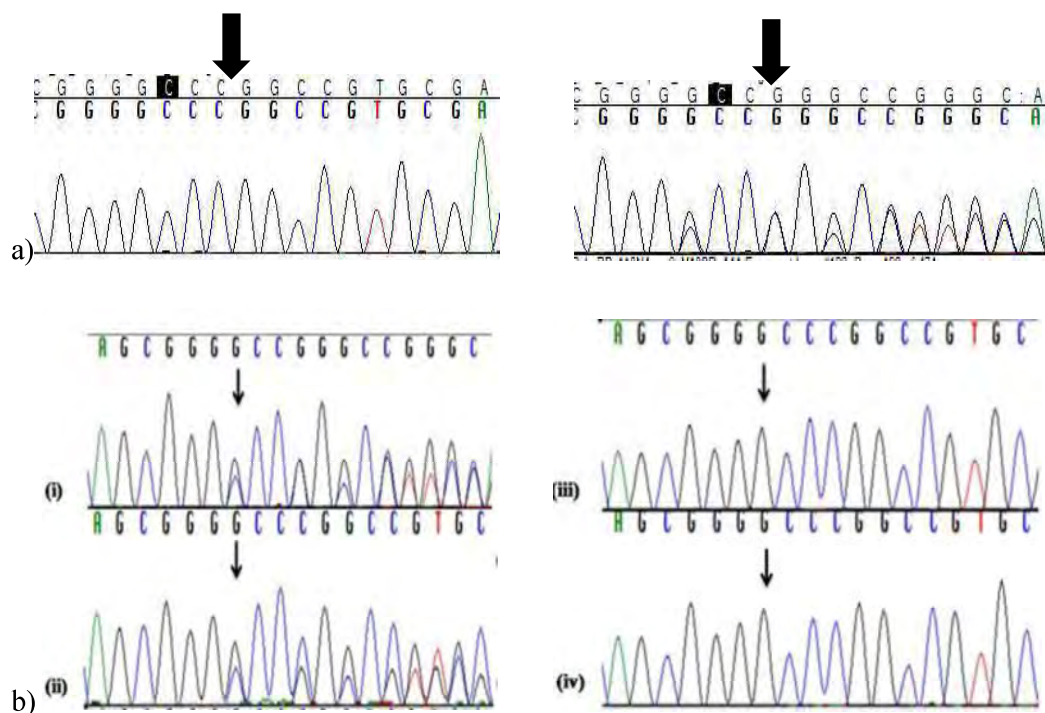


**Figure 3.48:** (A) Chromatogram of unaffected and affected individual. (b) Segregation testing for heterozygous variant c.109del; p.Ala37fs\*31 found in RP110 in PAX6 gene in two affected (i, ii) and two unaffected (iii, iv) family members.

This mutation is absent from the gnomAD database. Segregation testing for the family was carried out for two affected and two unaffected family members, confirming the segregation of the mutant allele with the disease phenotype (figure 3.48). This variant was listed as pathogenic on ClinVar. The family was recruited due to presence of 4 affected siblings and high consanguinity in family but molecular analysis revealed a dominant pattern of disease.

### 3.7.15. Family RP 112 and 113:

The same homozygous insertion that leads to a novel frameshift mutation, i.e., c.471dup causing p.Pro158Alafs\*39 in exon 5 of the SPATA7 gene, was found in two families, i.e., RP112 and RP113 (Figure 3.49, 3.50). This frameshift mutation has not been observed in the gnomAD database. A segregation test was carried out in families RP112 and RP113 for four affected and their parents (figure 3.51).

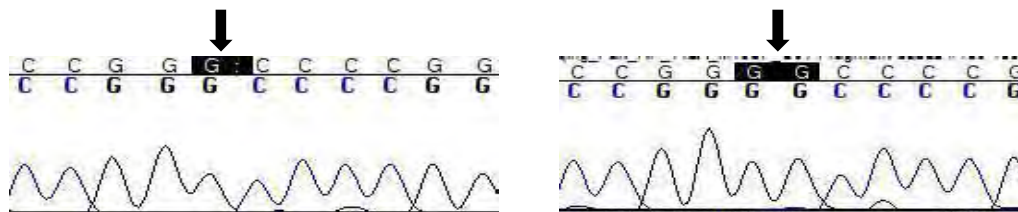
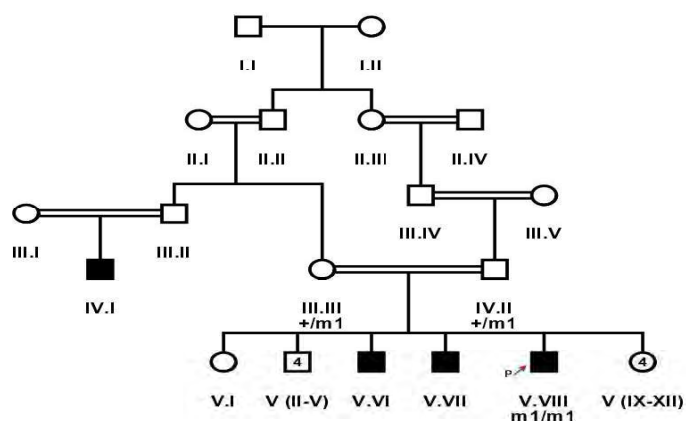


**Figure 3.49:** Chromatogram of unaffected and affected individual for variant c.471dup identified in family RP 112 and RP 113 in SPATA7 gene.



(A)

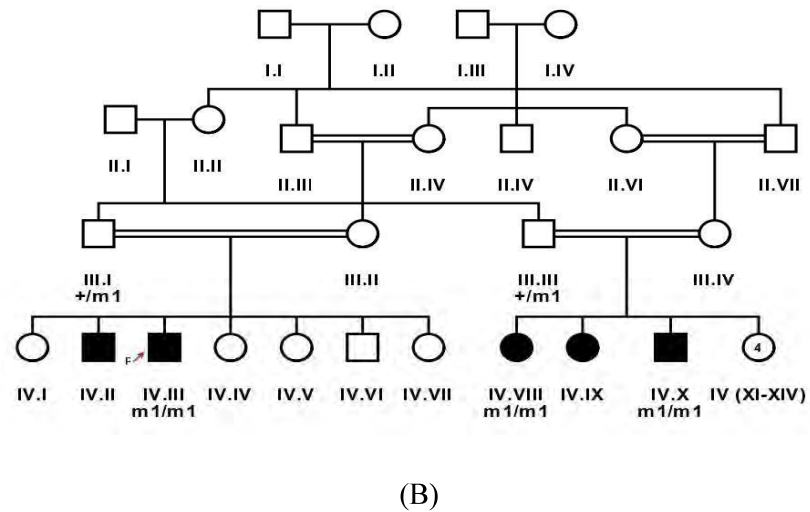


**Figure 3.50:** Pedigree diagram (A) RP 112 (B) RP 113 (m1: c.471dup)

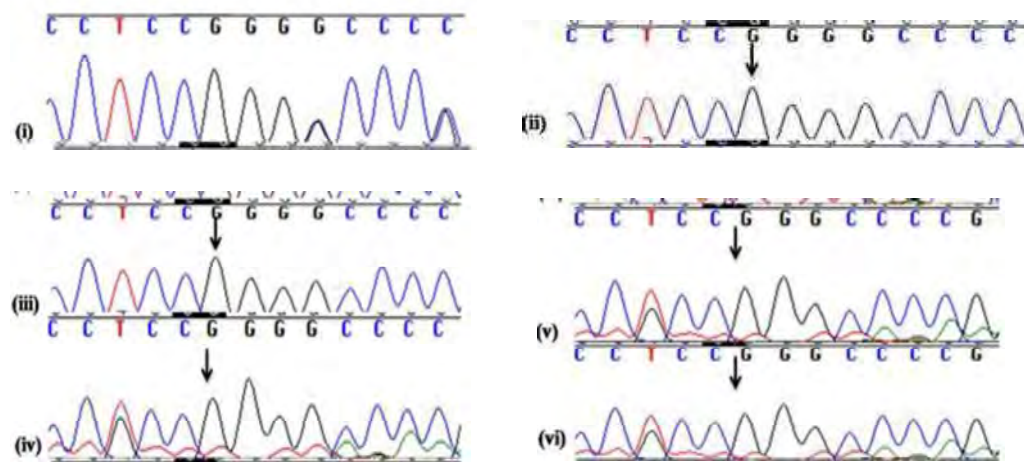


**Figure 3.51:** Segregation testing results for homozygous duplication c.471dupG: p.Pro158Alafs\*39 checked in RP113 in four affected (i, ii, iii, iv) and two unaffected (v, vi) family members.

All affected members are homozygous for the mutation, while unaffected parents are carriers of the mutant allele. The affected individuals of both families had severe phenotypes as all affected were suffering from LCA by birth. The age of affected individuals ranged from 5 to 50 years at the time of enrollment for this study. The youngest affected individual (IV.VIII) of RP113 was five years old at the time of enrollment for this study and had bilateral blindness with nystagmus.

### 3.7.16. Family RP 131:

On Exome analysis a missense variant c.1163A>G (p.Asp388Gly) was identified in proband IV.III (Figure 3.52) in *ACOX3* gene. At the time of recruitment for study patient was 34 years old and suffering from progressive bilateral night blindness and polydactyly (figure 3.53).

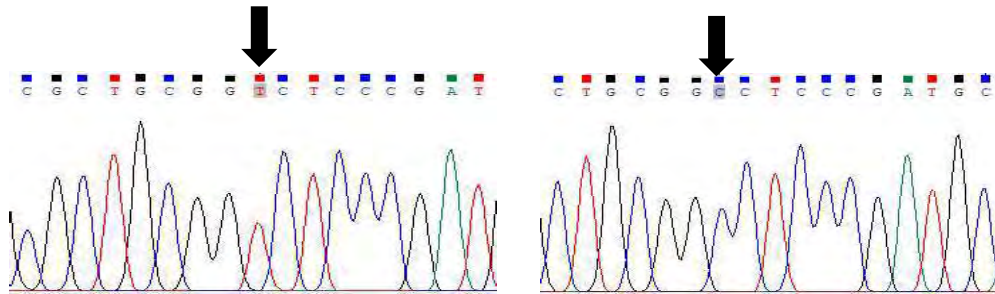


**Figure 3.52:** Chromatogram of unaffected and affected member of family RP 131 in *ACOX3* gene.

He had two affected siblings and consanguineous parents. Provean gave it score of -4.58 and Mutation taster listed it as disease causing. The REVEL value for this novel variant was not very high (0.271) and CADD score was 18.95. For confirmation this variant was segregated in unaffected parents, siblings and two affected siblings by direct Sanger sequencing (Figure 3.54).

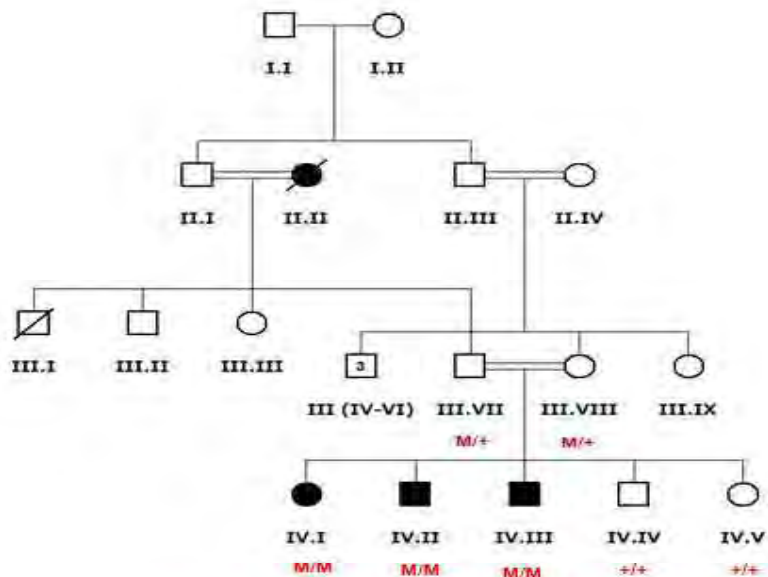


**Figure 3.53:** Pedigree diagram of RP 131.



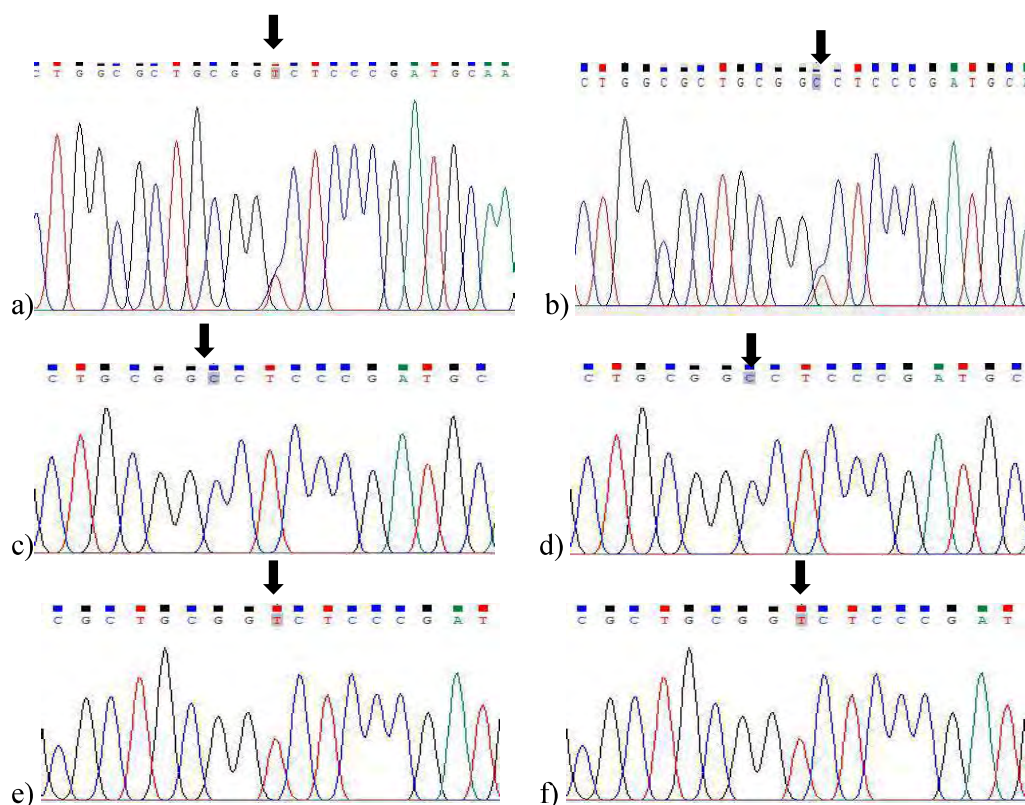


**Figure 3.54:** Segregation analysis of variant c.1459T>C in RP 131. (a,b,e,f) Unaffected (c,d) Affected.

When the change of amino acid p.Arg130Cys was analyzed in ACOX3 gene by iStable, it was predicted to cause decreased stability of protein structure (score 0.656). The DDG value was predicted as -1.59 that shows decrease in stability of protein structure due to amino acid change.

### 3.7.17. Family RP 144:

In family RP 144 eight individuals were affected from night blindness. Two individuals IV.VI and IV.VII also had hearing loss and speaking disability as well as slight mental disability (Figure 3.56). Whole exome analysis identified a reported homozygous missense variant c.1459T>C (p.Ser487Pro) with a high REVEL score 0.851 (Figure 3.55). This variant was also listed as likely pathogenic in ClinVar. SIFT predicted the variant as not tolerated and Provean gave it a score of -4.58. Segregation analysis confirmed the autosomal recessive pattern of inheritance of this variant in CRB1 gene.

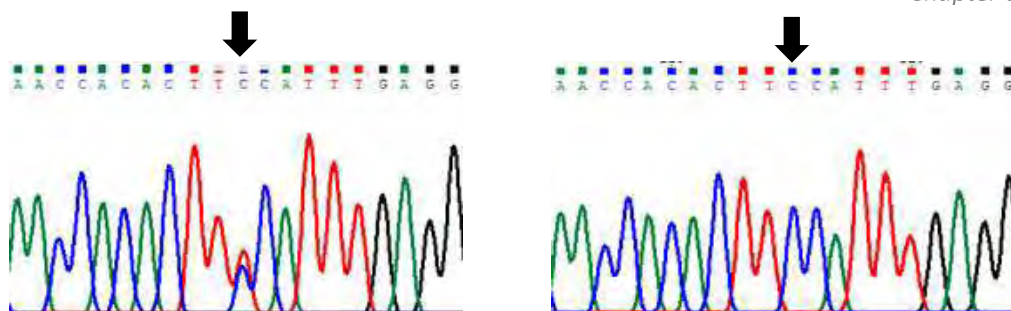


**Figure 3.55:** Chromatogram of affected IV.VI (right) and unaffected (left) III.II.

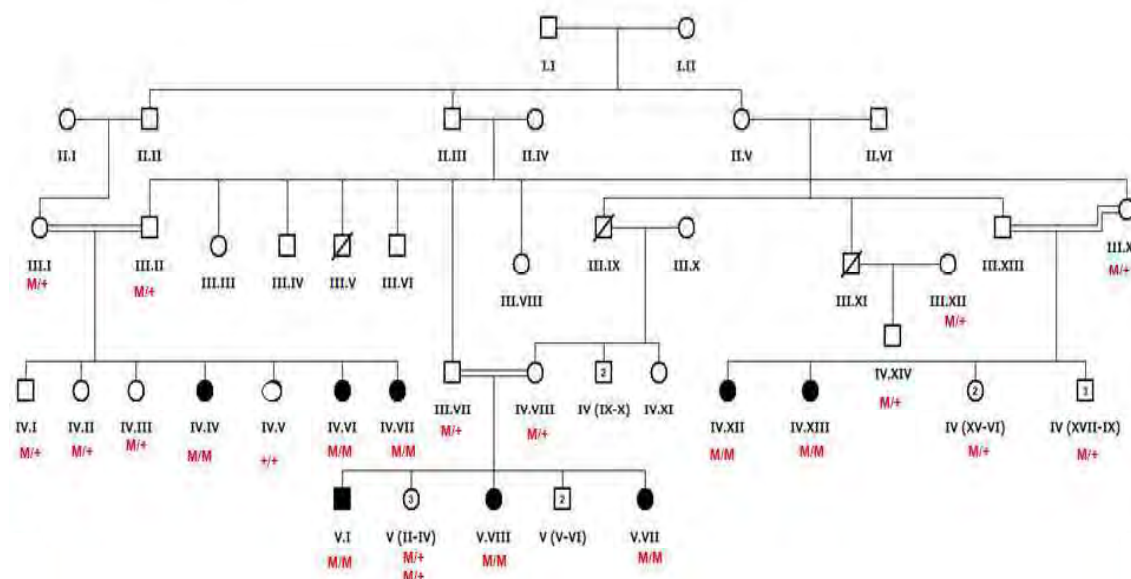


**Figure 3.56:** Pedigree diagram of RP 144.

### SECTION III:

A highly inbred family Micro-001 having three microphthalmia cases was recruited from Dera Ismail Khan, Khyber Pakhtunkhwa (KPK) Pakistan after clinical assessment by ophthalmologists following Declaration of Helsinki. The proband VI.VIII an 11 year old female (Figure3.57), her phenotypically normal mother V.XI, her two affected maternal uncles V.VII (40 years), V.II (35 years) and an unaffected maternal uncle V.III and his unaffected son VI.IV (9 year old).

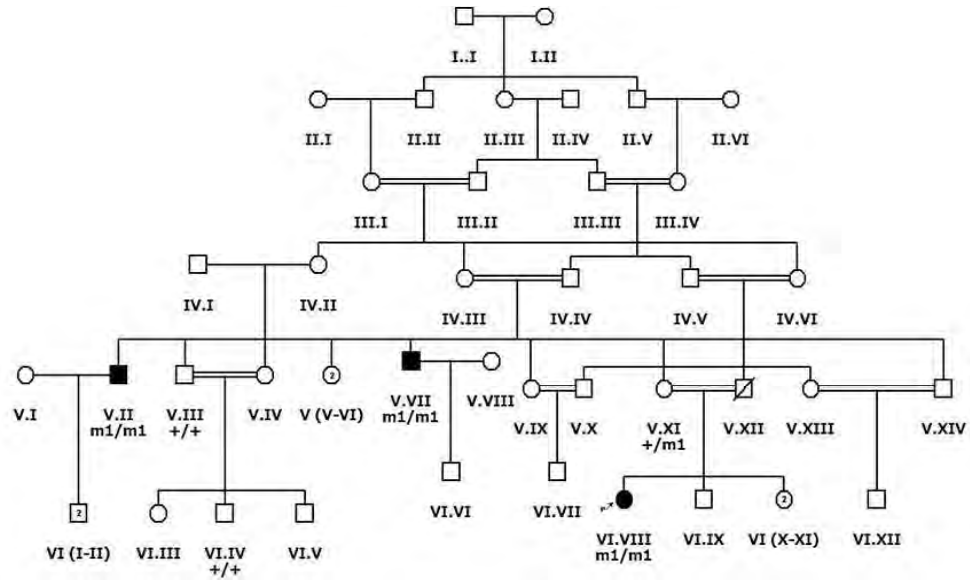


**Figure 3.57:** Pedigree drawing of microphthalmia family (Micro-001) enrolled in this study showing autosomal recessive inheritance pattern of disease phenotype.

### 3.8. Clinical analysis of microphthalmia:

The patient VI.VIII presented with congenital bilateral microphthalmia and total sclerocornea was completely blind (Figure 3.58 A). Siblings of proband, 2 sisters and one brother were phenotypically normal. Her other affected family members V.VII and V.II also had small eye orbit since birth and corneal opacities (Figure 3.58 B).

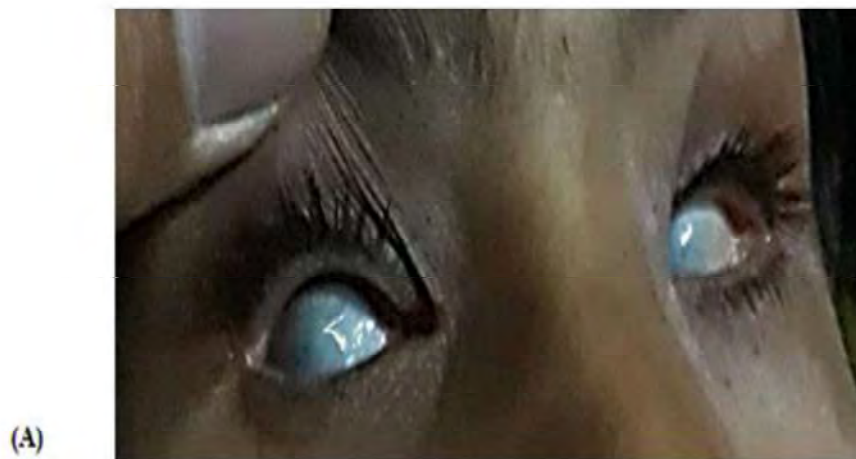




**Figure 3.58:** A) Proband (VI.VIII in figure 1) an eleven years old female having microphthalmia, total sclerocornea and total blindness. (B) Uncle (V.VII in figure 1) of proband suffering from corneal opacities and microphthalmia since birth.

### 3.9. Molecular analysis of Microphthalmia:

NGS capture panel sequencing revealed a previously reported pathogenic homozygous nonsense variant c.720C>A (p.Cys240\*) in *FOXE3* gene (Figure 3.59) (Table 3.10).

**Table 3.10:** Details of pathogenic variant identified in *FOXE3* encoding gene in current study

Proband ID	NM_ID	cDNA change	Protein change	Genotype status	Allele Type	ACMG classification	References PMID
V.I.VIII	NM_012186..3	c.720C>A	p.Cys240*	Homozygous	Known stop-gain	Pathogenic	20664696, 29314435, 27218149, 29769628,

This variant is very rare with a population frequency of 0.00016% according to the gnomAD database. Segregation testing was carried out for 4 family members of Micro-001 that confirmed co-segregation of variant with disease ACMG classified the variant as pathogenic.

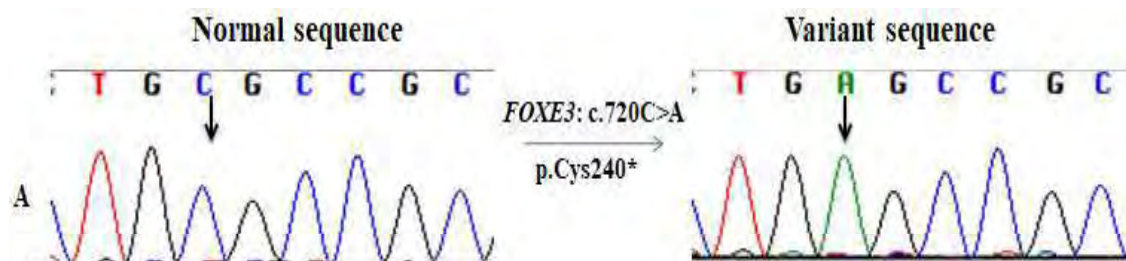


**Figure 3.59:** Chromatogram of reported disease causing variant i.e., c.720C>A identified in homozygous state in proband (VI.VIII). Normal sequence is shown on left side while variant sequence is shown on right side of figure.

Due to this splicing variant auxiliary sequence were altered breaking seven exonic splicing enhancer (ESE) sequences and creating four new ESE sequences and an exonic splicing silencer site (ESS) (Table 3.11). This stop gain mutation is previously reported for microphthalmia (Lopez Jimenez et al., 2011b), congenital primary aphakia (Sarkar, Moore, Leroy, & Moosajee, 2018; Valleix et al., 2006), pediatric cataract (Reis & Semina, 2019) and peter's anomaly (S. Y. Khan et al., 2016).

**Table 3.11:** List of exonic splicing sites (ESE), exonic splicing silencer (ESS) created and ESE sites broken due to c.720 C>A disease causing variant

Name	Position	Sequence	Status
<b>Exonic splicing enhancer site (ESE)</b>			
Exon-identity elements (EIE)	chr1:47417031	GCTGCG	Broken
Exon-identity elements (EIE)	chr1:47417032	CTGCGC	Broken
Pseudo exon ESE (PESE)	chr1:47417032	CTGCGCCG	Broken
ESE Serine/arginine-rich splicing factor 55 (ESE_SRp55)	chr1:47417033	TGCGCC	Broken
Pseudo exon ESE (PESE)	chr1:47417034	GCGCCGCG	Broken
ESE_ASFB	chr1:47417035	CGCCGCG	Broken
Pseudo exon ESE (PESE)	chr1:47417035	CGCCGCGC	Broken
Pseudo exon ESE (PESE)	chr1:47417028	CCTGCTGA	Created
ESE_ASFB	chr1:47417029	CTGCTGA	Created
Pseudo exon ESE (PESE)	chr1:47417029	CTGCTGAG	Created
ESE_9G8	chr1:47417031	GCTGAG	Created

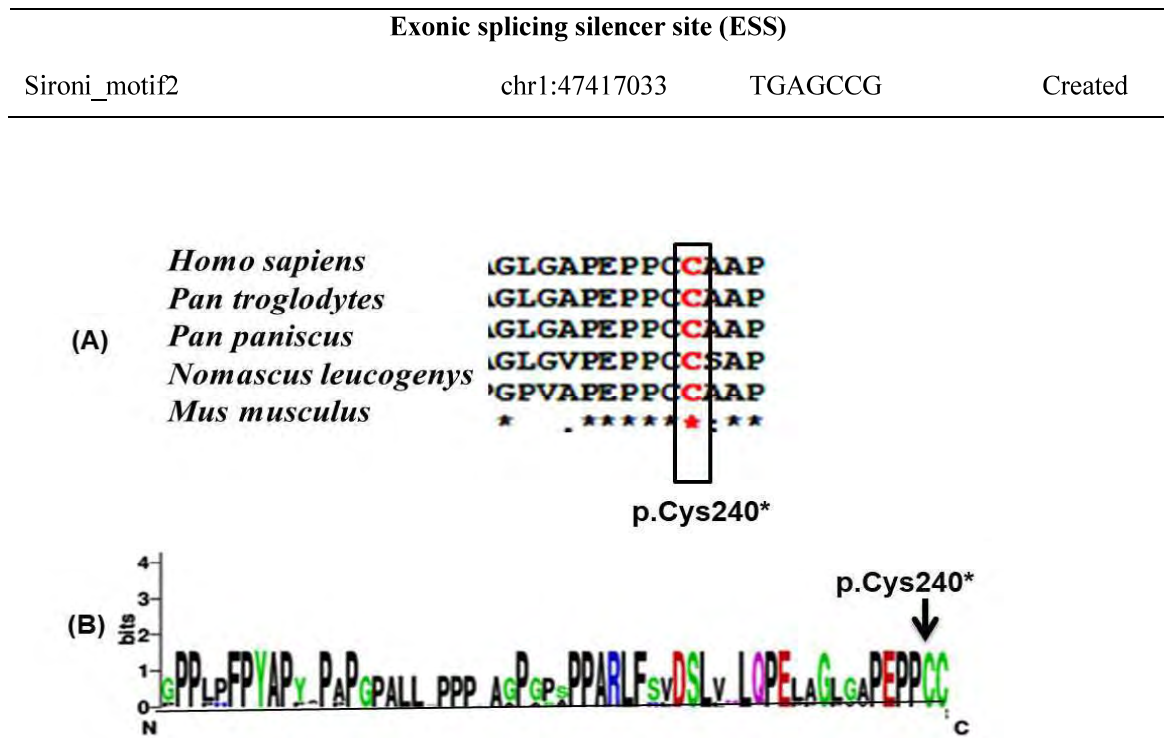


**Figure 3.60:** (A) Clustal omega results showing comparison of *FOXE3* gene sequence conservation among different homologs at variant site. (B) Web logo graphical representation of *FOXE3* sequence proposing 100% conservation at variant i.e., p.Cys240\* site. (Large size of amino acid abbreviation letter in Web logo result show full conservation while small size of letter shows less conserved position of amino acid among homologs).

Clustal omega predicted 100% conservation of amino acid at variant site in *FOXE3* gene among homologous sequences from different species having high similarity index to *Homo sapiens*, i.e., *Mus musculus* (NP\_001075448.1), *Pongoabelii* (XP\_009235654.1), *Nomascusleucogenys* (XP\_003262792.2) and *Pantroglodytes* (XP\_001167556.1) (Figure 3.60 A). Graphical representation of highly conserved sequence by Weblogo is shown in figure 3.57 B (Figure 3.60 B).

# **Chapter 4**

## **DISCUSSION**

In Pakistan very few national level or large-scale studies have been conducted to investigate the burden and molecular basis of visual impairments. Pakistan has one of the highest rates of inherited genetic diseases in the world, consistent with the prominence of consanguinity within the society, harboring one of the highest rates of blindness and vision impairment as well. Therefore, the current study was focused on identifying the molecular determinants of primary congenital glaucoma, inherited retinal dystrophies and microphthalmia inherited in an autosomal recessive pattern. To achieve these goal 20 families of primary congenital glaucoma, 35 families of inherited retinal dystrophies and one family of microphthalmia was enrolled from various hospitals of Pakistan after approval from Bioethical Committee of Quaid-i-Azam University Islamabad.

#### **4.1. Clinical and molecular study of primary congenital glaucoma in Pakistani population:**

High frequency i.e., 70–100% of consanguineous marriages (Abu-Amero & Edward, 2017) is the main cause of high prevalence of autosomal recessive disorders like PCG in Pakistan (Rauf et al., 2016). Mutated *CYP1B1* coded protein is reported to cause abnormal development of ocular structures resulting in impeded outflow of aqueous humor and PCG phenotype (Bagiyeva, Marfany, Gonzalez-Angulo, & Gonzalez-Duarte, 2007; Li, Zhou, Du, Wei, & Chen, 2011). Data retrieved through studies have shown that mutational spectrum of in *CYP1B1* gene varies among different populations i.e.; p. Ser476Pro is 44% prevalent in India, p.Arg469Trp, p.Arg368His, p.Arg390His, p.Gly61Glu and p.Glu173Arg are 70% prevalent in Iran, p.Gly61Glu, p. Arg390His and p.Glu229Lys are 80–100% prevalent in Saudi Arabia however p.Arg330Phe and p.Arg390His are predominantly reported from China (M. Shah, Bouhenni, & Benmerzouga, 2022).

Founder mutations reported from India c.1449G>A (R368H), Iran c.182G>A (p.Gly61Glu), Europe c.7996G>A (p.Glu387Lys), Saudi Arabia c.182G>A (p. Gly61Glu) and South Korea c.958G>T (p.Val320Leu) are not prevalent in Pakistan (Chouiter & Nadifi, 2017). Previous studies from Pakistan had reported p.Arg390His mutation to be implicated in more than 50% of analyzed PCG cases (Afzal et al., 2019; Micheal et al., 2015; Rashid et al., 2019; Rauf et al., 2016); however, in present study, we did not identify this mutation in any of the analyzed case. A possible



explanation of not detection of p.Arg390His mutation in our study cohort could be the differences in ethnicities of analyzed subjects. In previous studies, PCG cases belonging to Punjab and Sindh provinces of Pakistan were included (Rashid et al., 2019; Rauf et al., 2016) however in present study majority of the families i.e., 11/20 belonged to Baluchistan province of Pakistan. In present study CYP1B1 analysis in 20 cases enrolled through various regions of Punjab, Baluchistan and Khyber Pakhtunkhwa, Pakistan revealed a total of two frameshift, five missense and two silent disease-causing variations. Both frameshift variations c.758\_759insA and c.789dup detected in our study are not reported earlier from Pakistan or any other region.

All homozygous variants identified in this study showed a perfect segregation with phenotype of disease in all families. Previously, Ou et al., 2018 have shown that the active site residues of CYP1B1 are distributed from amino acid 126 to 510 of the protein therefore all truncations that omit one or more of these amino acids result in loss of protein function. Missense disease-causing variants found in family PCG049, 060, 062 and 067 and two silent disease-causing variants found in family PCG062, 063 are also previously unreported. In CYP1B1 protein, novel missense variant p.Arg153Gly is located in C-helix, p.Ser172Arg in D-helix, p.Phe421Leu in K-helix, and p.Asp242His in substrate recognition site 2 (Ou et al., 2018). The locations of residue replacements in conserved core structures highlight their possible severe effect on mutated protein structure and functionality hence causing disease phenotype (Achary et al., 2006; Firasat, Kaul, Ashfaq, & Idrees, 2018). Here in two families PCG049 and PCG062, we identified compound heterozygous mutations in CYP1B1 gene. Previously compound heterozygosity has been reported in developmental glaucoma, (Cai et al., 2021) and primary congenital glaucoma patients from China (Song et al., 2019). Cai et al., 2021 reported that two heterozygous mutations c.1310C>T (p.P437L) and c.3G>A (p.M11) are responsible for glaucoma in a Chinese family (Cai et al., 2021). In another study conducted on 13 Chinese PCG patients, two heterozygous mutations Ala330Phe and Arg390His were detected in a patient and reduced enzymatic activity due to these variants was reported to be the cause of disease (Song et al., 2019). Waryah et al., 2019 identified compound heterozygosity (p.Val364Met along with p.Pro350Thr) in two consanguineous families of PCG belonging to different ethnic groups of Pakistan (Waryah et al., 2019). Furthermore,

previous studies have also reported co-segregation of heterozygous variants of CYP1B1 with heterozygous TEK alleles in PCG cases (Kabra et al., 2017).

In present study, we identified a heterozygous variant p.Leu247Gln in a consanguineous family i.e., PCG060 and absence of any other heterozygous/homozygous variant in CYP1B1, recessive inheritance pattern and previously reported allelic interactions of two un linked genes for PCG phenotype (Chakrabarti et al., 2009; Kabra et al., 2017; K Kaur et al., 2005) necessitates genetic analysis of other glaucoma related genes including *MYOC*, *FOXC1* and *TEK* genes in PCG060 family. Due to epigenetic modifications and different environmental factors incomplete penetrance and increased variability could be observed in manifestation of CYP1B1 disease causing variations in PCG patients (Bejjani et al., 2000; Rashid et al., 2019). We could not identify homozygous or compound heterozygous disease-causing variants in fourteen analyzed families in this study that predicts the contribution of other genes like *LTBP2*, *TEK*, *MYOC*, *FOXC1* and regulatory effect of cis-acting elements, splicing elements or possible modifiers (K Kaur et al., 2005; Sheikh et al., 2014; Yousaf et al., 2018).

All single nucleotide polymorphisms (SNPs) identified in current study except one present in intronic region i.e., g.35710\_35711insT in homozygous state are previously reported. Four reported SNPs i.e., rs1056836 (c.1294G>C), rs1800400 (c.1358A>G), rs1056827 (c.355G>T) and rs10012 (c.142C>G) showed amino acid change while two polymorphisms rs1056837 (c.1347T>C) and rs4646431 (c.2244\_2245insT) were silent. Most prevalent polymorphism (45%) c.1347T>C in present study was also reported in other studies conducted on PCG cases from Pakistani population [51]. Afzal et al., 2019 (Afzal et al., 2019) reported SNP c.142C>G in 21.6%, c.1294G>C in 23.3% and c.355G>T in 50.2% cases while in current data they showed a frequency of 3.1%, 11.5% and 11.5% respectively.

#### **4.2.Clinical and molecular analysis of inherited retinal dystrophies:**

Despite the high prevalence of inherited retinal dystrophies in the population, limited studies on the genetic spectrum of IRDs have been undertaken in the region, likely because of underdevelopment, socio-economic limitations and lack of proper medical infrastructure or resources in the country. Furthermore, several studies in recent years

indicate that a large portion of mutations were highly specific to families of Pakistani descent. Therefore, the data represented in this study provides important insight into the genetic landscape of IRDs in Pakistan, providing valuable resources for both affected populations residing in the region and medical researchers from around the world. Results of this study will assist with future research of patients in this region, instigating the application of gene therapy techniques to assist families seeking treatment in this relatively underdeveloped country. In thirty-five enrolled families of IRDs all affected individuals had bilateral night blindness. Proband of eight families among these thirty-five families had speaking and hearing disability, one proband had mental retardation while proband in three families had polydactyly (Table 3.5).

The data presented in this study identified the disease-causing genetic variants in eighteen families among a cohort of thirty-five Pakistani families. A total of eighteen distinct pathogenic variants in fifteen genes were identified, including seven missense, six nonsense, four frameshift, and one splice variant. There is significant mutation heterogeneity within the population, considering that only the *SPATA7*, *CRB1* and *USH2A* genes were repeated in more than one family. This high heterogeneity within the cohort urges extensive studies involving Pakistani families using comprehensive molecular diagnostic approaches to further explore genetic components to form a better understanding of disease mechanisms and identify founder mutations for the development of suitable treatment options (Shivanna, Anand, Chakrabarti, & Khanna, 2019). One interesting observation from this study was that two families carry the same novel *SPATA7* pathogenic mutations, in contrast to the general reported rarity of mutations in *SPATA7* as a cause of retinal dystrophy (Mackay et al., 2011). This data suggest a unique mutation spectrum of IRDs in the study population.

In family RP102, other phenotypic abnormalities such as mental retardation and acute leukemia were also observed, suggesting the involvement of some other genetic variant segregating in the family. Among the nineteen pathogenic mutations detected in this study, six of them have been reported. The missense variant c.842G>A: p.Arg281His identified in RP 004 in *AGBL5* gene was previously reported in a study on inherited retinal dystrophy patients from US in heterozygous condition (Branham et al., 2016). In ceramide kinase gene (*CERKL*) p.Arg477\* stop gain variant causes early truncation of protein and is reported (Ávila-Fernández et al., 2010; González-del

Pozo et al., 2011; Tuson, Marfany, & González-Duarte, 2004; van Huet et al., 2015). The loss of function variant p.Arg477\* in *GPR179* gene is previously reported for congenital stationary night blindness (Peachey et al., 2012). Premature translational stop signal p.Arg292\* in *SAG* gene was reported in patients affected from autosomal recessive retinitis pigmentosa and Oguchi disease (Nakamura et al., 2004; O'Sullivan et al., 2012). In RP 019 the dominant heterozygous variant p.Cys187Arg found in *RHO* gene is reported as likely pathogenic in ClinVar for retinitis pigmentosa 4 (Audo et al., 2010). The gnomAD frequency of the variant p.Ile94Thr in *ARL6* gene in RP 043 is 0.00002 and the variant is reported for Bardet-Biedl syndrome-3 and retinitis pigmentosa (Carss et al., 2017; S. Khan et al., 2013; Kim et al., 2021).

In crumbs cell polarity complex component 1 (*CRB1*) gene two compound heterozygous variants c.1252T>C and c.1728del in RP 044 and one homozygous disease-causing mutation c.1459T>C in family RP 144 was found. The heterozygous variant c.1728del (p.Asp576Glu>Ter20) is not reported previously while c.1252T>C and c.1459T>C are previously reported by Eisenberger et al., 2013 in patients with retinitis pigmentosa and Leber's congenital amaurosis (Eisenberger et al., 2013). Splice site acceptor variant c.413-1G>A will lead to a frameshift of -1 creating a premature termination codon as reported by Nicopoulos et al., 2016 (Nikopoulos et al., 2016).

The stop-gain variant c.187C>T: p.Arg63\* in *USH2A* is common and has been observed in individuals with Usher Syndrome (Dad et al., 2016; Dreyer et al., 2000; Perez-Carro et al., 2018). Previously, this variant has been reported from different regions of the world, i.e., China (T. K. Ng et al., 2019), Spain (Perez-Carro et al., 2018), Denmark (Dad et al., 2016) and Italy (Sodi et al., 2014). Another cytosine to adenine substitution, i.e., c.1560C>A (p.Cys520\*) in *USH2A* identified in family RP 105 in this study, was also reported previously in the Spanish population by González-del Pozo et al., in 2018 as a heterozygous allele in a non-syndromic retinitis pigmentosa patient along with another heterozygous variant c.2276G>T: p.Cys759Phe. Previous studies also indicate that mutations in *USH2A* can result in a broadly variable clinical outcome between patients varying from non-syndromic IRD to Usher phenotype (Zupan et al., 2019). The same observation is reported for the genes implicated in Bardet-Biedl syndrome. Interestingly, a frame shift mutation in

USH2A at the same position (p.Cys520Alafs\*71) has also been reported to be pathogenic (Dreyer et al., 2000; Lenassi et al., 2015; McGee, Seyedahmadi, Sweeney, Dryja, & Berson, 2010; Weston et al., 2000). A large deletion encompassing a ~41.1Kb region of the *ALMS1* gene, i.e., c.9911\_11550del identified in family RP109, has been previously reported by Nikopoulos et al. in 2016 in two affected siblings of a consanguineous Pakistani family (Nikopoulos et al., 2016). Interestingly, the family reported by Nikopoulos et al. in 2016 and RP109 both belonged to the KPK province of Pakistan but are unrelated. Upon comparison of disease phenotype, it was found that affected members of RP109 also had acanthosis nigricans, obesity, vision and hearing loss since early childhood; however, we could not get them tested for renal function, cardiomyopathy and hepatomegaly as patients refused to cooperate.

According to the Human Genome Mutation Database (<http://www.hgmd.cf.ac.uk> (accessed on 1 April, 2024)), there are 10 reported large deletions in the *ALMS1* gene, among which three include deletion of region comprising exons 13–16. Monzo et al. (2017) identified a 38Kb deletion comprising exon 13-16 of the *ALMS1* gene in a Pakistani female Alstrom-syndrome-affected case (Monzó et al., 2017). They used Sanger's sequencing and the SNPs/CNVs microarray approach to define the exact location of deleted nucleotides, as well as showed that a long contiguous stretch (8.24 Mb) of homozygosity is centered in *ALMS1* sequence from the Pakistani population. According to Monzo et al.'s (2017) findings, the deletion of exons 13-16 is fixed in Pakistani recurrent haplotype, specifically in cases from northern Pakistani areas, i.e., KPK (Monzó et al., 2017), and our findings support this notion. The heterozygous variant, i.e., c.109del leading to p.Ala37Profs17 detected in exon 5 of *PAX6* gene in family RP110, is reported to cause nonsense-mediated decay (Lagali et al., 2020). This disease-causing variant has previously been reported as causative of aniridia (A. O. Khan, Aldahmesh, & Alkuraya, 2011), and the same phenotype was detected in cases of the RP110 family. In the *PAX6* gene, most of the detected variants are in heterozygous condition that partially disrupts the protein, suggesting haplo-insufficiency is enough for loss of *PAX6* function (Lima Cunha, Arno, Corton, & Moosajee, 2019). The *ACOX3* missense variant c.1163A>G (p.Asp388Gly) is not reported in any study on retinal dystrophies. The role of peroxisomes lie *ACOX1* in lipid metabolism in retinal pigment epithelium is well established but more research is

needed to understand the distribution and function of *ACOX2* and *ACOX3* in retinal epithelium (Miller, 2000).

#### **4.3. Clinical and molecular analysis of microphthalmia:**

Microphthalmia is a severe disorder that decreases the axial length of eye orbit. Abnormal thickening of the sclera is a very common finding in affected individuals (Qidwai & Shaikh, 2015). Unfortunately inherited eye disorders are very common in Pakistan due to high consanguinity (Darr et al., 2016; Kaul et al., 2010; Ullah et al., 2016). The means and medical resources necessary for timely diagnosis of congenital disorders are not available due to economic limitations. This case study was conducted to provide genetic counseling and to understand molecular basis of microphthalmia in local population. The stop-gain homozygous variant i.e., p.Cys240\* has high allele frequency in South Asia as compared to other regions according to gnomAD. High ocular phenotypic diversity is observed in patients with disease variants in *FOXE3* gene (Iseri et al., 2009). In our study the proband is an eleven years old female child (VI.VIII) suffering from bilateral congenital microphthalmia and total sclerocornea. She was declared as complete blind by ophthalmologists. Genetic analysis of the family identified a pathogenic stop-gain variant that resulted in loss of function by premature truncation of mRNA that will probably undergo nonsense mediated decay (Coban-Akdemir et al., 2018). Segregation analysis confirmed the pathogenicity caused by p.Cys240\* variant of *FOXE3* in other affected members of family (V.II, V.VII). Another finding from the genotyping data was that the *FOXE3* genetic variant was not found in two maternal cousins (VI.IV, VI.V) manifesting symptoms like nystagmus, albinism and blur vision as both of them were homozygous for normal allele. According to Valleix et al., 2006 substitution of cytosine at position 240 induced clinical abnormalities i.e., bilateral aphakia, microphthalmia, complete aplasia, dysplasia and loss of iris in an infant and his two siblings (Valleix et al., 2006). In 2010, Reis et al, identified homozygous variant c.720C>A in a seven year old male from Bangladesh suffering from bilateral asymmetrical microphthalmia, aphakia, glaucoma (Reis et al., 2010) and Ali et al., 2010 identified the same variant in a Pakistani microphthalmia family from Multan, Punjab (Ali et al., 2010). Previously, peter's anomaly, a developmental disorder of lens, iris and cornea was found in cases carrying *FOXE3* homozygous substitution

c.720C>A altering *DNAJB1* expression in large consanguineous Pakistani family PKCC139 (S. Y. Khan et al., 2016). An experiment performed by Wada et al., 2011 on mice revealed a 22-bp deletion located 3.2-kb upstream of *FOXE3* start codon that showed reduced expression in lens and caused both microphthalmia and cataract in mice (Anjum, Eiberg, Baig, Tommerup, & Hansen, 2010). In another study gene mapping of 3.8 Mb interval of *ALDH1A3* in a multiplex highly inbred Pakistani microphthalmia family reported negative for variants in *FOXE3*, *OTX2*, *SOX2* and *PAX2* revealed a homozygous missense variant (Fares-Taie et al., 2013). Exome sequencing of three families from remote areas of Pakistan having bilateral microphthalmia, corneal opacities and dysgenesis of anterior eye segment revealed homozygous variants p.Ile97Val and p.Met71Ilefs\*216 in *FOXE3* gene. Premature stop codon causing variant c.21\_24delGGAT (p.Met71Ilefs\*216) was also identified in consanguineous microphthalmia families by Iseri et al., 2009 and Islam et al., 2015 (Iseri et al., 2009; Islam et al., 2015). Variable phenotypic presentation in patients with *FOXE3* disease causing variants could be due to position of variant in forkhead domain that can also affect its mode of transmission (Rashid et al., 2020).

#### **4.4. Conclusion and future perspective:**

In conclusion, during molecular screening we identified nine disease-causing variants in nine out of twenty PCG families, eighteen disease-causing variants in eighteen out of thirty five retinal dystrophies families and one disease causing variant segregating with disease phenotype in a microphthalmia family. No disease-causing variant was identified in eleven PCG families by Sanger sequencing and seventeen retinal dystrophies families by targeted panel sequencing highlighting genetic heterogeneity and need of whole genome sequencing of these families. The inheritance pattern of all disease-causing variants was autosomal recessive except for c.559T>C identified in *RHO* gene in RP 019. Given that known alleles are notably easier to interpret than novel alleles due to limitations from lack of data for the later, it is a requisite to construct a substantial database for Pakistani cohorts to improve the ability of interpretation for future studies. It is evident that additional screening of our population is essential for the future expansion of research and genetic counseling in Pakistan.

# **Chapter 5**

## **REFERENCES**



## References:

- Abu-Amero, K. K., & Edward, D. P. (2017). Primary congenital glaucoma.
- Achary, M. S., Reddy, A. B., Chakrabarti, S., Panicker, S. G., Mandal, A. K., Ahmed, N., . . . Nagarajaram, H. A. (2006). Disease-causing mutations in proteins: structural analysis of the CYP1B1 mutations causing primary congenital glaucoma in humans. *Biophysical journal*, *91*(12), 4329-4339.
- Acton, J. H., & Greenstein, V. C. (2013). Fundus-driven perimetry (microperimetry) compared to conventional static automated perimetry: similarities, differences, and clinical applications. *Canadian Journal of Ophthalmology*, *48*(5), 358-363.
- Adzhubei, I. A., Schmidt, S., Peshkin, L., Ramensky, V. E., Gerasimova, A., Bork, P., . . . Sunyaev, S. R. (2010). A method and server for predicting damaging missense mutations. *Nature methods*, *7*(4), 248-249.
- Afzal, R., Firasat, S., Kaul, H., Ahmed, B., Siddiqui, S. N., Zafar, S. N., . . . Afshan, K. (2019). Mutational analysis of the CYP1B1 gene in Pakistani primary congenital glaucoma patients: Identification of four known and a novel causative variant at the 3' splice acceptor site of intron 2. *Congenital anomalies*, *59*(5), 152-161.
- Ali, M., Buentello-Volante, B., McKibbin, M., Rocha-Medina, J. A., Fernandez-Fuentes, N., Koga-Nakamura, W., . . . Williams, G. (2010). Homozygous FOXE3 mutations cause non-syndromic, bilateral, total sclerocornea, aphakia, microphthalmia and optic disc coloboma. *Molecular Vision*, *16*, 1162.
- Ali, M., McKibbin, M., Booth, A., Parry, D. A., Jain, P., Riazuddin, S. A., . . . Shires, M. (2009). Null mutations in LTBP2 cause primary congenital glaucoma. *The American Journal of Human Genetics*, *84*(5), 664-671.
- Allwardt, B. A., Lall, A. B., Brockerhoff, S. E., & Dowling, J. E. (2001). Synapse formation is arrested in retinal photoreceptors of the zebrafish nrc mutant. *Journal of Neuroscience*, *21*(7), 2330-2342.
- Anderson, D. R., Drance, S. M., & Schulzer, M. (2003). Factors that predict the benefit of lowering intraocular pressure in normal tension glaucoma. *American journal of ophthalmology*, *136*(5), 820-829.
- Anholt, R. R., & Carbone, M. A. (2013). A molecular mechanism for glaucoma: endoplasmic reticulum stress and the unfolded protein response. *Trends in molecular medicine*, *19*(10), 586-593.
- Anjum, I., Eiberg, H., Baig, S. M., Tommerup, N., & Hansen, L. (2010). A mutation in the FOXE3 gene causes congenital primary aphakia in an autosomal recessive consanguineous Pakistani family. *Molecular Vision*, *16*, 549.
- Audo, I., Friedrich, A., Mohand-Saïd, S., Lancelot, M.-E., Antonio, A., Moskova-Doumanova, V., . . . Zeitze, C. (2010). An unusual retinal phenotype associated with a novel mutation in RHO. *Archives of Ophthalmology*, *128*(8), 1036-1045.
- Aung, T., Yong, V. H., Lim, M. C., Venkataraman, D., Toh, J.-Y., Chew, P. T., & Vithana, E. N. (2008). Lack of association between the rs2664538 polymorphism in the MMP-9 gene and primary angle closure glaucoma in Singaporean subjects. *Journal of glaucoma*, *17*(4), 257-258.
- Ávila-Fernández, A., Cantalapiedra, D., Aller, E., Vallespín, E., Aguirre-Lambán, J., Blanco-Kelly, F., . . . Trujillo-Tiebas, M. J. (2010). Mutation analysis of 272 Spanish families affected by autosomal recessive retinitis pigmentosa using a genotyping microarray. *Molecular Vision*, *16*, 2550.
- Awadalla, M. S., Burdon, K. P., Kuot, A., Hewitt, A. W., & Craig, J. E. (2011). Matrix metalloproteinase-9 genetic variation and primary angle closure glaucoma in a Caucasian population. *Molecular Vision*, *17*, 1420.

- Ayub, H., Khan, M. I., Micheal, S., Akhtar, F., Ajmal, M., Shafique, S., . . . Qamar, R. (2010). Association of eNOS and HSP70 gene polymorphisms with glaucoma in Pakistani cohorts. *Molecular Vision*, *16*, 18.
- Azam, M., Collin, R. W., Malik, A., Khan, M. I., Shah, S. T. A., Shah, A. A., . . . Ajmal, M. (2011). Identification of novel mutations in Pakistani families with autosomal recessive retinitis pigmentosa. *Archives of Ophthalmology*, *129*(10), 1377-1378.
- Bagiyeva, S., Marfany, G., Gonzalez-Angulo, O., & Gonzalez-Duarte, R. (2007). Mutational screening of CYP1B1 in Turkish PCG families and functional analyses of newly detected mutations. *Mol Vis*, *13*(13), 1458-1468.
- Barembaum, M., & Bronner-Fraser, M. (2005). *Early steps in neural crest specification*. Paper presented at the Seminars in cell & developmental biology.
- Barkan, O. (1955). Pathogenesis of congenital glaucoma: gonioscopic and anatomic observation of the angle of the anterior chamber in the normal eye and in congenital glaucoma. *American journal of ophthalmology*, *40*(1), 1-11.
- Beales, P., Elcioglu, N., Woolf, A., Parker, D., & Flinter, F. (1999). New criteria for improved diagnosis of Bardet-Biedl syndrome: results of a population survey. *Journal of medical genetics*, *36*(6), 437.
- Beck, A. D. (2011). Primary congenital glaucoma in the developing world. *Ophthalmology*, *118*(2), 229-230.
- Bejjani, B. A., Stockton, D. W., Lewis, R. A., Tomey, K. F., Dueker, D. K., Jabak, M., . . . Lupski, J. R. (2000). Multiple CYP1B1 mutations and incomplete penetrance in an inbred population segregating primary congenital glaucoma suggest frequent de novo events and a dominant modifier locus. *Human Molecular Genetics*, *9*(3), 367-374.
- Berson, E. L., Rosner, B., Sandberg, M. A., Weigel-DiFranco, C., Brockhurst, R. J., Hayes, K., . . . Gaudio, A. R. (2010). Clinical trial of lutein in patients with retinitis pigmentosa receiving vitamin A. *Archives of Ophthalmology*, *128*(4), 403.
- Black, G. C., Ashworth, J. L., & Sergouniotis, P. I. (2022). *Clinical ophthalmic genetics and genomics*: Academic Press.
- Bowne, S. J., Sullivan, L. S., Blanton, S. H., Cepko, C. L., Blackshaw, S., Birch, D. G., . . . Daiger, S. P. (2002). Mutations in the inosine monophosphate dehydrogenase 1 gene (IMPDH1) cause the RP10 form of autosomal dominant retinitis pigmentosa. *Human Molecular Genetics*, *11*(5), 559-568.
- Branham, K., Matsui, H., Biswas, P., Guru, A. A., Hicks, M., Suk, J. J., . . . Telenti, A. (2016). Establishing the involvement of the novel gene AGBL5 in retinitis pigmentosa by whole genome sequencing. *Physiological Genomics*, *48*(12), 922-927.
- Brennan, D., & Giles, S. (2014). Ocular involvement in fetal alcohol spectrum disorder: a review. *Current pharmaceutical design*, *20*(34), 5377-5387.
- Cai, S., Zhang, D., Jiao, X., Wang, T., Fan, M., Wang, Y., . . . Liu, X. (2021). Novel compound heterozygous mutations in CYP1B1 identified in a Chinese family with developmental glaucoma. *Molecular Medicine Reports*, *24*(5), 1-8.
- Canning, C., Greaney, M., Dewynne, J., & Fitt, A. (2002). Fluid flow in the anterior chamber of a human eye. *Mathematical Medicine and Biology: a Journal of the IMA*, *19*(1), 31-60.
- Capriotti, E., Fariselli, P., & Casadio, R. (2005). I-Mutant2. 0: predicting stability changes upon mutation from the protein sequence or structure. *Nucleic acids research*, *33*(suppl\_2), W306-W310.
- Carss, K. J., Arno, G., Erwood, M., Stephens, J., Sanchis-Juan, A., Hull, S., . . . Malka, S. (2017). Comprehensive rare variant analysis via whole-genome sequencing to determine the molecular pathology of inherited retinal disease. *The American Journal of Human Genetics*, *100*(1), 75-90.

- Chakrabarti, S., Devi, K. R., Komatireddy, S., Kaur, K., Parikh, R. S., Mandal, A. K., . . . Thomas, R. (2007). Glaucoma-associated CYP1B1 mutations share similar haplotype backgrounds in POAG and PACG phenotypes. *Investigative ophthalmology & visual science*, *48*(12), 5439-5444.
- Chakrabarti, S., Kaur, K., Rao, K. N., Mandal, A. K., Kaur, I., Parikh, R. S., & Thomas, R. (2009). The transcription factor gene FOXC1 exhibits a limited role in primary congenital glaucoma. *Investigative ophthalmology & visual science*, *50*(1), 75-83.
- Chawla, H., & Vohra, V. (2023). Retinal dystrophies *StatPearls [Internet]*: StatPearls Publishing.
- Chen, C.-W., Lin, M.-H., Liao, C.-C., Chang, H.-P., & Chu, Y.-W. (2020). iStable 2.0: predicting protein thermal stability changes by integrating various characteristic modules. *Computational and structural biotechnology journal*, *18*, 622-630.
- Chen, W., Stambolian, D., Edwards, A. O., Branham, K. E., Othman, M., Jakobsdottir, J., . . . Klein, M. L. (2010). Genetic variants near TIMP3 and high-density lipoprotein-associated loci influence susceptibility to age-related macular degeneration. *Proceedings of the National Academy of Sciences*, *107*(16), 7401-7406.
- Cheng, J., Randall, A., & Baldi, P. (2006). Prediction of protein stability changes for single-site mutations using support vector machines. *Proteins: Structure, Function, and Bioinformatics*, *62*(4), 1125-1132.
- Choi, Y., & Chan, A. P. (2015). PROVEAN web server: a tool to predict the functional effect of amino acid substitutions and indels. *Bioinformatics*, *31*(16), 2745-2747.
- Choi, Y., Sims, G. E., Murphy, S., Miller, J. R., & Chan, A. P. (2012). Predicting the functional effect of amino acid substitutions and indels.
- Chouiter, L., & Nadifi, S. (2017). Analysis of CYP1B1 gene mutations in patients with primary congenital glaucoma. *Journal of pediatric genetics*, *6*(04), 205-214.
- Coban-Akdemir, Z., White, J. J., Song, X., Jhangiani, S. N., Fatih, J. M., Gambin, T., . . . Punetha, J. (2018). Identifying genes whose mutant transcripts cause dominant disease traits by potential gain-of-function alleles. *The American Journal of Human Genetics*, *103*(2), 171-187.
- Collin, G., Cyr, E., Bronson, R., Marshall, J., Gifford, E., Hicks, W., . . . Nishina, P. (2005). Alms1-disrupted mice recapitulate human Alström syndrome. *Human Molecular Genetics*, *14*(16), 2323-2333.
- Crooks, G. E., Hon, G., Chandonia, J.-M., & Brenner, S. E. (2004). WebLogo: a sequence logo generator. *Genome research*, *14*(6), 1188-1190.
- Cvekl, A., & Wang, W.-L. (2009). Retinoic acid signaling in mammalian eye development. *Experimental eye research*, *89*(3), 280-291.
- Dad, S., Rendtorff, N. D., Tranebjærg, L., Grønsvov, K., Karstensen, H. G., Brox, V., . . . Jensen, H. (2016). Usher syndrome in Denmark: mutation spectrum and some clinical observations. *Molecular genetics & genomic medicine*, *4*(5), 527-539.
- Daiger, S. P., Bowne, S. J., & Sullivan, L. S. (2007). Perspective on genes and mutations causing retinitis pigmentosa. *Archives of Ophthalmology*, *125*(2), 151-158.
- Darr, A., Small, N., Ahmad, W. I., Atkin, K., Corry, P., & Modell, B. (2016). Addressing key issues in the consanguinity-related risk of autosomal recessive disorders in consanguineous communities: lessons from a qualitative study of British Pakistanis. *Journal of community genetics*, *7*(1), 65-79.
- Daufenbach, D. R., Ruttum, M. S., Pulido, J. S., & Keech, R. (1998). Chorioretinal colobomas in a pediatric population. *Ophthalmology*, *105*(8), 1455-1458.
- Davies, E. C., & Pineda II, R. (2017). Cataract surgery outcomes and complications in retinal dystrophy patients. *Canadian Journal of Ophthalmology*, *52*(6), 543-547.
- Demirci, H., Singh, A., Shields, J., Shields, C., & Eagle, R. (2003). Bilateral microphthalmos and orbital cyst. *Eye*, *17*(2), 273-276.

- den Hollander, A. I., Roepman, R., Koenekoop, R. K., & Cremers, F. P. (2008). Leber congenital amaurosis: genes, proteins and disease mechanisms. *Progress in retinal and eye research*, 27(4), 391-419.
- Desmet, F.-O., Hamroun, D., Lalande, M., Collod-Bérout, G., Claustres, M., & Bérout, C. (2009). Human Splicing Finder: an online bioinformatics tool to predict splicing signals. *Nucleic acids research*, 37(9), e67-e67.
- Dineen, B., Bourne, R., Jadoon, Z., Shah, S. P., Khan, M. A., Foster, A., . . . Khan, M. D. (2007). Causes of blindness and visual impairment in Pakistan. The Pakistan national blindness and visual impairment survey. *British journal of ophthalmology*, 91(8), 1005-1010.
- Dreyer, B., Tranebjærg, L., Rosenberg, T., Weston, M. D., Kimberling, W. J., & Nilssen, Ø. (2000). Identification of novel USH2A mutations: implications for the structure of USH2A protein. *European Journal of Human Genetics*, 8(7), 500-506.
- Ducker, L., & Rivera, R. Y. (2022). Anatomy, head and neck, eye lacrimal duct *StatPearls [Internet]*: StatPearls Publishing.
- Eisenberger, T., Neuhaus, C., Khan, A. O., Decker, C., Preising, M. N., Friedburg, C., . . . Holz, F. G. (2013). Increasing the yield in targeted next-generation sequencing by implicating CNV analysis, non-coding exons and the overall variant load: the example of retinal dystrophies. *PLoS one*, 8(11), e78496.
- Eker, M. B. H. K. (2023). Whole-Exome Sequencing in Turkish Patients with Inherited Retinal Dystrophies Reveals Novel Variants in Ten Genes.
- Fahim, A. T., Daiger, S. P., & Weleber, R. G. (2023). Nonsyndromic retinitis pigmentosa overview. *GeneReviews®[Internet]*.
- Fares-Taie, L., Gerber, S., Chassaing, N., Clayton-Smith, J., Hanein, S., Silva, E., . . . Baumann, C. (2013). ALDH1A3 mutations cause recessive anophthalmia and microphthalmia. *The American Journal of Human Genetics*, 92(2), 265-270.
- Ferrara, N. (2009). VEGF-A: a critical regulator of blood vessel growth. *European cytokine network*, 20(4), 158-163.
- Fields, R. R., Zhou, G., Huang, D., Davis, J. R., Möller, C., Jacobson, S. G., . . . Sumegi, J. (2002). Usher syndrome type III: revised genomic structure of the USH3 gene and identification of novel mutations. *The American Journal of Human Genetics*, 71(3), 607-617.
- Firasat, S., Kaul, H., Ashfaq, U. A., & Idrees, S. (2018). In silico analysis of five missense mutations in CYP1B1 gene in Pakistani families affected with primary congenital glaucoma. *International ophthalmology*, 38, 807-814.
- Firasat, S., Riazuddin, S. A., Hejtmancik, J. F., & Riazuddin, S. (2008). Primary congenital glaucoma localizes to chromosome 14q24. 2-24.3 in two consanguineous Pakistani families. *Molecular Vision*, 14, 1659.
- Flitcroft, D., Adams, G., Robson, A., & Holder, G. (2005). Retinal dysfunction and refractive errors: an electrophysiological study of children. *The British journal of ophthalmology*, 89(4), 484.
- Forsyth, R., & Gunay-Aygun, M. (2020). Bardet-Biedl syndrome overview.
- Glazer, L. C., & Dryja, T. P. (2002). Understanding the etiology of Stargardt's disease. *Ophthalmology clinics of North America*, 15(1), 93-100, viii.
- Goel, M., Picciani, R. G., Lee, R. K., & Bhattacharya, S. K. (2010). Aqueous humor dynamics: a review. *The open ophthalmology journal*, 4, 52.
- Gomes, A., & Korf, B. (2018). Genetic testing techniques. *Pediatric cancer genetics*, 47-64.
- González-del Pozo, M., Borrego, S., Barragan, I., Pieras, J. I., Santoyo, J., Matamala, N., . . . Antinolo, G. (2011). Mutation screening of multiple genes in Spanish patients with autosomal recessive retinitis pigmentosa by targeted resequencing. *PLoS one*, 6(12), e27894.

- Gould, D. B., & John, S. W. (2002). Anterior segment dysgenesis and the developmental glaucomas are complex traits. *Human Molecular Genetics*, *11*(10), 1185-1193.
- Gregory-Evans, K., Pennesi, M. E., & Weleber, R. G. (2012). Retinitis pigmentosa and allied disorders *Medical Retina* (pp. 761-835): Elsevier Inc.
- Hagemann, I. S. (2015). Overview of technical aspects and chemistries of next-generation sequencing. *Clinical genomics*, 3-19.
- Haim, M. (2002). Epidemiology of retinitis pigmentosa in Denmark. *Acta ophthalmologica Scandinavica. Supplement*(233), 1-34.
- Hamamy, H., Antonarakis, S. E., Cavalli-Sforza, L. L., Temtamy, S., Romeo, G., Ten Kate, L. P., . . . van Duijn, C. (2011). Consanguineous marriages, pearls and perils: Geneva international consanguinity workshop report. *Genetics in Medicine*, *13*(9), 841-847.
- Hamel, C. (2006). Retinitis pigmentosa. *Orphanet journal of rare diseases*, *1*(1), 1-12.
- Harding, P., & Moosajee, M. (2019). The molecular basis of human anophthalmia and microphthalmia. *Journal of developmental biology*, *7*(3), 16.
- Hingorani, M., Hanson, I., & Van Heyningen, V. (2012). Aniridia. *European Journal of Human Genetics*, *20*(10), 1011-1017.
- Hood, D. C., Ramachandran, R., Holopigian, K., Lazow, M., Birch, D. G., & Greenstein, V. C. (2011). Method for deriving visual field boundaries from OCT scans of patients with retinitis pigmentosa. *Biomedical optics express*, *2*(5), 1106-1114.
- Huang, T.-L., Huang, S.-P., Chang, C.-H., Lin, K.-H., Sheu, M.-M., & Tsai, R.-K. (2014). Protective effects of cerebrolysin in a rat model of optic nerve crush. *The Kaohsiung journal of medical sciences*, *30*(7), 331-336.
- Hussain, R., & Bittles, A. H. (1998). The prevalence and demographic characteristics of consanguineous marriages in Pakistan. *Journal of biosocial science*, *30*(2), 261-275.
- Insinna, C., & Besharse, J. C. (2008). Intraflagellar transport and the sensory outer segment of vertebrate photoreceptors. *Developmental dynamics: an official publication of the American Association of Anatomists*, *237*(8), 1982-1992.
- Ioannidis, N. M., Rothstein, J. H., Pejaver, V., Middha, S., McDonnell, S. K., Baheti, S., . . . Karyadi, D. (2016). REVEL: an ensemble method for predicting the pathogenicity of rare missense variants. *The American Journal of Human Genetics*, *99*(4), 877-885.
- Iseri, S. U., Osborne, R. J., Farrall, M., Wyatt, A. W., Mirza, G., Nürnberg, G., . . . Hussain, M. S. (2009). Seeing clearly: the dominant and recessive nature of FOXE3 in eye developmental anomalies. *Human mutation*, *30*(10), 1378-1386.
- Islam, L., Kelberman, D., Williamson, L., Lewis, N., Glindzicz, M. B., Nischal, K. K., & Sowden, J. C. (2015). Functional Analysis of FOXE 3 Mutations Causing Dominant and Recessive Ocular Anterior Segment Disease. *Human mutation*, *36*(3), 296-300.
- Jadoon, M. Z., Dineen, B., Bourne, R. R., Shah, S. P., Khan, M. A., Johnson, G. J., . . . Khan, M. D. (2006). Prevalence of blindness and visual impairment in Pakistan: the Pakistan National Blindness and Visual Impairment Survey. *Investigative ophthalmology & visual science*, *47*(11), 4749-4755.
- Jagger, D., Collin, G., Kelly, J., Towers, E., Nevill, G., Longo-Guess, C., . . . Marshall, J. (2011). Alström Syndrome protein ALMS1 localizes to basal bodies of cochlear hair cells and regulates cilium-dependent planar cell polarity. *Human Molecular Genetics*, *20*(3), 466-481.
- Jiang, J., Geroski, D. H., Edelhauser, H. F., & Prausnitz, M. R. (2006). Measurement and prediction of lateral diffusion within human sclera. *Investigative ophthalmology & visual science*, *47*(7), 3011-3016.
- Jonas, J. B., Aung, T., Bourne, R. R., Bron, A. M., Ritch, R., & Panda-Jonas, S. (2018). Glaucoma—Authors' reply. *The Lancet*, *391*(10122), 740.

- Kabra, M., Zhang, W., Rathi, S., Mandal, A. K., Senthil, S., Pyatla, G., . . . Marmamula, S. (2017). Angiopoietin receptor TEK interacts with CYP1B1 in primary congenital glaucoma. *Human genetics*, *136*, 941-949.
- Kaul, H., Riazuddin, S. A., Shahid, M., Kousar, S., Butt, N. H., Zafar, A. U., . . . Hejtmancik, J. F. (2010). Autosomal recessive congenital cataract linked to EPHA2 in a consanguineous Pakistani family. *Molecular Vision*, *16*, 511.
- Kaur, K., Mandal, A. K., & Chakrabarti, S. (2011). Primary congenital glaucoma and the involvement of CYP1B1. *Middle East African journal of ophthalmology*, *18*(1), 7.
- Kaur, K., Reddy, A., Mukhopadhyay, A., Mandal, A., Hasnain, S., Ray, K., . . . Chakrabarti, S. (2005). Myocilin gene implicated in primary congenital glaucoma. *Clinical genetics*, *67*(4), 335-340.
- Kels, B. D., Grzybowski, A., & Grant-Kels, J. M. (2015). Human ocular anatomy. *Clinics in dermatology*, *33*(2), 140-146.
- Khan, A. O., Aldahmesh, M. A., & Alkuraya, F. S. (2011). Genetic and genomic analysis of classic aniridia in Saudi Arabia. *Molecular Vision*, *17*, 708.
- Khan, K., Rudkin, A., Parry, D. A., Burdon, K. P., McKibbin, M., Logan, C. V., . . . Laurie, K. J. (2011). Homozygous mutations in PXDN cause congenital cataract, corneal opacity, and developmental glaucoma. *The American Journal of Human Genetics*, *89*(3), 464-473.
- Khan, S., Ullah, I., Touseef, M., Basit, S., Khan, M. N., & Ahmad, W. (2013). Novel homozygous mutations in the genes ARL6 and BBS10 underlying Bardet-Biedl syndrome. *Gene*, *515*(1), 84-88.
- Khan, S. Y., Vasanth, S., Kabir, F., Gottsch, J. D., Khan, A. O., Chaerkady, R., . . . Laux, J. (2016). FOXE3 contributes to Peters anomaly through transcriptional regulation of an autophagy-associated protein termed DNAJB1. *Nature communications*, *7*(1), 1-15.
- Kim, Y.-J., Kim, Y.-N., Yoon, Y.-H., Seo, E.-J., Seo, G.-H., Keum, C., . . . Lee, J.-Y. (2021). Diverse genetic landscape of suspected retinitis pigmentosa in a large Korean cohort. *Genes*, *12*(5), 675.
- Kimizuka, Y., Kiyosawa, M., Tamai, M., & Takase, S. (1993). Retinal changes in myotonic dystrophy. Clinical and follow-up evaluation. *Retina (Philadelphia, Pa.)*, *13*(2), 129-135.
- Knierim, E., Lucke, B., Schwarz, J. M., Schuelke, M., & Seelow, D. (2011). Systematic comparison of three methods for fragmentation of long-range PCR products for next generation sequencing. *PLoS one*, *6*(11), e28240.
- Koenekoop, R. K., Arriaga, M. A., Trzuppek, K. M., & Lentz, J. J. (2020). Usher syndrome type I.
- Koenig, R. (2003). Bardet-Biedl syndrome and Usher syndrome. *Developments in ophthalmology*, *37*, 126-140.
- Kohli, P., & Kaur, K. (2023). Stargardt disease *StatPearls [Internet]*: StatPearls Publishing.
- Kolb, H. (2011). Gross anatomy of the eye.
- Kopanos, C., Tsiolkas, V., Kouris, A., Chapple, C. E., Aguilera, M. A., Meyer, R., & Massouras, A. (2019). VarSome: the human genomic variant search engine. *Bioinformatics*, *35*(11), 1978.
- Kumar, M., Srivastava, S., & Muhammad, T. (2022). Relationship between physical activity and cognitive functioning among older Indian adults. *Scientific reports*, *12*(1), 2725.
- Lagali, N., Wowra, B., Fries, F. N., Latta, L., Moslemani, K., Utheim, T. P., . . . Käsmann-Kellner, B. (2020). PAX6 mutational status determines aniridia-associated keratopathy phenotype. *Ophthalmology*, *127*(2), 273-275.
- Lamba, D. A., Karl, M. O., Ware, C. B., & Reh, T. A. (2006). Efficient generation of retinal progenitor cells from human embryonic stem cells. *Proceedings of the National Academy of Sciences*, *103*(34), 12769-12774.

- Laver, T. W., De Franco, E., Johnson, M. B., Patel, K. A., Ellard, S., Weedon, M. N., . . . Wakeling, M. N. (2022). SavvyCNV: Genome-wide CNV calling from off-target reads. *PLoS Computational Biology*, *18*(3), e1009940.
- Lee, S. Y., Usui, S., Zafar, A. b., Oveson, B. C., Jo, Y. J., Lu, L., . . . Campochiaro, P. A. (2011). N-acetylcysteine promotes long-term survival of cones in a model of retinitis pigmentosa. *Journal of cellular physiology*, *226*(7), 1843-1849.
- Lefter, M., Vis, J. K., Vermaat, M., den Dunnen, J. T., Taschner, P. E., & Laros, J. F. (2021). Mutalyzer 2: next generation HGVS nomenclature checker. *Bioinformatics*, *37*(18), 2811-2817.
- Lenassi, E., Vincent, A., Li, Z., Saihan, Z., Coffey, A. J., Steele-Stallard, H. B., . . . Héon, E. (2015). A detailed clinical and molecular survey of subjects with nonsyndromic USH2A retinopathy reveals an allelic hierarchy of disease-causing variants. *European Journal of Human Genetics*, *23*(10), 1318-1327.
- Léveillard, T., Fridlich, R., Clérin, E., Ait-Ali, N., Millet-Puel, G., Jaillard, C., . . . Sahel, J.-A. (2014). Therapeutic strategy for handling inherited retinal degenerations in a gene-independent manner using rod-derived cone viability factors. *Comptes rendus biologies*, *337*(3), 207-213.
- Lewis, C. J., Hedberg-Buenz, A., DeLuca, A. P., Stone, E. M., Alward, W. L., & Fingert, J. H. (2017). Primary congenital and developmental glaucomas. *Human Molecular Genetics*, *26*(R1), R28-R36.
- Lewis, R. A., Christie, W. C., Day, D. G., Craven, E. R., Walters, T., Bejanian, M., . . . Whitcup, S. M. (2017). Bimatoprost sustained-release implants for glaucoma therapy: 6-month results from a phase I/II clinical trial. *American journal of ophthalmology*, *175*, 137-147.
- Li, N., Zhou, Y., Du, L., Wei, M., & Chen, X. (2011). Overview of Cytochrome P450 1B1 gene mutations in patients with primary congenital glaucoma. *Experimental eye research*, *93*(5), 572-579.
- Lima Cunha, D., Arno, G., Corton, M., & Moosajee, M. (2019). The spectrum of PAX6 mutations and genotype-phenotype correlations in the eye. *Genes*, *10*(12), 1050.
- López-Garrido, M. P., Blanco-Marchite, C., Sánchez-Sánchez, F., López-Sánchez, E., Chaqués-Alepuz, V., Campos-Mollo, E., . . . Escribano, J. (2010). Functional analysis of CYP1B1 mutations and association of heterozygous hypomorphic alleles with primary open-angle glaucoma. *Clinical genetics*, *77*(1), 70-78.
- Lopez Jimenez, N., Flannick, J., Yahyavi, M., Li, J., Bardakjian, T., Tonkin, L., . . . Slavotinek, A. M. (2011a). Targeted'next-generation'sequencing in anophthalmia and microphthalmia patients confirms SOX2, OTX2 and FOXE3 mutations. *BMC Medical Genetics*, *12*(1), 1-8.
- Lopez Jimenez, N., Flannick, J., Yahyavi, M., Li, J., Bardakjian, T., Tonkin, L., . . . Slavotinek, A. M. (2011b). Targeted'next-generation'sequencing in anophthalmia and microphthalmia patients confirms SOX2, OTX2 and FOXE3 mutations. *BMC Medical Genetics*, *12*, 1-8.
- Lyons, C. J., & Lambert, S. R. (2022). *Taylor and Hoyt's Pediatric Ophthalmology and Strabismus*: Elsevier Health Sciences.
- Mackay, D. S., Ocaka, L. A., Borman, A. D., Sergouniotis, P. I., Henderson, R. H., Moradi, P., . . . Moore, A. T. (2011). Screening of SPATA7 in patients with Leber congenital amaurosis and severe childhood-onset retinal dystrophy reveals disease-causing mutations. *Investigative ophthalmology & visual science*, *52*(6), 3032-3038.
- MacLaren, R. E., Pearson, R., MacNeil, A., Douglas, R., Salt, T., Akimoto, M., . . . Ali, R. (2006). Retinal repair by transplantation of photoreceptor precursors. *Nature*, *444*(7116), 203-207.

- Mahar, P., & Shahzad, M. A. (2008). Glaucoma burden in a public sector hospital. *Pakistan Journal of Ophthalmology*, 24(3).
- Marc, R. E., Jones, B. W., Watt, C. B., & Strettoi, E. (2003). Neural remodeling in retinal degeneration. *Progress in retinal and eye research*, 22(5), 607-655.
- Marshall, J. D., Bronson, R. T., Collin, G. B., Nordstrom, A. D., Maffei, P., Paisey, R. B., . . . Shea, S. E. (2005). New Alström syndrome phenotypes based on the evaluation of 182 cases. *Archives of internal medicine*, 165(6), 675-683.
- Marwan, M., Dawood, M., Ullah, M., Shah, I. U., Khan, N., Hassan, M. T., . . . Crosby, A. H. (2023). Unravelling the genetic basis of retinal dystrophies in Pakistani consanguineous families. *BMC ophthalmology*, 23(1), 205.
- Mauri, L., Franzoni, A., Scarcello, M., Sala, S., Garavelli, L., Modugno, A., . . . Del Longo, A. (2015). SOX2, OTX2 and PAX6 analysis in subjects with anophthalmia and microphthalmia. *European Journal of Medical Genetics*, 58(2), 66-70.
- McGee, T. L., Seyedahmadi, B. J., Sweeney, M. O., Dryja, T. P., & Berson, E. L. (2010). Novel mutations in the long isoform of the USH2A gene in patients with Usher syndrome type II or non-syndromic retinitis pigmentosa. *Journal of medical genetics*, 47(7), 499-506.
- Mi, H., Guo, N., Kejariwal, A., & Thomas, P. D. (2007). PANTHER version 6: protein sequence and function evolution data with expanded representation of biological pathways. *Nucleic acids research*, 35(suppl\_1), D247-D252.
- Micheal, S., Ayub, H., Zafar, S. N., Bakker, B., Ali, M., Akhtar, F., . . . den Hollander, A. I. (2015). Identification of novel CYP1B 1 gene mutations in patients with primary congenital and primary open-angle glaucoma. *Clinical & experimental ophthalmology*, 43(1), 31-39.
- Micheal, S., Qamar, R., Akhtar, F., Khan, M. I., Khan, W. A., & Ahmed, A. (2009). MTHFR gene C677T and A1298C polymorphisms and homocysteine levels in primary open angle and primary closed angle glaucoma. *Molecular Vision*, 15, 2268.
- Miller, A. C. (2000). *Vibrations of non-homogeneous media and the prediction of mechanical resonance in human tibia*. Texas Tech University.
- Monemi, S., Spaeth, G., DaSilva, A., Popinchalk, S., Ilitchev, E., Liebmann, J., . . . Child, A. (2005). Identification of a novel adult-onset primary open-angle glaucoma (POAG) gene on 5q22. 1. *Human Molecular Genetics*, 14(6), 725-733.
- Monzó, C., Gimeno-Ferrer, F., García, J. C. F., Amadoz, A., Albuquerque, D., Angueira, F. B., . . . Rodríguez-López, R. (2017). Alström syndrome caused by deletion in ALMS1 gene fixed in a Northern Pakistan recurrent haplotype. *Indian Journal of Case Reports*, 3(4), 171-174.
- Morle, L., Bozon, M., Zech, J.-C., Alloisio, N., Raas-Rothschild, A., Philippe, C., . . . Ederly, P. (2000). A locus for autosomal dominant colobomatous microphthalmia maps to chromosome 15q12-q15. *The American Journal of Human Genetics*, 67(6), 1592-1597.
- Moroi, S. E., Lark, K. K., Sieving, P. A., Nouri-Mahdavi, K., Schlötzer-Schrehardt, U., Katz, G. J., & Ritch, R. (2003). Long anterior zonules and pigment dispersion. *American journal of ophthalmology*, 136(6), 1176-1178.
- Musarella, M. A., & MacDonald, I. M. (2011). Current concepts in the treatment of retinitis pigmentosa. *Journal of Ophthalmology*, 2011.
- Nadeem, R., Kabir, F., Li, J., Gradstein, L., Jiao, X., Rauf, B., . . . Ayyagari, R. (2020). Mutations in CERKL and RP1 cause retinitis pigmentosa in Pakistani families. *Human genome variation*, 7(1), 14.
- Nakamura, M., Yamamoto, S., Okada, M., Ito, S., Tano, Y., & Miyake, Y. (2004). Novel mutations in the arrestin gene and associated clinical features in Japanese patients with Oguchi's disease. *Ophthalmology*, 111(7), 1410-1414.



- Narayan, D. S., Wood, J. P., Chidlow, G., & Casson, R. J. (2016). A review of the mechanisms of cone degeneration in retinitis pigmentosa. *Acta ophthalmologica*, *94*(8), 748-754.
- Nash, B. M., Wright, D. C., Grigg, J. R., Bennetts, B., & Jamieson, R. V. (2015). Retinal dystrophies, genomic applications in diagnosis and prospects for therapy. *Translational pediatrics*, *4*(2), 139.
- Ng, P. C., & Henikoff, S. (2003). SIFT: Predicting amino acid changes that affect protein function. *Nucleic acids research*, *31*(13), 3812-3814.
- Ng, T. K., Tang, W., Cao, Y., Chen, S., Zheng, Y., Xiao, X., & Chen, H. (2019). Whole exome sequencing identifies novel USH2A mutations and confirms Usher syndrome 2 diagnosis in Chinese retinitis pigmentosa patients. *Scientific reports*, *9*(1), 5628.
- Niederlova, V., Modrak, M., Tsyklauri, O., Huranova, M., & Stepanek, O. (2019). Meta-analysis of genotype-phenotype associations in Bardet-Biedl syndrome uncovers differences among causative genes. *Human mutation*, *40*(11), 2068-2087.
- Nikopoulos, K., Butt, G., Farinelli, P., Mudassar, M., Domènech-Estévez, E., Samara, C., . . . Rivolta, C. (2016). A large multiexonic genomic deletion within the ALMS1 gene causes Alström syndrome in a consanguineous Pakistani family. *Clinical genetics*, *89*(4), 510-511.
- Nongpiur, M. E., He, M., Amerasinghe, N., Friedman, D. S., Tay, W.-T., Baskaran, M., . . . Aung, T. (2011). Lens vault, thickness, and position in Chinese subjects with angle closure. *Ophthalmology*, *118*(3), 474-479.
- Nongpiur, M. E., Khor, C. C., Jia, H., Cornes, B. K., Chen, L.-J., Qiao, C., . . . George, R. (2014). ABCC5, a gene that influences the anterior chamber depth, is associated with primary angle closure glaucoma. *PLoS genetics*, *10*(3), e1004089.
- O'Sullivan, J., Mullaney, B. G., Bhaskar, S. S., Dickerson, J. E., Hall, G., O'Grady, A., . . . Black, G. C. (2012). A paradigm shift in the delivery of services for diagnosis of inherited retinal disease. *Journal of medical genetics*, *49*(5), 322-326.
- Ohnaka, M., Miki, K., Gong, Y. Y., Stevens, R., Iwase, T., Hackett, S. F., & Campochiaro, P. A. (2012). Long-term expression of glial cell line-derived neurotrophic factor slows, but does not stop retinal degeneration in a model of retinitis pigmentosa. *Journal of neurochemistry*, *122*(5), 1047-1053.
- Ou, Z., Liu, G., Liu, W., Deng, Y., Zheng, L., Zhang, S., & Feng, G. (2018). Bioinformatics analysis of CYP1B1 mutation hotspots in Chinese primary congenital glaucoma patients. *Bioscience reports*, *38*(4), BSR20180056.
- Park, S. J., Ahn, S., Woo, S. J., & Park, K. H. (2015). Extent of exacerbation of chronic health conditions by visual impairment in terms of health-related quality of life. *JAMA ophthalmology*, *133*(11), 1267-1275.
- Peachey, N. S., Ray, T. A., Florijn, R., Rowe, L. B., Sjoerdsma, T., Contreras-Alcantara, S., . . . Iuvone, P. M. (2012). GPR179 is required for depolarizing bipolar cell function and is mutated in autosomal-recessive complete congenital stationary night blindness. *The American Journal of Human Genetics*, *90*(2), 331-339.
- Pejaver, V., Urresti, J., Lugo-Martinez, J., Pagel, K. A., Lin, G. N., Nam, H.-J., . . . Iakoucheva, L. M. (2020). Inferring the molecular and phenotypic impact of amino acid variants with MutPred2. *Nature communications*, *11*(1), 5918.
- Perez-Carro, R., Blanco-Kelly, F., Galbis-Martinez, L., Garcia-Garcia, G., Aller, E., Garcia-Sandoval, B., . . . Martin-Merida, I. (2018). Unravelling the pathogenic role and genotype-phenotype correlation of the USH2A p.(Cys759Phe) variant among Spanish families. *PLoS one*, *13*(6), e0199048.
- Perez-Lanzon, M., Kroemer, G., & Maiuri, M. C. (2018). Organoids for modeling genetic diseases. *International review of cell and molecular biology*, *337*, 49-81.

- Perkins, B. D., Fadool, J. M., & Dowling, J. E. (2004). Photoreceptor structure and development: analyses using GFP transgenes *Methods in cell biology* (Vol. 76, pp. 315-331): Elsevier.
- Pierrottet, C., Zuntini, M., Digiuni, M., Bazzanella, I., Ferri, P., Paderni, R., . . . Bertelli, M. (2014). Syndromic and non-syndromic forms of retinitis pigmentosa: a comprehensive Italian clinical and molecular study reveals new mutations. *Genet Mol Res*, *13*(4), 8815-8833.
- Pineles, S. L., Volpe, N. J., Miller-Ellis, E., Galetta, S. L., Sankar, P. S., Shindler, K. S., & Maguire, M. G. (2006). Automated combined kinetic and static perimetry: an alternative to standard perimetry in patients with neuro-ophthalmic disease and glaucoma. *Archives of Ophthalmology*, *124*(3), 363-369.
- Punzo, C., Kornacker, K., & Cepko, C. L. (2009). Stimulation of the insulin/mTOR pathway delays cone death in a mouse model of retinitis pigmentosa. *Nature neuroscience*, *12*(1), 44-52.
- Qiao, Y., Shao, T., Chen, Y., Chen, J., Sun, X., & Chen, X. (2023). Screening of candidate genes at GLC3B and GLC3C loci in Chinese primary congenital glaucoma patients with targeted next generation sequencing. *Ophthalmic Genetics*, *44*(2), 133-138.
- Qidwai, N., & Shaikh, K. (2015). Posterior Microphthalmia, A Challenging Diagnosis. *Pakistan Journal of Ophthalmology*, *31*(4).
- Qin, D. (2019). Next-generation sequencing and its clinical application. *Cancer biology & medicine*, *16*(1), 4.
- Radtke, N. D., Aramant, R. B., Petry, H. M., Green, P. T., Pidwell, D. J., & Seiler, M. J. (2008). Vision improvement in retinal degeneration patients by implantation of retina together with retinal pigment epithelium. *American journal of ophthalmology*, *146*(2), 172-182. e171.
- Ragge, N., Subak-Sharpe, I., & Collin, J. (2007). A practical guide to the management of anophthalmia and microphthalmia. *Eye*, *21*(10), 1290-1300.
- Rashid, M., Qasim, M., Ishaq, R., Bukhari, S. A., Sajid, Z., Ashfaq, U. A., . . . Ahmed, Z. M. (2020). Pathogenic variants of AIPL1, MERTK, GUCY2D, and FOXE3 in Pakistani families with clinically heterogeneous eye diseases. *PLoS one*, *15*(9), e0239748.
- Rashid, M., Yousaf, S., Sheikh, S. A., Sajid, Z., Shabbir, A. S., Kausar, T., . . . Ali, M. (2019). Identities and frequencies of variants in CYP1B1 causing primary congenital glaucoma in Pakistan. *Molecular Vision*, *25*, 144.
- Rauf, B., Irum, B., Kabir, F., Firasat, S., Naeem, M. A., Khan, S. N., . . . Riazuddin, S. (2016). A spectrum of CYP1B1 mutations associated with primary congenital glaucoma in families of Pakistani descent. *Human genome variation*, *3*(1), 1-4.
- Reis, L. M., & Semina, E. V. (2019). Genetic landscape of isolated pediatric cataracts: extreme heterogeneity and variable inheritance patterns within genes. *Human genetics*, *138*(8), 847-863.
- Reis, L. M., Tyler, R. C., Schneider, A., Bardakjian, T., Stoler, J. M., Melancon, S. B., & Semina, E. V. (2010). FOXE3 plays a significant role in autosomal recessive microphthalmia. *American Journal of Medical Genetics Part A*, *152*(3), 582-590.
- Rentzsch, P., Witten, D., Cooper, G. M., Shendure, J., & Kircher, M. (2019). CADD: predicting the deleteriousness of variants throughout the human genome. *Nucleic acids research*, *47*(D1), D886-D894.
- Rezaie, T., Child, A., Hitchings, R., Brice, G., Miller, L., Coca-Prados, M., . . . Kreutzer, D. (2002). Adult-onset primary open-angle glaucoma caused by mutations in optineurin. *Science*, *295*(5557), 1077-1079.
- Richardson, R., Tracey-White, D., Webster, A., & Moosajee, M. (2017). The zebrafish eye—a paradigm for investigating human ocular genetics. *Eye*, *31*(1), 68-86.

- Rodrigues, C. H., Pires, D. E., & Ascher, D. B. (2018). DynaMut: predicting the impact of mutations on protein conformation, flexibility and stability. *Nucleic acids research*, *46*(W1), W350-W355.
- Ronquillo, C., Bernstein, P., & Baehr, W. (2012). Senior-Løken syndrome: A syndromic form of retinal dystrophy associated with nephronophthisis. *Vision research*, *75*, 88-97.
- Russell, S., Bennett, J., Wellman, J. A., Chung, D. C., Yu, Z.-F., Tillman, A., . . . McCague, S. (2017). Efficacy and safety of voretigene neparvovec (AAV2-hRPE65v2) in patients with RPE65-mediated inherited retinal dystrophy: a randomised, controlled, open-label, phase 3 trial. *The Lancet*, *390*(10097), 849-860.
- Russnes, H. G., Navin, N., Hicks, J., & Borresen-Dale, A.-L. (2011). Insight into the heterogeneity of breast cancer through next-generation sequencing. *The Journal of clinical investigation*, *121*(10), 3810-3818.
- Sadeghi, M., Cohn, E. S., Kelly, W. J., Kimberling, W. J., Tranebjoerg, L., & Möller, C. (2004). Audiological findings in Usher syndrome types IIa and II (non-IIa). *International Journal of Audiology*, *43*(3), 136-143.
- Sarfarazi, M., & Stoilov, I. (2000). Molecular genetics of primary congenital glaucoma. *Eye*, *14*(3), 422-428.
- Sarfarazi, M., Stoilov, I., & Schenkman, J. B. (2003). Genetics and biochemistry of primary congenital glaucoma. *Ophthalmology clinics of North America*, *16*(4), 543-554, vi.
- Sarkar, H., Moore, W., Leroy, B. P., & Moosajee, M. (2018). CUGC for congenital primary aphakia. *European Journal of Human Genetics*, *26*(8), 1234-1237.
- Schilter, K., Schneider, A., Bardakjian, T., Soucy, J. F., Tyler, R. C., Reis, L. M., & Semina, E. V. (2011). OTX2 microphthalmia syndrome: four novel mutations and delineation of a phenotype. *Clinical genetics*, *79*(2), 158-168.
- Schum, U. (2013). Fluorescenzangiographie bei vitelliformer Maculadegeneration. *Auge und Immunologie: Bericht über die 70. Zusammenkunft der Deutschen Ophthalmologischen Gesellschaft in Heidelberg 1969*, *70*, 252.
- Schwarz, J. M., Cooper, D. N., Schuelke, M., & Seelow, D. (2014). MutationTaster2: mutation prediction for the deep-sequencing age. *Nature methods*, *11*(4), 361-362.
- Searle, A., Shetty, P., Melov, S., & Alahakoon, T. (2018). Prenatal diagnosis and implications of microphthalmia and anophthalmia with a review of current ultrasound guidelines: two case reports. *Journal of Medical Case Reports*, *12*(1), 1-7.
- Seddon, J. M., Reynolds, R., Yu, Y., Daly, M. J., & Rosner, B. (2011). Risk models for progression to advanced age-related macular degeneration using demographic, environmental, genetic, and ocular factors. *Ophthalmology*, *118*(11), 2203-2211.
- Semina, E. V., Brownell, I., Mintz-Hittner, H. A., Murray, J. C., & Jamrich, M. (2001). Mutations in the human forkhead transcription factor FOXE3 associated with anterior segment ocular dysgenesis and cataracts. *Human Molecular Genetics*, *10*(3), 231-236.
- Shah, B. R., Xu, W., & Mraz, J. (2019). Cytochrome P450 1B1: role in health and disease and effect of nutrition on its expression. *RSC advances*, *9*(36), 21050-21062.
- Shah, M., Bouhenni, R., & Benmerzouga, I. (2022). Geographical variability in CYP1B1 mutations in primary congenital glaucoma. *Journal of Clinical Medicine*, *11*(7), 2048.
- Shah, S. P., Taylor, A. E., Sowden, J. C., Ragge, N. K., Russell-Eggitt, I., Rahi, J. S., . . . Group, S. o. E. A. S. I. (2011). Anophthalmos, microphthalmos, and typical coloboma in the United Kingdom: a prospective study of incidence and risk. *Investigative ophthalmology & visual science*, *52*(1), 558-564.
- Sheikh, S. A., Waryah, A. M., Narsani, A. K., Shaikh, H., Gilal, I. A., Shah, K., . . . Shaikh, N. (2014). Mutational spectrum of the CYP1B1 gene in Pakistani patients with primary congenital glaucoma: novel variants and genotype-phenotype correlations. *Molecular Vision*, *20*, 991.

- Shihab, H. A., Rogers, M. F., Gough, J., Mort, M., Cooper, D. N., Day, I. N., . . . Campbell, C. (2015). An integrative approach to predicting the functional effects of non-coding and coding sequence variation. *Bioinformatics*, *31*(10), 1536-1543.
- Shivanna, M., Anand, M., Chakrabarti, S., & Khanna, H. (2019). Ocular ciliopathies: genetic and mechanistic insights into developing therapies. *Current medicinal chemistry*, *26*(17), 3120-3131.
- Shoemark, A., Dixon, M., Beales, P. L., & Hogg, C. L. (2015). Bardet Biedl syndrome: motile ciliary phenotype. *Chest*, *147*(3), 764-770.
- Shumway, C. L., Motlagh, M., & Wade, M. (2018). Anatomy, head and neck, eye conjunctiva.
- Sievers, F., Wilm, A., Dineen, D., Gibson, T. J., Karplus, K., Li, W., . . . Söding, J. (2011). Fast, scalable generation of high-quality protein multiple sequence alignments using Clustal Omega. *Molecular systems biology*, *7*(1), 539.
- Singh, M., & Tyagi, S. C. (2018). Genes and genetics in eye diseases: a genomic medicine approach for investigating hereditary and inflammatory ocular disorders. *International journal of ophthalmology*, *11*(1), 117.
- Sinn, R., & Wittbrodt, J. (2013). An eye on eye development. *Mechanisms of development*, *130*(6-8), 347-358.
- Skalicky, S. E., White, A. J., Grigg, J. R., Martin, F., Smith, J., Jones, M., . . . Jamieson, R. V. (2013). Microphthalmia, anophthalmia, and coloboma and associated ocular and systemic features: understanding the spectrum. *JAMA ophthalmology*, *131*(12), 1517-1524.
- Slavotinek, A. (2019). Genetics of anophthalmia and microphthalmia. Part 2: Syndromes associated with anophthalmia–microphthalmia. *Human genetics*, *138*(8-9), 831-846.
- Sodi, A., Mariottini, A., Passerini, I., Murro, V., Tachyla, I., Bianchi, B., . . . Torricelli, F. (2014). MYO7A and USH2A gene sequence variants in Italian patients with Usher syndrome. *Molecular Vision*, *20*, 1717.
- Solomon, D. A. (2018). Integrating molecular diagnostics with surgical neuropathology *Practical surgical neuropathology: a diagnostic approach* (pp. 71-89): Elsevier.
- Song, N., Leng, L., Yang, X.-J., Zhang, Y.-Q., Tang, C., Chen, W.-S., . . . Yang, X. (2019). Compound heterozygous mutations in CYP1B1 gene leads to severe primary congenital glaucoma phenotype. *International journal of ophthalmology*, *12*(6), 909.
- Souma, T., Tompson, S. W., Thomson, B. R., Siggs, O. M., Kizhatil, K., Yamaguchi, S., . . . Maurer-Stroh, S. (2016). Angiopoietin receptor TEK mutations underlie primary congenital glaucoma with variable expressivity. *The Journal of clinical investigation*, *126*(7), 2575-2587.
- Steinhaus, R., Proft, S., Schuelke, M., Cooper, D. N., Schwarz, J. M., & Seelow, D. (2021). MutationTaster2021. *Nucleic acids research*, *49*(W1), W446-W451.
- Stoilov, I., Akarsu, A. N., & Sarfarazi, M. (1997). Identification of three different truncating mutations in cytochrome P4501B1 (CYP1B1) as the principal cause of primary congenital glaucoma (Buphthalmos) in families linked to the GLC3A locus on chromosome 2p21. *Human Molecular Genetics*, *6*(4), 641-647.
- Stone, E. M., Fingert, J. H., Alward, W. L., Nguyen, T. D., Polansky, J. R., Sunden, S. L., . . . Nichols, B. E. (1997). Identification of a gene that causes primary open angle glaucoma. *Science*, *275*(5300), 668-670.
- Strong, S., Liew, G., & Michaelides, M. (2016). Retinitis pigmentosa-associated cystoid macular oedema: pathogenesis and avenues of intervention. *British journal of ophthalmology*.
- Sturm, V., Leiba, H., Menke, M. N., Valente, E. M., Poretti, A., Landau, K., & Boltshauser, E. (2010). Ophthalmological findings in Joubert syndrome. *Eye*, *24*(2), 222-225.

- Sultana, A. (2023). Role of fundus fluorescein angiography in identifying the unexplained visual loss due to macular edema in peripheral retinal diseases. *Indian Journal of Clinical and Experimental Ophthalmology*, 9(1), 53-59.
- Sunderland, D. K., & Sapra, A. (2022). Physiology, aqueous humor circulation. *StatPearls [Internet]*.
- Take-uchi, M., Clarke, J. D., & Wilson, S. W. (2003). Hedgehog signalling maintains the optic stalk-retinal interface through the regulation of Vax gene activity.
- Talib, M., Van Cauwenbergh, C., & Boon, C. J. (2022). Non-syndromic retinitis pigmentosa. *Clinical Ophthalmic Genetics and Genomics*, 162.
- Taqi, U., Fasih, U., Jafri, S. F. A., & Sheikh, A. (2011). Frequency of primary open angle glaucoma from Abbasi Shaheed Hospital. *JPMA-Journal of the Pakistan Medical Association*, 61(8), 778.
- Thenappan, A., Nanda, A., Lee, C. S., & Lee, S. Y. (2023). Retinitis Pigmentosa Masquerades: Case Series and Review of the Literature. *Journal of Clinical Medicine*, 12(17), 5620.
- Thiadens, A. A., Somervuo, V., van den Born, L. I., Roosing, S., van Schooneveld, M. J., Kuijpers, R. W., . . . Klaver, C. C. (2010). Progressive loss of cones in achromatopsia: an imaging study using spectral-domain optical coherence tomography. *Investigative ophthalmology & visual science*, 51(11), 5952-5957.
- Thiele, H., & Nürnberg, P. (2005). HaploPainter: a tool for drawing pedigrees with complex haplotypes. *Bioinformatics*, 21(8), 1730-1732.
- Thomson, B. R., Souma, T., Tompson, S. W., Onay, T., Kizhatil, K., Siggs, O. M., . . . Kalaydjieva, L. (2017). Angiopoietin-1 is required for Schlemm's canal development in mice and humans. *The Journal of clinical investigation*, 127(12), 4421-4436.
- Tibrewal, S., & Kekunnaya, R. (2018). Risk of anterior segment ischemia following simultaneous three rectus muscle surgery: results from a single tertiary care centre. *Strabismus*, 26(2), 77-83.
- Topper, S., Ober, C., & Das, S. (2011). Exome sequencing and the genetics of intellectual disability. *Clinical genetics*, 80(2), 117-126.
- Traverso, V., Kinkl, N., Grimm, L., Sahel, J., & Hicks, D. (2003). Basic fibroblast and epidermal growth factors stimulate survival in adult porcine photoreceptor cell cultures. *Investigative ophthalmology & visual science*, 44(10), 4550-4558.
- Tripathy, K., & Salini, B. (2023). Aniridia *StatPearls [Internet]*: StatPearls Publishing.
- Tsin, A., Betts-Obregon, B., & Grigsby, J. (2018). Visual cycle proteins: structure, function, and roles in human retinal disease. *Journal of Biological Chemistry*, 293(34), 13016-13021.
- Tuson, M., Marfany, G., & González-Duarte, R. (2004). Mutation of CERKL, a novel human ceramide kinase gene, causes autosomal recessive retinitis pigmentosa (RP26). *The American Journal of Human Genetics*, 74(1), 128-138.
- Ullah, E., Saqib, M. A. N., Sajid, S., Shah, N., Zubair, M., Khan, M. A., . . . Danda, S. (2016). Genetic analysis of consanguineous families presenting with congenital ocular defects. *Experimental eye research*, 146, 163-171.
- Untergasser, A., Cutcutache, I., Koressaar, T., Ye, J., Faircloth, B. C., Remm, M., & Rozen, S. G. (2012). Primer3—new capabilities and interfaces. *Nucleic acids research*, 40(15), e115-e115.
- Valleix, S., Niel, F., Nedelec, B., Algros, M.-P., Schwartz, C., Delbosc, B., . . . Kantelip, B. (2006). Homozygous nonsense mutation in the FOXE3 gene as a cause of congenital primary aphakia in humans. *The American Journal of Human Genetics*, 79(2), 358-364.
- van Huet, R. A., Pierrache, L. H., Meester-Smoor, M. A., Klaver, C. C., van den Born, L. I., Hoyng, C. B., . . . Klevering, B. J. (2015). The efficacy of microarray screening for

- autosomal recessive retinitis pigmentosa in routine clinical practice. *Molecular Vision*, 21, 461.
- Vargas, M., Mitchell, A., Yang, P., & Weleber, R. (2019). Bietti crystalline dystrophy.
- Vasiliou, V., & Gonzalez, F. J. (2008). Role of CYP1B1 in glaucoma. *Annu. Rev. Pharmacol. Toxicol.*, 48, 333-358.
- Venkatesh, A., Ma, S., Le, Y. Z., Hall, M. N., Rüegg, M. A., & Punzo, C. (2015). Activated mTORC1 promotes long-term cone survival in retinitis pigmentosa mice. *The Journal of clinical investigation*, 125(4), 1446-1458.
- Venselaar, H., Te Beek, T. A., Kuipers, R. K., Hekkelman, M. L., & Vriend, G. (2010). Protein structure analysis of mutations causing inheritable diseases. An e-Science approach with life scientist friendly interfaces. *BMC bioinformatics*, 11(1), 1-10.
- Verbakel, S. K., van Huet, R. A., Boon, C. J., den Hollander, A. I., Collin, R. W., Klaver, C. C., . . . Klevering, B. J. (2018). Non-syndromic retinitis pigmentosa. *Progress in retinal and eye research*, 66, 157-186.
- Verma, A. S., & FitzPatrick, D. R. (2007). Anophthalmia and microphthalmia. *Orphanet journal of rare diseases*, 2, 1-8.
- Vithana, E. N., Khor, C.-C., Qiao, C., Nongpiur, M. E., George, R., Chen, L.-J., . . . Low, S. (2012). Genome-wide association analyses identify three new susceptibility loci for primary angle closure glaucoma. *Nature genetics*, 44(10), 1142-1146.
- Wang, F., Wang, H., Tuan, H.-F., Nguyen, D. H., Sun, V., Keser, V., . . . Zhao, L. (2014). Next generation sequencing-based molecular diagnosis of retinitis pigmentosa: identification of a novel genotype-phenotype correlation and clinical refinements. *Human genetics*, 133, 331-345.
- Wang, I.-J., Lin, S., Chiang, T.-H., Chen, Z. T.-Y., Lin, L. L., Hung, T., & Shih, Y.-F. (2008). The association of membrane frizzled-related protein (MFRP) gene with acute angle-closure glaucoma—a pilot study. *Molecular Vision*, 14, 1673.
- Wang, X., Gregory-Evans, K., Wasan, K. M., Sivak, O., Shan, X., & Gregory-Evans, C. Y. (2017). Efficacy of postnatal in vivo nonsense suppression therapy in a Pax6 mouse model of aniridia. *Molecular Therapy-Nucleic Acids*, 7, 417-428.
- Waryah, Y. M., Iqbal, M., Sheikh, S. A., Baig, M. A., Narsani, A. K., Atif, M., . . . Pirzado, M. S. (2019). Two novel variants in CYP1B1 gene: a major contributor of autosomal recessive primary congenital glaucoma with allelic heterogeneity in Pakistani patients. *International journal of ophthalmology*, 12(1), 8.
- Weinreb, R. N., Aung, T., & Medeiros, F. A. (2014). The pathophysiology and treatment of glaucoma: a review. *Jama*, 311(18), 1901-1911.
- Weston, M., Eudy, J. D., Fujita, S., Yao, S.-F., Usami, S., Cremers, C., . . . Moller, C. (2000). Genomic structure and identification of novel mutations in usherin, the gene responsible for Usher syndrome type IIa. *The American Journal of Human Genetics*, 66(4), 1199-1210.
- Williamson, K. A., & FitzPatrick, D. R. (2014). The genetic architecture of microphthalmia, anophthalmia and coloboma. *European Journal of Medical Genetics*, 57(8), 369-380.
- Wong, W. L., Su, X., Li, X., Cheung, C. M. G., Klein, R., Cheng, C.-Y., & Wong, T. Y. (2014). Global prevalence of age-related macular degeneration and disease burden projection for 2020 and 2040: a systematic review and meta-analysis. *The Lancet Global Health*, 2(2), e106-e116.
- Wyatt, A., Bakrania, P., Bunyan, D. J., Osborne, R. J., Crolla, J. A., Salt, A., . . . Collin, J. R. O. (2008). Novel heterozygous OTX2 mutations and whole gene deletions in anophthalmia, microphthalmia and coloboma. *Human mutation*, 29(11), E278-E283.
- Yadav, V. (2019). Impact of Environmental Factors on Eye Health. *Mediterranean Journal of Basic and Applied Sciences (MJBAS), (Quarterly International Journal)*, 3(4), 37-46.

- Yang, H., Lu, W., & Sun, X. (2023). Primary congenital glaucoma: we are always on the way. *Taiwan Journal of Ophthalmology*.
- Yang, J., Wang, L., Song, H., & Sokolov, M. (2012). Current understanding of usher syndrome type II. *Frontiers in bioscience: a journal and virtual library*, 17, 1165.
- Yanoff, M., & Sassani, J. W. (2018). *Ocular pathology*: Elsevier Health Sciences.
- Yoon, C. K. (2022). Syndromic Retinitis Pigmentosa *Inherited Retinal Disease* (pp. 99-108): Springer.
- Yousaf, R., Ahmed, Z. M., Giese, A. P., Morell, R. J., Lagziel, A., Dabdoub, A., . . . Riazuddin, S. (2018). Modifier variant of METTL13 suppresses human GAB1-associated profound deafness. *The Journal of clinical investigation*, 128(4), 1509-1522.
- Zagozewski, J., Zhang, Q., & Eisenstat, D. (2014). Genetic regulation of vertebrate eye development. *Clinical genetics*, 86(5), 453-460.
- Zhang, P., Seth, A., & Fernandes, H. (2014). Other post-PCR detection technologies.
- Zhao, Y., Wang, S., Sorenson, C. M., Teixeira, L., Dubielzig, R. R., Peters, D. M., . . . Sheibani, N. (2013). Cyp1b1 mediates periostin regulation of trabecular meshwork development by suppression of oxidative stress. *Molecular and cellular biology*, 33(21), 4225-4240.
- Zupan, A., Fakin, A., Battelino, S., Jarc-Vidmar, M., Hawlina, M., Bonnet, C., . . . Glavač, D. (2019). Clinical and haplotypic variability of Slovenian USH2A patients homozygous for the c. 11864G> A nonsense mutation. *Genes*, 10(12), 1015.

# **ANNEXURE I**





قاہد اعظم یونیورسٹی

**QUAID-I-AZAM UNIVERSITY**

Faculty of Biological Sciences

Bioethics Committee

No. #BEC-FBS-QAU2017-

Date: 13-10-2017

**Dr. Sabika Firasat**  
**Assistant Professor**  
**Department of Animal Sciences**  
**Q.A.U Islamabad**

Subject:- **Molecular genetic characterization of prevalent eye disorders in children from Pakistani population**

Dear Dr. Sabika Firasat

We wish to inform you that your subject research study had been reviewed and is hereby granted approval for implementation by Bio-Ethical Committee (BEC) of Quaid-i-Azam University, Your study had been assigned protocol #BEC-FBS-QAU2017-

While the study is in progress, please inform us of any adverse events or new, relevant information about risks associated with the research. In case changes have to be made to the study procedure, the informed consent from and or informed consent process, the BEC must review and approve any to these changes prior to implementation.

Sincerely,

**Prof. Dr. Bushra Mirza**  
**Chairperson Bioethics Committee**

**Cc:**  
**Dean, F.B.S**

# **ANNEXURE II**



**QUAID-E-AZAM UNIVERSITY**

**Faculty of Biological Sciences**

**ISLAMABAD, PAKISTAN**

**Molecular Biology Lab**

**The Record of patients presented at Hospital is as follows:**

- Name: \_\_\_\_\_
- Father's name: \_\_\_\_\_
- Hospital file number: \_\_\_\_\_
- District \_\_\_\_\_ Tehsil \_\_\_\_\_ City \_\_\_\_\_
- Address:  
\_\_\_\_\_  
\_\_\_\_\_  
\_\_\_\_\_
- Phone number: \_\_\_\_\_
- Age \_\_\_\_\_
- Gender \_\_\_\_\_
- Cast \_\_\_\_\_
- Diagnosis \_\_\_\_\_
- Treatment \_\_\_\_\_
- Other associated eye problems \_\_\_\_\_
- Any other disease \_\_\_\_\_

**Annexure - B**

**Clinical Examination**

1. V/A<sub>sc</sub> (Vision Assessment Without Glasses):
2. V/A<sub>cc</sub> (Vision Assessment With Glasses):
3. Refractive Error:

i. Hyperopia

ii. Myopia

iii. Astigmatism

4. Signs and Symptoms: \_\_\_\_\_

5. Age of Onset: \_\_\_\_\_

6. Associated Systemic Features: \_\_\_\_\_

7. Eye Examination:

a. Nystagmus: Yes / No

b. Keratoconus: Yes / No

c. Squint: Yes / No

8. Intraocular Pressure (I.O.P): \_\_\_\_\_

9. Anterior Segment Findings: \_\_\_\_\_

10. Retinal Findings:

a. Disc: \_\_\_\_\_





b. Macula: \_\_\_\_\_

c. Pigmentary Changes: \_\_\_\_\_

11. Fundus Photographs:

Article

# Exome Sequencing Identified Molecular Determinants of Retinal Dystrophies in Nine Consanguineous Pakistani Families

Raeesa Tehreem <sup>1</sup>, Iris Chen <sup>2</sup>, Mudassar Raza Shah <sup>1</sup>, Yumei Li <sup>2</sup>, Muzammil Ahmad Khan <sup>3,4</sup>, Kiran Afshan <sup>1</sup>, Rui Chen <sup>2,\*</sup> and Sabika Firasat <sup>1,\*</sup>

<sup>1</sup> Department of Zoology, Faculty of Biological Sciences, Quaid-i-Azam University, University Road, Islamabad 45320, Pakistan

<sup>2</sup> Department of Molecular and Human Genetics, Baylor College of Medicine, Houston, TX 77030, USA

<sup>3</sup> Gomal Center of Biochemistry and Biotechnology, Gomal University, Dera Ismail Khan 29111, Pakistan

<sup>4</sup> Department of Human Genetics, Sidra Medicine, Doha P.O. Box 26999, Qatar

\* Correspondence: ruichen@bcm.edu (R.C.); sabika.firasat@qau.edu.pk (S.F.);  
Tel.: +(713)-798-5194 (R.C.); +92-51-9064-4410 (S.F.)

**Abstract:** Inherited retinal dystrophies (IRDs) are a heterogeneous group of degenerative disorders of the retina. Retinitis Pigmentosa (RP) is a common type of IRD that causes night blindness and loss of peripheral vision and may progress to blindness. Mutations in more than 300 genes have been associated with syndromic and non-syndromic IRDs. Recessive forms are more frequent in populations where endogamy is a social preference, such as Pakistan. The aim of this study was to identify molecular determinants of IRDs with the common presentation of night blindness in consanguineous Pakistani families. This study included nine consanguineous IRD-affected families that presented autosomal recessive inheritance of the night blindness phenotype. DNA was extracted from blood samples. Targeted exome sequencing of 344 known genes for retinal dystrophies was performed. Screening of nine affected families revealed two novel (c.5571\_5576delinsCTAGATand c.471dup in *EYS* and *SPATA7* genes, respectively) and six reported pathogenic mutations (c.304C>A, c.187C>T, c.1560C>A, c.547C>T, c.109del and c.9911\_11550del in *PDE6A*, *USH2A*, *USH2A*, *NMNAT1*, *PAX6* and *ALMS1* genes, respectively) segregating with disease phenotype in each respective family. Molecular determinants of hereditary retinal dystrophies were identified in all screened families. Identification of novel variants aid future diagnosis of retinal dystrophies and help to provide genetic counseling to affected families.

**Keywords:** retinaldystrophies; night blindness; homozygous sequence variants; autosomal recessive



**Citation:** Tehreem, R.; Chen, I.; Shah, M.R.; Li, Y.; Khan, M.A.; Afshan, K.; Chen, R.; Firasat, S. Exome Sequencing Identified Molecular Determinants of Retinal Dystrophies in Nine Consanguineous Pakistani Families. *Genes* **2022**, *13*, 1630. <https://doi.org/10.3390/genes13091630>

Academic Editors: Christina Zeitz and Selvarangan Ponnazhagan

Received: 3 June 2022

Accepted: 7 September 2022

Published: 10 September 2022

**Publisher's Note:** MDPI stays neutral with regard to jurisdictional claims in published maps and institutional affiliations.



**Copyright:** © 2022 by the authors. Licensee MDPI, Basel, Switzerland. This article is an open access article distributed under the terms and conditions of the Creative Commons Attribution (CC BY) license (<https://creativecommons.org/licenses/by/4.0/>).

## 1. Introduction

Inherited retinal dystrophies (IRDs) are degenerative eye disorders causing substantial loss of vision and even blindness [1]. The most common inheritable retinal dystrophy is retinitis pigmentosa (RP), which is characterized by the degradation of photoreceptors, predominantly rods and secondarily tightly packed cones [2]. In the initial stage of disease, night vision is reduced, followed by loss of peripheral vision in the diseased individuals [3]. Different values of prevalence are reported from various regions worldwide; from 1:372 in rural regions of South India [4] to 1:9000 in Korea [5]. RP can be present in both non-syndromic and syndromic forms. In non-syndromic forms, it can be inherited in autosomal pattern (dominant/recessive), X-linked pattern (dominant/recessive), mitochondrial inheritance or sporadic cases [6]. Syndromic forms of RP such as Bardet–Biedl syndrome (MIM no. 209900) and Usher syndrome (MIM no. 276901) are associated with extra ocular abnormalities and are reported in almost 20–30% cases [3].

Significant overlap at both the clinical and molecular level is observed between different forms of IRDs. For example, early onset RP can be detected at the age of 2 years and could overlap with Leber's congenital amaurosis (LCA) (MIM # 204000) [2], but in

most cases symptoms manifest in adolescence [1]. LCA is a severe autosomal recessive retinopathy [7] that presents in children by birth or in early years of life [8]. Nyctalopia is the earliest clinical symptom experienced by a patient, followed by photophobia, loss of visual acuity, abnormal fundus, bone spicules deposition, tunnel vision, waxy pallor of optic nerve, attenuated retinal vessels and abnormal or absent a- and b- wave amplitudes in electroretinogram (ERG) [9]. Heterogeneity of clinical findings in IRDs is partially due to the involvement of different genes and alleles. Until now, more than 80 genes have been associated with non-syndromic forms of RP, which function in diverse pathways [1]. Similarly, fourteen genes are reported to cause LCA, encoded proteins which are involved in the development and physiology of the visual pathway such as CRB1 (photoreceptor morphogenesis), CRX (retinal development), MERTK (RPE phagocytosis), RDH12 (retinal reductase), LRAT (Lecithin Retinol Acyltransferase), RPE65 (vitamin A metabolism) RPGRIP1L (cilium formation) [10,11] NMNAT1 (protein multimerization) [12], GUCY2D (Guanylate Cyclase 2D) and AIPL1 (phototransduction) [13]. In families of Pakistani origin, most of the mutations in IRDs patients are reported in genes encoding the PDE6A, PDE6B, ABCA4, RHO, SPATA7, TULP1 and RP1 protein [14].

Syndromic forms of IRDs also show heterogeneity, as 15 genes are associated with Usher syndrome [15] and 20 genes (BBS1-BBS20) are reported for Bardet-Biedl syndrome [16]. Usher syndrome (USH) is an autosomal recessive form of RP that is accompanied by hearing impairment and functional abnormality of the vestibular system [17]. Characterization into subtypes USH type I (MIM no. 276900), USH type II (MIM no. 276901) and USH type III (MIM no. 276902) is based on intensity of hearing loss, onset of RP and presence or absence of vestibular dysfunction. Although USH is heterogeneous [18], the *USH2A* gene is the most frequently mutated and accounts for 74% to 90% cases of UHS type II [19]. Proteins coded by Usher genes are usually expressed in transmembrane regions, scaffolding proteins and in motor transport. Predominantly, nonsense and splice site mutations result in syndromic conditions in affected cases [20,21].

Prevalence of consanguinity is very high in Pakistan [4], resulting in the high prevalence of recessive forms of IRD. Due to the high genetic heterogeneity, the conventional molecular diagnostic method, e.g., Sanger's sequencing, is not cost effective. Therefore, the current study was designed to investigate the molecular determinants of IRD phenotypes in the Pakistani population using Next Generation Sequencing (NGS) technology to perform panel sequencing targeting exons of 344 known inherited retinal disease genes. In this study, nine consanguineous families suffering from IRDs, each having at least three or more affected individuals, were analyzed.

## 2. Materials and Methods

### 2.1. Enrollment of Patients for Study

Nine familial cases of inherited retinal dystrophies, clinically assessed by ophthalmologists, were recruited from Dera Ismail Khan, Khyber Pakhtunkhwa (KPK) Pakistan following the Declaration of Helsinki [22,23]. Approval was received from the Bioethical review Committee (BEC) of Quaid-i-Azam University (QAU) Islamabad before beginning the study. Blood samples were collected from patients and phenotypically normal family members. Clinical data of each proband, family history of disease and data regarding any other disorder in family member/s were also recorded after informed consent (Table 1). Inclusion criteria for patients recruited after ophthalmological assessment was based on the symptom of night blindness and recessive mode of inheritance. HaploPainter (<http://haploPainter.sourceforge.net/index.html> (accessed on 5 April 2021)) [24] was used to draw pedigrees of all families, with a unique identification number given to each family (Figures 1 and 2 and Supplementary Figures S1 and S2).

**Table 1.** Demographic and clinical data of nine inherited retinal dystrophies affected families enrolled for this study.

Family ID	Proband ID	Age of Onset	Age at Enrollment	No of Affecteds	Consanguinity	Family History	Disease Progression	Symptoms
RP 101	III.IV	By birth	41 years	5	YES	Positive	Stationary	Night blind
RP102	IV.I	9 years	40 years	3	YES	Positive	Progressive	Night blind, Hearing loss
RP105	V.IV	14 years	26 Years	3	YES	Positive	Progressive	Night blind, Myopia, Hearing loss
RP106	V.II	By birth	7 Years	6	YES	Positive	Stationary	Night blind, Uncontrolled body movements
RP107	IV.XIII	12 years	30 years	9	YES	Positive	Progressive	Night blind, Epiphora, Myopia, Blurred vision
RP109	IV.I	2–6 years	15 years	3	YES	Positive	Progressive	Night blind, Nystagmus, Hearing problem, Poor day vision
RP110	V.IV	By birth	32 years	5	YES	Positive	Progressive	Night blind, Photosensitive, Nystagmus, Poor day vision
RP112	V.VIII	By birth	45 years	4	YES	Positive	Progressive	Night blind, Maculopathy
RP113	IV.III	By birth	22 years	5	YES	Positive	Progressive	Night blind, Maculopathy

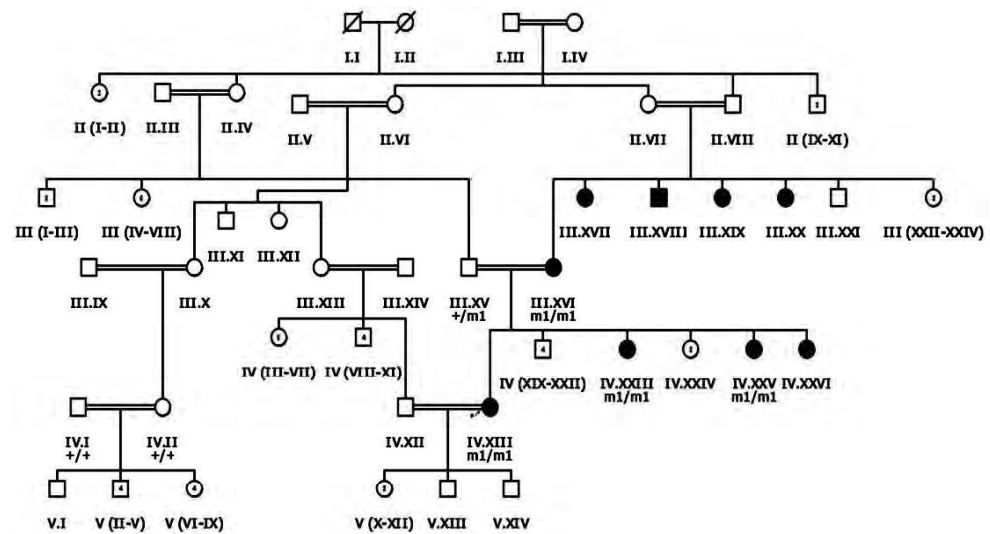


**Figure 1.** Pedigree drawing of inherited retinal dystrophy family, i.e., RP107 showing autosomal recessive pattern of phenotype in which the novel disease-causing variant in the EYS gene was detected. Squares and circles denote males and females, respectively. Filled symbols show affected, while unfilled symbols show unaffected individuals. Double lines indicate consanguineous union. M1/m1 refers to the homozygous disease-causing variant, whereas m1/+ and +/+ refers to heterozygous carrier and homozygous normal status, respectively.

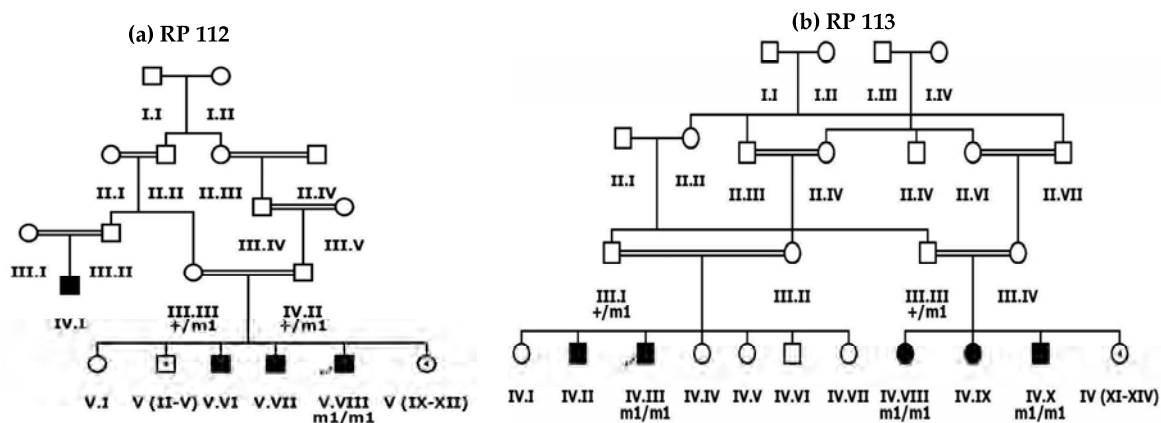


**Figure 2.** Pedigree drawings of inherited retinal dystrophies families, i.e., (a) RP112 and (b) RP113 showing autosomal recessive pattern of phenotype in which the novel disease-causing variant in the *SPATA7* gene was detected. Squares and circles denote males and females, respectively. Filled symbols show affected, while unfilled symbols show unaffected individuals. Double lines indicate consanguineous union. m1/m1 refers to the homozygous disease-causing variant, whereas m1/+ refers to heterozygous carrier status.

### 2.2. Sample Collection, DNA Extraction and Targeted Exome Sequencing

Peripheral blood samples were collected in 5ml ethylene diamine tetra acetic acid (EDTA) vacutainers and stored at  $-20^{\circ}\text{C}$ . To extract genomic DNA from blood samples, a non-organic method of DNA extraction described by Kaul et al., 2010 [25] was used. Nano Drop (Thermo Scientific NanoDrop spectrophotometers, Waltham, MA, USA) was performed to quantify DNA and assess its purity at the Department of Zoology, Quaid-i-Azam University, Islamabad, Pakistan. For NGS panel capture sequencing, DNA samples were shipped to Baylor College of Medicine, USA. The sequencing library was generated using KAPA HyperPrep Kit (Roche, Basel, Switzerland) following the manufacturer's protocol, then pooled together for targeted enrichment of a panel of 344 known and candidate inherited retinal diseases related genes (Supplementary Table S1) with the SureSelect Target Enrichment System for the Illumina Platform (Agilent, Santa Clara, CA, USA) [23]. Captured DNA was quantified and sequenced using a Novaseq 6000 (Illumina, San Diego, CA, USA). All these procedures were conducted at the Functional Genomics Core at Baylor College of Medicine, USA.

### 2.3. Bioinformatics Analysis

Sequencing data was processed following the previous methods [23]. Briefly, the fastq read files were aligned to the hg19 human reference genome using bwa. Aligned reads were recalibrated and realigned using GATK. Variants were called using GATK. All variants were filtered against dbSNP, 1000 Genome Projects, gnomAD V2.1.1 and BCM\_HGSC internal database. Variants passing the filtering steps were evaluated according to the ACMG standards and guidelines for variant interpretation. Previously reported pathogenic mutations were identified through searching HGMD, ClinVar and LOVD databases. Novel variants were evaluated for their potential impact on protein function using various in silico tools. Nonsense, frame-shift and splicing mutations were classified as likely loss-of-function alleles. Missense variants were evaluated based on features such as sequence conservation and in silico predictions.

### 2.4. Sanger's Validation and Segregation Test

Each candidate pathogenic variant was validated via direct Sanger's sequencing. Primers were designed using the Primer3 software (<https://bioinfo.ut.ee/primer3-0.4.0/>) (accessed on 15 September 2021) to amplify the region containing the variant with at least



50 flanking base pairs. Sanger's sequencing and segregation test was performed on the amplified fragments for the affected proband, other affected members and non-affected members of each family based on availability of DNA samples. For the confirmation of previously reported large deletion, primers were adopted from Nikopoulos et al., 2015 [26] to exactly define the break points for the deleted region in a control and an affected individual of family RP109. Furthermore, for segregation testing of a large deletion identified in RP109, primers were designed using the Primer3 software to amplify the deleted region in a control and affected samples (Supplementary Table S2).

### 3. Results

In the current study, nine large multigenerational consanguineous families with inherited retinal dystrophies were enrolled from different regions of Dera Ismail Khan, KPK, Pakistan. Each enrolled family has multiple affected individuals (Figures 1 and 2 and Supplementary Figures S1 and S2).

Families RP105 and RP109 had three affected individuals, while RP112 had four, RP101, RP110 and RP113 had five, RP102 and RP106 had six and RP107 had nine affected members. The phenotypic onset of disease in proband of enrolled families ranged from birth to the second decade of life (Table 1). In families RP101, RP106, RP110, RP112 and RP113, probands (III.IV, V.II, V.IV, V.VIII and IV.III, respectively) were affected by birth (Figure 2 and Supplementary Figure S1). Individual IV.I in family RP102 and IV.I in family RP109 were affected in the first decade of life, while V.IV in family RP105 and IV.XIII in family RP107 were affected in the second decade of life (Figure 1 and Supplementary Figures S1 and S2). Average age of proband at the time of enrollment was 28 years (Table 1).

In addition to the retinal phenotypes shared by affected individuals of all families, such as night blindness, poor day vision and photosensitivity, three (RP102, RP105 and RP109) out of nine families were suffering from syndromic disease. The affected individuals of families RP102, RP105 and RP109 were also suffering from progressive hearing loss. Nystagmus is observed in the affected individuals of family RP109. Fundus examination of probands of all affected families showed typical symptoms, including bone spicule formation, waxy pale discs and attenuation of vessels. Fundus photograph and audiometry findings of one affected individual (V.II) of family RP105 are shown in Figure 3 (Figure 3a,b).

To identify the underlying mutations of these families, NGS capture panel sequencing was performed on the proband of each family to screen for mutations in known inherited retinal diseases related genes. A total of 8 diverse types of pathogenic mutations from 7 different genes were identified, including 2 missense, 3 nonsense, 2 frameshift indel and 1 large deletion (Table 2, Figure 4 and Supplementary Figure S2).

Among them, six pathogenic variants were previously reported, while the remaining two were novel. Consistent with the nature of consanguineous families, 7 of 8 variants are homozygous mutations in recessive genes. Surprisingly, a heterozygous pathogenic mutation in *PAX6* is identified in family RP110 (Figure 4F).

The proband III.IV from the RP101 family was 41 years old at the time of enrollment for this study. Detailed interview of the patient revealed onset of RP phenotype in early childhood with initial complaints of poor night vision and then progressive loss of day vision. Mutation screening identified a homozygous missense variant c.304C>A (p.Arg102Ser) in the *PDE6A* gene which affects a highly conserved residue (Figure 4A). This variant is rare, with a population frequency of 0.016% according to the gnomAD database. Consistently, segregation testing in five affected family members indicated that mutation co-segregates with the retinal disease phenotype.

**Table 2.** List of previously reported and novel pathogenic variants identified in nine unrelated inherited retinal dystrophies families segregating with disease phenotype in recessive form.

Family ID	Disease	NM_ID	cDNA Change	Protein Change	Gene	Genotype Status	Allele Type	Reference	ACMG Prediction
RP101	RP	NM_000440	c.304C>A	p.Arg102Ser	<i>PDE6A</i>	Homozygous	Known missense	[27,28]	Likely Pathogenic
RP102	USH	NM_206933	c.187C>T	p.Arg63 *	<i>USH2A</i>	Homozygous	Known stop-gain	[29]	Pathogenic
RP105	USH	NM_206933	c.1560C>A	p.Cys520 *	<i>USH2A</i>	Homozygous	Known stop-gain	[30]	Pathogenic
RP106	LCA	NM_022787	c.547C>T	p.Leu183Phe	<i>NMNAT1</i>	Homozygous	Known missense	rs1337014971	Likely Pathogenic
RP107	RP	NM_001142800	c.5571_5576 delinsCTAGAT	p.Leu1858 *	<i>EYS</i>	Homozygous	Novel stop-gain	N/A	Pathogenic
RP109	AS	NM_015120	c.9911_11550 del	p.Asn3306Lysfs *7	<i>ALMS1</i>	Homozygous	Known deletion	[26]	Pathogenic
RP110	Aniridia	NM_001258465	c.109del	p.Ala37Profs *17	<i>PAX6</i>	Heterozygous	Known frameshift	[31]	Pathogenic
RP112	LCA	NM_001040428	c.471dup	p.Pro158Alafs *39	<i>SPATA7</i>	Homozygous	Novel frameshift	N/A	Pathogenic
RP113	LCA	NM_001040428	c.471dup	p.Pro158Alafs *39	<i>SPATA7</i>	Homozygous	Novel frameshift	N/A	Pathogenic

\* RP: Retinitis Pigmentosa, USH: Usher Syndrome, LCA: Leber's Congenital Amaurosis, AS: Alstrom Syndrome, N/A: Not Available.

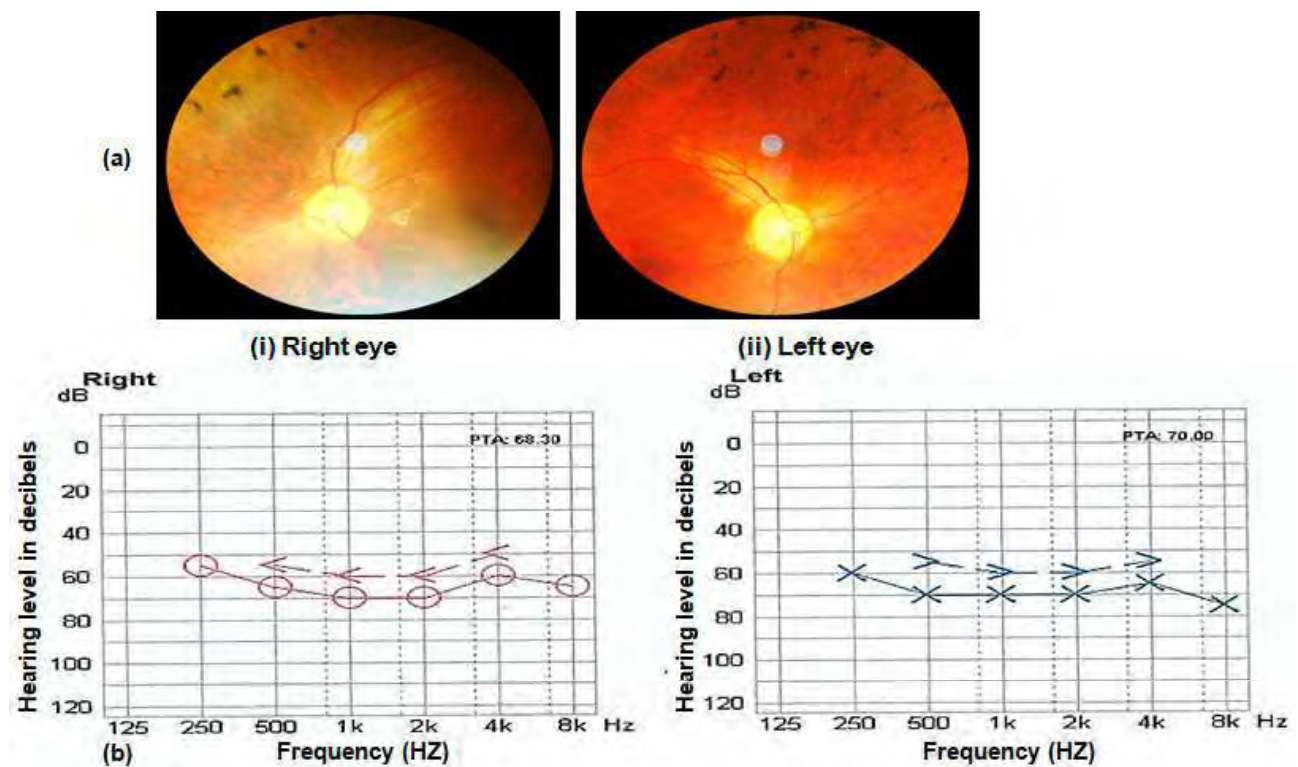


**Figure 3.** (a) Fundus photograph of left and right eye of an affected individual (V.II of RP105) showing pale optic disc, bony spicules and thin blood vessels characteristic of RP phenotype. (b) Audiometry report of an affected individual (V.II of RP105) performed at 14 years. The x-axis on graphs shows the frequency in hertz, and the y-axis shows hearing level in decibels (dB). Note the hearing loss in the range of 50–80 dB in both ears of the Usher patient.

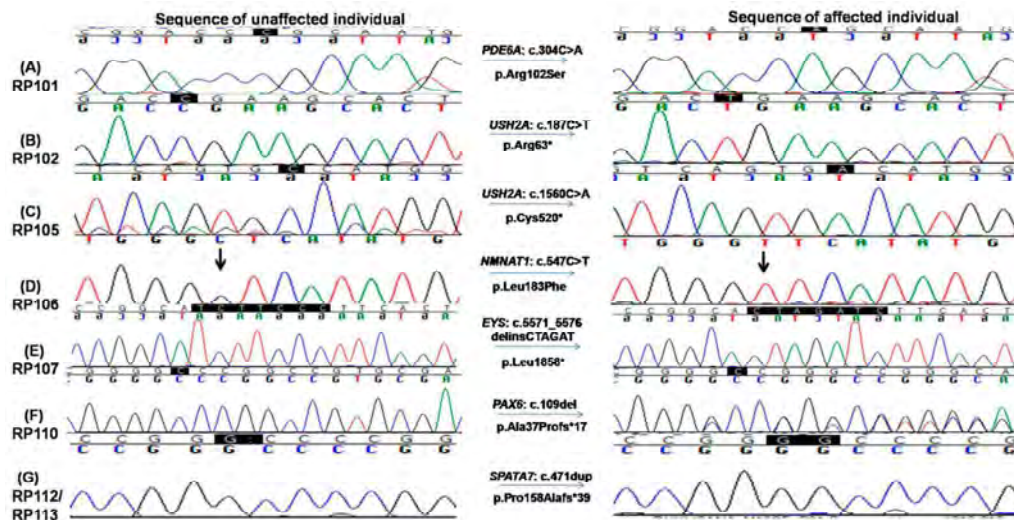


**Figure 4.** Chromatograms of known and novel disease causing variants (single nucleotide substitution/s, deletion, duplication and small INDELS) identified in this study, i.e., (A) c.304C>A in RP101, the homozygous sequence is shown on the left and homozygous mutated on the right (proband III.IV), (B) c.187C>T in RP102 showing homozygous normal on the left side and homozygous mutated on the right (proband IV.I) and (C) c.1560C>A in RP105 the homozygous wild-type sequence is shown on the left, whereas homozygous mutated on the right side (proband V.IV). (D) c.547C>T in RP106, homozygous mutated sequence is shown on the right, while homozygous normal sequence is present on the left (proband V.II); (E) c.5571\_5576delinsCTAGAT in RP107 is shown on the right, whereas the sequence of normal individuals is shown on the left side; (F) c.109del in RP110 showing heterozygous mutated sequence on the right while wild-type sequence is shown on the left; and (G) c.471dup in RP112 and RP113, heterozygous mutated sequence is shown on the right, while normal sequence is on the left side.

Two homozygous nonsense mutations in the *USH2A* gene, i.e., c.187C>T: p.Arg63\* and c.1560C>A: p.Cys520\*, were found in RP102 and RP105, respectively (Figure 4B,C). Consistent with the molecular diagnosis, patients from both families exhibit RP and hearing loss. The p.Arg63\* variant in RP102 is a reported pathogenic mutation with a low population frequency of 0.001% in gnomAD. Segregation testing was carried out for the three affected and five unaffected family members, and perfect segregation between the mutations with the disease phenotype was observed (Figure 4B). One RP-affected (V.I) and two unaffected (V.III and a paternal aunt of IV.I) family members had mental retardation phenotype, which needs further investigation to find its causes. The stop-gain mutation p.Cys520\* identified in family RP105 suffering from Usher syndrome is also previously reported [30,32] and likely to be pathogenic as it is predicted to result in a truncated protein that is approximately 10% of the normal size. As a premature truncation, the mRNA is likely to undergo nonsense-mediated decay. Segregation testing for the RP105 family was carried out in three affected and three phenotypically normal family members, and the mutation co-segregated with all patients (Figure 4C and Supplementary Figure S1).

The affected individual of family RP106 carried a known homozygous missense variant, i.e., c.547C>T; p.Leu183Phe in the *NMNAT1* gene (Figure 4D). This variant is likely to be pathogenic as (1) it is rare in population and is only observed once in the gnomAD database with an estimated frequency of 0.0004%; (2) the variant is conserved from chicken to human; (3) multiple in silico prediction programs suggested it is deleterious with a CADD score of 22. Consistently, segregation testing in four affected and five unaffected members of the family showed that this variant co-segregates with the disease phenotype (Figure 4D and Supplementary Figure S1).

A novel homozygous variant in exon 6 in the *EYS* gene, i.e., c.5571\_5576delinsCTAGAT: p.Leu1858\*, that leads to a premature stop codon was identified in RP107 (Figure 4E). This variant is likely to be pathogenic as the early termination removes approximately 40% of the protein, including all the laminin G-like domains. Alternatively, due to the premature stop codon, the mRNA may undergo nonsense-mediated decay. This variant is rare in population, and it has not been observed in the gnomAD database. Segregation of the mutation with the disease is observed for this family by genotyping four affected and three unaffected family members, further supporting the pathogenicity of this variant (Figure 4E, Supplementary Figure S3A).

One homozygous previously reported large deletion, i.e., c.9911\_11550del, resulting in loss of four exons (exons 13–16) causing p.Asn3306Lys\*7 was identified in the *ALMS1* gene in family RP109. This deletion was validated by performing PCR testing using a pair of primers adopted from Nikopoulos et al., 2015 (Supplementary Figure S2c) [26] and four primer pairs, one for each of exon 13–16 (Supplementary Table S2). These PCRs confirmed the exact break points of the deleted sequence (chr2: 73,772,326–73,813,432, Supplementary Figure S2c) as well as failure to obtain the band of the targeted region with patients' DNA as a template confirmed segregation of mutation (Supplementary Figure S2b). This variant has not been observed in the gnomAD database and is pathogenic according to ACMG classification. The affected patient in RP110 carried a known heterozygous frameshift mutation, i.e., c.109del; p.Ala37Profs\*17 in *PAX6* gene (Figure 4F). This mutation is absent from the gnomAD database. Segregation testing for the family was carried out for two affected and two unaffected family members, confirming the segregation of the mutant allele with the disease phenotype (Figure 4F, Supplementary Figure S3B).

The same homozygous insertion that leads to a novel frameshift mutation, i.e., c.471dup causing p.Pro158Alafs\*39 in exon 5 of the *SPATA7* gene, was found in two families, i.e., RP112 and RP113 (Figure 4G). This frameshift mutation has not been observed in the gnomAD database. A segregation test was carried out in families RP112 and RP113 for four affected and their parents. All affected members are homozygous for the mutation, while unaffected parents are carriers of the mutant allele (Figure 4G, Supplementary Figure S3C). The affected individuals of both families had severe phenotypes as all affected were suffering from LCA by birth. The age of affected individuals ranged from 5 to 50 years at the time of enrollment for this study. The youngest affected individual (IV.VIII) of RP113 was five years old at the time of enrollment for this study and had bilateral blindness with nystagmus.

#### 4. Discussion

Pakistan has one of the highest rates of inherited genetic diseases in the world, consistent with the prominence of consanguinity within the society, harboring one of the highest rates of blindness and vision impairment as well. However, despite the high prevalence of IRDs in the population, limited studies on the genetic spectrum of IRDs have been undertaken in the region, likely because of underdevelopment, socio-economic limitations and lack of proper medical infrastructure or resources in the country. Furthermore, several studies in recent years indicate that a large portion of mutations were highly specific to families of Pakistani descent [33]. Therefore, the data represented in this study provides important insight into the genetic landscape of IRDs in Pakistan, providing valuable resources for both affected populations residing in the region and medical researchers from around the world. Results of this study will assist with future research of patients in this region, instigating the application of gene therapy techniques to assist families seeking treatment in this relatively underdeveloped country.

The data presented in this study identified the disease-causing genetic variants in a cohort of nine Pakistani families. A total of eight distinct pathogenic variants in seven genes were identified, including two missense, three nonsense, one frameshift indel and one deletion allele (Figure 4, Supplementary Figures S2 and S3). There is significant mutation heterogeneity within the population, considering that only the *SPATA7* and *USH2A*

genes were repeated in more than one family. This high heterogeneity within the cohort urges extensive studies involving Pakistani families using comprehensive molecular diagnostic approaches to further explore genetic components to form a better understanding of disease mechanisms and identify founder mutations for the development of suitable treatment options [34]. One interesting observation from this study was that two families carry the same novel *SPATA7* pathogenic mutations, in contrast to the general reported rarity of mutations in *SPATA7* as a cause of retinal dystrophy [35]. These data suggest a unique mutation spectrum of IRDs in the study population. In family RP102, other phenotypic abnormalities such as mental retardation and acute leukemia were also observed, suggesting the involvement of some other genetic variant running in the family (Supplementary Figure S1b).

Among the eight pathogenic mutations detected in this study, six of them have been reported. A variant c.304C>A: p.Arg102Ser in *PDE6A* detected in RP101 is rare and was previously reported by Maria et al., 2015, Ullah et al., 2016 and Khan et al., 2021 [28,36] in families from Pakistan. This variant has been reported as a pathogenic mutation as it has been observed in multiple patients with autosomal recessive retinitis pigmentosa [27,28,36,37]. The stop-gain variant c.187C>T: p.Arg63\* in *USH2A* is common and has been observed in individuals with Usher Syndrome [29,38,39]. Previously, this variant has been reported from different regions of the world, i.e., China [37], Spain [38], Denmark [39] and Italy [40]. Another cytosine to adenine substitution, i.e., c.1560C>A (p.Cys520\*) in *USH2A* identified in family RP 105 in this study, was also reported previously in the Spanish population by González-del Pozo et al. in 2018 as a heterozygous allele in a non-syndromic retinitis pigmentosa patient along with another heterozygous variant c.2276G>T: p.Cys759Phe. Previous studies also indicate that mutations in *USH2A* can result in a broadly variable clinical outcomes between patients varying from non-syndromic IRD to Usher phenotype [41]. The same observation is reported for the genes implicated in Bardet–Biedl syndrome. Interestingly, a frame shift mutation in *USH2A* at the same position (p.Cys520Alafs\*71) has also been reported to be pathogenic [29,42–44].

A large deletion encompassing a ~41.1Kb region of the *ALMS1* gene, i.e., c.9911\_11550del identified in family RP109, has been previously reported by Nikopouloset al. in 2015 in two affected siblings of a consanguineous Pakistani family [26]. Interestingly, the family reported by Nikopouloset al. in 2015 and RP109 both belonged to the KPK province of Pakistan but are unrelated. Upon comparison of disease phenotype, it was found that affected members of RP109 also had acanthosis nigricans, obesity, vision and hearing loss since early childhood; however, we could not get them tested for renal function, cardiomyopathy and hepatomegaly as patients refused to cooperate. According to the Human Genome Mutation Database (<http://www.hgmd.cf.ac.uk> (accessed on 1 September, 2022)), there are 10 reported large deletions in the *ALMS1* gene, among which three include deletion of region comprising exons 13–16. Monzo et al. (2017) identified a 38Kb deletion comprising exon 13-16 of the *ALMS1* gene in a Pakistani female Alstrom-syndrome-affected case [45]. They used Sanger's sequencing and the SNPs/CNVs microarray approach to define the exact location of deleted nucleotides, as well as showed that a long contiguous stretch (8.24 Mb) of homozygosity is centered in *ALMS1* sequence from the Pakistani population. According to Monzo et al.'s (2017) findings, the deletion of exons 13-16 is fixed in Pakistani recurrent haplotype, specifically in cases from northern Pakistani areas, i.e., KPK [45], and our findings support this notion.

The heterozygous variant, i.e., c.109del leading to p.Ala37Profs17 detected in exon 5 of *PAX6* gene in family RP110, is reported to cause nonsense-mediated decay [46]. This disease-causing variant has previously been reported as causative of aniridia [47], and the same phenotype was detected in cases of the RP110 family. In the *PAX6* gene, most of the detected variants are in heterozygous condition that partially disrupts the protein, suggesting haplo-insufficiency is enough for loss of *PAX6* function [48].

As 25% of the pathogenic variants identified in this study are novel, however, future studies using a large number of familial cases are required to reveal population-specific

disease-causing variants. Given that known alleles are notably easier to interpret than novel alleles due to limitations from lack of data for the latter, it is a requisite to construct a substantial database for Pakistani cohorts to improve the ability of interpretation for future studies. It is evident that additional sequencing of this population is essential for the future expansion of research and genetic counseling in Pakistan.

**Supplementary Materials:** The following supporting information can be downloaded at: <https://www.mdpi.com/article/10.3390/genes13091630/s1>, Figure S1: Pedigree drawings of inherited retinal dystrophy families in which known mutations were detected, i.e., RP101 RP102, RP105, RP106 and RP110 showing autosomal recessive pattern of phenotype. Squares and circles denote males and females, respectively. Filled symbols show affected, while unfilled symbols show unaffected individuals. Double lines indicate consanguineous union. m1/m1, m2/m2, m3/m3, m4/m4 and m5/m5 refer to the homozygous disease-causing variants c.304C > A, c.187C>T, c.1560C>A, c.547C>T and c.109del, respectively, whereas m/+and +/+ refer to heterozygous carrier and homozygous normal status. Figure S2: (a) Pedigree drawing of inherited retinal dystrophy family RP109 showing autosomal recessive pattern of phenotype. Squares and circles denote males and females, respectively. Filled symbols show affected, while unfilled symbols show unaffected individuals. m1/m1 refers to the homozygous disease-causing variant, whereas m1/+ refers to heterozygous carrier status. (b) Validation of deletion, i.e., c.9911\_11550del found in RP109 in the *ALMS1* gene by PCR testing. Four pairs of primers for exonic region 13–16 were used. Four primer pairs, i.e., Exon 13, Exon 15, Exon 16-1 and Exon 16-2, failed to amplify the region in patient DNA due to this deletion, however, in positive control, both the DNA of the patient and wild-type individual were amplified, as shown in the last wells of the gel photograph. (c) Sanger sequencing results confirming the exact breakpoints of gross deletion, i.e., c.9911\_11550del found in RP109 in the *ALMS1* gene. Figure S3: (A) Segregation testing for novel homozygous deletion variant c.5571\_5576delinsCTAGAT: p.Leu1858\* found in RP107 in four affected (i–iv) and three unaffected (v–vii) family members. (B) Segregation testing for heterozygous variant c.109del: p.Ala37Profs\*17 found in RP110 in two affected (i,ii) and two unaffected (iii,iv) family members. (C) Segregation testing results for homozygous duplication c.471dup: p.Pro158Alafs\*39 checked in RP113 in four affected (i–iv) and two unaffected (v,vi) family members. Table S1: List of 344 genes screened through targeted exome sequencing in this study. Table S2: A list of primers used to amplify *ALMS1* gene exonic region (exon 13–16) to confirm gross deletion, i.e., c.9911\_11550del in RP109.

**Author Contributions:** S.F., K.A. and R.C. contributed to the study conception and design. M.R.S. and M.A.K. enrolled families and collected data. R.T., I.C., M.R.S. and Y.L. performed experiments. R.T., I.C., M.R.S., Y.L. and S.F. performed data analysis. R.T., I.C., Y.L., K.A., S.F. and R.C. prepared the first draft of the manuscript. All authors have read and agreed to the published version of the manuscript.

**Funding:** This study was financially supported (in part) by the University Research Fund (URF) for the year 2020–2021 (NO.DFBS/2021-URF/ZOO), Quaid-i-Azam University, Islamabad, Pakistan and Retina Research Foundation to R.C.

**Institutional Review Board Statement:** The study was conducted in accordance with the Declaration of Helsinki and approved by the Bio Ethics Committee of Faculty of Biological Sciences, Quaid-i-Azam University, Islamabad, Pakistan (BEC-FBS-QAU2017-52 on 14 October 2017) for studies involving humans.

**Informed Consent Statement:** Informed consent was obtained from all subjects involved in the study.

**Data Availability Statement:** All data relevant to the study are included in the manuscript.

**Acknowledgments:** We thank patients and their families for their participation in this study.

**Conflicts of Interest:** The authors declare no conflict of interest.

## References

1. Verbakel, S.K.; van Huet, R.A.; Boon, C.J.; den Hollander, A.I.; Collin, R.W.; Klaver, C.C.; Hoyng, C.B.; Roepman, R.; Klevering, B.J. Non-syndromic retinitis pigmentosa. *Prog. Retin. Eye Res.* **2018**, *66*, 157–186. [[CrossRef](#)] [[PubMed](#)]
2. Hamel, C. Retinitis pigmentosa. *Orphanet J. Rare Dis.* **2006**, *1*, 40. [[CrossRef](#)] [[PubMed](#)]

3. Musarella, M.A.; MacDonald, I.M. Current concepts in the treatment of retinitis pigmentosa. *J. Ophthalmol.* **2011**, *2011*, 753547. [[CrossRef](#)]
4. Sen, P.; Bhargava, A.; George, R.; Ramesh, S.V.; Hemamalini, A.; Prema, R.; Kumaramanickavel, G.; Vijaya, L. Prevalence of retinitis pigmentosa in South Indian population aged above 40 years. *Ophthalmic Epidemiol.* **2008**, *15*, 279–281. [[CrossRef](#)] [[PubMed](#)]
5. Na, K.-H.; Kim, H.J.; Kim, K.H.; Han, S.; Kim, P.; Hann, H.J.; Ahn, H.S. Prevalence, age at diagnosis, mortality, and cause of death in Retinitis Pigmentosa in Korea—A nationwide population-based study. *Am. J. Ophthalmol.* **2017**, *176*, 157–165. [[CrossRef](#)]
6. Daiger, S.P.; Bowne, S.J.; Sullivan, L.S. Perspective on genes and mutations causing retinitis pigmentosa. *Arch. Ophthalmol.* **2007**, *125*, 151–158. [[CrossRef](#)] [[PubMed](#)]
7. Koenekoop, R.K. An overview of Leber congenital amaurosis: A model to understand human retinal development. *Surv. Ophthalmol.* **2004**, *49*, 379–398. [[CrossRef](#)]
8. Hanein, S.; Perrault, I.; Gerber, S.; Tanguy, G.; Hamel, C.; Dufier, J.-L.; Rozet, J.-M.; Kaplan, J. Amaurose congénitale de Leber: Le point sur l'hétérogénéité génétique, actualisation de la définition clinique. *J. Français D'ophtalmol.* **2005**, *28*, 98–105. [[CrossRef](#)]
9. Ferrari, S.; Di Iorio, E.; Barbaro, V.; Ponzin, D.; Sorrentino, F.; Parmeggiani, F. Retinitis pigmentosa: Genes and disease mechanisms. *Curr. Genom.* **2011**, *12*, 238–249.
10. Dryja, T.P.; Adams, S.M.; Grimsby, J.L.; McGee, T.L.; Hong, D.-H.; Li, T.; Andréasson, S.; Berson, E.L. Null RPGRIP1 alleles in patients with Leber congenital amaurosis. *Am. J. Hum. Genet.* **2001**, *68*, 1295–1298. [[CrossRef](#)]
11. Gerber, S.; Perrault, I.; Hanein, S.; Barbet, F.; Ducroq, D.; Ghazi, I.; Martin-Coignard, D.; Leowski, C.; Homfray, T.; Dufier, J.-L. Complete exon-intron structure of the RPGR-interacting protein (RPGRIP1) gene allows the identification of mutations underlying Leber congenital amaurosis. *Eur. J. Hum. Genet.* **2001**, *9*, 561–571. [[CrossRef](#)] [[PubMed](#)]
12. Falk, M.J.; Zhang, Q.; Nakamaru-Ogiso, E.; Kannabiran, C.; Fonseca-Kelly, Z.; Chakarova, C.; Audo, I.; Mackay, D.S.; Zeitz, C.; Borman, A.D. NMNAT1 Mutations Cause Leber Congenital Amaurosis. *Nat. Genet.* **2012**, *44*, 1040–1045. [[CrossRef](#)] [[PubMed](#)]
13. Den Hollander, A.I.; Roepman, R.; Koenekoop, R.K.; Cremers, F.P. Leber congenital amaurosis: Genes, proteins and disease mechanisms. *Prog. Retin. Eye Res.* **2008**, *27*, 391–419. [[CrossRef](#)] [[PubMed](#)]
14. Zafar, S.; Ahmed, K.; Ali, A.; Baig, R. Retinitis pigmentosa genes implicated in South Asian populations: A systematic review. *J. Pak. Med. Assoc.* **2017**, *67*, 1734.
15. Daiger, S.; Sullivan, L.; Bowne, S. Genes and mutations causing retinitis pigmentosa. *Clin. Genet.* **2013**, *84*, 132–141. [[CrossRef](#)]
16. Priya, S.; Nampoothiri, S.; Sen, P.; Sripriya, S. Bardet-Biedl syndrome: Genetics, molecular pathophysiology, and disease management. *Indian J. Ophthalmol.* **2016**, *64*, 620. [[CrossRef](#)]
17. Dreyer, B.; Brox, V.; Tranebjærg, L.; Rosenberg, T.; Sadeghi, A.M.; Möller, C.; Nilssen, Ø. Spectrum of USH2A mutations in Scandinavian patients with Usher syndrome type II. *Hum. Mutat.* **2008**, *29*, 451. [[CrossRef](#)] [[PubMed](#)]
18. Ebermann, I.; Scholl, H.P.; Issa, P.C.; Becirovic, E.; Lamprecht, J.; Jurklics, B.; Millán, J.M.; Aller, E.; Mitter, D.; Bolz, H. A novel gene for Usher syndrome type 2: Mutations in the long isoform of whirlin are associated with retinitis pigmentosa and sensorineural hearing loss. *Hum. Genet.* **2007**, *121*, 203–211. [[CrossRef](#)]
19. Weston, M.D.; Luijendijk, M.W.; Humphrey, K.D.; Möller, C.; Kimberling, W.J. Mutations in the VLGR1 gene implicate G-protein signaling in the pathogenesis of Usher syndrome type II. *Am. J. Hum. Genet.* **2004**, *74*, 357–366. [[CrossRef](#)]
20. Bademci, G.; Foster, J.; Mahdieh, N.; Bonyadi, M.; Duman, D.; Cengiz, F.B.; Menendez, I.; Diaz-Horta, O.; Shirkavand, A.; Zeinali, S. Comprehensive analysis via exome sequencing uncovers genetic etiology in autosomal recessive nonsyndromic deafness in a large multiethnic cohort. *Genet. Med.* **2016**, *18*, 364–371. [[CrossRef](#)] [[PubMed](#)]
21. French, L.S.; Mellough, C.B.; Chen, F.K.; Carvalho, L.S. A review of gene, drug and cell-based therapies for Usher syndrome. *Front. Cell. Neurosci.* **2020**, *14*, 183. [[CrossRef](#)] [[PubMed](#)]
22. World Medical Association. World Medical Association Declaration of Helsinki: Ethical principles for medical research involving human subjects. *JAMA* **2013**, *310*, 2191–2194. [[CrossRef](#)] [[PubMed](#)]
23. Wang, F.; Wang, H.; Tuan, H.-F.; Nguyen, D.H.; Sun, V.; Keser, V.; Bowne, S.J.; Sullivan, L.S.; Luo, H.; Zhao, L. Next generation sequencing-based molecular diagnosis of retinitis pigmentosa: Identification of a novel genotype-phenotype correlation and clinical refinements. *Hum. Genet.* **2014**, *133*, 331–345. [[CrossRef](#)] [[PubMed](#)]
24. Thiele, H.; Nürnberg, P. HaploPainter: A tool for drawing pedigrees with complex haplotypes. *Bioinformatics* **2005**, *21*, 1730–1732. [[CrossRef](#)]
25. Kaul, H.; Riazuddin, S.A.; Shahid, M.; Kousar, S.; Butt, N.H.; Zafar, A.U.; Khan, S.N.; Husnain, T.; Akram, J.; Hejtmancik, J.F. Autosomal recessive congenital cataract linked to EPHA2 in a consanguineous Pakistani family. *Mol. Vis.* **2010**, *16*, 511.
26. Nikopoulos, K.; Butt, G.; Farinelli, P.; Mudassar, M.; Domènech-Estévez, E.; Samara, C.; Kausar, M.; Masroor, I.; Chrast, R.; Rivolta, C. A large multiexonic genomic deletion within the ALMS1 gene causes Alström syndrome in a consanguineous Pakistani family. *Clin. Genet.* **2016**, *89*, 510–511. [[CrossRef](#)]
27. Dryja, T.P.; Rucinski, D.E.; Chen, S.H.; Berson, E.L. Frequency of mutations in the gene encoding the  $\alpha$  subunit of rod cGMP-phosphodiesterase in autosomal recessive retinitis pigmentosa. *Investig. Ophthalmol. Vis. Sci.* **1999**, *40*, 1859–1865.
28. Maria, M.; Ajmal, M.; Azam, M.; Waheed, N.K.; Siddiqui, S.N.; Mustafa, B.; Ayub, H.; Ali, L.; Ahmad, S.; Micheal, S. Homozygosity mapping and targeted sanger sequencing reveal genetic defects underlying inherited retinal disease in families from Pakistan. *PLoS ONE* **2015**, *10*, e0119806. [[CrossRef](#)]

29. Dreyer, B.; Tranebjærg, L.; Rosenberg, T.; Weston, M.D.; Kimberling, W.J.; Nilssen, Ø. Identification of novel *USH2A* mutations: Implications for the structure of USH2A protein. *Eur. J. Hum. Genet.* **2000**, *8*, 500–506. [[CrossRef](#)]
30. González-del Pozo, M.; Martín-Sánchez, M.; Bravo-Gil, N.; Méndez-Vidal, C.; Chimenea, Á.; Rodríguez-de la Rúa, E.; Borrego, S.; Antiñolo, G. Searching the second hit in patients with inherited retinal dystrophies and monoallelic variants in *ABCA4*, *USH2A* and *CEP290* by whole-gene targeted sequencing. *Sci. Rep.* **2018**, *8*, 13312. [[CrossRef](#)]
31. Grønskov, K.; Olsen, J.H.; Sand, A.; Pedersen, W.; Carlsen, N.; Jylling, A.; Lyngbye, T.; Brøndum-Nielsen, K.; Rosenberg, T. Population-based risk estimates of Wilms tumor in sporadic aniridia. *Hum. Genet.* **2001**, *109*, 11–18. [[CrossRef](#)]
32. Audo, I.; Sahel, J.A.; Mohand-Saïd, S.; Lancelot, M.E.; Antonio, A.; Moskova-Doumanova, V.; Nandrot, E.F.; Doumanov, J.; Barragan, I.; Antinolo, G. EYS is a major gene for rod-cone dystrophies in France. *Hum. Mutat.* **2010**, *31*, E1406–E1435. [[CrossRef](#)] [[PubMed](#)]
33. Ur Rehman, A.; Peter, V.G.; Quinodoz, M.; Rashid, A.; Khan, S.A.; Superti-Furga, A.; Rivolta, C. Exploring the genetic landscape of retinal diseases in North-Western Pakistan reveals a high degree of autozygosity and a prevalent founder mutation in *ABCA4*. *Genes* **2019**, *11*, 12. [[CrossRef](#)] [[PubMed](#)]
34. Shivanna, M.; Anand, M.; Chakrabarti, S.; Khanna, H. Ocular Ciliopathies: Genetic and mechanistic insights into developing therapies. *Curr. Med. Chem.* **2019**, *26*, 3120–3131. [[CrossRef](#)] [[PubMed](#)]
35. Mackay, D.S.; Ocaka, L.A.; Borman, A.D.; Sergouniotis, P.I.; Henderson, R.H.; Moradi, P.; Robson, A.G.; Thompson, D.A.; Webster, A.R.; Moore, A.T. Screening of *SPATA7* in patients with Leber congenital amaurosis and severe childhood-onset retinal dystrophy reveals disease-causing mutations. *Investig. Ophthalmol. Vis. Sci.* **2011**, *52*, 3032–3038. [[CrossRef](#)]
36. Ullah, I.; Kabir, F.; Gottsch, C.B.S.; Naeem, M.A.; Guru, A.A.; Ayyagari, R.; Khan, S.N.; Riazuddin, S.; Akram, J.; Riazuddin, S. Mutations in phosphodiesterase 6 identified in familial cases of retinitis pigmentosa. *Hum. Genome Var.* **2016**, *3*, 16036. [[CrossRef](#)]
37. Ng, T.K.; Tang, W.; Cao, Y.; Chen, S.; Zheng, Y.; Xiao, X.; Chen, H. Whole exome sequencing identifies novel *USH2A* mutations and confirms Usher syndrome 2 diagnosis in Chinese retinitis pigmentosa patients. *Sci. Rep.* **2019**, *9*, 5628. [[CrossRef](#)]
38. Perez-Carro, R.; Blanco-Kelly, F.; Galbis-Martinez, L.; Garcia-Garcia, G.; Aller, E.; Garcia-Sandoval, B.; Minguez, P.; Corton, M.; Mahillo-Fernandez, I.; Martin-Merida, I. Unravelling the pathogenic role and genotype-phenotype correlation of the *USH2A* p.(Cys759Phe) variant among Spanish families. *PLoS ONE* **2018**, *13*, e0199048. [[CrossRef](#)]
39. Dad, S.; Rendtorff, N.D.; Tranebjærg, L.; Grønskov, K.; Karstensen, H.G.; Brox, V.; Nilssen, Ø.; Roux, A.F.; Rosenberg, T.; Jensen, H. Usher syndrome in Denmark: Mutation spectrum and some clinical observations. *Mol. Genet. Genom. Med.* **2016**, *4*, 527–539. [[CrossRef](#)]
40. Sodi, A.; Mariottini, A.; Passerini, I.; Murro, V.; Tachyla, I.; Bianchi, B.; Menchini, U.; Torricelli, F. *MYO7A* and *USH2A* gene sequence variants in Italian patients with Usher syndrome. *Mol. Vis.* **2014**, *20*, 1717. [[PubMed](#)]
41. Zupan, A.; Fakin, A.; Battelino, S.; Jarc-Vidmar, M.; Hawlina, M.; Bonnet, C.; Petit, C.; Glavač, D. Clinical and haplotypic variability of Slovenian *USH2A* patients homozygous for the c. 11864G>A nonsense mutation. *Genes* **2019**, *10*, 1015. [[CrossRef](#)] [[PubMed](#)]
42. Weston, M.; Eudy, J.D.; Fujita, S.; Yao, S.-F.; Usami, S.; Cremers, C.; Greenburg, J.; Ramesar, R.; Martini, A.; Moller, C. Genomic structure and identification of novel mutations in usherin, the gene responsible for Usher syndrome type IIa. *Am. J. Hum. Genet.* **2000**, *66*, 1199–1210. [[CrossRef](#)]
43. McGee, T.L.; Seyedahmadi, B.J.; Sweeney, M.O.; Dryja, T.P.; Berson, E.L. Novel mutations in the long isoform of the *USH2A* gene in patients with Usher syndrome type II or non-syndromic retinitis pigmentosa. *J. Med. Genet.* **2010**, *47*, 499–506. [[CrossRef](#)] [[PubMed](#)]
44. Lenassi, E.; Vincent, A.; Li, Z.; Saihan, Z.; Coffey, A.J.; Steele-Stallard, H.B.; Moore, A.T.; Steel, K.P.; Luxon, L.M.; Héon, E. A detailed clinical and molecular survey of subjects with nonsyndromic *USH2A* retinopathy reveals an allelic hierarchy of disease-causing variants. *Eur. J. Hum. Genet.* **2015**, *23*, 1318–1327. [[CrossRef](#)]
45. Monzó, C.; Gimeno-Ferrer, F.; García, J.C.F.; Amadoz, A.; Albuquerque, D.; Angueira, F.B.; Marcaida, G.; Rodríguez-López, R. Alström syndrome caused by deletion in *ALMS1* gene fixed in a Northern Pakistan recurrent haplotype. *Indian J. Case Rep.* **2017**, *3*, 171–174. [[CrossRef](#)]
46. Lagali, N.; Wowra, B.; Fries, F.N.; Latta, L.; Moslemani, K.; Utheim, T.P.; Wylegala, E.; Seitz, B.; Käsmann-Kellner, B. PAX6 mutational status determines aniridia-associated keratopathy phenotype. *Ophthalmology* **2020**, *127*, 273–275. [[CrossRef](#)] [[PubMed](#)]
47. Khan, A.O.; Aldahmesh, M.A.; Alkuraya, F.S. Genetic and genomic analysis of classic aniridia in Saudi Arabia. *Mol. Vis.* **2011**, *17*, 708. [[PubMed](#)]
48. Lima Cunha, D.; Arno, G.; Corton, M.; Moosajee, M. The spectrum of PAX6 mutations and genotype-phenotype correlations in the eye. *Genes* **2019**, *10*, 1050. [[CrossRef](#)]



## RESEARCH ARTICLE

# Mutation screening of the *CYP1B1* gene reveals thirteen novel disease-causing variants in consanguineous Pakistani families causing primary congenital glaucoma

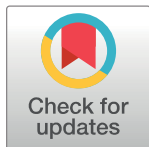
Raeesa Tehreem<sup>1</sup>, Anam Arooj<sup>1</sup>, Sorath Noorani Siddiqui<sup>2</sup>, Shagufta Naz<sup>3</sup>, Kiran Afshan<sup>1</sup>, Sabika Firasat<sup>1\*</sup>

**1** Department of Zoology, Faculty of Biological Sciences, Quaid-i-Azam University, Islamabad, Pakistan,

**2** Department of Pediatric Ophthalmology and Strabismus, Al-Shifa Trust Eye Hospital, Rawalpindi, Pakistan,

**3** Department of Zoology, Lahore College for Women University, Lahore, Pakistan

\* [sabika.firasat@qau.edu.pk](mailto:sabika.firasat@qau.edu.pk)



## Abstract

### Background

Primary congenital glaucoma (PCG) is a heterogeneous rare recessively inherited disorder prevalent in regions with high consanguinity. Disease phenotype is associated with increased intra ocular pressure and is a major cause of childhood blindness. Sequence variations in *Cytochrome P450 1B1* (*CYP1B1*) gene are a major cause of PCG. Current study was conducted to screen *CYP1B1* gene in highly consanguineous PCG affected families from Pakistani population consistent with the autosomal recessive pattern of PCG inheritance.

### Methods

For this study, patients and controls (clinically unaffected individuals of each family) from 25 consanguineous families belonging to Punjab, Baluchistan and Khyber Pakhtunkhwa, Pakistan were recruited through ophthalmologists. DNA was isolated from collected blood samples. Genetic screening of *CYP1B1* gene was done for all enrolled families. In-silico analysis was performed to identify and predict the potential disease-causing variations.

### Results

Pathogenicity screening revealed sequence variants segregating with disease phenotype in homozygous or compound heterozygous form in eleven out of 25 analyzed families. We identified a total of sixteen disease causing variants among which five frameshift i.e., c.629dup (p.Gly211Argfs\*13), c.287dup (p.Leu97Alafs\*127), c.662dup (p.Arg222Profs\*2), c.758\_759insA (p.Val254Glyfs\*73) and c.789dup (p.Leu264Alafs\*63), two silent c.1314G>A, c.771T>G and six missense variations c.457C>G (p.Arg153Gly), c.516C>A (p.Ser172Arg), c.722T>A (p.Val241Glu), c.740T>A (p.Leu247Gln), c.1263T>A (p.Phe421-Leu), and c.724G>C (p.Asp242His) are previously un reported. However two frameshift

## OPEN ACCESS

**Citation:** Tehreem R, Arooj A, Siddiqui SN, Naz S, Afshan K, Firasat S (2022) Mutation screening of the *CYP1B1* gene reveals thirteen novel disease-causing variants in consanguineous Pakistani families causing primary congenital glaucoma. PLoS ONE 17(9): e0274335. <https://doi.org/10.1371/journal.pone.0274335>

PLoS ONE 17(9): e0274335. <https://doi.org/10.1371/journal.pone.0274335>

**Editor:** Muhammad Qasim, Government College University Faisalabad, PAKISTAN

**Received:** June 28, 2022

**Accepted:** August 25, 2022

**Published:** September 9, 2022

**Copyright:** © 2022 Tehreem et al. This is an open access article distributed under the terms of the [Creative Commons Attribution License](https://creativecommons.org/licenses/by/4.0/), which permits unrestricted use, distribution, and reproduction in any medium, provided the original author and source are credited.

**Data Availability Statement:** All relevant data are within the article.

**Funding:** The author(s) received no specific funding for this work.

**Competing interests:** The authors have declared that no competing interests exist.

c.868dup (p.Arg290Profs\*37), c.247del (p.Asp83Thrfs\*12) and one missense variant c.732G>A (p.Met244Ile), is previously reported. Furthermore, six polymorphisms c.1347T>C, c.2244\_2245insT, c.355G>T, c.1294G>C, c.1358A>G and c.142C>G were also identified. In the intronic region, a novel silent polymorphism i.e., g.35710\_35711insT was found in homozygous state. All the newly detected disease-causing variants were negative in 96 ethnically matched controls.

## Conclusion

Among twenty-five screened families, eight families (PCG50, 52–54, 58, 59, 63 and 67) were segregating disease causing variants in recessive manner. Two families (PCG049 and PCG062) had compound heterozygosity. Our data confirms genetic heterogeneity of PCG in Pakistani population however we did not find molecular variants segregating with PCG in fifteen families in coding exons and intron-exon boundaries of *CYP1B1* gene. Genetic counseling was provided to families to refrain from practicing consanguinity and perform premarital screening as a PCG control measure in upcoming generations.

## Introduction

Glaucoma is characterized by impaired vision due to increased intraocular pressure, a primary risk factor for irreversible optic nerve damage. This disorder can be categorized according to etiology (primary glaucoma/secondary glaucoma), onset (congenital/adult) and iridocorneal angle (open/close) [1]. Primary congenital glaucoma (PCG; OMIM 231300) manifests during the first three years of life due to developmental defects of trabecular meshwork and Schlemm's canal resulting in hindrance to outflow of aqueous humour and increased intraocular pressure [2]. Clinical manifestation of PCG includes buphthalmos, epiphora, photophobia, hyperlacrimation, optic nerve damage, blepharospasm (uncontrolled eyelid movement), enlarged and opaque cornea [3]. Worldwide prevalence of PCG is 1:10,000 to 18,000 live births [4] with males (65%) being more affected than females (35%) [5] but there is variability of incidence between populations [1, 6]. Genetically PCG is heterogeneous with incomplete penetrance and four genetic loci are reported until now including *GLC3A* [7], *GLC3B* [8], *GLC3C* [9] and *GLC3D* [10] at position 2p21, 1p36, 14q24.3 and 14q24.2-q24.3 respectively [10]. Among these loci, mutations in cytochrome P4501B1 (*CYP1B1*) at *GLC3A* and Latent Transforming growth factor- $\beta$ -binding Protein-2 (*LTBP2*) at *GLC3D* have been reported to cause PCG [11]. However, variants in myocilin (*MYOC*) [12], Forkhead Box C1 (*FOXC1*) [13], and the angiopoietin receptor (*TEK*) [14] have also been reported to be implicated in PCG phenotype.

*CYP1B1* gene has three exons out of which the last 2 codes for a 543 amino acid (a.a) protein [15]. Cytochrome P4501B1 is a heme-thiolate monooxygenases that oxidizes multiple compounds including xenobiotics, steroids, retinoic acid and melatonin [5, 15]. This membrane bound protein has a transmembrane domain at amino terminal (53 a.a) and a highly conserved cytoplasmic region (480 a.a) that is connected to amino terminal by a proline rich hinge (10 a.a) [16]. Exact function of *CYP1B1* in development of eye is uncertain however it is believed that due to mutations in this gene, generation of some important morphogens is affected leading to structural defects in trabecular meshwork and the aqueous humour outflow pathways [5, 6, 17, 18]. Up till now almost 270 mutations are reported in *CYP1B1* gene

including missense, small deletions, indels, gross deletions and regulatory mutations [19]. Studies have revealed several genetic mutations causing PCG from Pakistani population, but this data is still too limited as compared to high prevalence of this disorder in our population due to consanguinity [6, 10, 15, 20]. In an ongoing effort of mutation screening of *CYP1B1* gene in PCG cases belonging to consanguineous Pakistani families, we enrolled and screened twenty-five families for *CYP1B1* variants. Each family had at least one child affected with primary congenital glaucoma.

## Materials and methods

### Assessment and enrollment of patients

Based on clinical assessment provided by ophthalmologists, 25 diagnosed families of PCG were enrolled belonging to Khyber Pakhtunkhwa (KPK), Baluchistan and South Punjab. Clinical data, family history and blood samples of patients and each available family member was collected after informed written consent following the principles of world medical association of Helsinki [21]. The study was approved by Bioethical review Committee (BEC) of Quaid-i-Azam University (QAU) Islamabad, Pakistan. Inclusion criteria for patients was diagnosis of PCG through ophthalmologist based on symptoms like buphthalmos, edema and corneal cloudiness. Patients with other eye diseases and PCG patients that did not belong to consanguineous couples were excluded from the study. Each family was given a unique identification number (PCG047-PCG069 and PCG101, PCG102). To draw pedigrees of affected families haploPainter program (<http://haploPainter.sourceforge.net/about.html>) [22] was used.

### Extraction of genomic DNA

Average 4ml of peripheral blood sample was taken from each participating individual and stored in 5ml EDTA (Ethylene Diamine Tetra Acetic acid) vacutainer. Extraction was performed using non-organic method of DNA extraction described by Kaul *et al.*, 2010 [23]. To check purity and quantify DNA, Nanodrop was used (Thermo Scientific Nanodrop spectrophotometers).

### Amplification and sequencing of *CYP1B1* gene

Amplification of coding regions and at least 50 base pairs of flanking non-coding regions was performed using primers reported previously by Afzal *et al.*, 2019 [20]. 25µl polymerase chain reaction (PCR) was performed for both affected and non-affected individuals following protocol described by Afzal *et al.*, 2019 [20]. After amplification, 1.5% agarose gel was prepared to load samples and controls along with DNA ladder (1kb) to separate bands according to their sizes. Purification was done using instructions provided by manufacturer of PCR purification kit (Wiz Bio Solutions, Seongnam, Korea). Finally, each amplified product was sequenced using big dye terminator ready reaction mix (Applied Biosystems, Foster City, CA, USA) in an automated ABI 3100 genetic analyzer. Sequencing results were analyzed by aligning them to reference sequence NM\_000104.4 using Sequencher software (5.4.6) and Codon Code Aligner program to identify sequence variations. After identification of each variant, their disease causing potential was checked using Mutation taster (<https://www.mutationtaster.org/>) [24]. Furthermore, segregation with disease phenotype was confirmed by sequencing other available family members. Each novel identified sequence variant was checked in 96 control samples.

## In silico analysis of variants

For significance of each variant and to check their nomenclature according to Human Genome Variation Society HGVS (<http://www.hgvs.org/>) guidelines, Mutalyzer (2.0.35) (<https://mutalyzer.nl/>) [25] was used. Varsome (<https://varsome.com/>) [26] was used to evaluate the effect of variations and HSF (Human Splicing Finder version 3.1) (<https://www.genomnis.com/access-hsf>) was used to determine pathogenicity due to disruption of splicing signals because of sequence variants.

## Prediction of variant effect on protein structure and stability

PolyPhen-2 (Polymorphism Phenotyping v2) (<http://genetics.bwh.harvard.edu/pph2/>) [27], SIFT (Sorting Intolerant From Tolerant) (<https://sift.bii.a-star.edu.sg/>) [28] and PROVEAN (Protein Variation Effect Analyzer) ([http://provean.jcvi.org/seq\\_submit.php](http://provean.jcvi.org/seq_submit.php)) [29] were used to predict the effect of amino acid substitution on protein structure and function based on sequence homology. I-Mutant v2.0 (<https://folding.biofold.org/i-mutant/i-mutant2.0.html>) [30] and MUpro (<http://mupro.proteomics.ics.uci.edu/>) [31] softwares were used which predict protein stability by analyzing thermodynamics based on SVM (support vector method). Both these softwares give Gibbs free energy ( $\Delta\Delta G = \Delta G_f^{wt} - \Delta G_f^{mut}$ ) of protein structure that corresponds to stabilizing or destabilizing effect of variations. To check the conservation between different mammalian species, Clustal omega (<https://www.ebi.ac.uk/Tools/msa/clustalo/>) [32] was used and for generation of graphical representation of amino acids WebLogo software (<https://weblogo.berkeley.edu/>) [33] was used. HOPE software (<https://www3.cmbi.umcn.nl/hope/>) [22] was used to predict the biochemical changes in structure of protein due to sequence variation.

## Results

In this study, twenty-five PCG segregating consanguineous Pakistani families were enrolled. Among these families i.e., 09 belonged to Punjab province of Pakistan, 01 to Azad Kashmir whereas 12 and 03 belonged to Khyber Pakhtunkhwa and Baluchistan respectively. At the time of enrollment, seventeen families (PCG047, PCG048, PCG052-PCG056, PCG059-PCG063, PCG065-PCG067, PCG101 and PCG102) had a single PCG affected individual, three families (PCG049, PCG057, and PCG065) had two, one family (PCG058) had three, three families (PCG064, PCG051 and PCG067) had four whereas family PCG050 had six affected members respectively (Fig 1).

Average age of proband of each enrolled family was  $10 \pm 6$  years. Ophthalmological findings confirmed diagnosis of congenital glaucoma for each proband. Proband of each enrolled family had consanguineous mating parents. Molecular screening of *CYP1B1* coding regions and at least 50 base pairs of flanking noncoding region using DNA of each proband revealed thirteen novel disease-causing variations in coding regions according to mutation taster (Table 1, Figs 2 and 3).

Among these variations seven were found in homozygous state and six in heterozygous state. In addition to novel disease-causing variations three already reported mutations (c.868dup), (c.247del), (c.732G>A) and six reported polymorphisms (c.1347T>C), (c.1294G>C), (c.1358A>G), (c.2244\_2245insT), (c.355G>T), (c.142C>G) were also found. Another polymorphism g.35710\_35711insT was also found in intronic region in family PCG062 that has not been reported previously. Out of the novel disease-causing variants, five were frame shift variations c.629dup (p.Gly211Argfs\*13), c.287dup (p.Leu97Alafs\*127), c.662dup (p.Arg222Profs\*2), c.758\_759insA (p.Val254Glyfs\*73) and c.789dup (p.Leu264Alafs\*63). Other novel disease-causing variants include six missense variants

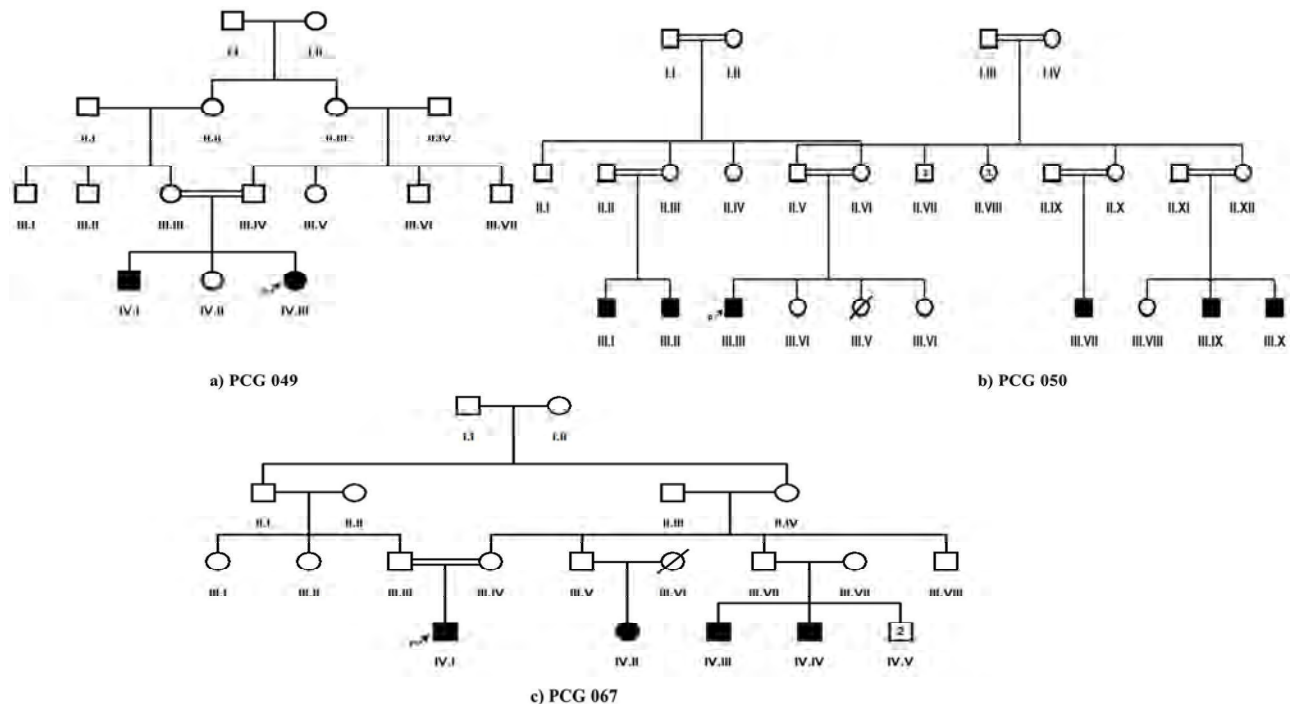


**Fig 1. Pedigrees of three PCG families (PCG049, PCG050 and PCG067) having more than one affected member and segregating novel disease causing variant/s in *CYP1B1* gene.** Filled squares and circles indicate affected members of family. Cousin marriage is indicated by double line.

<https://doi.org/10.1371/journal.pone.0274335.g001>

c.457C>G (p.Arg153Gly), c.516C>A (p.Ser172Arg), c.722T>A (p.Val241Glu), c.740T>A (p.Leu247Gln), c.1263T>A (p.Phe421Leu), and c.724G>C (p.Asp242His) and two silent variations c.1314G>A and c.771T>G. In addition to disease causing variants, seven polymorphisms were also detected (Table 2).

**Table 1. List of reported and novel disease-causing variants detected in this study upon sequencing of *CYP1B1* gene in PCG patients.**

Family ID	Position	Nucleotide change	Protein change	Zygoty	Mutation taster prediction	dbSNP Status
PCG049	EXON 2	c.457C>G	p.Arg153Gly	Heterozygous	Disease causing	Not reported
	EXON 2	c.516C>A	p.Ser172Arg	Heterozygous	Disease causing	Not reported
PCG050	EXON 2	c. 629dup	p.Gly211Argfs*13	Homozygous	Disease causing	Not reported
PCG052	EXON 2	c.722T>A	p.Val241Glu	Homozygous	Disease causing	Not reported
	EXON 2	c.732G>A	p.Met244Ile	Homozygous	Disease causing	Reported
PCG053	EXON 2	c. 287dup	p.Leu97Alafs*127	Homozygous	Disease causing	Not reported
PCG054	EXON 2	c.662dup	p.Arg222Profs*2	Homozygous	Disease causing	Not reported
	EXON 2	c.868dup	p.Arg290Profs*37	Homozygous	Disease causing	rs67543922
PCG058	EXON 2	c.247del	p.Asp83Thrfs*12	Homozygous	Disease causing	Reported
PCG059	EXON 2	c.758-759insA	p.Val254Glyfs*73	Homozygous	Disease causing	Not reported
PCG060	EXON 2	c.740T>A	p.Leu247Gln	Heterozygous	Disease causing	Not reported
PCG062	EXON 3	c.1263T>A	p.Phe421Leu	Heterozygous	Disease causing	Not reported
	EXON 3	c.1314G>A	p. (=)	Heterozygous	Disease causing	Not reported
PCG063	EXON 2	c.771T>G	p. (=)	Heterozygous	Disease causing	Not reported
	EXON 2	c.789dup	p.Leu264Alafs*63	Homozygous	Disease causing	Not reported
PCG067	EXON 2	c.724G>C	p.Asp242His	Homozygous	Disease causing	Not reported

<https://doi.org/10.1371/journal.pone.0274335.t001>

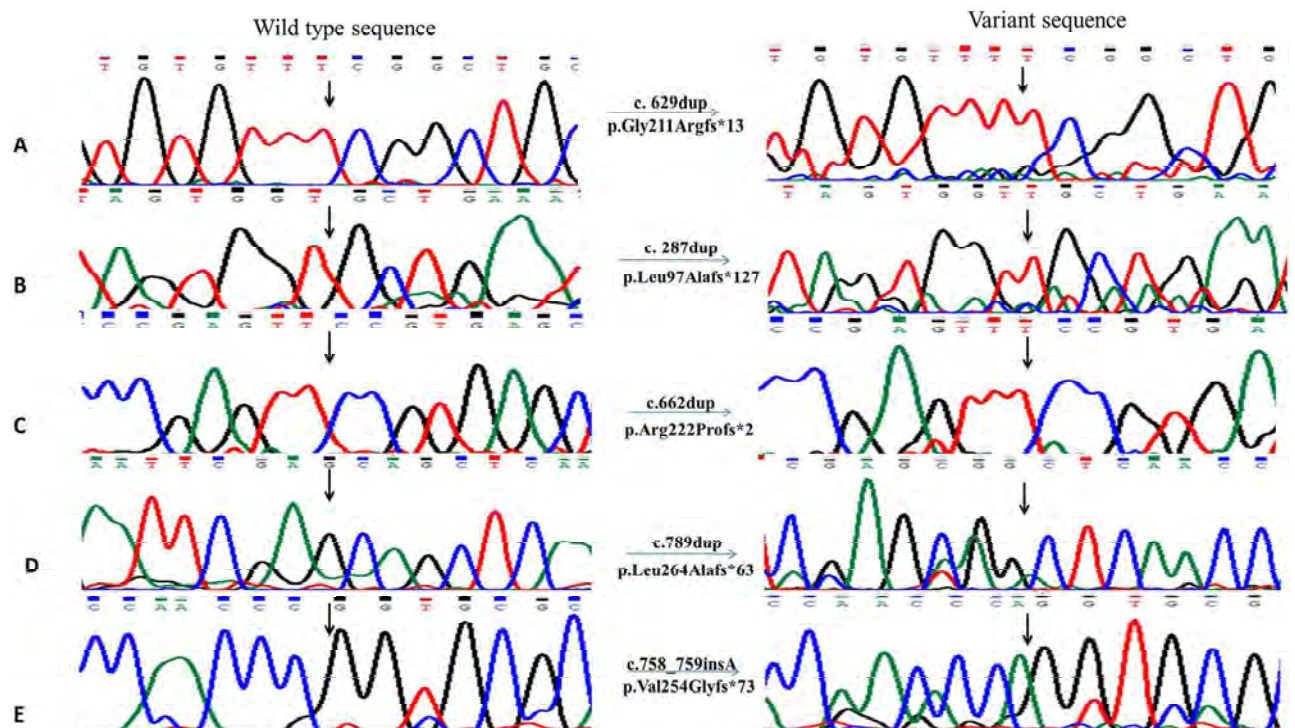


**Fig 2. Chromatograms of novel duplications and an insertion detected in PCG patients.** A) A homozygous variant c.629dup detected in PCG050 leading to p.Gly211Argfs\*13. B) Chromatogram of homozygous variant c.287dup detected in PCG053 that resulted in protein change i.e., p.Leu97Alafs\*127. C) Sequence chromatogram of homozygous variant c.662dup leading to protein change p.Arg222Profs\*2 in PCG054. D) Chromatogram showing c.789dup homozygous variant in PCG063 leading to a p.Leu264Alafs\*63. E) Homozygous insertion c.758\_759insA detected in PCG059 resulting in p.Val254Glyfs\*73. All the chromatograms on left side indicate normal sequence while right side of figure shows mutated chromatograms.

<https://doi.org/10.1371/journal.pone.0274335.g002>

### *CYP1B1* disease causing variations segregating in families with PCG

In family PCG049, two disease causing variations were detected. A single nucleotide substitution i.e., c.457C>G was present in heterozygous condition, it changed arginine at position 153 to glycine and was deleterious according to PROVEAN and Polyphen-2 with a score of -5.21 and 1.00 respectively (Fig 3A) (Table 3). The other missense heterozygous variant i.e., c.516C>A resulted in substitution of arginine at position 172 (Fig 3B). Human splicing finder predicted that addition of glycine at position 172 will create new sites for auxiliary factors like exonic splicing enhancer (ESE) 9G8, exonic splicing suppresser (ESS) hnRNPA1, IIE, Fas ESS, Sironi\_motif2 and break sites for EIE, ESE\_SRp55 and Sironi\_motif1 that might affect the protein structure.

Insertion of thymine (T) in PCG050 in exon 2 at position 629–630 (Fig 2A) changed amino acid glycine to arginine resulting in frameshift and in-frame stop codon leading to truncated protein after 13 residues (Table 1). This homozygous variant was predicted as damaging for the protein structure according to in-silico analysis (PROVEAN -6.66 and polyphen-2 1.00) (Table 3). Varsome predicted it as pathogenic and negative values determined by I-Mutant and MUpro showed destabilizing effect. HSF analysis for c.629dup predicted alteration of auxiliary sequences i.e., SRp55/SRSF6 (Serine and Arginine Rich Splicing Factor 6) ESE site TTCGGC and Fas ESS site TGTTTC was broken. Two new ESS sites TTTTCG and GTTTTC were created for IIE and one TGTGTTTT for PESS (putative exonic splicing silencer).

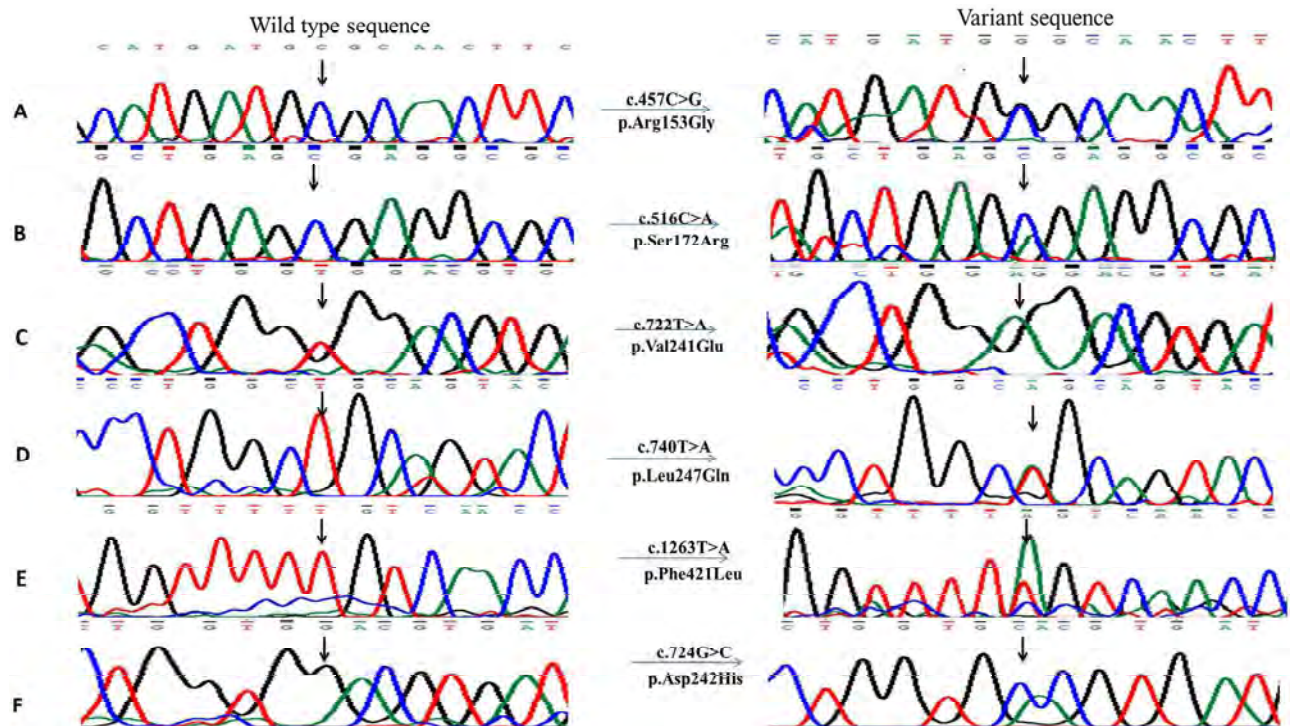


**Fig 3. Chromatograms of novel disease-causing single nucleotide substitutions detected in PCG patients upon sequencing of *CYP1B1* gene.** Right side of figure shows substituted nucleotides in chromatograms. A) A heterozygous variant c.457C>G detected in PCG049 leading to p.Arg153Gly. B) Second heterozygous variant c.516C>A detected in PCG049 resulting in p.Ser172Arg. C) Variant c.722T>A detected in homozygous condition in PCG052 leading to protein change p.Val241Glu. D) A heterozygous variant c.740T>A leading to p.Leu247Gln detected in PCG060. E) Sequence chromatogram of heterozygous variant c.1263T>A detected in PCG062 resulting in p.Phe421Leu. F) A homozygous variant c.724G>C leading to p.Asp242His detected in PCG067.

<https://doi.org/10.1371/journal.pone.0274335.g003>

In family PCG052, two homozygous variants c.722T>A (Fig 3C) and c.732G>A were found in second exon of *CYP1B1* gene (Table 1). Variation c.732G>A was previously reported and described as less lethal than other variation according to pathogenicity prediction softwares. I-Mutant and MUpro gave negative values for both variations that depicts unstable protein structure ( $\Delta\Delta G$  (kcal/mol) -0.62, -0.11 and -1.5608, -0.5974 respectively) (Table 3). In family PCG053, insertion of single nucleotide at position c.287dup (Fig 2B) resulted in a frameshift and in-frame stop codon at 127 position i.e., p.Leu97Alafs\*127. This homozygous variant had deleterious effect on protein structure (PROVEAN score -4.09) and was predicted as pathogenic by Varsome (Table 3). This variation was predicted to create ESE/ESS site GGTTCCTG, GTGGTT and TAGTGGTT for factors ESE\_SC35, Fas ESS and PESS respectively. Thermodynamics softwares predicted this variation as destabilizing but HOPE described that it might not cause disease because in rare cases this mutant residue was observed in homologous proteins. Two disease causing variants in homozygous condition were present in proband of family PCG054 among which one was already reported i.e., c.868dup that shifted the reading frame and truncated the protein after 37 residues i.e., p.Arg290Profs\*37 (Table 1). The other variant was a novel frameshift variation c.662dup (p.Arg222Profs\*2) (Fig 2C). Decrease in the stability of protein structure was predicted by I-Mutant and MUpro giving negative energy values -0.51 and -0.852 respectively.

A reported homozygous frameshift variation was found in family PCG058 i.e., c.247del (p.Asp83Thrfs\*12) that replaced aspartic acid at position 83 to threonine shifting reading frame

**Table 2. List of reported and a previously unreported single nucleotide polymorphism detected in *CYP1B1* gene in PCG patients analyzed in this study.**

Family ID	Position	Nucleotide change	Zygoty	Protein change	Mutation taster	Polyphen-2	SIFT	Provean	dbSNP
PCG047-054, 056, 058, 060-064069, 102	EXON 3	c.1347T>C	Homozygous	p.(=)	Polymorphism	N/A	N/A	N/A	rs1056837
PCG049, 055, 057	EXON 3	c.1294G>C	Homozygous	p.Val432Leu	Polymorphism	Benign 0.00	Tolerant 1.00	N/A	rs1056836
PCG051, 063	EXON 3	c.1358A>G	Homozygous	p.Asn453Ser	Polymorphism	Possibly damaging 0.906	Tolerant 1.00	Deleterious-3.24	rs1800400
PCG052, 064, 065, 102	3'UTR	c.2244_2245insT	Homozygous	p.(=)	Polymorphism	N/A	N/A	N/A	rs4646431
PCG053, 056, 069	EXON 2	c.355G>T	Homozygous	p.Ala119Ser	Polymorphism	Benign 0.00	Tolerant 1.00	Neutral 1.51	rs1056827
PCG056	EXON 2	c.142C>G	Homozygous	p.Arg48Gly	Polymorphism	Benign 0.00	Tolerant 0.82	Neutral -0.085	rs10012
PCG062	Intron	g.35710_35711insT	Homozygous	p.(=)	Polymorphism	N/A	N/A	N/A	Not reported

<https://doi.org/10.1371/journal.pone.0274335.t002>

and creating stop codon after 12 residues (Table 1). I-Mutant and MUpro gave negative  $\Delta\Delta G$  (kcal/mol) values (-0.79, -1.289) for c.247del that corresponds to slightly unstable structure. Insertion of adenine at position c.758-759insA (Fig 2E) resulted in frame shift of 73 bases replacing valine at position 254 to glycine in family PCG059. In-silico analysis described this variant as highly pathogenic (polyphen-2 1.00, PROVEAN -3.95). Highest value (-3.18 kcal/mol) of negative Gibbs free energy was obtained by I-Mutant and by MUpro (-2.691) for this variant (Table 3). Missense variations present in family PCG060 i.e., c.740T>A (p.Leu247Gln) and PCG067 i.e., c.724G>C (p.Asp242His) (Fig 3D and 3F) were predicted to be highly deleterious (PROVEAN score: -5.45 and -6.50) by pathogenicity prediction tools. Change of aspartate at position 242 to histidine resulted in creation and destruction of many sites for auxiliary factors that help in splicing. Sites for ESE\_9G8, EIE, Sironi\_motif2, PESE, Sironi\_motif1 were broken and new site was created for ESE\_SRP55CACGTG according to HSF.

Family PCG062 had two different heterozygous variants including c.1263T>A (Fig 3E) and c.1314G>A in coding regions (Table 1) showing compound heterozygosity. One of the detected variant c.1263T>A changed phenylalanine at position 421 to leucine and was reported as probably damaging by Polyphen-2. Human splicing finder predicted that a new acceptor site will be created CTGTGGTTTTTGTGTC>CTGTGGTTTTTAGTC changing consensus value (CV) from 50.91 to 78.78. CV for newly created site showed that it is not a very strong site (strong site CV> 80). PCG063 had two unreported mutations, a silent heterozygous mutation c.771T>G and a frameshift homozygous mutation c.789dup (Fig 2D). Shifting the frame by 63 amino acids replaced leucine at position 264 to alanine and resulted in a short protein (Table 3). HSF analysis showed that CAGGCT site was created for ESS\_hnRNPA1, CAGGCTCA for PESE, GCAGGC for ESE\_9G8 and AGCAGC, AGCAGCTC sites were broken that are required for auxiliary factors ESE\_SRP55 and PESE respectively.

Amino acid conservation was analyzed by using Clustal Omega multiple sequence alignment tool among *CYP1B1* homologous sequences from different species i.e.: *Mus musculus* (NP\_001075448.1), *Nomascus leucogenys* (XP\_003262792.2), *Pongo abelii* (XP\_009235654.1) and *Pan troglodytes* (XP\_001167556.1) with high similarity index to *Homo sapiens* (Fig 4a-4k). Structures predicted by HOPE software showed the position of mutant residues and their possible impact on conservation of protein structure (Fig 5a-5l) (Table 3).



Table 3. In-silico analysis data of disease-causing variants identified in this study.

Nucleotide change	Protein change	Polyphen-2	PROVEAN	Varsome	I mutant		MUpro		HOPE Conservation prediction
					$\Delta\Delta G$ (kcal/mol) DDG value	Stability Prediction SVM2	$\Delta\Delta G$ (kcal/mol)	Stability Prediction SVM2	
c.457C>G	p.Arg153Gly	Probably damaging 1.00	Deleterious -5.21	Likely Pathogenic	-1.47	Decreased Stability	-1.1669	Decreased Stability	Probably stable
c.516C>A	p.Ser172Arg	Possibly damaging 0.685	Neutral -1.167	Pathogenic	-0.03	Decreased Stability	-0.2848	Decreased Stability	Probably stable
c.629dup	p. Gly211Argfs*13	Probably damaging 1.00	Deleterious -6.66	Pathogenic	-1.26	Decreased Stability	-0.6032	Decreased Stability	Probably stable
c.722T>A	p.Val241Glu	Probably damaging 1.00	Deleterious -4.11	Likely Pathogenic	-0.62	Decreased Stability	-1.5608	Decreased Stability	Damaging
c.732G>A	p.Met244Ile	Benign 0.338	Neutral -0.98	Likely Pathogenic	-0.11	Decreased Stability	-0.5974	Decreased Stability	Probably stable
c.287dup	p. Leu97Alafs*127	Probably damaging 1.00	Deleterious -4.09	Pathogenic	-0.72	Decreased Stability	-1.9697	Decreased Stability	Probably stable
c.662dup	p. Arg222Profs*2	Probably damaging 0.998	Neutral -2.367	Pathogenic	-0.51	Decreased Stability	-0.8527	Decreased Stability	Damaging
c.868dup	p. Arg290Profs*37	Probably damaging 1.00	Deleterious -6.40	Pathogenic	-1.91	Decreased Stability	-0.9609	Decreased Stability	Damaging
c.247del	p. Asp83Thrfs*12	Possibly damaging 0.732	Deleterious -4.11	Likely Pathogenic	-0.79	Decreased Stability	-1.2898	Decreased Stability	Probably stable
c.758-759insA	p. Val254Glyfs*73	Probably damaging 1.00	Deleterious -3.95	Pathogenic	-3.18	Decreased Stability	-2.691	Decreased Stability	Damaging
c.740T>A	p.Leu247Gln	Probably damaging 1.00	Deleterious -5.45	Likely Pathogenic	-2.14	Decreased Stability	-1.1804	Decreased Stability	Probably stable
c.1263T>A	p.Phe421Leu	Probably damaging 1.00	Deleterious -5.43	Likely Pathogenic	-1.06	Decreased Stability	-0.4212	Decreased Stability	Stable
c.1314G>A	p. (=)	N/A	N/A	Likely Benign	N/A	N/A	N/A	N/A	N/A
c.771T>G	p. (=)	N/A	N/A	Likely Benign	N/A	N/A	N/A	N/A	N/A
c.789dup	p. Leu264Alafs*63	Probably damaging 0.998	Deleterious -3.62	Likely Pathogenic	-1.59	Decreased Stability	-1.5125	Decreased Stability	Deleterious
c.724G>C	p.Asp242His	Probably damaging 1.00	Deleterious -6.50	Likely Pathogenic	-2.35	Decreased Stability	-0.7293	Decreased Stability	Probably stable

\*N/A Not available

<https://doi.org/10.1371/journal.pone.0274335.t003>

### CYP1B1 polymorphisms in families with PCG

A single nucleotide polymorphism, c.1347T>C (rs1056837) (Table 2) was found in homozygous state in highest frequency 44% in enrolled families (PCG047, 054, 056, 058, 060, 061, 062, 063, 064, 069 and PCG102). Second variation c.1294G>C (rs1056836) (Table 2) was found in PCG049, 055 and 057 (12%) also showed amino acid change p.Val432Leu that was described as Benign 0.00 by PolyPhen-2. Family PCG051 and 063 (8%) showed SNP c.1358A>G (rs1800400) (Table 2) in coding region that changed amino acid at position 453 from asparagine to serine. This polymorphism was predicted as possibly damaging with a score of 0.906 by PolyPhen-2 and deleterious with a score of -3.24 by PROVEAN. Insertion of T

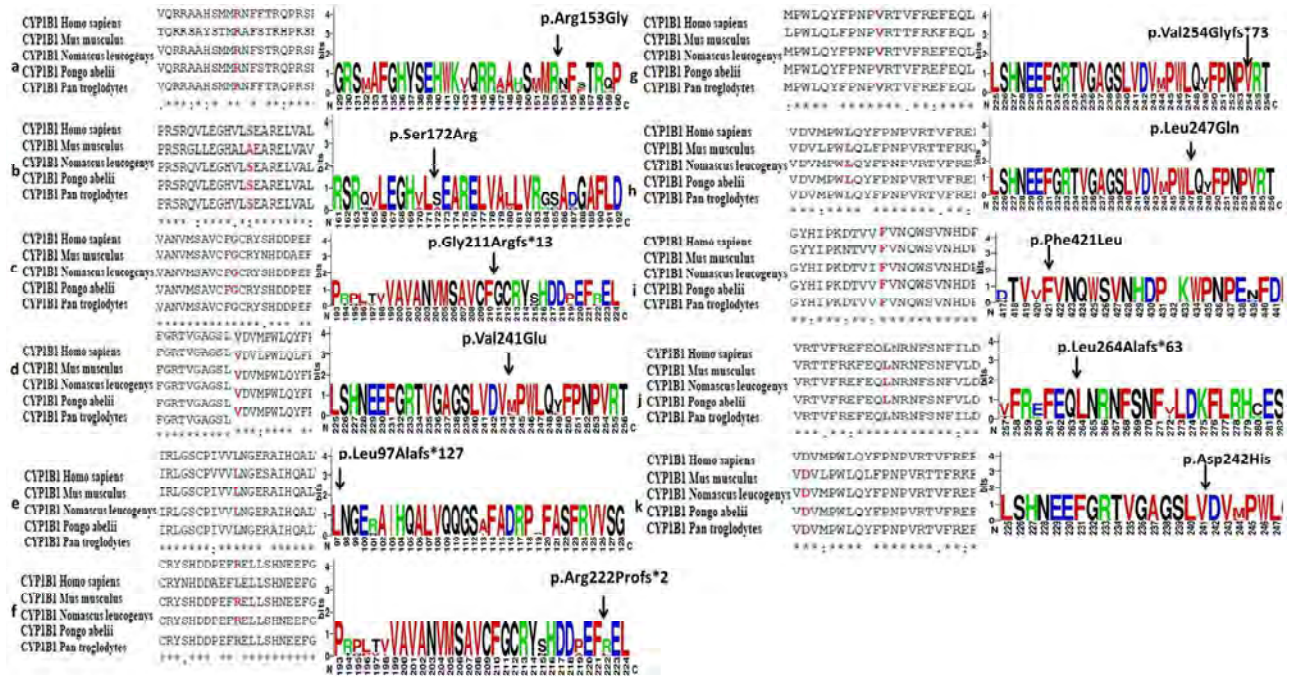


**Fig 4. A comparison of *CYP1B1* gene conservation among different homologs for novel variants detected in this study.** a) Clustal Omega multiple sequence alignment (MSA) (Shown in red) for p.Arg153Gly detected in PCG049. b) Multiple sequence alignment (MSA) for p. Ser172Arg among homologs detected in PCG049 showing less conservation in *Mus musculus*. c) MSA result for p.Gly211Argfs\*13 among homologs detected in PCG050. d) MSA result for variant p.Val241Glu detected in PCG052. e) MSA result for p.Leu97Ala\*127 among homologs detected in PCG053. f) MSA result for p.Arg222Profs\*2 detected in PCG054 showing less conservation in *Mus musculus*. g) MSA result for variant p.Val254Glyfs\*73 detected on PCG059 showing complete conservation among homologs. h) MSA result for p. Leu247Gln among homologs detected in PCG060. i) MSA result for p. Phe421Leu detected in PCG062. j) MSA result for p.Leu264Alafs\*63 detected in PCG063. k) MSA result for p.Asp242His detected in PCG067. a-k) WebLogo results of all novel *CYP1B1* protein variants showing comparison of conservation among homologs are on right side of the figure. All the variants except p.Ser172Arg and p.Arg222Profs\*73 show 100% conservation among different mammals (Large size of amino acid abbreviation letter show full conservation while small size show less conserved position among homologs).

<https://doi.org/10.1371/journal.pone.0274335.g004>

(c.2244\_2245insT) (rs4646431) (Table 2) was found in family PCG052, 064, 065 and 102 (16%) in 3' untranslated region (3'UTR). In exon 2 a substitution of G by T (c.355G>T) (rs1056827) was detected in proband of family PCG053, 056, 069 (12%) (Table 2) in homozygous condition leading to protein change i.e., p.Ala119Ser with no pathogenic effect as predicted by in-silico analysis. Family PCG056 showed SNPs c.142C>G (rs10012) in addition to most prevalent variation c.1347T>C in coding region. This polymorphism was considered as benign and neutral by pathogenicity prediction tools. In this variation arginine at position 48 is replaced by glycine (p.Arg48Gly). Family PCG062 also revealed a previously unreported polymorphism g.35710\_35711insT (Table 2) in intronic region.

## Discussion

High frequency i.e., 70–100% of consanguineous marriages [34] is the main cause of high prevalence of autosomal recessive disorders like PCG in Pakistan [6]. Mutated *CYP1B1* coded protein is reported to cause abnormal development of ocular structures resulting in impeded outflow of aqueous humor and PCG phenotype [35, 36]. Data retrieved through studies have shown that mutational spectrum of in *CYP1B1* gene varies among different populations i.e.; p. Ser476Pro is 44% prevalent in India, p.Arg469Trp, p.Arg368His, p.Arg390His, p.Gly61Glu and p.Glu173Arg are 70% prevalent in Iran, p.Gly61Glu, p. Arg390His and p.Glu229Lys are

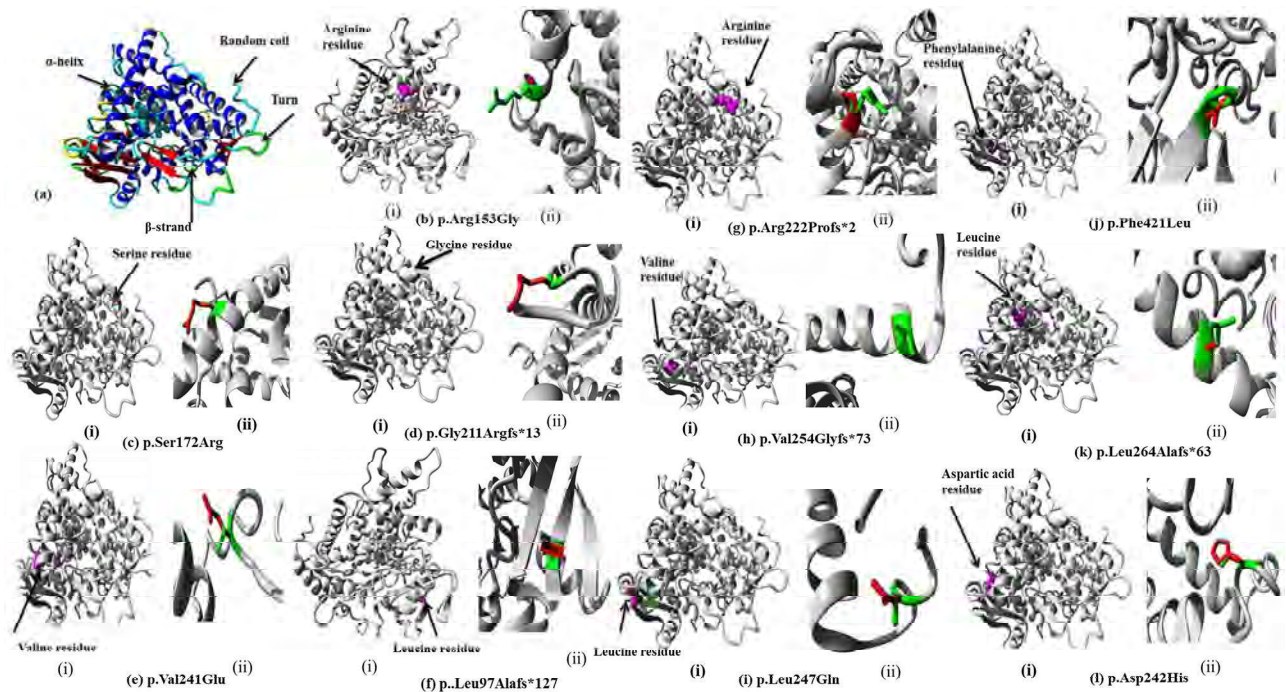


**Fig 5.** (a) Overview of CYP1B1 wild type protein in ribbon-presentation (b-l) In-silico protein prediction regarding variant protein structures for all detected variants by HOPE software. (b-l) i: for each variant show the position of amino acid in protein structure. (b-l) ii: for each detected variant show the zoomed in change in protein structure due to each respective variant (Wild type amino acid residue is colored as green while mutant is colored as red).

<https://doi.org/10.1371/journal.pone.0274335.g005>

80–100% prevalent in Saudi Arabia however p.Arg330Phe and p.Arg390His are predominantly reported from China [37]. Founder mutations reported from India c.1449G>A (R368H), Iran c.182G>A (p.Gly61Glu), Europe c.7996G>A (p.Glu387Lys), Saudi Arabia c.182G>A (p.Gly61Glu) and South Korea c.958G>T (p.Val320Leu) are not prevalent in Pakistan [15]. Previous studies from Pakistan had reported p.Arg390His mutation to be implicated in more than 50% of analyzed PCG cases [6, 20, 38, 39]; however, in present study, we did not identify this mutation in any of the analyzed case. A possible explanation of non-detection of p.Arg390His mutation in our study cohort could be the differences in ethnicities of analyzed subjects. In previous studies, PCG cases belonging to Punjab and Sindh provinces of Pakistan were included [6, 38] however in present study majority of the families i.e., 13/25 belonged to Baluchistan province of Pakistan.

In present study *CYP1B1* analysis in 25 cases enrolled through various regions of Punjab, Baluchistan and Khyber Pakhtunkhwa, Pakistan revealed a total of seven frameshift, seven missense and two silent disease-causing variations. Among seven frameshift variations five are novel however two are previously reported in patients of different ethnicities. The variant c.868dup (p.Arg290Profs\*37) (rs67543922) was initially identified in PCG affected Pakistani family by Sheikh *et al.*, 2014 [40] and then in another family by Micheal *et al.*, 2015 [39]. Mutational analysis of *CYP1B1* conducted on population of Sindh and Punjab province of Pakistan by Rashid *et al.*, 2019 [38] reported that out of total 427 individuals, c.868dup was found in two families that resulted in premature stop codon and eventually truncation.

Second reported frame shift variant c.247del (p.Asp83Thrfs\*12) was initially identified in a study conducted on Indian population by Tanwar *et al.*, 2009 [41]. According to the study a stop codon TAG was introduced at position 94 due to frameshift after codon 82 [41]. Five

homozygous frameshift variants including c.629dup, c.287dup, c.662dup, c.4\_5insT, c.758\_759insA and c.789dup detected in our study are not reported earlier from Pakistan or any other region. All homozygous variants identified in this study showed a perfect segregation with phenotype of disease in all families (Fig 2). Previously, Ou *et al.*, 2018 [42] have shown that the active site residues of CYP1B1 are distributed from amino acid 126 to 510 of the protein therefore all truncations that omit one or more of these amino acids result in loss of protein function [43].

Missense disease-causing variants found in family PCG049, 052, 060, 062 and 067 and two silent disease-causing variants found in family PCG062, 063 are also previously unreported (Fig 3, Table 3). In CYP1B1 protein, novel missense variant p.Arg153Gly is located in C-helix, p.Ser172Arg in D-helix, p.Phe421Leu in K-helix, p.Val241Glu, p.Asp242His and p.Leu247Glu in substrate recognition site 2 [42]. The locations of residue replacements in conserved core structures highlight their possible severe affect on mutated protein structure and functionality hence causing disease phenotype [43, 44]. Here in two families PCG049 and PCG062, we identified compound heterozygous mutations in *CYP1B1* gene. Previously compound heterozygosity has been reported in developmental glaucoma, [45] and primary congenital glaucoma patients from China [46]. Cai *et al.*, 2021 reported that two heterozygous mutations c.1310C>T (p.P437L) and c.3G>A (p.M1I) are responsible for glaucoma in a Chinese family [45]. In another study conducted on 13 Chinese PCG patients, two heterozygous mutations Ala330Phe and Arg390His were detected in a patient and reduced enzymatic activity due to these variants was reported to be the cause of disease [46]. Waryah *et al.*, 2019 identified compound heterozygosity (p.Val364Met along with p.Pro350Thr) in two consanguineous families of PCG belonging to different ethnic groups of Pakistan [47]. Furthermore, previous studies have also reported co-segregation of heterozygous variants of *CYP1B1* with heterozygous *TEK* alleles in PCG cases [48]. In present study, we identified a heterozygous variant p.Leu247Gln in a consanguineous family i.e., PCG060 and absence of any other heterozygous/homozygous variant in *CYP1B1*, recessive inheritance pattern and previously reported allelic interactions of two un linked genes for PCG phenotype [12, 13, 48] necessitates genetic analysis of other glaucoma related genes including MYOC, FOXC1 and TEK genes in PCG060 family.

Due to epigenetic modifications and different environmental factors incomplete penetrance and increased variability could be observed in manifestation of *CYP1B1* disease causing variations in PCG patients [38, 49]. We could not identify homozygous or compound heterozygous disease-causing variants in fifteen analyzed families in this study that predicts the contribution of other genes like *LTBP2*, *TEK*, *MYOC*, *FOXC1* and regulatory effect of cis-acting elements, splicing elements or possible modifiers [12, 13, 40, 50].

All single nucleotide polymorphisms (SNPs) identified in current study except one present in intronic region i.e., g.35710\_35711insT in homozygous state are previously reported. Four reported SNPs i.e., rs1056836 (c.1294G>C), rs1800400 (c.1358A>G), rs1056827 (c.355G>T) and rs10012 (c.142C>G) showed amino acid change while two polymorphisms rs1056837 (c.1347T>C) and rs4646431 (c.2244\_2245insT) were silent. Most prevalent polymorphism (45%) c.1347T>C in present study was also reported in other studies conducted on PCG cases from Pakistani population [51]. Afzal *et al.*, 2019 [20] reported SNP c.142C>G in 23.6%, c.1294G>C in 25.3% and c.355G>T in 53.2% cases while in current data they showed a frequency of 4.1%, 12.5% and 12.5% respectively.

## Conclusion

In conclusion we identified thirteen previously unreported and three reported mutations as well as six SNPs (one novel) in PCG probands born to parents having consanguineous

marriages highlighting the autosomal recessive pattern of disease. Proper genetic testing and counseling should be provided to people in high consanguinity areas to help ophthalmologists in disease management and treatment. Mass screening and additional studies are required to better understand the heterogeneous pattern and contribution of *CYP1B1* gene to PCG pathophysiology in our population.

## Acknowledgments

We thank patients and their families for their participation in this study.

## Author Contributions

**Conceptualization:** Shagufta Naz, Kiran Afshan, Sabika Firasat.

**Data curation:** Anam Arooj, Sorath Noorani Siddiqui.

**Formal analysis:** Raeesa Tehreem, Anam Arooj, Shagufta Naz, Sabika Firasat.

**Funding acquisition:** Sabika Firasat.

**Investigation:** Raeesa Tehreem, Anam Arooj, Sorath Noorani Siddiqui.

**Methodology:** Raeesa Tehreem, Anam Arooj, Kiran Afshan, Sabika Firasat.

**Project administration:** Sabika Firasat.

**Resources:** Kiran Afshan, Sabika Firasat.

**Supervision:** Sabika Firasat.

**Validation:** Raeesa Tehreem, Anam Arooj, Shagufta Naz, Sabika Firasat.

**Visualization:** Raeesa Tehreem, Anam Arooj, Sorath Noorani Siddiqui, Sabika Firasat.

**Writing – original draft:** Raeesa Tehreem, Sabika Firasat.

**Writing – review & editing:** Raeesa Tehreem, Anam Arooj, Sorath Noorani Siddiqui, Shagufta Naz, Kiran Afshan, Sabika Firasat.

## References

1. Sarfarazi M., Stoilov I., and Schenkman J.B., Genetics and biochemistry of primary congenital glaucoma. *Ophthalmology clinics of North America*, 2003. 16(4): p. 543–54, vi. [https://doi.org/10.1016/s0896-1549\(03\)00062-2](https://doi.org/10.1016/s0896-1549(03)00062-2) PMID: 14740995
2. Ko F., Papadopoulos M., and Khaw P.T., Primary congenital glaucoma. *Progress in brain research*, 2015. 221: p. 177–189. <https://doi.org/10.1016/bs.pbr.2015.06.005> PMID: 26518078
3. Barkan O., Pathogenesis of congenital glaucoma: gonioscopic and anatomic observation of the angle of the anterior chamber in the normal eye and in congenital glaucoma. *American journal of ophthalmology*, 1955. 40(1): p. 1–11. PMID: 14388087
4. Rulli E., et al., Visual field loss and vision-related quality of life in the Italian Primary Open Angle Glaucoma Study. *Scientific reports*, 2018. 8(1): p. 1–12.
5. Vasiliou V. and Gonzalez F.J., Role of *CYP1B1* in glaucoma. *Annu. Rev. Pharmacol. Toxicol.*, 2008. 48: p. 333–358. <https://doi.org/10.1146/annurev.pharmtox.48.061807.154729> PMID: 17914928
6. Rauf B., et al., A spectrum of *CYP1B1* mutations associated with primary congenital glaucoma in families of Pakistani descent. *Human genome variation*, 2016. 3(1): p. 1–4. <https://doi.org/10.1038/hgv.2016.21> PMID: 27508083
7. Stoilov I., Akarsu A.N., and Sarfarazi M., Identification of three different truncating mutations in cytochrome P4501B1 (*CYP1B1*) as the principal cause of primary congenital glaucoma (Buphthalmos) in families linked to the *GLC3A* locus on chromosome 2p21. *Human molecular genetics*, 1997. 6(4): p. 641–647. <https://doi.org/10.1093/hmg/6.4.641> PMID: 9097971

8. Akarsu A.N., et al., A second locus (GLC3B) for primary congenital glaucoma (Buphthalmos) maps to the 1p36 region. *Human molecular genetics*, 1996. 5(8): p. 1199–1203. <https://doi.org/10.1093/hmg/5.8.1199> PMID: [8842741](https://pubmed.ncbi.nlm.nih.gov/8842741/)
9. Stoilov I. and Sarfarazi M., The third genetic locus (GLC3C) for primary congenital glaucoma (PCG) maps to chromosome 14q24.3. *Investigative ophthalmology & visual science*, 2002. 43(13): p. 3015–3015.
10. Firasat S., et al., Primary congenital glaucoma localizes to chromosome 14q24.2–24.3 in two consanguineous Pakistani families. *Molecular vision*, 2008. 14: p. 1659. PMID: [18776954](https://pubmed.ncbi.nlm.nih.gov/18776954/)
11. Ali M., et al., Null mutations in LTBP2 cause primary congenital glaucoma. *The American Journal of Human Genetics*, 2009. 84(5): p. 664–671. <https://doi.org/10.1016/j.ajhg.2009.03.017> PMID: [19361779](https://pubmed.ncbi.nlm.nih.gov/19361779/)
12. Kaur K., et al., Myocilin gene implicated in primary congenital glaucoma. *Clinical genetics*, 2005. 67(4): p. 335–340. <https://doi.org/10.1111/j.1399-0004.2005.00411.x> PMID: [15733270](https://pubmed.ncbi.nlm.nih.gov/15733270/)
13. Chakrabarti S., et al., The transcription factor gene FOXC1 exhibits a limited role in primary congenital glaucoma. *Investigative ophthalmology & visual science*, 2009. 50(1): p. 75–83. <https://doi.org/10.1167/iovs.08-2253> PMID: [18708620](https://pubmed.ncbi.nlm.nih.gov/18708620/)
14. Souma T., et al., Angiopoietin receptor TEK mutations underlie primary congenital glaucoma with variable expressivity. *The Journal of clinical investigation*, 2016. 126(7): p. 2575–2587. <https://doi.org/10.1172/JCI85830> PMID: [27270174](https://pubmed.ncbi.nlm.nih.gov/27270174/)
15. Chouiter L. and Nadifi S., Analysis of *CYP1B1* gene mutations in patients with primary congenital glaucoma. *Journal of pediatric genetics*, 2017. 6(04): p. 205–214. <https://doi.org/10.1055/s-0037-1602695> PMID: [29142762](https://pubmed.ncbi.nlm.nih.gov/29142762/)
16. Acharya, M. and M. Walter, *Molecular Genetics of Congenital and Juvenile Glaucoma*. 2010.
17. Haddad A., et al., Meta-analysis of *CYP1B1* gene mutations in primary congenital glaucoma patients. *European journal of ophthalmology*, 2021. 31(6): p. 2796–2807. <https://doi.org/10.1177/11206721211016308> PMID: [34020567](https://pubmed.ncbi.nlm.nih.gov/34020567/)
18. Zhao Y., Sorenson C.M., and Sheibani N., Cytochrome P450 1B1 and primary congenital glaucoma. *Journal of ophthalmic & vision research*, 2015. 10(1): p. 60. <https://doi.org/10.4103/2008-322X.156116> PMID: [26005555](https://pubmed.ncbi.nlm.nih.gov/26005555/)
19. Database, T.H.G.M. *CYP1B1 Gene mutations*. 2021; <http://www.hgmd.cf.ac.uk/ac/gene.php?gene=CYP1B1>.
20. Afzal R., et al., Mutational analysis of the *CYP1B1* gene in Pakistani primary congenital glaucoma patients: Identification of four known and a novel causative variant at the 3' splice acceptor site of intron 2. *Congenital anomalies*, 2019. 59(5): p. 152–161. <https://doi.org/10.1111/cga.12312> PMID: [30270463](https://pubmed.ncbi.nlm.nih.gov/30270463/)
21. Association W.M., World Medical Association Declaration of Helsinki: ethical principles for medical research involving human subjects. *Jama*, 2013. 310(20): p. 2191–2194. <https://doi.org/10.1001/jama.2013.281053> PMID: [24141714](https://pubmed.ncbi.nlm.nih.gov/24141714/)
22. Thiele H. and Nürnberg P., HaploPainter: a tool for drawing pedigrees with complex haplotypes. *Bioinformatics*, 2005. 21(8): p. 1730–1732. <https://doi.org/10.1093/bioinformatics/bth488> PMID: [15377505](https://pubmed.ncbi.nlm.nih.gov/15377505/)
23. Kaul H., et al., Autosomal recessive congenital cataract linked to EPHA2 in a consanguineous Pakistani family. *Molecular vision*, 2010. 16: p. 511. PMID: [20361013](https://pubmed.ncbi.nlm.nih.gov/20361013/)
24. Schwarz J.M., et al., MutationTaster evaluates disease-causing potential of sequence alterations. *Nature methods*, 2010. 7(8): p. 575–576. <https://doi.org/10.1038/nmeth0810-575> PMID: [20676075](https://pubmed.ncbi.nlm.nih.gov/20676075/)
25. Wildeman M., et al., Improving sequence variant descriptions in mutation databases and literature using the Mutalyzer sequence variation nomenclature checker. *Human mutation*, 2008. 29(1): p. 6–13. <https://doi.org/10.1002/humu.20654> PMID: [18000842](https://pubmed.ncbi.nlm.nih.gov/18000842/)
26. Kopanos C., et al., VarSome: the human genomic variant search engine. *Bioinformatics*, 2019. 35(11): p. 1978. <https://doi.org/10.1093/bioinformatics/bty897> PMID: [30376034](https://pubmed.ncbi.nlm.nih.gov/30376034/)
27. Adzhubei I.A., et al., A method and server for predicting damaging missense mutations. *Nature methods*, 2010. 7(4): p. 248–249. <https://doi.org/10.1038/nmeth0410-248> PMID: [20354512](https://pubmed.ncbi.nlm.nih.gov/20354512/)
28. Ng P.C. and Henikoff S., SIFT: Predicting amino acid changes that affect protein function. *Nucleic acids research*, 2003. 31(13): p. 3812–3814. <https://doi.org/10.1093/nar/gkg509> PMID: [12824425](https://pubmed.ncbi.nlm.nih.gov/12824425/)
29. Choi, Y., et al., *Predicting the functional effect of amino acid substitutions and indels*. 2012.
30. Rodrigues C.H., Pires D.E., and Ascher D.B., *DynaMut: predicting the impact of mutations on protein conformation, flexibility and stability*. *Nucleic acids research*, 2018. 46(W1): p. W350–W355.
31. Cheng J., Randall A., and Baldi P., Prediction of protein stability changes for single-site mutations using support vector machines. *Proteins: Structure, Function, and Bioinformatics*, 2006. 62(4): p. 1125–1132. <https://doi.org/10.1002/prot.20810> PMID: [16372356](https://pubmed.ncbi.nlm.nih.gov/16372356/)

32. Sievers F., et al., Fast, scalable generation of high-quality protein multiple sequence alignments using Clustal Omega. *Molecular systems biology*, 2011. 7(1): p. 539. <https://doi.org/10.1038/msb.2011.75> PMID: [21988835](https://pubmed.ncbi.nlm.nih.gov/21988835/)
33. Crooks G.E., et al., WebLogo: a sequence logo generator. *Genome research*, 2004. 14(6): p. 1188–1190. <https://doi.org/10.1101/gr.849004> PMID: [15173120](https://pubmed.ncbi.nlm.nih.gov/15173120/)
34. Abu-Amero K.K., et al., Screening of CYP1B1 and LTBP2 genes in Saudi families with primary congenital glaucoma: genotype-phenotype correlation. *Molecular vision*, 2011. 17: p. 2911. PMID: [22128238](https://pubmed.ncbi.nlm.nih.gov/22128238/)
35. Bagiyeva S., et al., Mutational screening of CYP1B1 in Turkish PCG families and functional analyses of newly detected mutations. *Mol Vis*, 2007. 13(13): p. 1458–1468. PMID: [17893647](https://pubmed.ncbi.nlm.nih.gov/17893647/)
36. Li N., et al., Overview of Cytochrome P450 1B1 gene mutations in patients with primary congenital glaucoma. *Experimental eye research*, 2011. 93(5): p. 572–579. <https://doi.org/10.1016/j.exer.2011.07.009> PMID: [21854771](https://pubmed.ncbi.nlm.nih.gov/21854771/)
37. Shah M., Bouhenni R., and Benmerzoug I., Geographical Variability in CYP1B1 Mutations in Primary Congenital Glaucoma. *Journal of clinical medicine*, 2022. 11(7): p. 2048. <https://doi.org/10.3390/jcm11072048> PMID: [35407656](https://pubmed.ncbi.nlm.nih.gov/35407656/)
38. Rashid M., et al., Identities and frequencies of variants in CYP1B1 causing primary congenital glaucoma in Pakistan. *Molecular vision*, 2019. 25: p. 144. PMID: [30820150](https://pubmed.ncbi.nlm.nih.gov/30820150/)
39. Micheal S., et al., Identification of novel CYP1B 1 gene mutations in patients with primary congenital and primary open-angle glaucoma. *Clinical & experimental ophthalmology*, 2015. 43(1): p. 31–39.
40. Sheikh S.A., et al., Mutational spectrum of the CYP1B1 gene in Pakistani patients with primary congenital glaucoma: novel variants and genotype-phenotype correlations. *Molecular vision*, 2014. 20: p. 991. PMID: [25018621](https://pubmed.ncbi.nlm.nih.gov/25018621/)
41. Tanwar M., et al., Identification of four novel cytochrome P4501B1 mutations (p. I94X, p. H279D, p. Q340H, and p. K433K) in primary congenital glaucoma patients. *Molecular vision*, 2009. 15: p. 2926. PMID: [20057908](https://pubmed.ncbi.nlm.nih.gov/20057908/)
42. Ou Z., et al., Bioinformatics analysis of CYP1B1 mutation hotspots in Chinese primary congenital glaucoma patients. *Bioscience reports*, 2018. 38(4). <https://doi.org/10.1042/BSR20180056> PMID: [29903728](https://pubmed.ncbi.nlm.nih.gov/29903728/)
43. Firasat S., et al., In silico analysis of five missense mutations in CYP1B1 gene in Pakistani families affected with primary congenital glaucoma. *International ophthalmology*, 2018. 38(2): p. 807–814. <https://doi.org/10.1007/s10792-017-0508-4> PMID: [28386709](https://pubmed.ncbi.nlm.nih.gov/28386709/)
44. Achary M.S., et al., Disease-causing mutations in proteins: structural analysis of the CYP1B1 mutations causing primary congenital glaucoma in humans. *Biophysical journal*, 2006. 91(12): p. 4329–4339. <https://doi.org/10.1529/biophysj.106.085498> PMID: [16963504](https://pubmed.ncbi.nlm.nih.gov/16963504/)
45. Cai S., et al., Novel compound heterozygous mutations in CYP1B1 identified in a Chinese family with developmental glaucoma. *Molecular Medicine Reports*, 2021. 24(5): p. 1–8.
46. Song N., et al., Compound heterozygous mutations in CYP1B1 gene leads to severe primary congenital glaucoma phenotype. *International journal of ophthalmology*, 2019. 12(6): p. 909.
47. Waryah Y.M., et al., Two novel variants in CYP1B1 gene: a major contributor of autosomal recessive primary congenital glaucoma with allelic heterogeneity in Pakistani patients. *International Journal of Ophthalmology*, 2019. 12(1): p. 8. <https://doi.org/10.18240/ijo.2019.01.02> PMID: [30662834](https://pubmed.ncbi.nlm.nih.gov/30662834/)
48. Kabra M., et al., Angiopoietin receptor TEK interacts with CYP1B1 in primary congenital glaucoma. *Human genetics*, 2017. 136(8): p. 941–949. <https://doi.org/10.1007/s00439-017-1823-6> PMID: [28620713](https://pubmed.ncbi.nlm.nih.gov/28620713/)
49. Bejjani B.A., et al., Multiple CYP1B1 mutations and incomplete penetrance in an inbred population segregating primary congenital glaucoma suggest frequent de novo events and a dominant modifier locus. *Human molecular genetics*, 2000. 9(3): p. 367–374. <https://doi.org/10.1093/hmg/9.3.367> PMID: [10655546](https://pubmed.ncbi.nlm.nih.gov/10655546/)
50. Yousaf R., et al., Modifier variant of METTL13 suppresses human GAB1-associated profound deafness. *The Journal of clinical investigation*, 2018. 128(4): p. 1509–1522. <https://doi.org/10.1172/JCI97350> PMID: [29408807](https://pubmed.ncbi.nlm.nih.gov/29408807/)
51. Shan T., et al., Mutational Analysis of CYP1B1 gene in families with Primary Congenital glaucoma. *Ilkogretim Online*, 2021. 20(5): p. 5285–5292.

Turnitin Originality Report

Molecular Basis of Recessively Inherited Eye Disorders in Pakistani Population  
Raeesa Tehreem

by  turnitin

From Master PhD (Master PhD)

- Processed on 08-May-2024 14:24 PKT
- ID: 2374099280
- Word Count: 28107

Similarity Index  
14%  
Similarity by Source

*Sabit*  
ASSISTANT PROFESSOR  
Department of Zoology  
Quaid-i-Azam University  
Islamabad

Internet Sources:  
10%  
Publications:  
10%  
Student Papers:  
2%

*M. Sabit*  
Focal Person (Turnitin)  
Quaid-i-Azam University  
Islamabad

**sources:**

1 1% match (Internet from 21-Jul-2023)

<https://pubmed.ncbi.nlm.nih.gov/36083974/>

2 1% match (Internet from 14-May-2023)

[https://www.researchgate.net/figure/The-MYO7A-and-USH2A-sequence-variants-deleted-in-our-series\\_tbl1\\_270513083](https://www.researchgate.net/figure/The-MYO7A-and-USH2A-sequence-variants-deleted-in-our-series_tbl1_270513083)

3 < 1% match (Internet from 21-Jul-2023)

<https://pubmed.ncbi.nlm.nih.gov/36140798/>

4 < 1% match (Internet from 23-Apr-2024)

<https://pubmed.ncbi.nlm.nih.gov/37468087/?fc=None&ff=20230720091006&v=2.17.9.post6+86293pc>

5 < 1% match (Internet from 25-Jan-2024)

<https://pubmed.ncbi.nlm.nih.gov/28425126/>

6 < 1% match (Internet from 04-Jun-2023)

<https://www.researchgate.net/publication/367328563> In silico Tools Used to Predict the Impact of Missense Variants

7 < 1% match (Internet from 20-Mar-2024)

<https://www.frontiersin.org/journals/genetics/articles/10.3389/fgene.2022.969895/pdf?isPublishedV2=false>

8 < 1% match (Internet from 15-Sep-2023)

<https://www.frontiersin.org/articles/10.3389/fgene.2023.1154713/full>

9 < 1% match (Internet from 20-Mar-2024)